

Cellular substrates of arrhythmogenicity in inherited and acquired cardiomyopathies



Willem B. van Ham

Cellular substrates of arrhythmogenicity in inherited and acquired cardiomyopathies

Willem B. van Ham

ISBN: 978-94-6496-053-2

Cover design: Betzabel Cajiao Garcia

Printing: Gildeprint B.V. | www.gildeprint.nl



Copyright: © 2024 W.B. van Ham, Utrecht, The Netherlands. All rights reserved. No part of this thesis may be reproduced, stored in a retrieval system, or transmitted in any form or by any means without prior written permission of the author. The copyright of the publications has been transferred to the respective journals.

Cellular substrates of arrhythmogenicity in inherited and acquired cardiomyopathies

Cellulaire substraten van aritmogeniteit in erfelijke en verworven hartspierziekten
(met een samenvatting in het Nederlands)

Proefschrift

Ter verkrijging van de graad van doctor aan de Universiteit Utrecht
op gezag van de rector magnificus, prof. dr. H.R.B.M. Kummeling,
ingevolge het besluit van het college voor promoties
in het openbaar te verdedigen op

donderdag 11 april 2024
des middags te 2:15 uur

door

Willem Benjamin van Ham

geboren op 1 februari 1995
te Tilburg

Promotor:

Prof. dr. M.A. Vos

Copromotor:

Dr. A.A.B. van Veen

Beoordelingscommissie:

Prof. dr. ir. J.P.W.M. Bakkers (voorzitter)

Prof. dr. R. Masereeuw

Prof. dr. C.L. Mummery

Prof. dr. J.P.G. Sluijter

Prof. dr. A.A.M. Wilde

The research described in this thesis was performed in the Department of Medical Physiology from the Division Heart & Lungs of the University Medical Center Utrecht, within the PhD programme of Cardiovascular Research from the Graduate School of Life Sciences, Utrecht University.

The research described in this thesis was funded by the Netherlands Cardio Vascular Research Initiative (CVON): the Dutch Heart Foundation, Dutch Federation of University Medical Centers, the Netherlands Organization for Health Research and Development and the Royal Netherlands Academy of Sciences, CVON PREDICT2 and RECONNECT.

Financial support by the Dutch Heart Foundation for the publication of this thesis is gratefully acknowledged.

Voor ons mam
en ons pap

Contents

Chapter I	General introduction	9
	PART I CARDIORENAL SYNDROME	21
Chapter II	Uremic toxins in chronic kidney disease highlight a fundamental gap in understanding their detrimental effects on cardiac electrophysiology and arrhythmogenesis	23
Chapter III	Pro-arrhythmic potential of accumulated uremic toxins is mediated via vulnerability of action potential repolarization	48
	PART II PATIENT-SPECIFIC MODELING IN INHERITED AND ACQUIRED CARDIOMYOPATHIES	65
Chapter IIII	Maturation and function of the intercalated disc: report of two pediatric cases focusing on cardiac development and myocardial hyperplasia	67
Chapter V	An hiPSC-CM approach for electrophysiological phenotyping of a patient-specific case of short-coupled TdP	83
Chapter VI	Electrophysiological disturbances in inherited and acquired cardiomyopathies – Introduction	109
	Part A PITX2 induction leads to impaired cardiomyocyte function in arrhythmogenic cardiomyopathy	117
	Part B Desmosomal protein degradation as an underlying cause of arrhythmogenic cardiomyopathy	129
	Part C Hypoxia-responsive ZEB2 regulates a network of calcium handling genes in the injured heart	141
	Electrophysiological disturbances in inherited and acquired cardiomyopathies – Discussion	149
Chapter VII	Patient-specific modeling of disrupted calcium handling and cardiomyocyte electromechanics in arrhythmogenic cardiomyopathy	157
Chapter VIII	General discussion	187
Appendix		203
	Samenvatting in het Nederlands	205
	Dankwoord	211
	List of publications	218
	Curriculum vitae	221

Willem B. van Ham¹

¹Department of Medical Physiology, University Medical Center Utrecht, The Netherlands

Chapter I

General introduction

Electromechanics of the heart

The electrical activation of heart cells (cardiomyocytes) is an essential underlying mechanism to initiate contraction of the heart. To assure optimal organization and timing of the synchronized activation of all cardiomyocytes, conduction of the electrical signal (action potential, AP) throughout the cardiac tissue follows a conventional route. The AP is generated in the sinoatrial node, located in the right atrium, and is then propagated throughout both atria towards the atrioventricular node. Here, the conduction is temporarily delayed in order to facilitate an optimal filling of the ventricles. From the atrioventricular node the signal is, via the bundle of His and the bundle branches, directed along the ventricular septum towards the apex of the heart. Further transport of the AP across the ventricles following the Purkinje fibers finalizes the electrical activation (excitation) of the entire heart. Description of the human cardiac AP, often based on the ventricular AP, includes five phases that are the consequence of ions passing the membrane of the cardiomyocytes via specific ion channels. These phases consist of 0) depolarization (influx of Na^+), 1) initial repolarization (cease of Na^+ influx and initial K^+ efflux), 2) plateau (influx of Ca^{2+} and continuous K^+ efflux), 3) repolarization (arrest of all currents other than K^+ efflux), and 4) resting (termination of all but one K^+ current).

The Ca^{2+} influx during the excitation process in each cardiomyocyte also plays a role in the subsequent contraction process. The Ca^{2+} ions entering the cell by passing the membrane will simultaneously trigger the efflux of a much larger amount of Ca^{2+} from the cell storage (sarcoplasmic reticulum, SR) into the cytosol, a process named calcium-induced calcium release (CICR). This vast amount of Ca^{2+} binds to the troponin complex on the sarcomeres thereby creating space on the actin filaments for myosin binding, allowing the actin and myosin filaments to slide alongside one another, which facilitates the contraction of the sarcomeres. Upon release of Ca^{2+} from the sarcomeres, the cytosolic Ca^{2+} efflux is orientated towards the SR and the extracellular space, causing a period of relaxation. This sequence of calcium release and removal is reflected in the calcium transient (CaT). Altogether, this relationship between electrical activation and mechanical performance is described as excitation-contraction coupling (ECC)¹. This allows the heart to activate and contract in a controlled manner, functioning as a pump, and propagating blood through the entire circulatory system of the body.

The structure and organization of cardiomyocytes in the myocardial tissue are crucial for appropriate ECC. The oblong cardiomyocytes are firmly coupled to neighboring cells at their longitudinal ends. Here, at the intercalated disc (ID), molecular structures such as desmosomes, adherence junctions, and gap junctions can be found². As cardiomyocytes are tightly joined, electrical cell-to-cell conduction can occur at a fast pace without unexpected intermissions. However, in pathological situations these connections can weaken or disband, causing conduction blocks. Similarly, the internal organization of cardiomyocytes is vital as well. This includes a plethora of aspects like structural organization, metabolism, signal transduction

pathways, but also calcium homeostasis. Regarding the latter, the distance between the SR relative to the cell membrane, known as the dyad, influences the speed and intensity of CICR³. This is facilitated in cardiomyocytes by invaginations of the cell membrane (T-tubules), increasing the membrane surface in proximity to the SR. As such, Ca²⁺ influx through L-type calcium channels that particularly reside in the membranes of the T-tubules, enables the accumulation of Ca²⁺ in the dyad which subsequently is powerful enough to trigger CICR. Simultaneously, the sarcomeres are located closely alongside the SR to optimize contractility as this positioning enhances the chance that the released Ca²⁺ can bind to the nearby sarcomeric proteins.

Deviations in the electromechanical coupling can lead to rhythm disorders, called arrhythmias. The initiation and continuation of cardiac arrhythmias is a complicated assembly of triggers and substrates, with structural and electrical components. Specific electrophysiological mechanisms behind arrhythmias are spontaneous electrical activation (ectopic activity) and the perpetuation of uncontrolled electrical conduction (reentry). The former is mainly instigated by altered ion channel conduction and aberrant calcium homeostasis, while the latter is determined by cell-to-cell coupling and structural alterations of the heart. Amongst many pathological conditions that could predispose patients to these arrhythmias are chronic kidney failure and (non-)genetic diseases of the myocardium (cardiomyopathies).

Cardiorenal syndrome

As the heart and the kidneys are functionally intertwined, loss of function in one could result in damage to the other, which is called the cardiorenal syndrome (CRS)^{4,5}. The kidneys filter and excrete toxic materials and excess water from the blood. Prolonged damage to the kidneys, i.e. chronic kidney disease (CKD), affects the filtration function, causing the build-up of damaging waste products in the circulation. Both organs deteriorating over time creates a vicious circle, which eventually can end in multi-organ failure. Examples of damaging materials that can accumulate are uremic toxins (UTs), often metabolic intermediate structures of regular protein metabolism⁶. Many UTs are difficult to remove from the blood due to their protein binding properties, especially during kidney failure or by artificial filtration systems like hemodialysis^{7,8}. While the effects of elevated UT levels include already established factors like increased inflammation and collagen deposition in the heart and kidneys⁹, high rates of sudden cardiac death (SCD) in CKD patients suggest the direct involvement of disturbed cardiac electrophysiology¹⁰.

Most studies regarding UTs and the CRS involve cohorts of CKD patients focusing on correlations between UTs and disease outcome^{11,12}. Over time, most of these studies gave rise to similar lists of detrimental UTs, such as indoxyl sulfate and p-cresyl sulfate. Unfortunately, this also resulted in succeeding research emphasizing mainly these UTs, disregarding other potential toxins. Clinical research predominantly continues the efforts on improving or designing treatment options, e.g. dialysis membranes

that offer enhanced removal of UTs¹³. Direct effects of UTs in patients on cardiac electrophysiology are difficult to examine. The SCD prevalence is high in dialysis patients, but cause is primarily assigned to electrolyte disturbances due to fluid fluctuations¹⁴. Experimental studies investigating molecular mechanisms behind the effects that UTs directly exert on cardiac electrophysiology are very limited. This is partly due to systemic effects only being perceptible in whole organisms with kidney failure, which implies that isolating the individual impact of individual UTs then becomes impossible. Experimental strategies that would be able to achieve this generate the possibility to dissect the complexity as seen during CKD and allow to address the individual contribution of UTs and their potential pro-arrhythmic severity.

Arrhythmias in (non-)genetic cardiomyopathies

Genetic variants in genes encoding for proteins involved in cardiac ECC can increase susceptibility to arrhythmias. Examples of such variants that give rise to different forms of cardiomyopathies are found in patients that suffer from long QT syndrome (e.g. the *KCNH2* gene), Brugada syndrome (e.g. the *SCN5A* gene), phospholamban cardiomyopathy (the *PLN* gene), and hypertrophic cardiomyopathy (e.g. the *MYBPC3* gene)^{15,16}. Whereas alterations in ion channels can be explored rather straightforwardly, explaining arrhythmogenicity due to dysfunction of proteins that can affect cardiomyocyte structure and organization can often be difficult. However, in experimental models, a combination of expression analysis and bioinformatics can unmask the link between the primary dysfunction of an ion channel and the secondary pro-arrhythmic consequences. Furthermore, elucidating electrophysiological pathology in patients without known genetic alterations can even be more complicated. In those cases, broader experimental approaches are applicable, preferably covering electromechanics, structural studies, and molecular investigations. These are also often highly patient-specific, potentially prohibiting the general translational of scientific findings towards the clinic. This certainly accounts for rare cases in which the number of patients that can be studied provokes the robustness of the acquired findings.

A specific example of genetic cardiomyopathy is arrhythmogenic cardiomyopathy (ACM), an inherited disease of the desmosomes, with SCD often as the first devastating symptom that is presented, especially in young people and athletes¹⁷. The desmosomes function as anchors in cell-to-cell coupling and contain proteins such as plakophilin 2 (PKP2) and desmoplakin (DSP). Aberrancies in those proteins not only affect the integrity of the coupled cells, but can also cause calcium handling disturbances, mitochondrial dysfunction, and replacement of the myocardium by fibrofatty tissue¹⁷⁻²⁰. *PKP2* and *DSP* are also the most prevalent genes with pathogenic variants in ACM, but a genetic predisposition is not required for clinical diagnosis²¹. The clinical presentation of ACM patients is very heterogeneous, with incomplete penetrance of genetic variations and diverse cardiac structural involvement. Studying the molecular pathology of ACM remains important, with new genetic variants still being identified and only a partial understanding of disease pathology, as acquiring material from involved patients often occurs at advanced stages of the

disease²². Several animal and cell models of ACM have been and still are being developed, but often cover only a part of the disease development or are limited in clinical translationability.

Disease modeling and electrophysiological phenotyping

To investigate pathological mechanisms or to develop therapeutic interventions, different disease models can be used, naturally each having advantages and drawbacks. Obtaining cardiac tissue from human patients is limited in both availability and timepoint of the disease. Most often, sufficient material can only be obtained after death or heart transplantation, but include the most relevant representation of a disease. With exception of reconstructive interventions (like septal resection in hypertrophic cardiomyopathy), this also means that the obtained tissue is often reflecting the end-stage of the disease. Animal models can be created to allow for advanced modulation of genetics, inclusion of systemic effects, and increase of availability. Translationability towards the clinic becomes more difficult in animal models, as many physiological processes differ from the human situation. This especially accounts for the routinely applied mouse models given the fact that both physiology and pathophysiology substantially differ compared to humans. Cellular models are mainly applicable to study molecular and functional mechanisms of a small subset of cell types, also hampering translationability. However, these *in vitro* models do permit the complete control of culture environment, genetic manipulation, and unlimited access, all while being financially advantageous. The application of human induced pluripotent stem cell derived cardiomyocytes (hiPSC-CMs) has improved tremendously in the last decade, aiding in molecular and functional understanding of cardiac diseases. Unlike isolated cardiomyocytes from animals they can be cultured for longer periods of time, but they only partly mimic adult human ventricular cardiomyocytes. Finally, there are also computational models, which are often designed based on experimental data and aim to provide translationable predictions. Computational models can be beneficial in converting molecular data from other models into functional output, bridging and connecting the different disease modeling alternatives.

Electrophysiological phenotyping of cell and tissue models includes two options, being the quantification of absolute values for ion currents and membrane voltages using the patch clamping technique, or the relative representations of the AP and CaT using fluorescent dyes. While patch clamping allows for precise and absolute measurements, it can be a difficult and labor-intensive technique. Application of voltage and calcium sensitive dyes is much more tolerant, but no absolute voltages or calcium concentrations can be measured. However, the ability of high throughput can result in robust screenings of different genetic lines or drug responses. On top of that, in cases without a known genetic cause, general screenings are highly practical and provide indications for a more in-depth follow-up, rather than an elaborative initial approach of specific ion current measurements without a dedicated rationale. The increase and decrease in fluorescence signal represent the morphology of either an AP or CaT in e.g. hiPSC-CMs (**Figure 1A**). Time to reach the peak, return to the baseline, or overall peak width can be used to describe effects

between different conditions, including drug administration (**Figure 1B**). AP prolongation caused by the late repolarization blocker dofetilide, or CaT alterations instigated by the SR reuptake inhibitor thapsigargin and the β -adrenergic stimulator isoproterenol, all highlight the effects detectable using optical electrophysiology. From alterations in those signals can also be deduced which channel or transporter, or which combinations of these players involved in electrophysiological homeostasis are affected to guide further research.

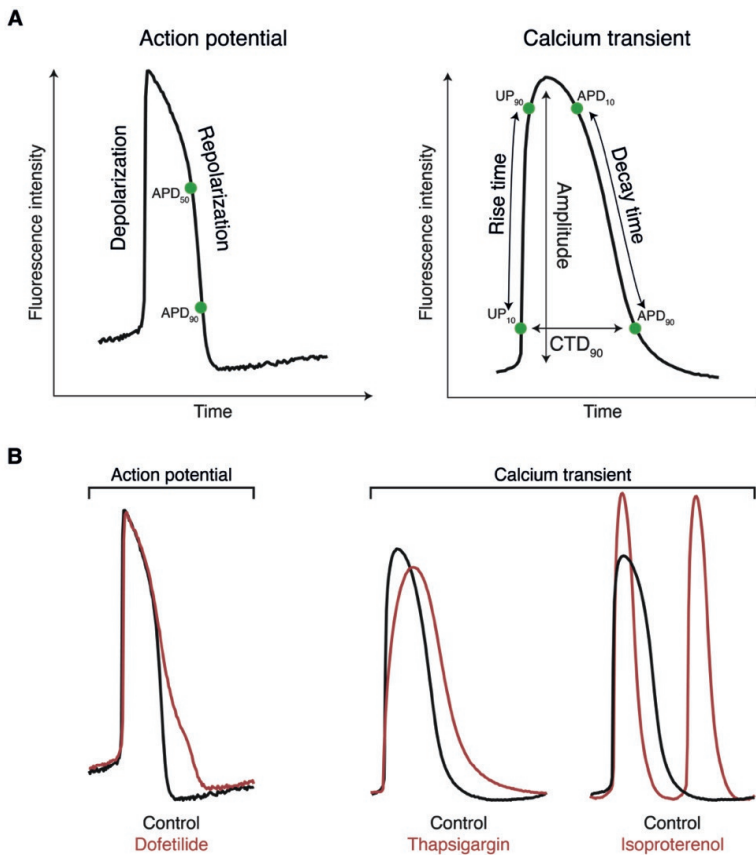


Figure 1. Representation of measured action potentials and calcium transients. Using fluorescent dyes, action potentials (APs) and calcium transients (CaTs) can be measured in cells and tissue. **(A)** Analysis of acquired traces, with definitions of up- and downstroke parameters of APs and CaTs. **(B)** Visualization of pharmacological effects on measurements, including the repolarization blocker dofetilide, SERCA inhibitor thapsigargin, and the β -adrenergic stimulator isoproterenol. Measurements originate from human induced pluripotent stem cell derived cardiomyocytes.

Thesis outline

This thesis consists of two parts that revolve around disease modeling and phenotyping, in which a variety of modeling systems are included to study cardiac electrophysiology. **Part I** reflects on the CRS and **Part II** includes patient-specific cases of several inherited and acquired cardiomyopathies.

Chapter II introduces the fundamental gap that exists between UTs and their direct influence on cardiac electrophysiology and arrhythmogenesis. Then, a broader introduction regarding cellular electrophysiology and the occurrence and perpetuation of arrhythmias will be described, followed by highlighting the existing clinical and experimental research that has been performed on cardiac effects of UTs. **Chapter III** continues with an experimental study describing a pro-arrhythmic mechanism caused by exposure to UTs. Here, it is shown that UTs can impede AP repolarization, increasing the potency for premature activation prevalence.

Chapter IIII presents a case report of two pediatric patients, encompassing pathological development of the heart. Formation of the ID is important for cell-to-cell interactions, but also impacts the shift from hyperplasia to hypertrophy of cardiomyocytes. **Chapter V** describes an investigation of arrhythmias in a patient without a known cardiac history. Analyzing calcium handling in patient-specific hiPSC-CMs indicated the emergence of premature calcium release as potential cause for the experienced arrhythmias.

Chapter VI includes various examples of electrophysiological phenotyping in both mouse and hiPSC-CM models. These studies stem from scientific collaborations, stressing the crucial involvement of functional data in disease modeling of arrhythmogenic and ischemic cardiomyopathy. **Chapter VII** presents the application of an experimental and computational approach to study cellular electromechanics in ACM patients. An important role for the sodium-calcium exchanger (NCX1) is emphasized, which further clarifies the mechanism of calcium overload and relaxation impairment in ACM cardiomyocytes.

Chapter VIII is a general discussion on all described chapters, focusing on electrophysiology, calcium handling, and myocardial development in inherited and acquired cardiomyopathies.

References

1. Bers DM. Cardiac excitation-contraction coupling. *Nature*. 2002;415(6868):198-205.
2. Vermij SH, Abriel H, van Veen TA. Refining the molecular organization of the cardiac intercalated disc. *Cardiovasc Res*. 2017;113(3):259-275.
3. Lu F, Pu WT. The architecture and function of cardiac dyads. *Biophys Rev*. 2020;12(4):1007-1017.
4. Ronco C, Haapio M, House AA, Anavekar N, Bellomo R. Cardiorenal syndrome. *J Am Coll Cardiol*. 2008;52(19):1527-1539.
5. Kumar U, Wettersten N, Garimella PS. Cardiorenal Syndrome: Pathophysiology. *Cardiol Clin*. 2019;37(3):251-265.
6. Lekawanvijit S, Kompa AR, Krum H. Protein-bound uremic toxins: a long overlooked culprit in cardiorenal syndrome. *Am J Physiol Renal Physiol*. 2016;311(1):F52-62.
7. Himmelfarb J, Ikizler TA. Hemodialysis. *N Engl J Med*. 2010;363(19):1833-1845.
8. Dhondt A, Vanholder R, Van Biesen W, Lameire N. The removal of uremic toxins. *Kidney Int Suppl*. 2000;76:S47-59.
9. Lekawanvijit S. Cardiotoxicity of Uremic Toxins: A Driver of Cardiorenal Syndrome. *Toxins (Basel)*. 2018;10(9).
10. Franczyk-Skora B, Gluba-Brzozka A, Wrancicz JK, Banach M, Olszewski R, Rysz J. Sudden cardiac death in CKD patients. *Int Urol Nephrol*. 2015;47(6):971-982.
11. Deltombe O, Van Biesen W, Glorieux G, Massy Z, Dhondt A, Eloot S. Exploring Protein Binding of Uremic Toxins in Patients with Different Stages of Chronic Kidney Disease and during Hemodialysis. *Toxins (Basel)*. 2015;7(10):3933-3946.
12. Liabeuf S, Druelle TB, Massy ZA. Protein-bound uremic toxins: new insight from clinical studies. *Toxins (Basel)*. 2011;3(7):911-919.
13. Pavlenko D, van Geffen E, van Steenberghe MJ, et al. New low-flux mixed matrix membranes that offer superior removal of protein-bound toxins from human plasma. *Sci Rep*. 2016;6:34429.
14. Ahmadmehrabi S, Tang WHW. Hemodialysis-induced cardiovascular disease. *Semin Dial*. 2018;31(3):258-267.
15. Behere SP, Weindling SN. Inherited arrhythmias: The cardiac channelopathies. *Ann Pediatr Cardiol*. 2015;8(3):210-220.
16. Kim KH, Pereira NL. Genetics of Cardiomyopathy: Clinical and Mechanistic Implications for Heart Failure. *Korean Circ J*. 2021;51(10):797-836.
17. Van der Voorn SM, Te Riele A, Basso C, Calkins H, Remme CA, van Veen TAB. Arrhythmogenic cardiomyopathy: pathogenesis, pro-arrhythmic remodelling, and novel approaches for risk stratification and therapy. *Cardiovasc Res*. 2020;116(9):1571-1584.
18. Cerrone M, Montnagh J, Lin X, et al. Plakophilin-2 is required for transcription of genes that control calcium cycling and cardiac rhythm. *Nat Commun*. 2017;8(1):106.
19. Van Opbergen CJM, Bagwan N, Maurya SR, et al. Exercise Causes Arrhythmogenic Remodeling of Intracellular Calcium Dynamics in Plakophilin-2-Deficient Hearts. *Circulation*. 2022;145(19):1480-1496.

20. Van Opbergen CJM, den Braven I, Delmar M, van Veen TAB. Mitochondrial Dysfunction as Substrate for Arrhythmogenic Cardiomyopathy: A Search for New Disease Mechanisms. *Front Physiol.* 2019;10:1496.
21. De Brouwer R, Bosman LP, Gripenstedt S, et al. Value of genetic testing in the diagnosis and risk stratification of arrhythmogenic right ventricular cardiomyopathy. *Heart Rhythm.* 2022;19(10):1659-1665.
22. Kim C, Wong J, Wen J, et al. Studying arrhythmogenic right ventricular dysplasia with patient-specific iPSCs. *Nature.* 2013;494(7435):105-110.

Part I

Cardiorenal syndrome

Willem B. van Ham¹
Carlijn M. Cornelissen¹
Toon A.B. van Veen¹

¹Department of Medical Physiology, University Medical Center Utrecht, The Netherlands

Chapter II

Uremic toxins in chronic kidney disease highlight a fundamental gap in understanding their detrimental effects on cardiac electrophysiology and arrhythmogenesis

Abstract

Chronic kidney disease (CKD) and cardiovascular disease (CVD) have an estimated 700-800 and 523 million cases worldwide, respectively, with CVD being the leading cause of death in CKD patients. The pathophysiological interplay between the heart and kidneys is defined as the cardiorenal syndrome (CRS), in which worsening of kidney function is represented by increased plasma concentrations of uremic toxins (UTs), culminating in dialysis patients. As there is a high incidence of CVD in CKD patients, accompanied by arrhythmias and sudden cardiac death, knowledge on electrophysiological remodeling would be instrumental for understanding the CRS. While the interplay between both organs is clearly of importance in the CRS, the involvement of UTs in pro-arrhythmic remodeling is only poorly investigated, especially regarding the mechanistic background. Currently, the clinical approach against potential arrhythmic events is mainly restricted to symptom treatment, stressing the need for fundamental research on UT in relation to electrophysiology. This review addresses the existing knowledge of UTs and cardiac electrophysiology, and the experimental research gap between fundamental research and clinical research of the CRS. Clinically, mainly absorbents like ibuprofen and AST-120 are studied, which show limited safe and efficient usability. Experimental research shows disturbances in cardiac electrical activation and conduction after inducing CKD or exposure to UTs, but are scarcely present or focus solely on already well-investigated UTs. Based on UTs data derived from CKD patient cohort studies, a clinically relevant overview of physiological and pathological UTs concentrations is created. Using this, future experimental research is stimulated to involve electrophysiologically translatable animals, such as rabbits, or *in vitro* engineered heart tissues.

Keywords: cardiac electrophysiology; cardiorenal syndrome; chronic kidney disease; uremic toxins

1. Introduction

Global prevalence of chronic kidney disease (CKD) is estimated at 700-800 million cases worldwide¹⁻³. Simultaneously, cardiovascular disease (CVD) is estimated to include 523 million cases², with CVD accounting for approximately 50% of all deaths in CKD patients⁴. In advanced staged CKD patients, the incidence of cardiac arrhythmias and sudden cardiac death (SCD) is estimated around 25%⁵⁻⁷. Under pathophysiological conditions this bidirectional interaction between the heart and kidneys is defined as the cardiorenal syndrome (CRS)^{8,9}. In the CRS the bidirectional dysfunction of heart and kidneys initiates a cascade of neurohormonal adaptations, hemodynamic changes, inflammation and oxidative stress, resulting in progressive damage to both organs (**Figure 1**)^{4,10,11}. The five ascending stages of CKD emphasize a gradual loss of kidney function, eventually deteriorating to end-stage renal disease (ESRD). Characteristic for CKD progression is the elevation of uremic toxins (UTs) concentrations and other damaging proteins, such as fibroblast growth factors¹²⁻¹⁴. Due to the damaged kidneys uremic solutes cannot be filtered and excreted sufficiently, with potentially pathological consequences that result from their accumulation¹⁵. Therefore, ESRD patients are mainly depending on dialysis, as transplantable kidneys are scarcely available. However, during dialysis small molecules diffuse rather quickly when compared to the larger molecules or protein-bound uremic toxins (PBUTs), resulting in accumulation of these toxins in the blood as they fail to be removed^{16,17}. The potential involvement of UTs in cardiac electrophysiological remodeling, and its underlying molecular mechanisms, remain poorly understood. Increased incidence of arrhythmias in dialysis patients has also been linked to fluid shifts and fluctuation of potassium concentrations^{5,18}, whereas correlations of elevated UT levels with worsened patient outcomes are also shown¹⁹⁻²¹. However, elaborative experimental studies investigating molecular and functional electrophysiological pathology are scarcely performed.

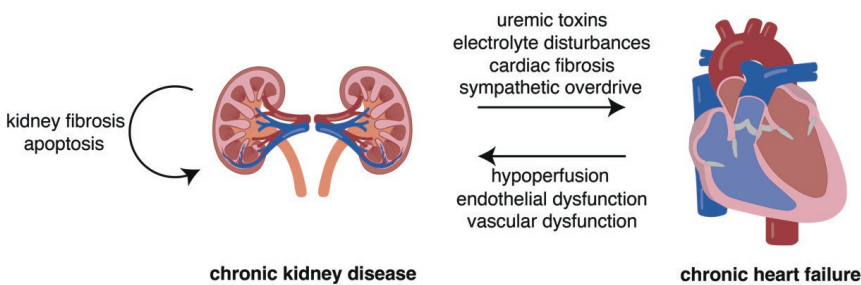


Figure 1. Progressive co-dysfunction of heart and kidneys defines the cardiorenal syndrome. Chronic kidney dysfunction progressively causes injury to the kidneys, while also leading to accumulation of uremic toxins and electrolyte disturbances, worsening functionality of the heart. Continuous dysfunction of the heart subsequently can cause vascular damage, and hypoperfusion in the kidneys, further establishing this vicious cycle of disease.

This review discusses electrophysiological research performed on UTs and CKD. First by briefly describing UTs and cardiac electrophysiology, the occurrence of arrhythmias in CKD and the roles of potassium concentrations and the autonomic nervous system. Then, clinically orientated studies will be listed, which mainly focus on improving UT filtering during dialysis in ESRD patients. Subsequently, experimental studies investigating electrophysiological mechanics are discussed, containing both *in vivo* and *in vitro* designs. Finally, there is an increasing need for future experimental UT research on cardiac electrophysiology to effectively address the consequences of UTs which ultimately would allow to develop treatment improvements for CKD patients.

2. Protein bound uremic toxins

In the past decade, UTs were uncovered as important regulators in the CRS, especially PBUTs^{12,15,20}. PBUTs are relatively small solutes (< 500 Dalton) which have a high affinity to plasma proteins such as albumin. While the majority of research is focused on two PBUTs, being indoxyl sulfate (IS) and p-cresyl sulfate (pCS), many other PBUTs exist²². Most of the PBUTs are liver or intestinal derived metabolic products that are released into the circulation and subsequently filtered from the blood by the kidneys²³. Several review manuscripts have been published describing the pathological effects of selected UTs in both heart and kidney, including increased inflammation, fibrosis formation, oxidative stress, and hypertrophy^{12,23,24}.

UTs, specifically IS, have been shown to increase both gene expression and protein levels of tumor necrosis factor alpha (TNF- α) and the interleukins 1 β and 6 (IL-1 β and IL-6)^{25,26}. Additionally, elevated gene expression of transforming growth factor beta (TGF- β) and connective tissue growth factor (CTGF) substantiated the increased fibrosis formation in the heart, as well as in the kidneys^{23,27}. Markers of myocardial hypertrophy, such as α -skeletal muscle actin and β myosin heavy chain, are also increased in nephrectomized rats, and isolated cardiomyocytes^{27,28}. All these processes are activated by signaling nodes that involve the nuclear factor kappa-light-chain-enhancer of activated B cells (NF κ B) and mitogen-activated protein kinase (MAPK)²⁶⁻²⁸, as a consequence of elevated oxidative stress^{23,29,30}. Although the effects evoked through elevation of individual concentrations of UTs are not often investigated in animal studies, as the serum contains an array of UTs and non-standardized concentrations, these pathological effects are directly associated to the detrimental activity of elevated levels of at least IS, pCS, but also indole-3 acetic acid (IAA)³¹.

2.1. Uremic concentrations in patients

Based on studies implementing clinical cohorts^{24,32-34}, as well as a comprehensive literature analysis by the European Uremic Toxin Work Group^{14,22}, concentration ranges can be made of physiological and pathological UT levels. While increasing UT concentrations can already be measured in early CKD

stages³², serum analysis is mainly performed in ESRD and dialysis patients. Based on these datasets, an overview of several PBUTs and their respective total concentrations was designed (**Figure 2**). Both physiological (shown in green) and pathological (shown in red) concentrations can highly vary between patients, complicating the establishment of a definitive toxic concentration of most UTs. The UTs with the highest pathological concentrations, including IS, pCS, and hippuric acid (HIP), also claim the majority of recognition in the scientific research field. This also accounts for the non-UT fibroblast growth factor 23 (FGF23). However, it could be advantageous to investigate UTs of which the physiological and pathological concentrations are relatively close, as the border to toxicity is crossed more easily.

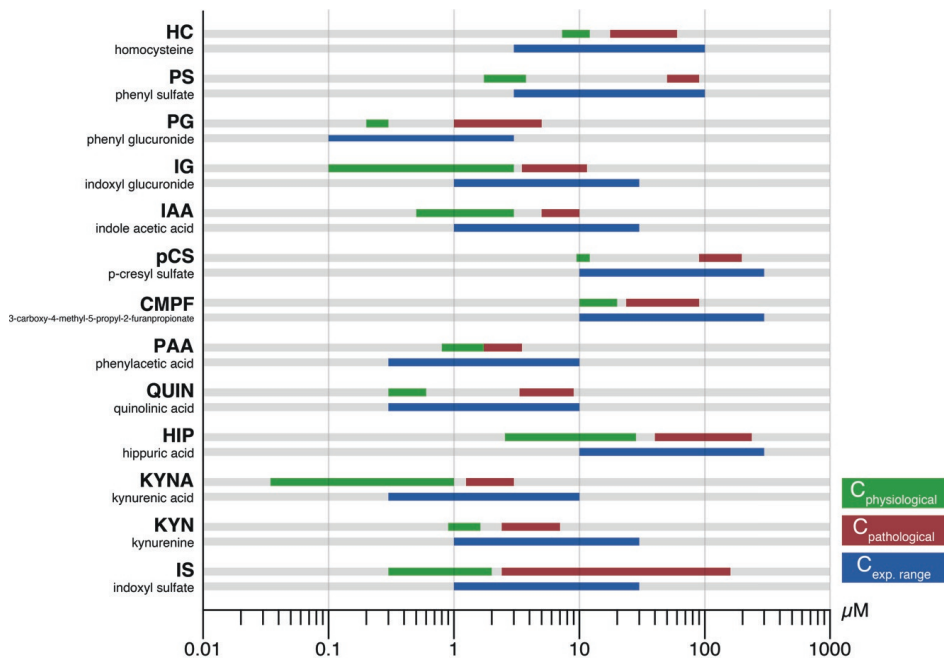


Figure 2. Overview of clinically relevant experimental total uremic toxin concentrations. Physiological (in green) and pathological (in red) serum concentrations of uremic toxins in patients vary extremely, but can be used to create an experimental (in blue) concentration range that spans both conditions. Using these concentrations, experiments can be designed to specifically define pathologic concentrations for individual uremic toxins.

3. Cardiac electrophysiology and arrhythmias

Alterations in cardiac electrophysiology underlying increased arrhythmic risk, can be investigated at different levels. The initiation and morphology of cardiac action potentials (APs), the intracellular calcium homeostasis, or the propagation of the APs from cell to cell can all be disturbed. Establishing the influence of PBUTs on any of the molecular pathways is valuable to understand the pro-arrhythmic risk in CKD patients. In the past decade the atria have been the most intensively investigated tissue regarding the relation between elevated UTs and arrhythmias, as the prevalence of atrial fibrillation (AF) is at least twice

as high in CKD patients compared to non-CKD populations^{21,35}, and especially this applies to the dialysis population³⁶⁻³⁸.

3.1. Action potentials, calcium transients, and impulse propagation

The cardiac action potential is the summation of multiple ion currents, originating from ions passing the cell membrane through specific ion channels, where shortening or prolongation of the action potential duration (APD) is the consequence of alterations in density of these currents (Figure 3)³⁹. The resting membrane potential of a cardiomyocyte is mainly stabilized by the inward rectifier K^+ current (I_{K1}), and is the main characteristic influencing excitability of a single cell (phase 4). Influx of Na^+ through sodium channels (I_{Na}) rapidly depolarizes the cell membrane, which is the first step of the AP (phase 0). The transient outward K^+ current (I_{to}) causes a small period of initial repolarization (phase 1), directly followed by the influx of Ca^{2+} ($I_{Ca,L}$), which temporarily leaves the membrane potential at a plateau phase because of a balance due to the simultaneous initiation of potassium efflux currents (phase 2).

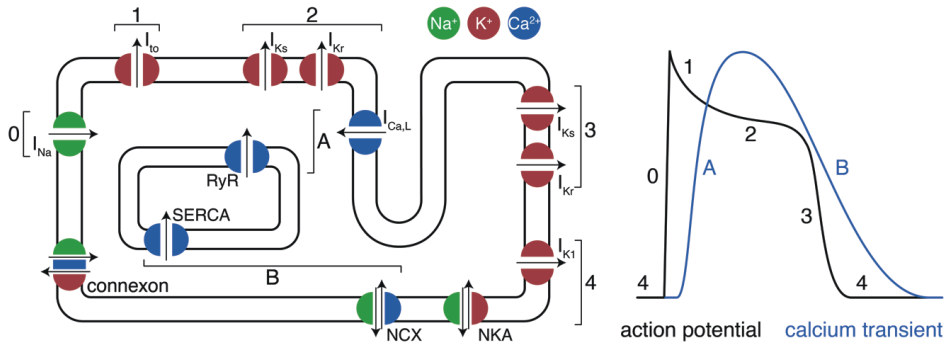


Figure 3. Representation of cardiac ion currents, orchestrating the morphology of action potentials and calcium transients. The cardiac action potential starts with an inflow of sodium ions (I_{Na}) depolarizing the cardiomyocyte (phase 0). As the sodium channels inactivate, the transient outward potassium current (I_{to}) causes an initial repolarization (phase 1). This is followed by the influx of calcium ions ($I_{Ca,L}$), as well as an efflux of potassium ions (I_{Kr} and I_{Ks}), which brings the membrane potential at a plateau (phase 2). Further conductance of I_{Kr} and I_{Ks} strongly repolarize the membrane potential (phase 3). Finally, the cell is brought to a resting membrane potential by the inward rectifier potassium current (I_{K1}), with support of the sodium/calcium exchanger (NCX1) and the sodium/potassium pump (phase 4). Simultaneously to causing the plateau phase, $I_{Ca,L}$ triggers the calcium release from the sarcoplasmic reticulum (SR) via activation of the ryanodine receptor (RyR2), a phenomenon which is described as calcium-induced calcium release, reflected through the rise of a calcium transient (phase A). Decay of cytosolic calcium during is mainly achieved by pumping the calcium back into the SR, via the sarco/endoplasmic reticulum Ca^{2+} ATPase (SERCA2a), or out of the cell via NCX1 (phase B). Propagation of action potentials to neighboring cells, is partly facilitated by connexon hemichannels.

Further conductance of these rapid and slow delayed rectifier potassium currents (I_{Kr} and I_{Ks} , respectively) repolarizes the membrane potential (phase 3), which is ultimately accomplished by the I_{K1} current that brings the cell back to its initial resting membrane potential. The sodium/calcium exchanger (NCX1) and the sodium/potassium ATPase (NKA) both support I_{K1} in maintaining the resting membrane potential until the next depolarization (phase 4).

Simultaneously to its role in the plateau phase, I_{CaL} triggers the Ca^{2+} release from the sarcoplasmic reticulum (SR) via activation of the ryanodine receptor (RyR2), a phenomenon which is described as calcium-induced calcium release. The subsequent large increase in cytosolic Ca^{2+} , reflected through the calcium transient (CaT), facilitates the calcium-dependent contraction of the sarcomeres. Lowering cytosolic Ca^{2+} during relaxation is mainly achieved by pumping the Ca^{2+} back into the SR, via the sarco/endoplasmic reticulum Ca^{2+} ATPase (SERCA2a), or out of the cell via NCX1⁴⁰.

Propagation of APs between cardiomyocytes facilitates the organized contraction of the myocardium. Pathophysiological remodeling resulting in an increased heterogeneity between cardiomyocytes, either in electrical or mechanical coupling, can affect conductivity⁴¹. The specific subcellular region that regulates electromechanical coupling between cardiomyocytes is named the intercalated disk (ID)^{42,43}. The ID consists of adherens junctions and desmosomes, which provide structural support between cardiomyocytes, and gap junctions, that provide electrical and metabolic coupling of cardiomyocytes. The gap junctions are formed by two connexon hemichannels, each of one delivered by the two connecting cells. These connexons are composed of six connexin (Cx) proteins, with Cx43 being the main isoform found in the ventricular myocardium⁴⁴. The normal spatio-temporal pattern of conduction throughout the heart is initiated in the sinus node in the right atrium, and runs via the atrio-ventricular node, through the ventricular septum, towards the free wall of both ventricles. The subsequent electrical activation of different parts of the heart in space and time is represented in an electrocardiogram (ECG), in which the direction and intensity of the electrical activity is shown in respect to electrodes attached to body.

3.2. Arrhythmias

Impaired integrity of the protein complexes at the ID and a reduction in intercellular electrical communication hampers coupling causing a decreased conductivity across the myocardium. Increased fibrosis formation, consisting of relatively poorly conductible tissue, can electrically insulate cardiomyocytes, which forms physical conduction barriers in addition to slowing intercellular AP propagation⁴⁵. This might lead to a conduction path that no longer follows the traditional propagation route, but rather disperses autonomously and repeatedly through a limited region, which is named a reentry arrhythmia.



Ion channel expression and protein levels, impeded intracellular trafficking and insertion into the sarcolemma, and channel kinetics or blockade all impact current densities, thereby influencing the morphology of the AP. An important example of channels that are sensitive to modulation are channels conducting I_{Kr} , as many chemicals and biological products have a high affinity for these channels⁴⁶. Blockade of this channel decreases I_{Kr} , which prolongs the repolarization phase and thus APD. During this period of prolongation, I_{Na} and $I_{Ca,L}$ can flow due to re-activated channels, giving rise to spontaneous early after depolarizations (EADs), often a characteristic of ectopic activity which is considered being pro-arrhythmic. Due to this, electrical activation can occur at locations other than the sinus node, indicating by an electrical storm on the ECG. Fortunately, under physiological conditions other potassium currents can compensate for the lack of e.g. I_{Kr} , which is considered as a ‘repolarization reserve’ of the myocardium.

Whereas prolonged existence of sodium or calcium currents during the repolarization can cause EADs, SR calcium leakage via RyR2 or calcium influx via Cx43 hemichannels during the resting phase can cause delayed afterdepolarizations (DADs)^{47,48}. While DADs can trigger ectopic activity similar to EADs, the premature activation of cardiac tissue can also cause electrical conduction block, which is, similar to a physical conduction block by increased collagen deposition, an instigator of reentry.

4. Arrhythmogenicity in chronic kidney disease

Alternative disturbances introduced by CKD that affect cardiac electrophysiology are also important pro-arrhythmic factors. In particular imbalance in serum potassium concentrations and autonomic nervous system dysfunction, indirectly can also partially be contributed to the accumulation of UTs. Before describing clinical and experimental research on cardiac electrophysiology induced by UTs, these mechanisms will be described to fully cover arrhythmogenicity in CKD.

4.1. Hypokalemia and hyperkalemia

High intracellular and low extracellular potassium are the main determinants of the negative resting membrane potential, which prevents spontaneous excitability of cardiomyocytes. Simultaneously, this balance establishes an outward driving force for potassium currents. Fluctuation of serum potassium concentrations to abnormal low and high extremes is a problematic clinical manifestation, especially in CKD patients⁴⁹. The kidney plays a pivotal role in the regulation of serum potassium levels, with a diminished kidney filtration being a predictor of hyperkalemia (> 5.0 mEq/L potassium)⁵⁰. Additionally, nutrition, medication, and dialysis also significantly influence serum potassium⁵¹, and can sway it to both hyperkalemia and hypokalemia (< 4.0 mEq/L potassium). Interestingly, while hyperkalemia is a widely acknowledged issue in CKD, the prevalence of both hyper- and hypokalemia is similar and estimated around 12-20% in the CKD population^{49,50}. Consequently, alterations in potassium metabolism can result in detrimental cardiac rhythm abnormalities. As in ESRD patients blood volume and electrolyte levels

alternate often after dialysis, this could partly explain the high incidence of arrhythmias in that population^{5,18}.

During hypokalemia the resting membrane potential is hyperpolarized, and a larger outward driving force for potassium is present. However, repolarization currents such as I_{K1} and I_{Kr} have alternate methods of regulation which result in a decreased outward current. I_{K1} is naturally blocked by voltage-dependent polyamines and magnesium, which in turn can be removed by extracellular potassium⁵². Low extracellular potassium would therefore stabilize I_{K1} block. The inactivation rate of I_{Kr} as well as its ion channel expression are influenced by potassium, with hypokalemia resulting in enhanced inactivation and decreased expression^{53,54}. These decreased currents lower the repolarization reserve and prolong the APD, thereby increasing susceptibility to EADs and triggered activity⁵⁵. Alternatively, the hyperpolarization of the membrane potential and lowered extracellular potassium inhibit NKA activity. This leads to increased cytosolic sodium, which diminishes NCX1 activity, eventually leading to increased cytosolic calcium⁵⁶. Ultimately, this calcium overload may induce DADs and associated rhythm abnormalities.

Opposite to that, during hyperkalemia the resting membrane potential depolarizes, initially leading to increased excitability due to the potential being closer to the activation potential of I_{Na} . However, the inactivation of sodium channels also increases at depolarizing potentials, leading to less channels contributing during every depolarization. Supplementary and opposed to hypokalemia, the repolarization reserve is increased, with a shorter APD as the consequence. Irregular activation of sodium channels and a chronic increase of the repolarization reserve can prolong the period of inexcitability of cardiomyocytes. In combination, this culminates into altered excitation, electrical recovery, and decreased conduction between cardiomyocytes^{55,57}, which in turn can lead to conduction block and reentrant arrhythmias.

4.2. Autonomic nervous system dysfunction

The communication between the autonomic nervous system (ANS) and the kidneys is crucial for an appropriate kidney function, e.g. regulating blood osmolarity and maintaining the sodium balance⁵⁸. The direct sympathetic innervation of the heart is mainly mediated by norepinephrine in concert with circulating adrenaline being produced by the adrenal gland, both targeting adrenergic receptors. Elevated sympathetic stimulation thereby leads to an increased heart rate and contractility. This is achieved via the effects on the sinoatrial node and the individual cardiomyocytes^{59,60}, where cyclic adenosine monophosphate (cAMP) enhances ion channel activity and other positive inotropic effects after adrenergic stimulation. This is counteracted by the parasympathetic nervous system, through acetylcholine binding to muscarinic receptors. A major player in autonomic modulation is acetylcholine signaling, being instigated by nitric oxide (NO)⁶¹. Cyclic guanosine monophosphate (cGMP) levels are mediated by NO, increasing cAMP breakdown via phosphodiesterases, resulting in negative inotropic effects⁶².



During CKD NO bioavailability is reduced, due to both increased oxidative stress and increasing asymmetric dimethylarginine (ADMA) levels^{59,63,64}, which results in a sympathetic overdrive^{64,65}. This is especially observed in ESRD patients⁶⁶. While oxidative stress can be promoted by elevated UT levels, UTs are also presumed to directly increase sympathetic activity by inducing inflammation and NO deficiency in the central nervous system⁵⁹. While further electrophysiological mechanisms are scarcely available in the setting of CKD, examples of increased NCX1 activity providing spontaneous calcium triggers are also observed⁶⁷. Augmented sympathetic activity can cause, or aggravate, existing rhythm disturbances leading to arrhythmias such as AF^{60,68,69}, again partially explaining high SCD rates in the ESRD and dialysis populations³⁶⁻³⁸.

5. Current clinically orientated uremic toxin research

The correlations between increased levels of PBUTs and diminished kidney function as well as cardiac dysfunction have been well established^{12,20,32}. Therefore, research on those UTs has mainly been focused on improving clinical outcome by adapting dialysis, but also through additionally decreasing UT concentrations in ESRD patients, through instrumentation of adsorbent and displacing chemicals. Investigations regarding the improvement of the applied dialysis method range from adjusting speed and frequency of dialysis sessions, to adjustments of the dialysate or physical conditions within the dialyzer⁷⁰. Additionally, alternative filtration techniques such as hemodiafiltration are studied to improve removal of PBUTs, e.g. in the recently initiated CONVINCE study⁷¹.

5.1. Clinical improvements

The addition of liposomes to the regimen of dialysis has experimentally been shown to increase the removal of PBUTs^{72,73}. These liposomes remain in the dialysate and act as adsorbent, taking up PBUTs. While still in the experimental phase, the natural components of the technique offer a potential safe and efficient addition to dialysis. The adsorptive effect of sevelamer, already prescribed for prevention of hyperphosphatemia in CKD patients, was also investigated in a trial with advanced staged CKD patients⁷⁴. However, a 12-week treatment with sevelamer did not show a decline in concentrations of IS, pCS, and IAA. Another well investigated chemical adsorbent is AST-120 (Kureha Company, Japan)⁷⁵⁻⁷⁸. AST-120 is an oral carbon adsorbent that binds UTs and retains them in the intestines, to decrease their concentrations in the circulation by limiting their uptake. It has been shown to effectively decrease concentrations of e.g. IS and pCS in patients⁷⁵, subsequently followed by decreased concentrations of IL-1 β and NF κ B⁷⁹. While it's not for optimal clearance of all UTs, AST-120 remains one of the most effective methods of reducing UT concentrations^{80,81}, but the effect on CKD progression remains uncertain thus far^{82,83}.

Alternative to absorbents are displacing agents like ibuprofen, which shares the binding site for albumin with PBUTs⁸⁴. By displacing the UTs on albumin, their free fraction increases, allowing a more easily filtration during regular hemodialysis. Unfortunately, the high concentration of ibuprofen that is needed to increase the free fraction of e.g. IS and pCS just 3-fold, can result in additional complications in CKD patients⁸⁵. On top of that, the binding site is not shared with all PBUTs, meaning that several displacing agents are needed for the entire set of PBUTs. Other more recently investigated displacing agents are salvianolic acids⁸⁶. While their mechanistic concept is similar to that of ibuprofen, the most effective salvianolic acids share a different binding site for albumin, which could also be beneficial. However, these chemicals also need to be cleared by the kidneys after their administration, which eventually could become detrimental for CKD patients.

As many UTs are dietary metabolites produced in the intestines, decreased protein intake and plant-based diets result in lower UT concentrations, potentially caused by modification of the gut microbiota⁸⁷⁻⁸⁹. Therefore, supplementation of the gut microbiota using probiotics to decrease UT production has also been investigated. Unfortunately, the supplement did not lower UT concentrations, but adversely increased serum potassium and urea levels⁹⁰. In conclusion, some additional clinical modes of intervention, and multiple absorbents and displacers are capable to improve PBUT filtration from the circulation. However, no methods have been established yet that are both safe and efficient⁸⁵. A more complete understanding of specific PBUTs and their contribution to disease pathology, could aid in targeting their effects in patients.

6. Current electrophysiological research

Arrhythmogenicity as the consequence of pathological cardiac electrical remodeling is rarely investigated in experimental studies of CKD, especially regarding the affected electrophysiological mechanisms which are at the basis of the arrhythmias seen in patients^{23,91}. *In vivo* experiments mainly consist of electrocardiogram (ECG) data, sometimes with a follow up on cellular electrophysiology, while *in vitro* studies that are considered as completely cell culture-based experiments are mostly lacking. Despite of that they would allow for a more detailed investigation into pathophysiology of single UTs. Mouse and rat models are often used for their reasonably low housing costs and increased availability compared to larger animals. While cardiomyocytes from these animals can technically be used very well for electrophysiological experiments, their species-specific electrophysiology significantly differs from human cardiomyocytes, whereas cellular electrophysiology in rabbits, dogs, and pigs is much more similar to humans⁹². An overview of studies that specifically included relevant parameters for arrhythmogenicity in CKD, are shown in **Table 1** (*in vivo*, see section 6.1) and **Table 2** (*in vitro*, see section 6.2).

6.1. *In vivo* CKD studies on cardiac electrophysiology

The most common approach to establish animal models of CKD is nephrectomy, either subtotal (SNx) or unilateral (UNx), removing 5/6 or 1/2 of the kidneys, respectively⁹³⁻¹⁰⁰. This abrupt reduction in nephron numbers causes kidney insufficiency, often followed by an inflammatory response and fibrosis formation, potentially systemically. Another approach is genetically inducing CKD, either by causing a defect in the *samcystin* gene, causing polycystic kidney disease (Cy/+)^{101,102}, or a defect in type 4 collagen alpha-3, resulting in increased FGF23 levels and renal fibrosis (Col4a3^{-/-})¹⁰³. Both initiate the substitution of functional kidney tissue, either with, or by increased collagen deposition. These CKD models show pro-arrhythmic parameters such as prolonged QTc, single cell APD prolongation, slowed conduction velocity, and increased tachyarrhythmias. Interestingly, mechanistic investigations always indicate a hampered calcium handling, fibrosis formation, and a decreased Cx43 expression as the main potentiators of the pro-arrhythmic parameters^{93-95,97-99,102,103}. Perfusion of a single toxin is an alternative method to specifically investigate its effects, which in case of the non-toxin FGF23 revealed to lead to increased arrhythmogenicity, via disturbed calcium handling^{94,104}. Unfortunately, the main drawback of these studies is that there is no data available on specific culprits for the electrophysiological changes and the mechanisms behind the effects have rarely been investigated. Ultimately, establishing a CKD model with consistent electrophysiological remodeling would be highly beneficial in the search for pharmacological interventions to treat or prevent the occurrence of arrhythmias.

6.2. *In vitro* CKD studies on cardiac electrophysiology

To study the maladaptive effects of individual UTs preferably should also be performed in *in vitro* experiments, where no systematic disease can be instigated that would influence the results. This has been performed, to a limited extent, in cardiomyocytes isolated from animals and in immortal cell lines (e.g. H9c2)^{48,105-110}. IS has been shown to cause Cx43 disruption, leading to a compromised intercellular gap junction communication^{48,105}. IS and pCS both decrease repolarizing potassium currents in a dose-dependent manner^{107,108}, which was subsequently proposed to prolong the APD in computer simulations¹⁰⁸. Chronic exposure to FGF23 can lead to calcium leakage from the SR, giving rise to uncontrolled calcium waves and contractions^{109,110}. In general, these alterations in conduction properties, AP formation and calcium handling, represent the pro-arrhythmogenicity corresponding to results from *in vivo* studies. Application of single toxins on cell cultures should be used to augment knowledge on molecular changes caused by each toxin, in parallel to strive for development of effective interventions.

Table 1. Studies on the effect of CKD and uremic toxins on cardiac electrophysiology *in vivo*.

Animal	CKD	Toxin	Outcome	Reference
Mouse	DOCA	-	Increased occurrence of arrhythmia, decreased conduction velocity, decreased Cx43 expression	93
Mouse	SNx	-	Increased occurrence of arrhythmia, decreased Cx43 expression	93
Mouse	SNx	-	No contractile dysfunction Hampered calcium handling	94
Rat	SNx	-	Prolonged QTc, increased ventricular arrhythmogenesis Hampered calcium handling	95
Rat	UNx	-	Prolonged QTc Increased action potential duration	96
Rat	SNx	-	Increased occurrence atrial fibrillation Cx43 redistribution Fibrosis formation	97
Rabbit	SNx	-	Increased occurrence of atrial arrhythmia Increased LA action potential duration and fibrosis formation	98
Rabbit	SNx	-	Increased ventricular arrhythmogenesis, fibrosis formation	99
Dog	SNx	-	Prolonged QTc, increased hypertrophy	100
Rat	Cy/+	-	Increased occurrence of arrhythmia and sudden cardiac death	101
Rat	Cy/+	-	Increased action potential duration, increased occurrence ventricular fibrillation, hampered calcium handling	102
Mouse	Col4a3 ^{-/-}	-	Contractile dysfunction, hampered calcium handling	103
Mouse	-	FGF23	Hampered calcium handling	94

7. Filling the gap in knowledge: future experimental studies

Currently, CKD patients are highly prone to cardiac arrhythmias, without existing preventive therapies being available. In the last two decades, clinical CVD treatment in CKD patients has improved importantly, with the exception of SCD¹¹¹. Clinically orientated research and experience show only treatments of symptoms, like application of antiarrhythmic drugs, atrial ablation strategies, and implantable cardioverter-defibrillator (ICD) therapy⁹¹. However, with limited understanding of the pathological mechanisms behind SCD in CKD patients, the applied clinical approaches to control deterioration of the disease remain rather non-specific and not always successful, as has been seen in the discontinued ICD2 trial¹¹². In this trial it was shown that prophylactic ICD implantation in dialysis patients did not decrease SCD occurrence, but resulted in an additional increased risk of adverse events related to the procedure of implantation. A major advantage for clinical progress would be a detailed and in-depth knowledge of UTs and their specific effects on the heart. Low protein diets decrease the production of UTs, but they remain

high in serum concentrations, especially in dialysis patients. Pro-fibrotic characteristics of UTs have already been investigated more extensively, but electrophysiological knowledge on the cause of ventricular arrhythmia triggering SCD remains elusive^{12,15,23}.

Table 2. Studies on the effect of CKD and uremic toxins on cardiac electrophysiology *in vitro*.

Cell type	CKD	Toxin	Outcome	Reference
Rat neonatal cardiomyocytes	-	Indoxyl sulfate	Cx43 redistribution, disruption of gap junction communication	105
Rat neonatal cardiomyocytes	-	P-cresol	Cx43 disassembly, disruption of gap junction communication	106
Rat ventricular cardiomyocytes (H9c2)	-	P-cresyl sulfate	Dose dependent decrease of I_{Kr}	107
Rat ventricular cardiomyocytes (H9c2)	-	Indoxyl sulfate	Dose dependent decrease of I_K	108
Rat adult ventricular cardiomyocytes	-	FGF23	Increased occurrence of spontaneous calcium waves, SR calcium leak	109
Rat adult ventricular cardiomyocytes	-	FGF23	Increased occurrence of spontaneous calcium waves, contractile dysfunction, decreased L-type calcium current	110
Rabbit atrial and pulmonary vein cardiomyocytes	-	Indoxyl sulfate	PV: Increased afterdepolarizations, SR calcium leakage. Atrial: increased occurrence of fibrillations	48

To design future electrophysiological experiments, clinically relevant UT concentrations should also be applied *in vitro*. Based on the overview of PBUTs and their respective total plasma concentrations as shown in **Figure 2**, an experimental concentration range (shown in blue) can be established, covering both clinical conditions. Doing this, not only effects of UTs can be investigated, but more refined clinical concentration boundaries can also be established. Importantly, in experimental designs of PBUTs it is of relevance to include 35-50 gr/L albumin in the experimentally applied protocols, as only the free fraction is effective¹¹³, which is established after including albumin with the concentrations as depicted in **Figure 2**.

To specifically investigate electrophysiologically relevant parameters, such as APD and calcium handling and their underlying mechanisms, experimental models should be carefully selected. While conduction disorders and rhythm abnormalities can be explored in mice, the proposed approach for mechanistic background studies are preferably performed in cardiomyocytes from rabbit, dog, or pig hearts, especially regarding repolarization of the action potential⁹². Moreover, the differences in natural sympathetic drive in different animals should be acknowledged. Beneficial in these *in vivo* models is the analysis of systemic effects after CKD initiation, on top of the subsequent cellular analysis. However, this method only allows to study the overall effects of CKD on cardiac electrophysiology, thereby still not elucidating the effects

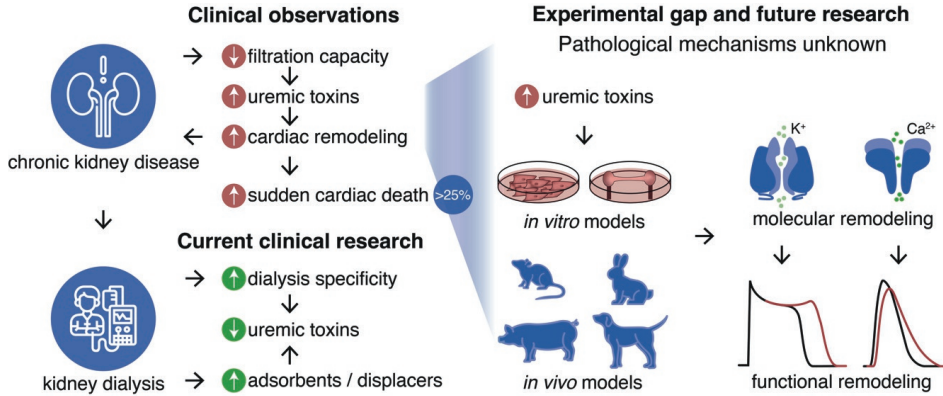
of individual UTs. Due to costs, availability, and ethical constraints for animal studies, it is of significant value to design and improve relevant *in vitro* models.

Human induced pluripotent stem cell derived cardiomyocytes (hiPSC-CMs) are often used as alternative electrophysiological relevant cell system. hiPSC-CMs are spontaneously active, contract, and parameters such as action potentials, calcium transients, and individual ion currents can be measured, with additional protein and gene analysis that can further explore the effects caused by exposure to individual or cocktails of clinically relevant concentrations of UTs. Drawback of these models is that hiPSC-CMs still have a rather immature electrical and morphological phenotype, which requires a skeptical perspective on their translational capabilities¹¹⁴. Additionally, preparation, culture, and differentiation of these cells remains generally inconsistent, lowering output both qualitatively and quantitatively.

Robust steps in the field of tissue engineering has led to improved maturation and applicability of hiPSC-CMs, producing engineered heart tissues (EHTs) and ventricular heart chambers¹¹⁵⁻¹¹⁷. EHTs can consist of combinations of multiple hiPSC derived cell types, such as cardiomyocytes, fibroblasts, and endothelial cells, and are much more reproducible compared to regular and commonly used (2-dimensional, only cardiomyocytes) cultures of hiPSC-CMs. Contraction of such constructs is unidirectional, improving cardiomyocyte orientation¹¹⁸.

8. Conclusion

This review describes the fundamental knowledge gap of the effects of uremic toxins on cardiac electrophysiology and arrhythmogenesis (**Central illustration**). The accumulation of UTs during advancing stages of CKD, especially PBUTs that are not filtered during dialysis, proved to be maladaptive with regards to cardiac structural remodeling. Apprehension of the involvement of UTs in remodeling of cardiac electrophysiology remains scarce, despite high prevalence of arrhythmias and SCD in CKD patients. Clinical UT research focusses mainly on adapting and improving dialysis. In contrast, pro-arrhythmic molecular mechanisms evoked by individual or combinations of UTs require unmet detailed investigations, preferably in state-of-the-art engineered cardiac tissues and relevant animal models.



Central illustration. Fundamental gap between clinical and experimental research of the cardiorenal syndrome, focused on cardiac electrophysiology and arrhythmogenesis. Development of a worsened cardiac function due to chronic kidney disease, leading to sudden cardiac death in approximately 25% of the latest stage chronic kidney disease patients. Clinical research mainly focusses on direct treatment options to reduce uremic toxins as important regulator in the cardiorenal syndrome. Experimental studies investigating the mechanisms underlying electrophysiological remodeling are lacking, complicating efficient research targeting treatment improvements.

References

1. Hill NR, Fatoba ST, Oke JL, et al. Global Prevalence of Chronic Kidney Disease - A Systematic Review and Meta-Analysis. *PLoS One*. 2016;11(7):e0158765.
2. Roth GA, Mensah GA, Johnson CO, et al. Global Burden of Cardiovascular Diseases and Risk Factors, 1990-2019: Update From the GBD 2019 Study. *J Am Coll Cardiol*. 2020;76(25):2982-3021.
3. Kovesdy CP. Epidemiology of chronic kidney disease: an update 2022. *Kidney Int Suppl (2011)*. 2022;12(1):7-11.
4. Cruz DN, Gheorghiade M, Palazzuoli A, Ronco C, Bagshaw SM. Epidemiology and outcome of the cardio-renal syndrome. *Heart Fail Rev*. 2011;16(6):531-542.
5. Franczyk-Skora B, Gluba-Brzozka A, Wrancicz JK, Banach M, Olszewski R, Rysz J. Sudden cardiac death in CKD patients. *Int Urol Nephrol*. 2015;47(6):971-982.
6. Green D, Roberts PR, New DI, Kalra PA. Sudden cardiac death in hemodialysis patients: an in-depth review. *Am J Kidney Dis*. 2011;57(6):921-929.
7. Wheeler DC, London GM, Parfrey PS, et al. Effects of cinacalcet on atherosclerotic and nonatherosclerotic cardiovascular events in patients receiving hemodialysis: the Evaluation Of Cinacalcet HCl Therapy to Lower CardioVascular Events (EVOLVE) trial. *J Am Heart Assoc*. 2014;3(6):e001363.
8. Gnanaraj J, Radhakrishnan J. Cardio-renal syndrome. *F1000Res*. 2016;5.
9. Ronco C, Haapio M, House AA, Anavekar N, Bellomo R. Cardiorenal syndrome. *J Am Coll Cardiol*. 2008;52(19):1527-1539.
10. Kumar U, Wettersten N, Garimella PS. Cardiorenal Syndrome: Pathophysiology. *Cardiol Clin*. 2019;37(3):251-265.
11. Uduman J. Epidemiology of Cardiorenal Syndrome. *Adv Chronic Kidney Dis*. 2018;25(5):391-399.
12. Lekawanvijit S. Cardiotoxicity of Uremic Toxins: A Driver of Cardiorenal Syndrome. *Toxins (Basel)*. 2018;10(9):352.
13. Jankowski J, Floege J, Fliser D, Bohm M, Marx N. Cardiovascular Disease in Chronic Kidney Disease: Pathophysiological Insights and Therapeutic Options. *Circulation*. 2021;143(11):1157-1172.
14. Vanholder R, De Smet R, Glorieux G, et al. Review on uremic toxins: classification, concentration, and interindividual variability. *Kidney Int*. 2003;63(5):1934-1943.
15. Lekawanvijit S, Kompa AR, Krum H. Protein-bound uremic toxins: a long overlooked culprit in cardiorenal syndrome. *Am J Physiol Renal Physiol*. 2016;311(1):F52-62.
16. Dhondt A, Vanholder R, Van Biesen W, Lameire N. The removal of uremic toxins. *Kidney Int Suppl*. 2000;76:S47-59.
17. Himmelfarb J, Ikizler TA. Hemodialysis. *N Engl J Med*. 2010;363(19):1833-1845.
18. Ahmadmehrabi S, Tang WHW. Hemodialysis-induced cardiovascular disease. *Semin Dial*. 2018;31(3):258-267.

19. Chinnappa S, Tu YK, Yeh YC, Glorieux G, Vanholder R, Mooney A. Association between Protein-Bound Uremic Toxins and Asymptomatic Cardiac Dysfunction in Patients with Chronic Kidney Disease. *Toxins (Basel)*. 2018;10(12):520.
20. Liabeuf S, Drucke TB, Massy ZA. Protein-bound uremic toxins: new insight from clinical studies. *Toxins (Basel)*. 2011;3(7):911-919.
21. Yamagami F, Tajiri K, Yumino D, Ieda M. Uremic Toxins and Atrial Fibrillation: Mechanisms and Therapeutic Implications. *Toxins (Basel)*. 2019;11(10):597.
22. Durantou F, Cohen G, De Smet R, et al. Normal and pathologic concentrations of uremic toxins. *J Am Soc Nephrol*. 2012;23(7):1258-1270.
23. Savira F, Magaye R, Hua Y, et al. Molecular mechanisms of protein-bound uremic toxin-mediated cardiac, renal and vascular effects: underpinning intracellular targets for cardiorenal syndrome therapy. *Toxicol Lett*. 2019;308:34-49.
24. Vanholder R, Pletinck A, Schepers E, Glorieux G. Biochemical and Clinical Impact of Organic Uremic Retention Solutes: A Comprehensive Update. *Toxins (Basel)*. 2018;10(1):33.
25. Lekawanvijit S, Adrahtas A, Kelly DJ, Kompa AR, Wang BH, Krum H. Does indoxyl sulfate, a uraemic toxin, have direct effects on cardiac fibroblasts and myocytes? *Eur Heart J*. 2010;31(14):1771-1779.
26. Lv J, Chen J, Wang M, Yan F. Klotho alleviates indoxyl sulfate-induced heart failure and kidney damage by promoting M2 macrophage polarization. *Aging (Albany NY)*. 2020;12(10):9139-9150.
27. Lekawanvijit S, Kompa AR, Manabe M, et al. Chronic kidney disease-induced cardiac fibrosis is ameliorated by reducing circulating levels of a non-dialysable uremic toxin, indoxyl sulfate. *PLoS One*. 2012;7(7):e41281.
28. Savira F, Cao L, Wang I, et al. Apoptosis signal-regulating kinase 1 inhibition attenuates cardiac hypertrophy and cardiorenal fibrosis induced by uremic toxins: Implications for cardiorenal syndrome. *PLoS One*. 2017;12(11):e0187459.
29. Fujii H, Nishijima F, Goto S, et al. Oral charcoal adsorbent (AST-120) prevents progression of cardiac damage in chronic kidney disease through suppression of oxidative stress. *Nephrol Dial Transplant*. 2009;24(7):2089-2095.
30. Yisireyili M, Shimizu H, Saito S, Enomoto A, Nishijima F, Niwa T. Indoxyl sulfate promotes cardiac fibrosis with enhanced oxidative stress in hypertensive rats. *Life Sci*. 2013;92(24-26):1180-1185.
31. Dou L, Sallee M, Cerini C, et al. The cardiovascular effect of the uremic solute indole-3 acetic acid. *J Am Soc Nephrol*. 2015;26(4):876-887.
32. Deltombe O, Van Biesen W, Glorieux G, Massy Z, Dhondt A, Eloit S. Exploring Protein Binding of Uremic Toxins in Patients with Different Stages of Chronic Kidney Disease and during Hemodialysis. *Toxins (Basel)*. 2015;7(10):3933-3946.
33. Itoh Y, Ezawa A, Kikuchi K, Tsuruta Y, Niwa T. Protein-bound uremic toxins in hemodialysis patients measured by liquid chromatography/tandem mass spectrometry and their effects on endothelial ROS production. *Anal Bioanal Chem*. 2012;403(7):1841-1850.

34. Lin CN, Wu IW, Huang YF, Peng SY, Huang YC, Ning HC. Measuring serum total and free indoxyl sulfate and p-cresyl sulfate in chronic kidney disease using UPLC-MS/MS. *J Food Drug Anal.* 2019;27(2):502-509.
35. Huang SY, Chen YA, Chen SA, Chen YJ, Lin YK. Uremic Toxins - Novel Arrhythmogenic Factor in Chronic Kidney Disease - Related Atrial Fibrillation. *Acta Cardiol Sin.* 2016;32(3):259-264.
36. Genovesi S, Pogliani D, Faini A, et al. Prevalence of atrial fibrillation and associated factors in a population of long-term hemodialysis patients. *Am J Kidney Dis.* 2005;46(5):897-902.
37. Winkelmayr WC, Patrick AR, Liu J, Brookhart MA, Setoguchi S. The increasing prevalence of atrial fibrillation among hemodialysis patients. *J Am Soc Nephrol.* 2011;22(2):349-357.
38. Wizemann V, Tong L, Satayathum S, et al. Atrial fibrillation in hemodialysis patients: clinical features and associations with anticoagulant therapy. *Kidney Int.* 2010;77(12):1098-1106.
39. De Git KC, de Boer TP, Vos MA, van der Heyden MA. Cardiac ion channel trafficking defects and drugs. *Pharmacol Ther.* 2013;139(1):24-31.
40. Bers DM. Cardiac excitation-contraction coupling. *Nature.* 2002;415(6868):198-205.
41. Kessler EL, Boulaksil M, van Rijen HV, Vos MA, van Veen TA. Passive ventricular remodeling in cardiac disease: focus on heterogeneity. *Front Physiol.* 2014;5:482.
42. Zhao G, Qiu Y, Zhang HM, Yang D. Intercalated discs: cellular adhesion and signaling in heart health and diseases. *Heart Fail Rev.* 2019;24(1):115-132.
43. Vermij SH, Abriel H, van Veen TA. Refining the molecular organization of the cardiac intercalated disc. *Cardiovasc Res.* 2017;113(3):259-275.
44. Jansen JA, van Veen TA, de Bakker JM, van Rijen HV. Cardiac connexins and impulse propagation. *J Mol Cell Cardiol.* 2010;48(1):76-82.
45. De Jong S, van Veen TA, van Rijen HV, de Bakker JM. Fibrosis and cardiac arrhythmias. *J Cardiovasc Pharmacol.* 2011;57(6):630-638.
46. Jonsson MK, van der Heyden MA, van Veen TA. Deciphering hERG channels: molecular basis of the rapid component of the delayed rectifier potassium current. *J Mol Cell Cardiol.* 2012;53(3):369-374.
47. Song Z, Ko CY, Nivala M, Weiss JN, Qu Z. Calcium-voltage coupling in the genesis of early and delayed afterdepolarizations in cardiac myocytes. *Biophys J.* 2015;108(8):1908-1921.
48. Chen WT, Chen YC, Hsieh MH, et al. The uremic toxin indoxyl sulfate increases pulmonary vein and atrial arrhythmogenesis. *J Cardiovasc Electrophysiol.* 2015;26(2):203-210.
49. Kovesdy CP, Matsushita K, Sang Y, et al. Serum potassium and adverse outcomes across the range of kidney function: a CKD Prognosis Consortium meta-analysis. *Eur Heart J.* 2018;39(17):1535-1542.
50. Gilligan S, Raphael KL. Hyperkalemia and Hypokalemia in CKD: Prevalence, Risk Factors, and Clinical Outcomes. *Adv Chronic Kidney Dis.* 2017;24(5):315-318.
51. Yamada S, Inaba M. Potassium Metabolism and Management in Patients with CKD. *Nutrients.* 2021;13(6):1751.

52. Ishihara K, Ehara T. Two modes of polyamine block regulating the cardiac inward rectifier K⁺ current IK1 as revealed by a study of the Kir2.1 channel expressed in a human cell line. *J Physiol.* 2004;556(Pt 1):61-78.
53. Yang T, Snyders DJ, Roden DM. Rapid inactivation determines the rectification and [K⁺]_o dependence of the rapid component of the delayed rectifier K⁺ current in cardiac cells. *Circ Res.* 1997;80(6):782-789.
54. Sanguinetti MC, Jurkiewicz NK. Role of external Ca²⁺ and K⁺ in gating of cardiac delayed rectifier K⁺ currents. *Pflügers Arch.* 1992;420(2):180-186.
55. Weiss JN, Qu Z, Shivkumar K. Electrophysiology of Hypokalemia and Hyperkalemia. *Circ Arrhythm Electrophysiol.* 2017;10(3):e004667.
56. Skogestad J, Aronsen JM. Hypokalemia-Induced Arrhythmias and Heart Failure: New Insights and Implications for Therapy. *Front Physiol.* 2018;9:1500.
57. Hunter RW, Bailey MA. Hyperkalemia: pathophysiology, risk factors and consequences. *Nephrol Dial Transplant.* 2019;34(Suppl 3):iii2-iii11.
58. Tanaka S, Okusa MD. Crosstalk between the nervous system and the kidney. *Kidney Int.* 2020;97(3):466-476.
59. Soomro QH, Charytan DM. Cardiovascular autonomic nervous system dysfunction in chronic kidney disease and end-stage kidney disease: disruption of the complementary forces. *Curr Opin Nephrol Hypertens.* 2021;30(2):198-207.
60. Franciosi S, Perry FKG, Roston TM, Armstrong KR, Claydon VE, Sanatani S. The role of the autonomic nervous system in arrhythmias and sudden cardiac death. *Auton Neurosci.* 2017;205:1-11.
61. Chowdhary S, Marsh AM, Coote JH, Townend JN. Nitric oxide and cardiac muscarinic control in humans. *Hypertension.* 2004;43(5):1023-1028.
62. Petrashevskaya NN, Koch SE, Bodi I, Schwartz A. Calcium cycling, historic overview and perspectives. Role for autonomic nervous system regulation. *J Mol Cell Cardiol.* 2002;34(8):885-896.
63. Hamaguchi S, Kawakami Y, Honda Y, et al. Developmental changes in excitation-contraction mechanisms of the mouse ventricular myocardium as revealed by functional and confocal imaging analyses. *J Pharmacol Sci.* 2013;123(2):167-175.
64. Ewen S, Ukena C, Linz D, Schmieder RE, Bohm M, Mahfoud F. The sympathetic nervous system in chronic kidney disease. *Curr Hypertens Rep.* 2013;15(4):370-376.
65. Grassi G, Seravalle G, Ghiadoni L, et al. Sympathetic nerve traffic and asymmetric dimethylarginine in chronic kidney disease. *Clin J Am Soc Nephrol.* 2011;6(11):2620-2627.
66. Converse RL, Jr., Jacobsen TN, Toto RD, et al. Sympathetic overactivity in patients with chronic renal failure. *N Engl J Med.* 1992;327(27):1912-1918.
67. Patterson E, Lazzara R, Szabo B, et al. Sodium-calcium exchange initiated by the Ca²⁺ transient: an arrhythmia trigger within pulmonary veins. *J Am Coll Cardiol.* 2006;47(6):1196-1206.

68. Herring N, Kalla M, Paterson DJ. The autonomic nervous system and cardiac arrhythmias: current concepts and emerging therapies. *Nat Rev Cardiol.* 2019;16(12):707-726.
69. Haissaguerre M, Jais P, Shah DC, et al. Spontaneous initiation of atrial fibrillation by ectopic beats originating in the pulmonary veins. *N Engl J Med.* 1998;339(10):659-666.
70. Vanholder RC, Eloit S, Glorieux GL. Future Avenues to Decrease Uremic Toxin Concentration. *Am J Kidney Dis.* 2016;67(4):664-676.
71. Vernooij RWM, Bots ML, Strippoli GFM, et al. CONVINCe in the context of existing evidence on haemodiafiltration. *Nephrol Dial Transplant.* 2022;37(6):1006-1013.
72. Shi Y, Wang Y, Ma S, et al. Increasing the removal of protein-bound uremic toxins by liposome-supported hemodialysis. *Artif Organs.* 2019;43(5):490-503.
73. Shen Y, Wang Y, Shi Y, et al. Improving the clearance of protein-bound uremic toxins using cationic liposomes as an adsorbent in dialysate. *Colloids Surf B Biointerfaces.* 2020;186:110725.
74. Bennis Y, Cluet Y, Titeca-Beauport D, et al. The Effect of Sevelamer on Serum Levels of Gut-Derived Uremic Toxins: Results from In Vitro Experiments and A Multicenter, Double-Blind, Placebo-Controlled, Randomized Clinical Trial. *Toxins (Basel).* 2019;11(5):279.
75. Lee CT, Hsu CY, Tain YL, et al. Effects of AST-120 on blood concentrations of protein-bound uremic toxins and biomarkers of cardiovascular risk in chronic dialysis patients. *Blood Purif.* 2014;37(1):76-83.
76. Sato E, Saigusa D, Mishima E, et al. Impact of the Oral Adsorbent AST-120 on Organ-Specific Accumulation of Uremic Toxins: LC-MS/MS and MS Imaging Techniques. *Toxins (Basel).* 2017;10(1):19.
77. Yoshifuji A, Wakino S, Irie J, et al. Oral adsorbent AST-120 ameliorates gut environment and protects against the progression of renal impairment in CKD rats. *Clin Exp Nephrol.* 2018;22(5):1069-1078.
78. Asanuma H, Chung H, Ito S, et al. AST-120, an Adsorbent of Uremic Toxins, Improves the Pathophysiology of Heart Failure in Conscious Dogs. *Cardiovasc Drugs Ther.* 2019;33(3):277-286.
79. Shen WC, Chou YH, Shi LS, et al. AST-120 Improves Cardiac Dysfunction in Acute Kidney Injury Mice via Suppression of Apoptosis and Proinflammatory NF-kappaB/ICAM-1 Signaling. *J Inflamm Res.* 2021;14:505-518.
80. Saar-Kovrov V, Zidek W, Orth-Alampour S, et al. Reduction of protein-bound uraemic toxins in plasma of chronic renal failure patients: A systematic review. *J Intern Med.* 2021;290(3):499-526.
81. Takkavatakarn K, Wuttiputinun T, Phannajit J, Praditpornsilpa K, Eiam-Ong S, Susantitaphong P. Protein-bound uremic toxin lowering strategies in chronic kidney disease: a systematic review and meta-analysis. *J Nephrol.* 2021;34(6):1805-1817.
82. Schulman G, Berl T, Beck GJ, et al. Randomized Placebo-Controlled EPPIC Trials of AST-120 in CKD. *J Am Soc Nephrol.* 2015;26(7):1732-1746.
83. Asai M, Kumakura S, Kikuchi M. Review of the efficacy of AST-120 (KREMEZIN) on renal function in chronic kidney disease patients. *Ren Fail.* 2019;41(1):47-56.

84. Madero M, Cano KB, Campos I, et al. Removal of Protein-Bound Uremic Toxins during Hemodialysis Using a Binding Competitor. *Clin J Am Soc Nephrol*. 2019;14(3):394-402.
85. Florens N, Yi D, Juillard L, Soulage CO. Using binding competitors of albumin to promote the removal of protein-bound uremic toxins in hemodialysis: Hope or pipe dream? *Biochimie*. 2018;144:1-8.
86. Li J, Wang Y, Xu X, et al. Improved dialysis removal of protein-bound uremic toxins by salvianolic acids. *Phytomedicine*. 2019;57:166-173.
87. Mocanu CA, Simionescu TP, Mocanu AE, Garneata L. Plant-Based versus Animal-Based Low Protein Diets in the Management of Chronic Kidney Disease. *Nutrients*. 2021;13(11):3721.
88. Lai S, Molfino A, Testorio M, et al. Effect of Low-Protein Diet and Inulin on Microbiota and Clinical Parameters in Patients with Chronic Kidney Disease. *Nutrients*. 2019;11(12):3006.
89. Black AP, Anjos JS, Cardozo L, et al. Does Low-Protein Diet Influence the Uremic Toxin Serum Levels From the Gut Microbiota in Nondialysis Chronic Kidney Disease Patients? *J Ren Nutr*. 2018;28(3):208-214.
90. Borges NA, Carmo FL, Stockler-Pinto MB, et al. Probiotic Supplementation in Chronic Kidney Disease: A Double-blind, Randomized, Placebo-controlled Trial. *J Ren Nutr*. 2018;28(1):28-36.
91. Turakhia MP, Blankestijn PJ, Carrero JJ, et al. Chronic kidney disease and arrhythmias: conclusions from a Kidney Disease: Improving Global Outcomes (KDIGO) Controversies Conference. *Eur Heart J*. 2018;39(24):2314-2325.
92. Kaese S, Frommeyer G, Verheule S, et al. The ECG in cardiovascular-relevant animal models of electrophysiology. *Herzschrittmacherther Elektrophysiol*. 2013;24(2):84-91.
93. Fontes MS, Papazova DA, van Koppen A, et al. Arrhythmogenic Remodeling in Murine Models of Deoxycorticosterone Acetate-Salt-Induced and 5/6-Subtotal Nephrectomy-Salt-Induced Cardiorenal Disease. *Cardiorenal Med*. 2015;5(3):208-218.
94. Verkaik M, Oranje M, Abdurrachim D, et al. High Fibroblast Growth Factor 23 concentrations in experimental renal failure impair calcium handling in cardiomyocytes. *Physiol Rep*. 2018;6(7):e13591.
95. Ke HY, Chin LH, Tsai CS, et al. Cardiac calcium dysregulation in mice with chronic kidney disease. *J Cell Mol Med*. 2020;24(6):3669-3677.
96. Lee AS, Chen WY, Chan HC, et al. Electronegative LDL-mediated cardiac electrical remodeling in a rat model of chronic kidney disease. *Sci Rep*. 2017;7:40676.
97. Qiu H, Ji C, Liu W, et al. Chronic Kidney Disease Increases Atrial Fibrillation Inducibility: Involvement of Inflammation, Atrial Fibrosis, and Connexins. *Front Physiol*. 2018;9:1726.
98. Huang SY, Chen YC, Kao YH, et al. Renal failure induces atrial arrhythmogenesis from discrepant electrophysiological remodeling and calcium regulation in pulmonary veins, sinoatrial node, and atria. *Int J Cardiol*. 2016;202:846-857.
99. Liu SH, Lo LW, Chou YH, et al. Renal denervation prevents myocardial structural remodeling and arrhythmogenicity in a chronic kidney disease rabbit model. *Heart Rhythm*. 2021;18(9):1596-1604.

100. Tang X, Shi L, Cui X, et al. Renal denervation decreases susceptibility of the heart to ventricular fibrillation in a canine model of chronic kidney disease. *Exp Physiol*. 2017;102(11):1414-1423.
101. Zhao Y, Chen NX, Shirazi JT, et al. Subcutaneous nerve activity and mechanisms of sudden death in a rat model of chronic kidney disease. *Heart Rhythm*. 2016;13(5):1105-1112.
102. Hsueh CH, Chen NX, Lin SF, et al. Pathogenesis of arrhythmias in a model of CKD. *J Am Soc Nephrol*. 2014;25(12):2812-2821.
103. Touchberry CD, Green TM, Tchikrizov V, et al. FGF23 is a novel regulator of intracellular calcium and cardiac contractility in addition to cardiac hypertrophy. *Am J Physiol Endocrinol Metab*. 2013;304(8):E863-873.
104. Graves JM, Vallejo JA, Hamill CS, et al. Fibroblast growth factor 23 (FGF23) induces ventricular arrhythmias and prolongs QTc interval in mice in an FGF receptor 4-dependent manner. *Am J Physiol Heart Circ Physiol*. 2021;320(6):H2283-H2294.
105. Changchien CY, Sung MH, Chang HH, Tsai WC, Peng YS, Chen Y. Uremic toxin indoxyl sulfate suppresses myocardial Cx43 assembly and expression via JNK activation. *Chem Biol Interact*. 2020;319:108979.
106. Peng YS, Ding HC, Lin YT, Syu JP, Chen Y, Wang SM. Uremic toxin p-cresol induces disassembly of gap junctions of cardiomyocytes. *Toxicology*. 2012;302(1):11-17.
107. Tsai IT, Hsu CC, Hung WC, et al. The Arrhythmogenic Effect of Protein-Bound Uremic Toxin p-Cresylsulfate: An In Vitro Study. *Acta Cardiol Sin*. 2019;35(6):641-648.
108. Tang WH, Wang CP, Chung FM, et al. Uremic retention solute indoxyl sulfate level is associated with prolonged QTc interval in early CKD patients. *PLoS One*. 2015;10(3):e0119545.
109. Lindner M, Mehel H, David A, et al. Fibroblast growth factor 23 decreases PDE4 expression in heart increasing the risk of cardiac arrhythmia; Klotho opposes these effects. *Basic Res Cardiol*. 2020;115(5):51.
110. Navarro-Garcia JA, Delgado C, Fernandez-Velasco M, et al. Fibroblast growth factor-23 promotes rhythm alterations and contractile dysfunction in adult ventricular cardiomyocytes. *Nephrol Dial Transplant*. 2019;34(11):1864-1875.
111. Wetmore JB, Li S, Molony JT, et al. Insights From the 2016 Peer Kidney Care Initiative Report: Still a Ways to Go to Improve Care for Dialysis Patients. *Am J Kidney Dis*. 2018;71(1):123-132.
112. Jukema JW, Timal RJ, Rotmans JI, et al. Prophylactic Use of Implantable Cardioverter-Defibrillators in the Prevention of Sudden Cardiac Death in Dialysis Patients. *Circulation*. 2019;139(23):2628-2638.
113. Vanholder R, Schepers E, Pletinck A, Nagler EV, Glorieux G. The uremic toxicity of indoxyl sulfate and p-cresyl sulfate: a systematic review. *J Am Soc Nephrol*. 2014;25(9):1897-1907.
114. Goversen B, van der Heyden MAG, van Veen TAB, de Boer TP. The immature electrophysiological phenotype of iPSC-CMs still hampers in vitro drug screening: Special focus on IK1. *Pharmacol Ther*. 2018;183:127-136.



115. Tiburcy M, Hudson JE, Balfanz P, et al. Defined Engineered Human Myocardium With Advanced Maturation for Applications in Heart Failure Modeling and Repair. *Circulation*. 2017;135(19):1832-1847.
116. Goldfracht I, Efraim Y, Shinnawi R, et al. Engineered heart tissue models from hiPSC-derived cardiomyocytes and cardiac ECM for disease modeling and drug testing applications. *Acta Biomater*. 2019;92:145-159.
117. Li RA, Keung W, Cashman TJ, et al. Bioengineering an electro-mechanically functional miniature ventricular heart chamber from human pluripotent stem cells. *Biomaterials*. 2018;163:116-127.
118. Camprostrini G, Windt LM, van Meer BJ, Bellin M, Mummery CL. Cardiac Tissues From Stem Cells: New Routes to Maturation and Cardiac Regeneration. *Circ Res*. 2021;128(6):775-801.



Willem B. van Ham¹

Carlijn M. Cornelissen¹

Elizaveta Polyakova¹

Stephanie M. van der Voorn¹

Merel L. Ligtermoet¹

Jantine Monshouwer-Kloots²

Marc A. Vos¹

Alexandre Bossu¹

Eva van Rooij²

Marcel A.G. van der Heyden¹

Toon A.B. van Veen¹

¹Department of Medical Physiology, University Medical Center Utrecht, The Netherlands

²Hubrecht Institute, KNAW, University Medical Center Utrecht, The Netherlands

Chapter III

**Pro-arrhythmic potential of
accumulated uremic toxins is
mediated via vulnerability of action
potential repolarization**

Abstract

Chronic kidney disease (CKD) is represented by a diminished filtration capacity of the kidneys. End-stage renal disease patients need dialysis treatment to remove waste and toxins from the circulation. However, endogenously produced uremic toxins (UTs) cannot always be filtered during dialysis. UTs are among the CKD-related factors that have been linked to maladaptive and pathophysiological remodeling of the heart. Importantly, 50% of the deaths in dialysis patients are cardiovascular related, with sudden cardiac death predominating. However, the mechanisms responsible remain poorly understood. The current study aimed to assess the vulnerability of action potential repolarization caused by exposure to pre-identified UTs at clinically relevant concentrations. We exposed human induced pluripotent stem cell-derived cardiomyocytes (hiPSC-CMs) and HEK293 chronically (48 h) to the UTs indoxyl sulfate, kynurenine, or kynurenic acid. We used optical and manual electrophysiological techniques to assess action potential duration (APD) in the hiPSC-CMs and recorded I_{Kr} currents in stably transfected HEK293 cells (HEK-hERG). Molecular analysis of $Kv11.1$, the ion channel responsible for I_{Kr} , was performed to further understand the potential mechanism underlying the effects of the UTs. Chronic exposure to the UTs resulted in significant APD prolongation. Subsequent assessment of the repolarization current I_{Kr} , often most sensitive and responsible for APD alterations, showed decreased current densities after chronic exposure to the UTs. This outcome was supported by lowered protein levels of $Kv11.1$. Finally, treatment with an activator of the I_{Kr} current, LUF7244, could reverse the APD prolongation, indicating the potential modulation of electrophysiological effects caused by these UTs. This study highlights the pro-arrhythmic potential of UTs and reveals a mode of action by which they affect cardiac repolarization.

Keywords: cellular electrophysiology; uremic toxins; chronic kidney disease; $Kv11.1$; cardiac repolarization

1. Introduction

Cardiorenal syndrome (CRS) is a global health care problem with high morbidity and mortality¹⁻³. The pathology of this syndrome is characterized by acute or chronic dysfunction of one of these organs, subsequently leading to malfunction of the other. CRS consists of a classification of five subtypes in which the bidirectional interaction between the heart and kidneys is displayed^{4,5}. Primary chronic kidney disease (CKD), a gradual loss of function of the kidneys that eventually may lead to end-stage renal disease (ESRD), contributes to reduced cardiac function and/or increased risk for adverse cardiovascular events⁶. Almost half of the deaths in CKD patients are caused by these cardiovascular events, particularly sudden cardiac death (SCD) in ESRD patients^{7,8}.

Due to the decline in kidney function, filtration of uremic solutes is compromised, leading to increased concentrations of uremic toxins (UTs) and other waste products in the circulation. In addition, the accumulation of UTs also further contributes to progressive damage to the kidneys, thereby worsening CKD^{4,9}. ESRD patients mainly rely on dialysis to filter their blood; however, dialysis only mimics the glomerular filtration of the kidneys and not the tubular section mediated by transporters. Protein-bound uremic toxins (PBUTs) are predominantly excreted by tubular secretion due to their strong protein-binding properties^{10,11}. This process results in accumulation of these toxins even in dialysis patients since only the free fraction of the UTs can be filtered in conventional dialysis therapies¹².

The high concentrations of UTs in ESRD, in association with the high SCD rates in these patients, suggests an important effect on cardiac electrophysiology that has been scarcely investigated in basic experimental studies¹³. Prolongation of the action potential duration (APD), as a trigger for increased susceptibility of early after depolarizations (EADs), is a known pro-arrhythmic parameter preceding SCD. Studying deviations in cardiac repolarization could prove beneficial in identifying electrophysiologically dangerous UTs, laying the ground for a more specific approach to UT removal. While some experimental studies have shown systemic effects evoking altered calcium handling and sodium currents in models of CKD¹⁴⁻¹⁶, the majority of data have predominately indicated effects on potassium currents, as recently reviewed by our group¹³. $K_v11.1$, or hERG, comprises one of the most important ion channels involved in repolarization of the action potential. These channels are highly sensitive to blockage by a variety of compounds and drugs, accounting for the high attrition rate during drug development. This sensitivity stresses the need to screen for potential pro-arrhythmogenicity of UTs by focusing on the repolarization current I_{K_r} ¹⁷.

The aim of this study was to identify the consequences on cardiac repolarization of UT exposure, using a subset of clinically relevant UTs, including indoxyl sulfate (IS), kynurenine (KYN), and kynurenic acid (KYNA). First, we determined the influence of acute and chronic UT exposure on APD in human induced

pluripotent stem cell-derived cardiomyocytes (hiPSC-CMs). Since chronic exposure resulted in APD prolongation, we measured current densities of the repolarization current I_{Kr} using a cell line stably expressing $K_v11.1$ (HEK-hERG). At the molecular level we analyzed levels of mRNA and protein of $K_v11.1$ after chronic UT exposure. Finally, we performed an intervention strategy using LUF7244, an activator of $K_v11.1$ channels, in an attempt to recover repolarization functionality in hiPSC-CMs after chronic UT exposure. In this study, we identified the negative effects of three UTs on cardiac repolarization, while distinguishing the more clinically relevant UTs and concentrations.

2. Materials and methods

2.1. Cell lines

2.1.1. hiPSCs culture

Commercially obtained ATCC hiPSC cells, originating from a healthy man (ATCC, CS-1026), were cultured daily with Essential 8™ medium (Gibco, A1517001, Waltham, MA, USA), in Geltrex™ LDEV-Free, hESC-Qualified, Reduced Growth Factor Basement Membrane Matrix-coated wells (Gibco, A1413302). The cells were passaged once the confluency reached 80–100%. They were dissociated with TrypLE Express Enzyme (Gibco, 12605010) for 5 min at 37 °C, after which Essential 8™ medium supplemented with 1 μM thiazovivin (Sigma, 420220, St. Louis, MI, USA) was added. The cell suspension was then transferred to a Falcon tube and centrifuged for 3 min at 300 RCF. Finally, the cells were seeded at 15,000 cells/cm² in Essential 8™ medium with 1 μM thiazovivin overnight, after which the medium was refreshed with plain Essential 8™ medium.

2.1.2. hiPSC cardiomyocyte differentiation

hiPSCs were cultured until 80–90% confluency and washed with dPBS (Gibco, 14190094). The cells were then provided with RPMI++ (bare RPMI-1640-Medium-GlutaMAX™ Supplement-HEPES (Gibco, 72400-021) supplemented with 0.5 mg/mL human recombinant albumin (Sigma, A9731), 0.2 mg/mL L-ascorbic acid 2-phosphate (Sigma, A8960)), and 4 μM CHIR99021 (Sigma, 361559). After 48 h, the medium was replaced with RPMI++ and 5 μM IWP2 (Sigma, 681671) after a single rinse with bare RPMI-1640. Then, the cells were refreshed every other day with RPMI++, for 4 days. Thereafter, the cells were cultured every 3–4 days with bare RPMI, supplemented with B-27™ Supplement (Gibco, 17504001). Prior to the optical experiments, the hiPSC-CMs were dissociated with TrypLE Select Enzyme without phenol red (Gibco, A1217703) and seeded on Geltrex™ coated coverslips.

2.1.3. HEK-hERG cells

Human embryonic kidney cells stably expressing $K_v11.1$ (HEK-hERG, generously obtained from C.T. January¹⁸) were cultured in Dulbecco's modified eagle medium, supplemented with 10% fetal calf serum,

1% L-glutamine, and 1% streptomycin/penicillin. The cells were passaged twice per week and cultured at 37 °C and 5% CO₂.

2.2. Drugs and toxins

The I_{Kr} blocker dofetilide (Sigma, PZ0016), as well as the three UTs — IS (Sigma, I3875), KYN (Sigma, K8625), and KYNA (Sigma, K3375) — were dissolved in DMSO to 10 mM. LUF7244 was custom synthesized at the Division of Drug Discovery and Safety, Leiden, the Netherlands, as described previously¹⁹, and was dissolved in DMSO to 100 mM. All stock solutions were filtered and stored at -20 °C. Clinically relevant total UT concentrations were identified previously¹⁵ and applied in all experiments. Albumin was present in all culture media to establish clinically relevant, free fraction concentrations of all UTs.

2.3. Electrophysiology

2.3.1. Optical action potential measurements

hiPSC-CMs were seeded at a density of approximately 150,000 per Geltrex™-coated coverslip, which facilitated the formation of cell clusters. Coverslips were incubated with Powerload and FluoVolt (ThermoFisher F10488, 1:1000, Waltham, MA, USA) in complete RPMI medium at 37 °C for 20 min. Action potentials were recorded at 37 °C, during which the coverslips were placed in a bath solution containing (mM): NaCl (130), KCl (4), CaCl₂ (1.8), MgCl₂ (1.2), NaHCO₃ (18), HEPES (10), and glucose (10), with a pH of 7.4. Fluorescent dye signals were recorded on a custom-built microscope (Cairn Research, Faversham, UK) using a 10× objective. Blue light was filtered using a 482/35 excitation filter and projected onto the objective with a 515-nm dichroic mirror. Fluorescent signals were captured via a 514 long-pass emission filter by a high-speed camera (Andor Zyla 5.5.CL3, Oxford Instruments, Abingdon, UK). Analysis of the data was performed using Fiji and Peaks, a custom-written Matlab script (DOI: 10.17605/OSF.IO/86UFE). APD of spontaneously beating hiPSC-CMs was determined at 90% repolarization and then adjusted for the beating rate using a modified Fredericia's correction: $APD_{corrected} = APD / (\sqrt[3]{60/BPM})$.

2.3.2. Patch clamp electrophysiology

HEK-hERG cells were cultured on poly-L-lysine-coated glass coverslips. Whole-cell voltage clamp recordings were performed at room temperature using an AxoPatch 200B patch clamp amplifier and pClamp software, v.10. Pipettes were pulled using a Sutter P2000 puller, with a resistance of 1.5–3 MΩ. Measurements were performed using an external bath solution containing (mM): NaCl (140), KCl (4), CaCl₂ (2), MgCl₂ (1), and HEPES (10) with a pH of 7.4 and an internal pipette solution containing (mM): KCl (110), CaCl₂ (5.17), MgCl₂ (1.42), HEPES (10), K₂ATP (4), and EGTA (10) with a pH of 7.2. I_{Kr} was measured from a holding potential of -80 mV, followed by a pulse protocol from -60 mV to +60 mV in

increments of 10 mV. Currents were analyzed using the pClamp software, with the maximum tail current at each voltage step being depicted in the current-voltage graphs.

2.4. Western immunoblotting

Cultured cells were harvested in RIPA lysis buffer (20 mM Tris, 150 mM NaCl, 10 mM Na₂HPO₄, 1 mM EDTA, 50 mM NaF, 1% Triton X100, 1% Na-deoxycholate, 0.1% SDS, supplemented with 0.2% aprotinin and 1 mM PMSF). SDS-PAGE was performed using 10–20 µg of protein per sample and subsequently transferred onto nitrocellulose membranes. Ponceau staining was used to determine equal loading. hERG primary antibody (Alomone, APC-062, Jerusalem, Israel) and the secondary HRP conjugated antibody (Bio-Rad, 170-6515, Hercules, CA, USA) were diluted in 5% protifar TBST (20 mM Tris, 150 mM NaCl, 0.05% Tween-20) and incubated at 4 °C overnight or at room temperature for 90 min. Data were imaged and analyzed using an ECL detection kit (Cytiva, RPN2232, Marlborough, MA, USA) and a ChemiDoc Molecular Imager and ImageLab software v.6.1. (Bio-Rad).

2.5. Quantitative PCR

Total RNA was extracted from HEK-hERG cells using TRIzol reagent (ThermoFisher). After DNase treatment, DNase-treated RNA was converted into complement DNA (cDNA) with reverse transcriptase (Invitrogen, Waltham, MA, USA) according to the manufacturer's protocol. RT-qPCR was performed using TaqMan gene expression assays (Applied Biosystems by Life Technologies Corp., Carlsbad, CA, USA). Relative mRNA levels were determined for KCNH2 (Hs00542479_g1). TATA-binding protein (Hs00427620_m1), 60S ribosomal protein L32 (Hs04194521_s1) and peptidylprolyl isomerase A (Hs00851655_g1) were used for internal controls. Fold changes were calculated using the $2^{(-\Delta\Delta CT)}$ method.

2.6. Statistical analysis

All statistical analysis was performed using GraphPad Prism software, v.9. Comparisons were performed using a two-way ANOVA, with Tukey's post-hoc test to correct for multiple comparisons. Data are reported as individual datapoints (optical electrophysiology), as means \pm SEM (manual electrophysiology), or as means \pm SD (western immunoblotting and quantitative PCR).

3. Results

3.1. Action potential prolongation caused by chronic toxin exposure

First, using the organic voltage-sensitive fluorescent dye FluoVolt, we measured APD in hiPSC-CMs (**Figure 1A**). Cardiomyocytes were exposed acutely (5 min) to one of two concentrations of each UT. Dofetilide, a well-known blocker of the cardiac repolarization hERG channel, was used as positive control (**Figure 1B**). Mean APD in the control group (304 ± 71 ms) remained similar upon exposure to all UT conditions, except for dofetilide, which significantly prolonged repolarization (APD 547 ± 206 ms). After

chronic exposure (48 h), the APD remained unchanged in the control group (297 ± 60 ms), while all other conditions significantly prolonged the APD (343 ± 77 and 353 ± 73 ms, 513 ± 95 and 460 ± 59 ms, and 375 ± 100 and 393 ± 112 ms for the low and high concentrations of IS, KYN, and KYNA respectively) (Figure 1C). This finding clearly suggests that chronic, but not acute, exposure to UTs is necessary to trigger a prolongation of repolarization in hiPSC-CMs. Therefore, it translates to the clinical settings, whereby patients are chronically exposed to high concentrations of UTs regardless of dialysis. Interestingly, no concentration-dependent effect was seen with any of the UTs, although the high concentrations of KYN and KYNA far exceeded the pathological concentrations measured in CKD patients. The lowest concentrations applied are in line with those measured in patients.

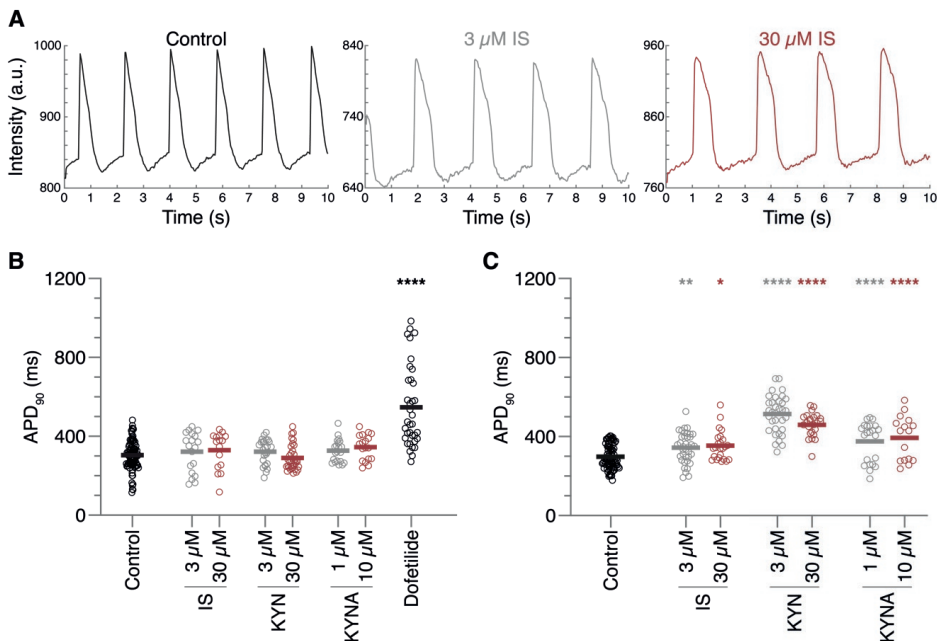


Figure 1. Action potential prolongation induced by chronic uremic toxin exposure. Action potential duration (APD) was measured in spontaneously beating cells, using a voltage sensitive dye, after exposure to two concentrations of indoxyl sulfate (IS), kynurenine (KYN), or kynurenic acid (KYNA). (A) Representative action potential traces of chronic exposure measurements in control, 3 μ M IS, and 30 μ M IS. (B) Quantified APD measurements after acute uremic toxin (UT) exposure of 5 min. (C) Quantified APD measurements after chronic 48 h UT exposure. Data are shown as means with individual measurements, and quantified APDs were corrected for beating rate. Measurements were obtained in three independent differentiations of hiPSC-CMs, with numbers of cells=16–99 (B), and 16–82 (C). * $p < 0.05$, ** $p < 0.01$, **** $p < 0.0001$ compared to control.

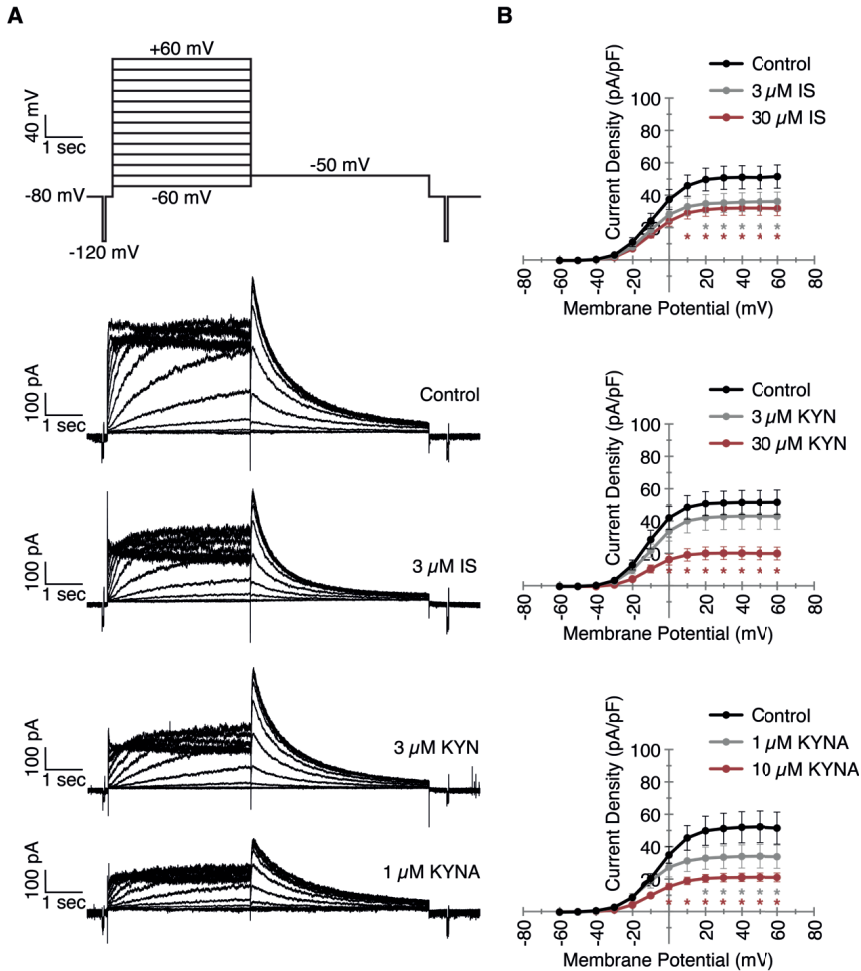


Figure 2. Chronic exposure to uremic toxins decreases I_{K_r} current density. HEK cells stably expressing the hERG ion channel were exposed to two concentrations of indoxyl sulfate (IS), kynurenine (KYN), and kynurenic acid (KYNA) for 48 h. I_{K_r} currents were measured using patch clamp electrophysiology. **(A)** Patch clamp measurement protocol and example traces of control, 3 μ M IS, 3 μ M KYN, and 1 μ M KYNA as clinically relevant concentrations. **(B)** Quantification of all measurements visualized in current-voltage curves. Data are shown as the mean \pm SEM. Number of cells=12–19. * $p < 0.05$ compared to control.

3.2. Decreased I_{K_r} current density after exposure to clinically relevant UT concentrations

Next, to elucidate the underlying mechanism of APD lengthening, we focused on the rapid delayed rectifier potassium repolarization current I_{K_r} . Using a voltage clamp in HEK-hERG cells, we measured I_{K_r} currents with or without chronic exposure (48 h) to the UT concentrations, including the clinically relevant concentrations, which are shown as example traces (**Figure 2A**). The current densities, which are comparable to relevant hERG channel activation during the repolarization, are covered between +20 mV

and +40 mV²⁰ (Figure 2B). Exposure to both concentrations of IS resulted in a diminished peak current density compared to control measurements (35 and 32 vs. 51 pA/pF for 3 and 30 μM respectively), again implying that no difference was observed between the clinically relevant and the exceeding concentration of IS. KYN only decreased the I_{Kr} current at 30 μM (20 vs. 51 pA/pF), whereas the clinically relevant concentration of 3 μM did not have an effect. Exposure to KYNA also resulted in smaller currents for both concentrations (34 and 21 vs. 52 pA/pF). Although not significant (p=0.08), 10 μM KYNA decreased the I_{Kr} current even further than the more clinically relevant 1 μM. While the hampered hERG channel functionality could explain the prolonged APDs as being caused by the UTs, the APD prolongation caused by 3 μM KYN did not seem to be disturbed in an I_{Kr}-dependent manner.

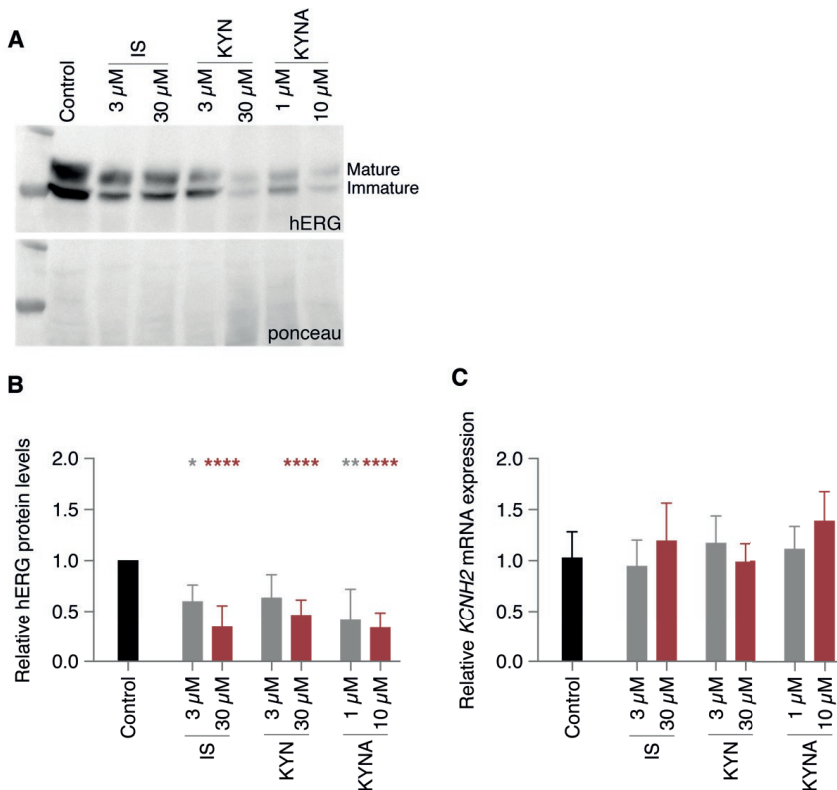


Figure 3. Diminished hERG protein levels caused by chronic uremic toxin exposure. HEK cells stably expressing the hERG ion channel were exposed to two concentrations of indoxyl sulfate (IS), kynurenine (KYN), and kynurenic acid (KYNA) for 48 h. (A and B) Example and quantification of protein levels. (C) Quantification of KCNH2 mRNA levels. Data are shown as the mean ± SD. Numbers of biological repeats=3–5 (B) and 5 (C).

* p < 0.05, ** p < 0.01, **** p < 0.0001 compared to control.

To gain more insight in the molecular events underlying this vulnerability in re-polarization, we quantified the protein and mRNA expression of the hERG channel as a potential cause of the diminished I_{Kr} current. Similar to the decreased currents, protein levels were reduced for the UT conditions in a dose-independent manner (**Figure 3A and 3B**). IS at a concentration of 30 μM and 10 μM KYNA exposure resulted in a reduction of approximately 70%. hERG protein decreases due to 3 μM KYN were nonsignificant compared to control. mRNA levels of the *KCNH2* gene were not altered in any of the conditions compared to control (**Figure 3C**), indicating a (post-)translational effect of the UTs that resulted in lower protein levels.

3.3. Action potential prolongation can be reversed by LUF7244

The reduced expression of functional protein could limit the possibility of recovering from prolonged UT exposure. We therefore attempted to reverse the APD prolongation by treatment with LUF7244, an activator of the $K_{V11.1}$ ion channel¹⁹. hiPSC-CMs were exposed for 48 h with a high concentration of the three UTs, followed by an additional 24 h of UT exposure either with or without supplementation of 10 μM LUF7244 (**Figure 4A and 4B**). UT exposure prolonged the APD for all three toxins, similar to the earlier described experiments (547 ± 139 , 522 ± 141 , and 601 ± 205 ms for IS, KYNA, and KYNA respectively). Control APDs were approximately 100 ms longer compared to previous measurements (390 ± 92 vs. 297 ± 60 ms), presumably due to known fluctuations between hiPSC-CMs differentiations. Addition of LUF7244 robustly shortened the APD for all groups (177 ± 79 , 170 ± 66 , 159 ± 57 , and 180 ± 78 ms for control, IS, KYN, and KYNA respectively).

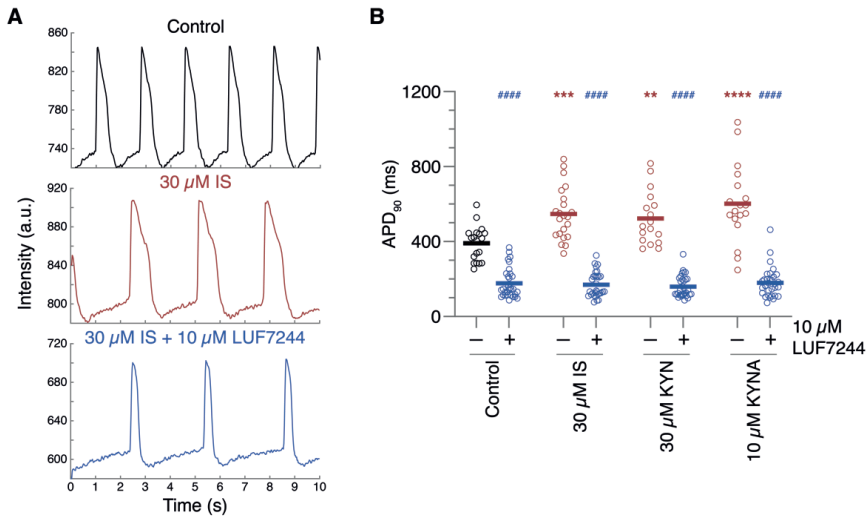


Figure 4. Reversal of uremic toxin-induced action potential prolongation by LUF7244. Action potential duration (APD) was measured in spontaneously beating cells, using a voltage sensitive dye. hiPSC-CMs were exposed to high concentrations of indoxyl sulfate (IS), kynurenine (KYN), and kynurenic acid (KYNA), for 48 h, followed by an additional 24 h of uremic toxin exposure in the absence or presence of LUF7244 (indicated by – and + respectively). **(A)** Example traces of APD measurements in control, 30 μM IS, and 30 μM IS + 10 μM LUF7244. **(B)** Quantification of APD measurements. Data are shown as the means with individual measurements, and quantified APDs were corrected for beating rate. Measurements were obtained in four independent differentiations of hiPSC-CMs with the number of cells=17–32. ** $p < 0.01$, *** $p < 0.001$, **** $p < 0.0001$ compared to control without LUF7244. ##### $p < 0.0001$ compared to control with LUF7244.

4. Discussion

In the present study we described the electrophysiological effect of UTs, which accumulate in the bloodstream of CKD patients. Chronic exposure to three clinically relevant UTs resulted in prolongation of the APD of hiPSC-CMs, although no acute effect was observed. These UTs also diminished the I_{K_r} current in HEK-hERG cells, indicating that this current, which is of major importance for adequate repolarization, could be responsible for lengthening of the APD. Additionally, chronic exposure to UTs appeared to lower $K_v11.1$ protein levels, an event not caused by alterations in *KCNH2* mRNA expression. Functional restoration of the APD in hiPSC-CMS could be achieved with LUF7244 treatment, indicating that sufficient repolarization current can be rescued to stabilize the action potential in the presence of the three UTs.

The high concentrations of UTs in CKD patients have been linked to inflammation and fibrosis formation in the past^{21,22}. However, there have been a limited number of studies that have investigated the potential direct electrophysiological effects of UTs. Previously, exposure to IS and another UT, p-cresyl sulfate, has

been shown to decrease repolarization currents in H9c2 rat ventricular cardiomyocytes and computer simulations^{23,24}. Additional studies, including *in vivo* studies, have shown pro-arrhythmic consequences but failed to delve into potential mechanisms of action¹³. With this current study, we have shown that UTs can additionally influence ion channel functionality, resulting in electrophysiological disturbances that might lead to increased susceptibility to arrhythmias in CKD patients. Future in-dept molecular analysis of the mechanisms triggered through exposure to different UTs could provide more specific targets to overcome the functional problems caused by any UT, rather than a solution against all toxins, which would demand a much broader and elaborative approach. While this study, as well as the majority of current electrophysiological research on UTs, only describes the repolarization current I_{Kr} , it is possible that other ion currents, such as late sodium, are also affected by the UTs and could be responsible for APD prolongation. This possibility is especially interesting for KYN since it showed a large APD lengthening but no effects on I_{Kr} . Future studies should also include sodium measurements, as well as calcium analysis, to fully elucidate the electrophysiological effects of UTs. However, based on current densities and protein levels of I_{Kr} , a distinction can already be made between the low and high concentrations of these three UTs.

While there are a large quantity and a variety of UTs present in CKD patients²⁵, we focused on a subset of PBUTs, including the well-known IS and two metabolites produced during tryptophan metabolism (KYN and KYNA). Since current dialysis regimens are still unable to specifically filter PBUTs, studies such as this one can contribute to the identification of UTs that are more harmful than others, thereby focusing on targets for potential adjustments in blood filtration approaches or adjustments in dietary programs. Recent clinical orientated studies have already shown superior improvements compared to conventional hemodialysis with the use of mixed matrix membranes to specifically filter out PBUTs^{26,27}.

In this study, we observed a concentration-dependent reduction in I_{Kr} current densities and hERG protein levels as caused by IS and KYNA, while KYN had mild effects. Unfortunately, these differences were not reproducible in either of the hiPSC-CM experiments, in which all three UTs were equally detrimental under all conditions. While it is possible that these three UTs ultimately do not cause different electrophysiological responses, it is important to note that measuring ion currents using patch clamp electrophysiology can be more sensitive to small differences in compound concentrations compared to optical electrophysiological measurements. Unfortunately, patch clamp electrophysiology is also much more labor intensive, restricting applicability of this latter approach for the large-scale reproducibility of these experiments for other UTs in the future.

The allosteric modulator LUF7244 acts as a specific activator of the I_{Kr} current^{19,28,29}. Previously, application of LUF7244 resulted in increased I_{Kr} currents, even independent of changes in protein levels³⁰.

Here, we used LUF7244 as a proof-of-concept method to investigate whether repolarization functionality could be rescued while simultaneously showing the potential of an alternative treatment option for specific electrophysiological effects caused by UTs. LUF7244 completely reversed the APD prolongation caused by all three UTs at their highest concentrations to a similar APD seen in control conditions. This outcome importantly indicates that, regardless of the specific effects of UTs on ion channels other than I_{Kr} , the ultimate electrophysiological disturbances can be modulated to stabilize APD repolarization in cardiomyocytes.

5. Conclusions

In this study, we have identified the detrimental effects of three UTs on cardiac repolarization. The consequences of clinically relevant concentrations of IS, KYN, and KYNA could be distinguished based on their molecular and functional effects after chronic exposure. Together, these data accentuate the need for further in-dept analysis of the electrophysiological disturbances triggered by UT exposure during CKD. Similar studies in the future could aid in providing a clinically relevant overview of (patho-)physiological concentrations of specific UTs. With this knowledge, research into UTs and potential methods for their removal from the bloodstream can be specified for the most detrimental UTs. Meanwhile, there is validity in modulating APD stability using, e.g., repolarization activators to prevent electrophysiological disturbances caused by UTs.



References

1. Roth GA, Mensah GA, Johnson CO, et al. Global Burden of Cardiovascular Diseases and Risk Factors, 1990-2019: Update From the GBD 2019 Study. *J Am Coll Cardiol.* 2020;76(25):2982-3021.
2. Hill NR, Fatoba ST, Oke JL, et al. Global Prevalence of Chronic Kidney Disease - A Systematic Review and Meta-Analysis. *PLoS One.* 2016;11(7):e0158765.
3. Kovesdy CP. Epidemiology of chronic kidney disease: an update 2022. *Kidney Int Suppl (2011).* 2022;12(1):7-11.
4. Ronco C, Haapio M, House AA, Anavekar N, Bellomo R. Cardiorenal syndrome. *J Am Coll Cardiol.* 2008;52(19):1527-1539.
5. Savira F, Magaye R, Liew D, et al. Cardiorenal syndrome: Multi-organ dysfunction involving the heart, kidney and vasculature. *Br J Pharmacol.* 2020;177(13):2906-2922.
6. Cruz DN, Gheorghiadu M, Palazzuoli A, Ronco C, Bagshaw SM. Epidemiology and outcome of the cardio-renal syndrome. *Heart Fail Rev.* 2011;16(6):531-542.
7. Franczyk-Skora B, Gluba-Brzozka A, Wrancicz JK, Banach M, Olszewski R, Rysz J. Sudden cardiac death in CKD patients. *Int Urol Nephrol.* 2015;47(6):971-982.
8. Green D, Roberts PR, New DI, Kalra PA. Sudden cardiac death in hemodialysis patients: an in-depth review. *Am J Kidney Dis.* 2011;57(6):921-929.
9. Kumar U, Wettersten N, Garimella PS. Cardiorenal Syndrome: Pathophysiology. *Cardiol Clin.* 2019;37(3):251-265.
10. Masereeuw R, Mutsaers HA, Toyohara T, et al. The kidney and uremic toxin removal: glomerulus or tubule? *Semin Nephrol.* 2014;34(2):191-208.
11. Van Gelder MK, Middel IR, Vernooij RWM, et al. Protein-Bound Uremic Toxins in Hemodialysis Patients Relate to Residual Kidney Function, Are Not Influenced by Convective Transport, and Do Not Relate to Outcome. *Toxins (Basel).* 2020;12(4):234.
12. Dhondt A, Vanholder R, Van Biesen W, Lameire N. The removal of uremic toxins. *Kidney Int Suppl.* 2000;76:S47-59.
13. van Ham WB, Cornelissen CM, van Veen TAB. Uremic toxins in chronic kidney disease highlight a fundamental gap in understanding their detrimental effects on cardiac electrophysiology and arrhythmogenesis. *Acta Physiol (Oxf).* 2022;236(3):e13888.
14. King BMN, Mintz S, Lin X, et al. Chronic Kidney Disease Induces Proarrhythmic Remodeling. *Circ Arrhythm Electrophysiol.* 2023;16(1):e011466.
15. Huang SY, Chen YC, Kao YH, et al. Redox and Activation of Protein Kinase A Dysregulates Calcium Homeostasis in Pulmonary Vein Cardiomyocytes of Chronic Kidney Disease. *J Am Heart Assoc.* 2017;6(7):e005701.
16. Ke HY, Chin LH, Tsai CS, et al. Cardiac calcium dysregulation in mice with chronic kidney disease. *J Cell Mol Med.* 2020;24(6):3669-3677.

17. Redfern WS, Carlsson L, Davis AS, et al. Relationships between preclinical cardiac electrophysiology, clinical QT interval prolongation and torsade de pointes for a broad range of drugs: evidence for a provisional safety margin in drug development. *Cardiovasc Res.* 2003;58(1):32-45.
18. Zhou Z, Gong Q, Epstein ML, January CT. HERG channel dysfunction in human long QT syndrome. Intracellular transport and functional defects. *J Biol Chem.* 1998;273(33):21061-21066.
19. Yu Z, van Veldhoven JP, t Hart IM, Kopf AH, Heitman LH, AP IJ. Synthesis and biological evaluation of negative allosteric modulators of the Kv11.1(hERG) channel. *Eur J Med Chem.* 2015;106:50-59.
20. Kiehn J, Karle C, Thomas D, Yao X, Brachmann J, Kubler W. HERG potassium channel activation is shifted by phorbol esters via protein kinase A-dependent pathways. *J Biol Chem.* 1998;273(39):25285-25291.
21. Vanholder R, Pletinck A, Schepers E, Glorieux G. Biochemical and Clinical Impact of Organic Uremic Retention Solutes: A Comprehensive Update. *Toxins (Basel).* 2018;10(1):33.
22. Savira F, Magaye R, Hua Y, et al. Molecular mechanisms of protein-bound uremic toxin-mediated cardiac, renal and vascular effects: underpinning intracellular targets for cardiorenal syndrome therapy. *Toxicol Lett.* 2019;308:34-49.
23. Tsai IT, Hsu CC, Hung WC, et al. The Arrhythmogenic Effect of Protein-Bound Uremic Toxin p-Cresylsulfate: An In Vitro Study. *Acta Cardiol Sin.* 2019;35(6):641-648.
24. Tang WH, Wang CP, Chung FM, et al. Uremic retention solute indoxyl sulfate level is associated with prolonged QTc interval in early CKD patients. *PLoS One.* 2015;10(3):e0119545.
25. Durantou F, Cohen G, De Smet R, et al. Normal and pathologic concentrations of uremic toxins. *J Am Soc Nephrol.* 2012;23(7):1258-1270.
26. Pavlenko D, van Geffen E, van Steenberghe MJ, et al. New low-flux mixed matrix membranes that offer superior removal of protein-bound toxins from human plasma. *Sci Rep.* 2016;6:34429.
27. Ter Beek OEM, van Gelder MK, Lokhorst C, et al. In vitro study of dual layer mixed matrix hollow fiber membranes for outside-in filtration of human blood plasma. *Acta Biomater.* 2021;123:244-253.
28. Yu Z, Liu J, van Veldhoven JP, et al. Allosteric Modulation of Kv11.1 (hERG) Channels Protects Against Drug-Induced Ventricular Arrhythmias. *Circ Arrhythm Electrophysiol.* 2016;9(4):e003439.
29. Qile M, Beekman HDM, Sprenkeler DJ, et al. LUF7244, an allosteric modulator/activator of K(v) 11.1 channels, counteracts dofetilide-induced torsades de pointes arrhythmia in the chronic atrioventricular block dog model. *Br J Pharmacol.* 2019;176(19):3871-3885.
30. Qile M, Ji Y, Golden TD, et al. LUF7244 plus Dofetilide Rescues Aberrant K(v)11.1 Trafficking and Produces Functional I(Kv11.1). *Mol Pharmacol.* 2020;97(6):355-364.

Part II

**Patient-specific modeling in inherited
and acquired cardiomyopathies**

Willem B. van Ham¹

Esmeralda E.M. Meijboom¹

Merel L. Ligtermoet¹

Peter G.J. Nikkels²

Toon A.B. van Veen¹

¹Department of Medical Physiology, University Medical Center Utrecht, The Netherlands

²Department of Pathology, University Medical Center Utrecht, The Netherlands

Chapter III

**Maturation and function of the
intercalated disc:
report of two pediatric cases
focusing on cardiac development and
myocardial hyperplasia**

Abstract

The development of the normal human heart, ranging from gestational age to the mature adult heart, relies on a very delicate and timely orchestrated order of processes. One of the most striking alterations in time is the gradual extinction of the ability for cardiomyocytes to proliferate. Once passing this event, cardiomyocytes grow and increase in contractile strength by means of physiological hypertrophy. This process, importantly, seems to depend on an adequate development of electromechanical coupling that is achieved by the appropriate formation of the intercellular junction named the intercalated disc (ID). In this report, we describe two sudden death cases of young and apparently healthy-born individuals without external abnormalities compared to an age-matched control. Histological examination, including the comparison with the age-matched and histology-matched controls, showed a disturbed formation of the protein machinery composing the electromechanical junctions at the ID and an increased nuclei count for both patients. As a cause or consequence, cardiomyocytes in both sudden death cases showed signs of a delayed developmental stage, presumably resulting in an exaggerated degree of hyperplasia.

Keywords: intercalated disc; myocardial hyperplasia; sudden death

1. Introduction

The interconnection of cardiomyocytes in the adult human heart is the basis for myocardial stability and function, resulting in the synchronous electromechanical activation of the heart. The area at which the cardiomyocytes are connected in a longitudinal orientation is named the intercalated disk (ID). It consists of a plethora of components that are structured in a sophisticated manner, thereby forming a network of neighboring proteins and the cytoskeleton of the cell¹. The intricate complex of junctional proteins, ion channels, and connexin channels is also defined as the area composita. Proteins such as N-cadherin (N-CAD), β -catenin, and plakoglobin (JUP) play an important role in the mechanical coupling of the cardiomyocytes. As cardiac workload increases during fetal and neonatal development², mechanical reliability becomes imperative. The absence of N-CAD during embryogenesis is therefore also resulting in compromise of the myocardium, delayed development, and embryonically lethal^{3,4}. During cardiomyocyte maturation, these ID proteins, as well as gap junction proteins (connexins), are initially dispersed across the entire cell. Over time, they localize on the lateral sites of the cell and finally on the longitudinal ends^{5,6}. Altered expression or localization of these proteins has been connected to cardiomyopathies and is linked to an increased incidence of arrhythmias^{7,8}. This highlights the significant relationship between mechanical and electrophysiological integrity.

One of the first organs to develop and function during embryogenesis is the heart. Throughout the subsequent phases of embryonic and fetal cardiac development, cells proliferate and migrate to form a heart tube, and due to the looping process of the tube over a timespan of around 7 weeks, they form a four-chamber system². In mammalian hearts, this proliferative capacity rapidly diminishes around birth, upon which the cardiomyocytes undergo physiological hypertrophy to increase cell size, protein expression, and support sarcomere organization⁹. In the human heart, hyperplasia also ceases gradually postnatally, leading to a negligible role in determining heart size after the age of 20^{10,11}. This process leads to terminal differentiation of the cardiomyocytes, which coincides with a general arrest of the capacity for cell division. Instead, cardiomyocytes undergo an alternate cell cycle, named endomitosis, during which the genome is replicated without finishing karyokinesis during mitosis^{12,13}. This results in polyploid nuclei in cardiomyocytes, which is presumed to facilitate increased protein production, growth, and ID stabilization in the hypertrophic cells. Interestingly, when karyokinesis does ensue but subsequent cytokinesis fails, cardiomyocytes end up multinucleated. This is mainly observed in animals like mice, dogs, and pigs, while human cardiomyocytes are predominantly mononucleated^{10,14}. During genome replication, the chromosomes are protected by the Ki67 protein, which can therefore be used as a marker for cells that are or have relatively recently been proliferating¹⁵. The shift from proliferation towards hypertrophy is a complex and not fully understood mechanism, but the process of polyploidy is thought to be connected. Furthermore, the ID components N-CAD and β -catenin have also been associated with playing a role in this transition^{16,17}.



Here we report an observational study of two pediatric patients who died of asphyxia without any known cause. Both cases presented during autopsy with enlarged hearts and an indication of malformed ID structures. We performed an immunohistological study of cardiac tissue obtained from those two patients, in which we identified immaturely formed ID structures. Additionally, patient material indicated persistent hyperplasia of the cardiomyocytes, which presumably could be responsible for insufficient contractile function and enhanced susceptibility to cardiac arrhythmias.

2. Materials and methods

Cardiac specimens of both patients (S and T, 4 and 6 weeks postnatal, respectively), an age-matched control (R, 5 weeks postnatal), and a histology-matched control (Q, 39 weeks in utero) were acquired via the biobank from the Department of Pathology of the University Medical Center Utrecht, the Netherlands. Both patients and the 5-week age-matched control were full term infants. Patient material was cryofrozen in liquid nitrogen. Tissues were then sectioned onto glass slides and post-fixed in 4% paraformaldehyde prior to immunohistology. Tissues were washed once with PBST (0.2% tween-20 in PBS) and once with TBST (20 mM tris, 150 mM NaCl, and 0.2% tween-20 in PBS, pH=8.0). Triton X-100 (0.2% in PBS) was used to permeabilize the cell membranes, followed by a brief wash with PBST. Samples were then blocked with BSA (4% BSA in PBS) for 60 min at room temperature. Incubation of the first antibodies was done overnight at 4 °C in 2% BSA in PBS. The next day, tissues were washed five times for 5 min with PBST, and secondary antibody incubation was again performed in 2% BSA in PBS for 120 min at room temperature. Afterwards, tissues were washed two times for 5 min with TNT (100 mM tris, 150 mM NaCl, and 0.1% tween-20 in ddH₂O, pH=8.0), as well as three times with PBST. Finally, slices were dried, covered, and stored at -20 °C. Labeling was performed against N-CAD (Sigma, St. Louis, MO, USA, C3678, 1:800), JUP (Sigma, P8087, 1:500), Ki67 (Invitrogen, Carlsbad, USA, PA519462, 1:500), α -actinin (Sigma, A7811, 1:1000), β -catenin (BD Transduction, Franklin Lakes, NJ, USA, 610154), and DAPI (Life Technologies, Carlsbad, CA, USA, D1306, 1:100) as counterstain to visualize the nuclei. Images were captured on a Nikon Eclipse Ti2 microscope with 40x and 60x objectives, and MetaMorph software (v.7). In total, 6–8 images taken from 4 independent tissue slice stainings per experiment were processed using ImageJ with the “cell counter” and “quickfigures” plugins. GraphPad Prism (v.10) was used for data visualization and to statistically compare nuclei counts with a One-way ANOVA with Tukey’s test for multiple comparisons.

3. Case history

Patient S was a 4-week-old male without a personal or familial medical history. The day prior to his death, the patient experienced tachypnea and was admitted to the ER, where resuscitation was later started due to apnea without shockable heart rhythm. The infant had normal proportions, weighing 4060 g and a

length of 57.5 cm. The heart was enlarged, weighing 42 g, with normal anatomy and the absence of dilation or inflammation. Patient T was a 6-week-old male with no previous medical history. The patient suffered from an irregular breathing pattern, which culminated in the need for resuscitation, during which asystole was noticed. Again, the infant had no external abnormalities, weighing 5600 g and a length of 57 cm. The heart was also enlarged, weighing 35.6 g, without inflammation or deformations. No abnormalities were identified in the other organs of either patient.

The histology-matched control (control Q) was a male fetus of 39 weeks that died in utero due to late-stage defective placental maturation. Aside from signs of recent hypoxia, such as mild aspiration of amniotic fluid and the absence of increased erythropoiesis, the fetus had no congenital abnormalities. The body weight was 3240 g with a length of 52 cm. No anatomical anomalies were identified, and the heart weight was 20.4 g. The age-matched control (control R) was a 5-week-old female patient with Pierre Robin sequence who suffered from severe cerebral ischemia during surgery and had treatment withheld based on a very poor prognosis. Beyond the classical signs of the Pierre Robin sequence, the infant had no other congenital anomalies and normal proportions, weighing 4400 g and having a length of 56 cm. Cardiac anatomy was normal, and the heart weight was 25.3 g. Autopsy reports of both patients highlighted the similarities of enlarged hearts without dilation as well as an initial indication of malformation of the ID structures. Immunohistological labeling of both hearts was performed to determine the nuclei count and the presence of the proliferation marker Ki67. These data were compared with control Q and control R, which both died without evidence of cardiac involvement. Cardiomyocyte-specific α -actinin signals indicated well-organized fibers of larger cardiomyocytes in tissue of control R without the presence of Ki67-positive immunolabeling (**Figure 1A**). In contrast, both patients showed an increased number of seemingly smaller-sized cardiomyocytes, highlighted by the combination of α -actinin-positive labeling and total nuclei counts (**Figure 1B**), suggesting the absence of hypertrophy during development. Furthermore, both hearts displayed an increased number of Ki67-positive nuclei, indicating increased cell proliferation, suggesting myocardial hyperplasia as the causative explanation for the enlarged but not dilated hearts. Interestingly, these labelings of patient material are similar to control Q, which indicates that the patients were in a hyperplastic phase comparable to 39 weeks of gestation.

Additional stainings identifying mechanical components of the ID (N-CAD and JUP) were performed. N-CAD labeling in control R shows mainly complete and normal-formed ID structures, with scarce labeling found at the lateral side of cardiomyocytes (**Figure 2**). Also, a consistent overlap between N-CAD, JUP, and β -catenin was seen, demonstrating the intertwined trafficking processes of these ID proteins (**Figure S1**). Whereas patient S presented seemingly decreased protein levels and an absence of ID formation, patient T showed several appropriate IDs but also much labeling in a diffuse pattern. Again, these patterns are more comparable to control Q. Overlap between both of the ID proteins remained

similar, as seen in both controls. These results highlight the differences between both patients and the controls, resembling more premature maturation patterns of both the ID and cardiomyocyte proliferation, with patient T being two weeks older and showing more advanced ID expression and structure compared to patient S.

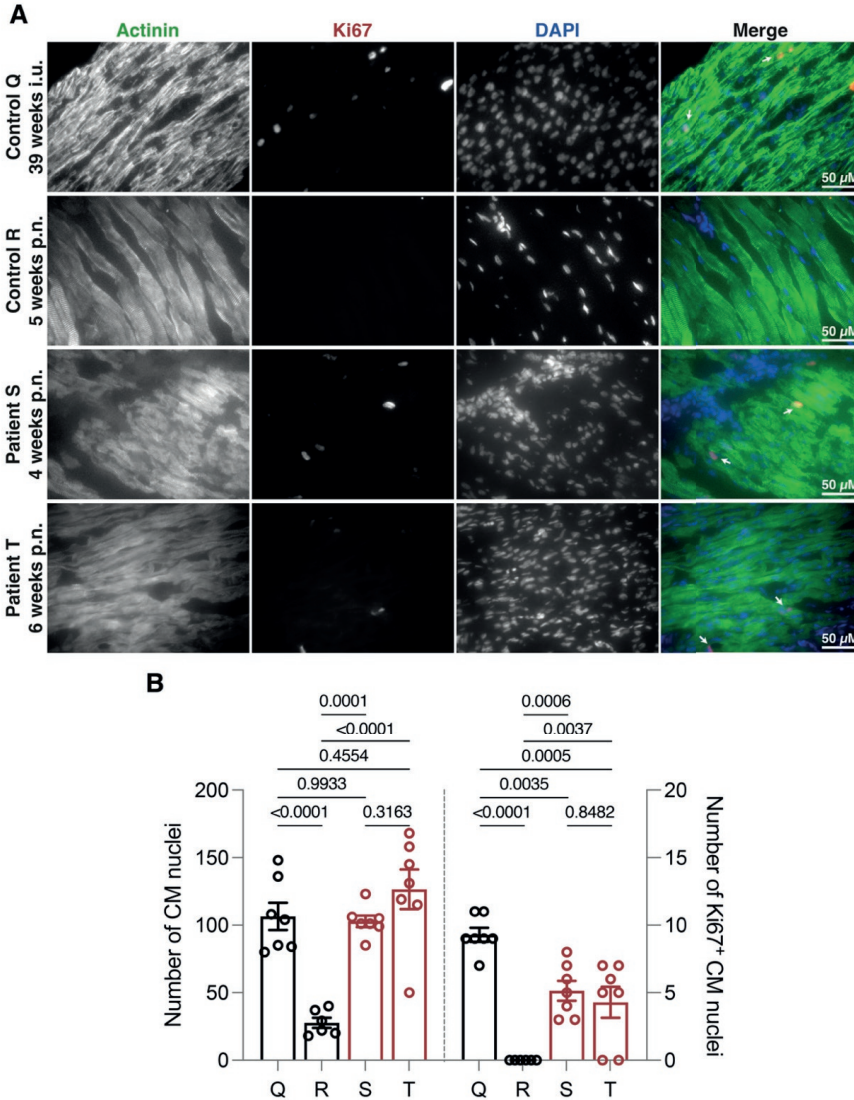


Figure 1. Hyperplasia and cardiomyocyte proliferation in pediatric patient tissues. (A) Immunohistochemical labeling of cardiomyocytes (α -actinin), proliferating cells (Ki67), and nuclei (DAPI), at 40x. (B) Comparison of two pediatric patients (patient S, 4 weeks postnatal; patient T, 6 weeks postnatal) to age-matched (control R, 5 weeks postnatal) and histology-matched (control Q, 39 weeks in utero) controls showed increased nuclei count and proliferation-positive nuclei (white arrows). CM—Cardiomyocyte. A total of 6–8 images were analyzed based on 4 independent tissue slice stainings per individual. The scale bar represents 50 μ M.

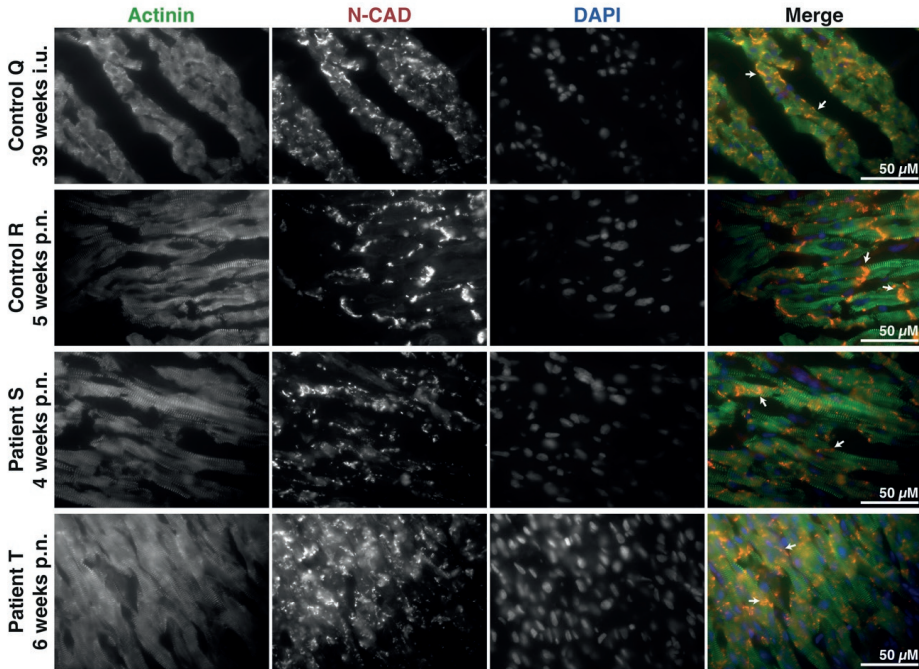


Figure 2. Immature intercalated disc maturation in pediatric patient tissues. Immunohistochemical labeling of cardiomyocytes (α -actinin), N-cadherin (N-CAD), and nuclei (DAPI) at 60x. Comparison of two pediatric patients (patient S, 4 weeks postnatal; patient T, 6 weeks postnatal) to age-matched (control R, 5 weeks postnatal) and histology-matched (control Q, 39 weeks in utero) controls showed increased diffuse and lateral expression of the intercalated disc (white arrows). A total of 6–8 images were captured based on 4 independent tissue slice stainings per individual; representative images are shown. The scale bar represents 50 μ M.

Finally, to exclude the involvement of increased fibrosis formation in these patients, Masson's trichrome stainings were performed (Figure 3). All individuals showed only a mild amount of collagen deposition, suggesting a limited contribution of fibrosis to the enlargement of these pediatric hearts.



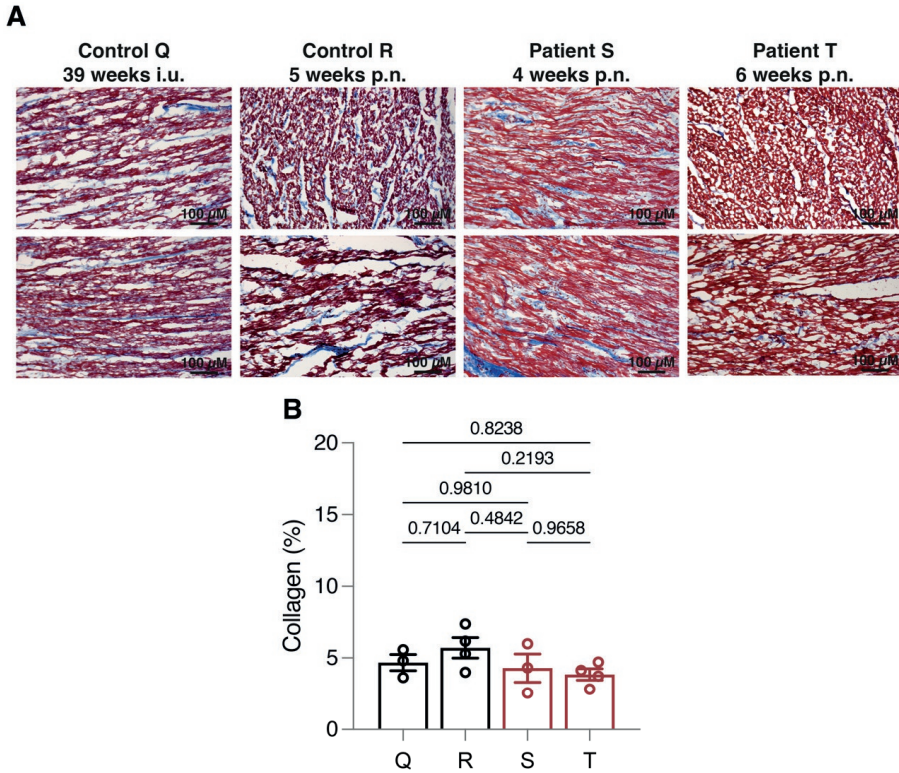


Figure 3. Limited fibrosis formation in pediatric patient tissues. (A) Masson's trichrome staining of myocardial tissues. (B) A quantitative comparison of two pediatric patients (patient S, 4 weeks postnatal; patient T, 6 weeks postnatal) to age-matched (control R, 5 weeks postnatal) and histology-matched (control Q, 39 weeks in utero) controls did not show overt collagen deposition (depicted in blue). A total of 3–4 images were captured based on 2 independent tissue slice stainings per individual; representative images are shown. The scale bar represents 100 μ M.

4. Discussion

During postnatal cardiac maturation, the cardiomyocytes lose the ability to proliferate, and muscle mass is almost entirely increased by hypertrophy of existing cardiomyocytes^{9,11,16}. Simultaneously, the protein network of the ID and the sarcomeres is formed in stages that can be identified by diffuse (unorganized) intracellular protein localization, followed by lateral expression of proteins designated to form the ID, and eventually resulting in the formation of a clear ID at the longitudinal contacts¹⁸.

Interestingly, N-CAD is presumed to be one of the first proteins to be trafficked and anchored at the forming ID, followed by the transportation of other junctional proteins^{17,18}. Furthermore, ion channels and connexins (composing gap junctions) that are also part of the area composite will follow afterwards and are therefore affected in situations of N-CAD mislocalization or absence¹⁹. Also, part of this area composita are catenin proteins, such as JUP (gamma-catenin), α -catenin, and β -catenin, that mainly

anchor the cytoskeleton to the ID thereby providing mechanical strength to the myocardium. Interestingly, both α - and β -catenin are involved in signaling pathways that regulate cardiomyocyte proliferation. Destabilization of the ID proteins can result in aggregation for α -catenin, or in translocation for β -catenin. Loss of α -catenin results in increased YAP protein accumulation in the nucleus, initiating cell proliferation, as seen during inactive Hippo signaling^{16,20}. Similarly, when β -catenin is not sequestered at the area composita due to disturbed N-CAD binding, it translocates into the nucleus as part of the Wnt-signaling pathway, also leading to cell proliferation²¹. While we did not observe clear nuclear β -catenin labeling, protein localization was also disturbed, similarly to JUP and NCAD. In cases of inappropriate N-CAD localization and ID formation, these overlapping mechanisms stimulate cardiomyocyte proliferation, leading to hyperplastic rather than hypertrophic development of the myocardium.

The consequences are weakened cell-to-cell conduction of mechanical force propagation and altered electrical activity patterns in the myocardium. This can directly be translated to increased arrhythmogenicity, as that could result in the occurrence of conduction blocks or premature reactivation during cardiac repolarization, leading to reentry or ectopic activity, respectively. The importance of proper ID formation is accentuated by the incidence of a specific disease named arrhythmogenic cardiomyopathy (ACM), a life-threatening disease that involves variations in genes encoding major desmosomal proteins in more than half of the patient population²². ACM is specifically known for the high occurrence of sudden cardiac death (SCD). Unfortunately, the ACM phenotypes vary between patients and show incomplete penetrance. As proper localization of most of the desmosomal proteins is preceded by proper localization of N-CAD, decreased N-CAD expression could result in a phenotype reminiscent of ACM. This has recently been studied in a subset of ACM patients, showing a comparable variation in *CDH2* (the gene encoding N-CAD) in genotype-negative ACM patients^{23,24}, which has previously also been shown for α -catenin²⁵.

In the presented patient cases, we observed and quantified a vast increase in nuclei counts, as well as increased Ki67-positive nuclei, compared to the age-matched control R. This suggests cardiomyocyte hyperplasia equivalent to control Q tissue at 39 weeks gestation, in which the switch towards physiological hypertrophy has yet to occur. Likely, this shift has not taken place in the patients, resulting in persistent hyperplasia. This manifested in increased heart sizes, which could precipitously be identified as hypertrophy. Simultaneously, the formation of the ID was not comparable to the age-matched control R, but rather to earlier gestation phases, such as control Q, indicating a delayed cardiac development in the patients. The difference between both patients consisted mainly of the seemingly increased expression and localization of N-CAD in patient T. This is at least partially caused by the older age of the patient, as two weeks of cardiac development can include major changes in terms of ID formation¹⁸. Due to N-CAD's



leading role in ID formation and structuring, the area composita of both patients was still immature. Hyperplastic cardiomyocytes lack the properties of well-organized sarcomere structures as seen in mature cardiomyocytes²⁶, consequently suggesting a limiting contractile function of these pediatric hearts. Additionally, fragmented formation of the ID includes dysfunction of ion channels and gap junctions^{7,18}, which could fuel worsened electrical conduction and increase susceptibility to arrhythmias in these patients.

While it is not a certainty that our two patients suffered from cardiac arrhythmias, the aberrancies regarding the proteins involved in mechanical coupling cannot be disregarded. As genetic variations in these proteins are linked to life-threatening symptoms, it would be advisable to monitor related and future family members. With future pediatric sudden death cases demonstrating an enlarged heart similar to our cases, it could be medically worthwhile to conduct more in-depth studies in order to reveal more details about the underlying etiology.

5. Conclusions

In conclusion, we described two cases in which pediatric patients died within the first 6 weeks after birth. The direct cause of asphyxia remains unclear in these patients, although tissue analysis dictates a leading role for the underdeveloped heart. While the morphological adaptation of the hearts is not comparable with that of ACM patients, potentially due to the very early onset of molecular remodeling, the overlap between alterations of the underlying ID protein mechanics in ACM and those in these patients remains striking.

References

1. Vermij SH, Abriel H, van Veen TA. Refining the molecular organization of the cardiac intercalated disc. *Cardiovasc Res*. 2017;113(3):259-275.
2. Tan CMJ, Lewandowski AJ. The Transitional Heart: From Early Embryonic and Fetal Development to Neonatal Life. *Fetal Diagn Ther*. 2020;47(5):373-386.
3. Piven OO, Kostetskii IE, Macewicz LL, Kolomiets YM, Radice GL, Lukash LL. Requirement for N-cadherin-catenin complex in heart development. *Exp Biol Med (Maywood)*. 2011;236(7):816-822.
4. Radice GL, Rayburn H, Matsunami H, Knudsen KA, Takeichi M, Hynes RO. Developmental defects in mouse embryos lacking N-cadherin. *Dev Biol*. 1997;181(1):64-78.
5. Kessler EL, Nikkels PG, van Veen TA. Disturbed Desmoglein-2 in the intercalated disc of pediatric patients with dilated cardiomyopathy. *Hum Pathol*. 2017;67:101-108.
6. Peters NS, Severs NJ, Rothery SM, Lincoln C, Yacoub MH, Green CR. Spatiotemporal relation between gap junctions and fascia adherens junctions during postnatal development of human ventricular myocardium. *Circulation*. 1994;90(2):713-725.
7. Noorman M, Hakim S, Kessler E, et al. Remodeling of the cardiac sodium channel, connexin43, and plakoglobin at the intercalated disk in patients with arrhythmogenic cardiomyopathy. *Heart Rhythm*. 2013;10(3):412-419.
8. Nielsen MS, van Opbergen CJM, van Veen TAB, Delmar M. The intercalated disc: a unique organelle for electromechanical synchrony in cardiomyocytes. *Physiol Rev*. 2023;103(3):2271-2319.
9. Leone M, Magadum A, Engel FB. Cardiomyocyte proliferation in cardiac development and regeneration: a guide to methodologies and interpretations. *Am J Physiol Heart Circ Physiol*. 2015;309(8):H1237-1250.
10. Mollova M, Bersell K, Walsh S, et al. Cardiomyocyte proliferation contributes to heart growth in young humans. *Proc Natl Acad Sci U S A*. 2013;110(4):1446-1451.
11. Bergmann O, Zdunek S, Felker A, et al. Dynamics of Cell Generation and Turnover in the Human Heart. *Cell*. 2015;161(7):1566-1575.
12. Swift SK, Purdy AL, Kolell ME, et al. Cardiomyocyte ploidy is dynamic during postnatal development and varies across genetic backgrounds. *Development*. 2023;150(7):dev201318.
13. Gilsbach R, Schwaderer M, Preissl S, et al. Distinct epigenetic programs regulate cardiac myocyte development and disease in the human heart in vivo. *Nat Commun*. 2018;9(1):391.
14. Velayutham N, Alfieri CM, Agnew EJ, et al. Cardiomyocyte cell cycling, maturation, and growth by multinucleation in postnatal swine. *J Mol Cell Cardiol*. 2020;146:95-108.
15. Sun X, Kaufman PD. Ki-67: more than a proliferation marker. *Chromosoma*. 2018;127(2):175-186.
16. Gunthel M, Barnett P, Christoffels VM. Development, Proliferation, and Growth of the Mammalian Heart. *Mol Ther*. 2018;26(7):1599-1609.
17. Linask KK, Knudsen KA, Gui YH. N-cadherin-catenin interaction: necessary component of cardiac cell compartmentalization during early vertebrate heart development. *Dev Biol*. 1997;185(2):148-164.



18. Vreeker A, van Stuijvenberg L, Hund TJ, Mohler PJ, Nikkels PG, van Veen TA. Assembly of the cardiac intercalated disk during pre- and postnatal development of the human heart. *PLoS One*. 2014;9(4):e94722.
19. Vite A, Radice GL. N-cadherin/catenin complex as a master regulator of intercalated disc function. *Cell Commun Adhes*. 2014;21(3):169-179.
20. Vite A, Zhang C, Yi R, Emms S, Radice GL. alpha-Catenin-dependent cytoskeletal tension controls Yap activity in the heart. *Development*. 2018;145(5):dev149823.
21. Fan Y, Ho BX, Pang JKS, et al. Wnt/beta-catenin-mediated signaling re-activates proliferation of matured cardiomyocytes. *Stem Cell Res Ther*. 2018;9(1):338.
22. Van der Voorn SM, Te Riele A, Basso C, Calkins H, Remme CA, van Veen TAB. Arrhythmogenic cardiomyopathy: pathogenesis, pro-arrhythmic remodelling, and novel approaches for risk stratification and therapy. *Cardiovasc Res*. 2020;116(9):1571-1584.
23. Ghidoni A, Elliott PM, Syrris P, et al. Cadherin 2-Related Arrhythmogenic Cardiomyopathy: Prevalence and Clinical Features. *Circ Genom Precis Med*. 2021;14(2):e003097.
24. Mayosi BM, Fish M, Shaboodien G, et al. Identification of Cadherin 2 (CDH2) Mutations in Arrhythmogenic Right Ventricular Cardiomyopathy. *Circ Cardiovasc Genet*. 2017;10(2):e001605.
25. Van Hengel J, Calore M, Bauce B, et al. Mutations in the area composita protein alphaT-catenin are associated with arrhythmogenic right ventricular cardiomyopathy. *Eur Heart J*. 2013;34(3):201-210.
26. Schaub MC, Hefli MA, Zuellig RA, Morano I. Modulation of contractility in human cardiac hypertrophy by myosin essential light chain isoforms. *Cardiovasc Res*. 1998;37(2):381-404.

Supplementary Material

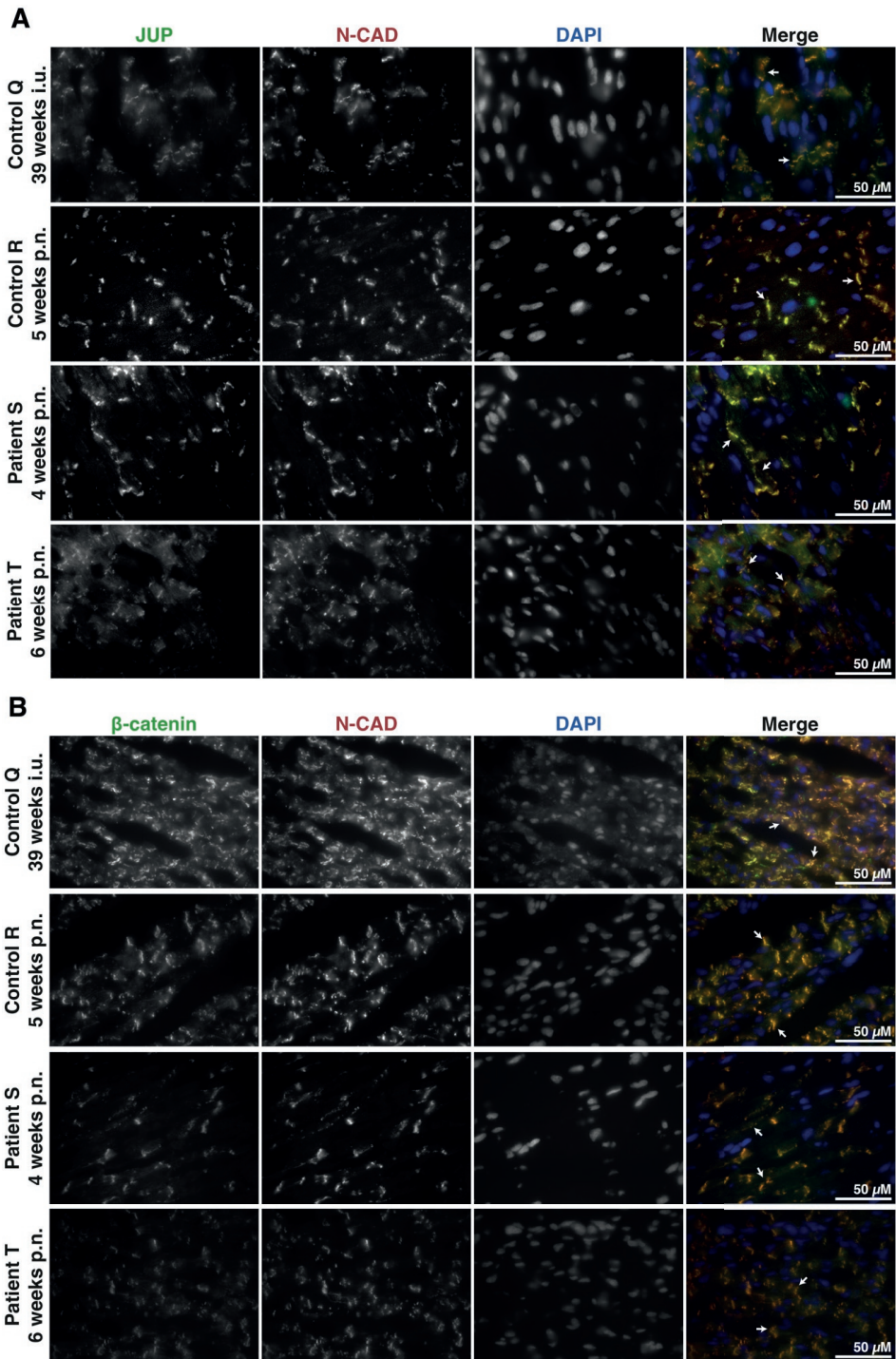


Figure S1. Immature intercalated disc maturation in pediatric tissues. Immunohistochemical labeling of N-cadherin (N-CAD) and nuclei (DAPI) in combination with either plakoglobin (JUP, **A**) or β -catenin (**B**), at 60x. Intercalated disc proteins JUP and β -catenin are expressed in similar patterns as N-CAD. The two pediatric patients (patient S, 4 weeks postnatal; patient T, 6 weeks postnatal) when compared to age-matched (control R, 5 weeks postnatal) and histology-matched (control Q, 39 weeks in utero) controls showed increased diffuse and lateral expression of the intercalated disc, alongside several completely formed intercalated discs (white arrows). Four images were captured based on four independent tissue slice stainings per individual; representative images are shown. The scale bar represents 50 μ M.



Willem B. van Ham¹

Esmeralda E.M. Meijboom¹

Merel L. Ligtermoet¹

Jantine Monshouwer-Kloots²

Anneline S.J.M. te Riele^{3,#}

Folkert W. Asselbergs^{3,4}

Eva van Rooij²

Mimount Bourfiss^{3,*}

Toon A.B. van Veen^{1,*}

¹Department of Medical Physiology, University Medical Center Utrecht, The Netherlands

²Hubrecht Institute, KNAW, and University Medical Center Utrecht, The Netherlands

³Department of Cardiology, University Medical Center Utrecht, The Netherlands

⁴Department of Cardiology, Amsterdam University Medical Center, The Netherlands

[#]Member of the European Reference Network for rare, low prevalence and complex diseases of the heart: ERN GUARD-Heart (ERN GUARD HEART; <http://guardheart.ern-net.eu>)

*Mimount Bourfiss and Toon A.B. van Veen are shared senior authors

Chapter V

**An hiPSC-CM approach for
electrophysiological
phenotyping of a patient-specific
case of short-coupled TdP**

In preparation

Abstract

A healthy young woman, age 26 without prior cardiac complications, experienced an out-of-hospital cardiac arrest caused by ventricular fibrillation (VF), which coincided with a fever. Comprehensive diagnostics including echo, MRI, exercise testing, and genetic sequencing, did not identify any potential cause. This led to the diagnosis of idiopathic VF and installment of an implantable cardioverter defibrillator, which six months later appropriately intervened another VF episode under conditions comparable to the first event. A second diagnostic opinion concluded short-coupled Torsade de Pointes (scTdP), and the patient was started on a verapamil treatment. Human induced pluripotent stem cell cardiomyocyte (hiPSC-CM) lines were generated to study cellular electrophysiology. Without a known genetic variation, no isogenic control line could be produced, therefore an age- and sex-matched control hiPSC-CM line was used. Additionally, hiPSC-CMs of the sister were generated from blood that was isolated at the same age as the patient. Cellular electrophysiology was studied in these cardiomyocytes using calcium- and voltage sensitive fluorescent dyes and measurements were carried out at 37 and 39 degrees, to mimic the condition of hyperthermia in the patient. Calcium transients measured in both patient and sister lines at a physiological temperature indicated the occurrence of early after transients (EATs). Strikingly, at 39 degrees the incidence of EATs further increased. These EATs suggest the premature release of calcium during diastole, which could be responsible for the extrasystoles in the patient. Membrane potential data from the patient also revealed shorter action potentials that, combined with the EATs, indicate the premature release of calcium during diastole, which could be responsible for the extrasystoles in the patient. Gene expression profiles did not differ between the patient and sister, and could not aid in unraveling a mechanism behind the occurrence of EATs. Pharmacological screening was performed to evaluate the treatment regimen and to determine a mechanisms of action of EATs. While both verapamil and dantrolene did not decrease the incidence of EATs, calcium handling parameters were affected indicating functionality of the drugs. This patient-specific case of electrophysiological phenotyping resulted in a hypothesis of the possible mechanism behind the scTdP arrhythmias, but also accentuates the applicability of patient-specific hiPSC-CM disease modeling and phenotyping.

Keywords: short-coupled Torsade de Pointes; hiPSC-CM; patient-specific; phenotyping; calcium handling dysfunction

1. Introduction

The complete list of inherited cardiomyopathies and cardiac channelopathies is comprised of a considerable number of cardiac diseases with various genetic predisposition, disease progression, and clinical presentation¹⁻⁴. These diseases are often introduced due to genetic variations, including complex variations like compound and digenic heterozygosity⁵. However, a primary clinical phenotype can also be present in patients without (or unknown) genetic predisposition, or patients can carry gene variations without developing symptoms due to incomplete penetrance or variable expressivity^{6,7}. Unfortunately, the most common and often first symptom in arrhythmogenic forms of cardiomyopathy is sudden cardiac death (SCD), caused by severe cardiac arrhythmias. The unlimited use of human induced pluripotent stem cell derived cardiomyocytes (hiPSC-CMs) has facilitated numerous possibilities for physiological studies, disease phenotyping, and pharmacological safety screenings. Additionally, it might help to identify relatives at risk⁸. Studying alternate gene variations in hiPSC-CM models can aid in understanding not only the mechanistic involvement of these genes in a disease, but it also provides a method to predict potential clinical presentations based on experimental phenotypes.

At the basis of cardiac arrhythmias stands the formation of the cardiac action potential (AP) and calcium handling within the cardiomyocytes⁹. Conduction of the AP across the myocardium activates the cardiomyocytes in a synchronized manner, followed by the calcium release from the sarcoplasmic reticulum (SR) within the individual cells, which then results in the contraction of the myocardial tissue¹⁰. Any of these processes can be disrupted by decreased or increased function of the proteins involved. Pharmacological interventions can be applied to modulate the effects of disturbed ion transport, by blocking, altering kinetics, or activating different ion channels and transporters.

In this study we included a 26 year-old female patient without prior cardiac or related family history, who suffered from out of hospital sudden cardiac arrest due to ventricular fibrillation (VF) while she was having a fever. Extensive clinical diagnostics, including cardiac echo and MRI, genetic sequencing, and exercise testing, did not identify a cause for the VF. The ectopy originated from the lower left septal segment and was suggested to be Purkinje fiber related. Given the fact that no extensive electrophysiological testing has been performed this could however not be confirmed after which she was diagnosed with short-coupled Torsade de Pointes (sTdp). An implanted cardioverter defibrillator (ICD) was installed, which several months later had to intervene another VF again during a second period of hyperthermia. The patient was instrumented on verapamil. Blood was taken from the patient and hiPSC-CMs were produced. In the absence of a genetic variation, a healthy age- and sex-matched donor was used as a control. In addition, and in an identical fashion, hiPSC-CMs were generated from the patient's sister, who at the time of blood withdrawal was the same age as the patient during her first event. The sister also had no cardiac complications and therefore no extensive diagnostic screening has been performed.

We investigated the experimental electrophysiological phenotype of the hiPSC-CMs of the three individuals, in an attempt to discover a potential mechanism for the VF occurrence in the patient. We were able to identify a potential calcium handling disturbance, which was even worsened by a hyperthermic condition, both in the patient and to a minor extent in her sister.

2. Methods

2.1. Drugs

Dantrolene (Sigma-Aldrich, D9175) was dissolved in DMSO to 10 mM, filtered, and stored at -20 °C. Verapamil (Centrafarm) was diluted at 2.5 mg/mL HCl and stored at room temperature. Drugs were added to the culture medium for 24 hours prior to experiments, DMSO was used for vehicle measurements.

2.2. Generation of human hiPSC clones

hiPSC lines were generated from isolated peripheral blood mononuclear cells derived from the patient, the sister, and a healthy age- and sex-matched control at the Leiden University Medical Center hiPSC core facility. Three independent clones were produced for the patient and the sister, and one clone for the healthy individual. Clones were obtained frozen in liquid nitrogen.

2.3. Bulk karyo-sequencing

Approximately 1000 hiPSCs were collected as pellet to which 5 µl of 2 µg Proteinase K (NEB) in 1x CutSmart Buffer (NEB) was added for 2 hours at 55 °C followed by 10 minutes at 80 °C. DNA was digested using 10 µl of 10 U NlaIII (NEB) in 1x CutSmart Buffer for 2 hours at 37 °C followed by 20 minutes at 80 °C. DNA fragments were ligated to adapters by adding 20 µl of 800 U T4 DNA ligase (NEB), 1 mM ATP (ThermoFisher) and 50 nM adapter in 1x T4 DNA ligase buffer (NEB) and incubating at 16 °C overnight. The library preparation, sequencing and analysis was performed as described previously¹¹.

2.4. Cell culture

hiPSCs were cultured on Geltrex™-coated wells (Gibco, A1413302). Cells were refreshed daily with Essential 8™ Medium (Gibco, A1517001), and passaged once they reached 80-100% confluency. Briefly, medium was aspirated and TrypLE Express Enzyme (Gibco, 12605010) was added for 5 minutes at 37 °C. After incubation, 4 mL of Essential 8™ Medium, supplemented with 1 µM thiazovivin (Sigma-Aldrich, 420220), was added to the dissociated cells and the cell suspension was transferred to a 15 mL Falcon tube. Cells were centrifuged at 300 RCF for 3 minutes. Subsequently, cells were seeded at a density of 15,000 cells/cm² in Essential 8™ Medium, supplemented with 1 µM thiazovivin. Medium was refreshed the next day with plain Essential 8™.

2.5. Cardiomyocyte differentiation

hiPSCs were grown until 80-90% confluency and washed once with dPBS (Gibco, 14190094). Cells were then cultured with RPMI++ (bare RPMI-1640-Medium-GlutaMAX™ Supplement-HEPES (Gibco, 72400-021) supplemented with 0.5 mg/mL human recombinant albumin (Sigma-Aldrich, A9731) and 0.2 mg/mL L-Ascorbic Acid 2-Phosphate (Sigma, A8960)), added with 4 μM CHIR99021 (Sigma, 361559). After 48 hours, medium was replaced with RPMI++ added with 5 μM IWP2 (Sigma, 681671), following a single rinse with bare RPMI-1640. Cells were then refreshed every other day with RPMI++, for four days. From there, cells were cultured every three to four days with complete RPMI medium (bare RPMI-1640, supplemented with B-27™ Supplement (Gibco, 17504001)). Prior to optical experiments, the hiPSC-CMs were dissociated with TrypLE Select Enzyme without phenol red (Gibco, A1217703) and seeded on Geltrex™-coated coverslips. Three to four independent differentiations were produced of each hiPSC line.

2.6. Optical electrophysiology

hiPSC-CMs were seeded at a density of 150.000 cells per Geltrex™-coated coverslip to allow formation of monolayered clusters. Coverslips were incubated with either Powerload and FluoVolt (ThermoFisher, F10488, 1:1000) or Fluo-4-AM (ThermoFisher, F14201, 1:1000) in complete RPMI medium for 20 minutes at 37 °C. Clusters were recorded at 37 °C and 39 °C (the latter to mimic fever) during which the coverslips were placed in a bath solution containing (mM): NaCl (130), KCl (4), CaCl₂ (1.8), MgCl₂ (1.2), NaHCO₃ (18), HEPES (10), Glucose (10), with pH 7.4. Fluorescent signals were recorded using a custom-built microscope (Cairn Research, UK) using a 10x objective. Blue light was filtered using an excitation filter (482/35 nm), and projected on the objective with a dichroic mirror (515 nm). Fluorescent signals were captured, via a long-pass emission filter (514 nm), by a high-speed camera (Andor Zula 5.5.CL3). Analysis of the data was performed using Fiji and Peaks, a custom-written Matlab script (DOI: 10.17605/OSF.IO/86UFE). Analyzed signals of the spontaneously beating hiPSC-CMs were then adjusted for beating rate using a modified Fredericia's correction: $APD_{corrected} = APD / \sqrt[3]{(60/BPM)}$.

2.7. Quantitative PCR

Total RNA was isolated from hiPSC-derived cardiomyocytes using the RNeasy Mini Kit (Qiagen, 74104) following the protocol supplied by the manufacturer. Total RNA was reverse transcribed using the iScript™ cDNA Synthesis Kit (Bio Rad, 1708891). Quantitative PCR (qPCR) reactions were performed on a Bio Rad CFX96 Real-Time PCR Detection System using the iQ SYBR Green Supermix kit (Bio Rad, 170-8885). Primers used for amplification can be found in **Table S1**. The $2^{-\Delta\Delta CT}$ method was used to analyze the data.

2.8. Statistical analysis

All statistical analysis was executed using GraphPad Prism v.9 software. Comparisons were analyzed using a Student's T-test (action potential data), One-Way ANOVA, with Tukey's post-hoc test to correct for multiple comparisons (mRNA expression data) or Two-Way ANOVA, with Tukey's post-hoc test to correct for multiple comparisons (calcium handling data). Data is shown as individual datapoints.

3. Results

3.1. Electrophysiological disturbances

In order to uncover a potential cause for the ventricular arrhythmias experienced by the patient, hiPSCs were generated from the patient, her sister, and an age- and sex-matched healthy control. hiPSC characterization and karyotyping data are shown in **Figure S1, S2**. Optical screening of calcium transients (CaTs) was performed using a fluorescent calcium sensitive dye, which resides in the cytosol. Release of SR calcium via the ryanodine receptor (RyR2) and removal via mainly the sarco-endoplasmic reticulum calcium ATPase (SERCA2A) and the sodium-calcium exchanger (NCX1) are represented in recordings as peak up- and downstrokes, respectively. In both the patient and the sister initial calcium releases were followed by additional releases, which were defined as early after transients (EATs) (**Figure 1A**). Under normothermic conditions, these EATs were observed in 8.14% and 4.31% of the measurements in the patient and sister respectively, compared to 0% in the healthy control cells (**Figure 1B**). The occurrence of these EATs was even further increased during hyperthermia, resulting in 17.99% and 8.33% in the patient and sister respectively, compared to 2.94% in the healthy control.

Interestingly, the single EAT in the control line that was observed in only one CaT during the recording displayed an amplitude that was smaller than the initial calcium release. However, the recorded EATs originating from the patient and sister lines mainly occurred in every CaT of those recordings, while also having amplitudes that matched the original released ones (**Figure S3**).

Morphology of CaTs were analyzed to quantify release and removal times of cytosolic calcium in these measurements (**Figure 2A**). An increased number of calcium releases, as well as increased amplitudes were detected in both the patient and sister, without displaying a prolonged release time (**Figure 2B-2D**). While cytosolic removal was not lengthened, overall CaT duration was increased for both patient and control (**Figure 2E, 2F**). This was mainly driven by extreme CaT durations corresponding to EAT measurements.

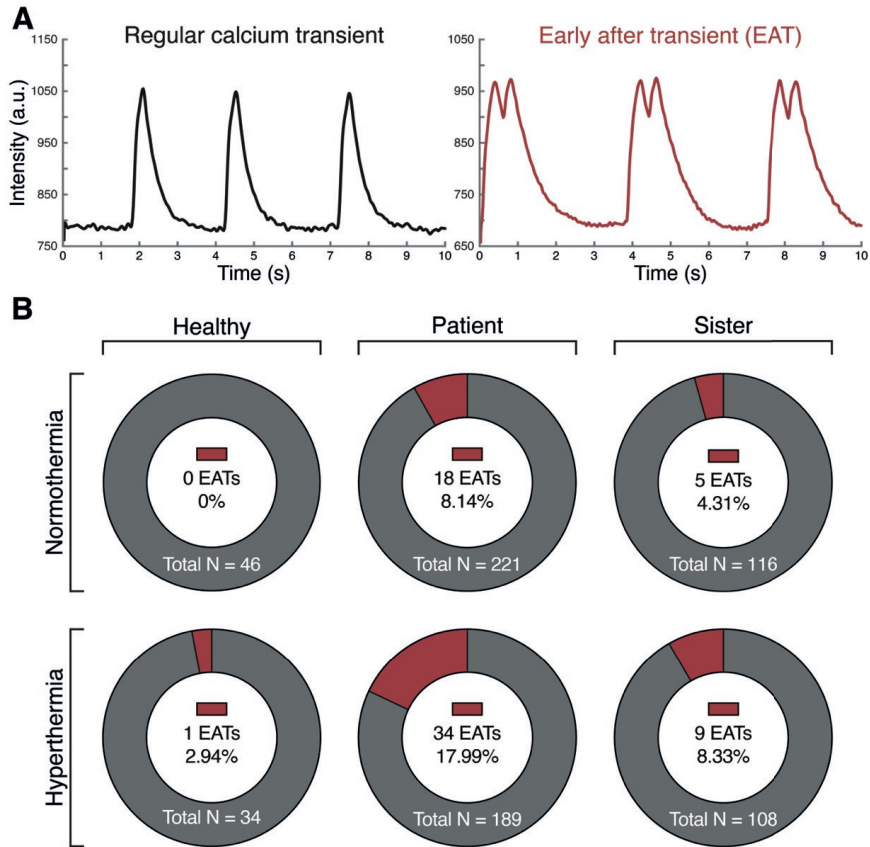


Figure 1. Occurrence of early after transients in patient and sister hiPSC-CMs. Calcium transient measurements were performed in hiPSC-CMs from the patient, sister, and a healthy control during normo- and hyperthermia. **(A)** During measurements of hiPSC-CMs of the patient and sister extra calcium releases, termed early after transients (EATs), were observed during normo- and hyperthermia. **(B)** Quantification of the EATs highlighted the increased occurrence in the patient and sister, especially after hyperthermia. n=number of measured cell clusters, originating from one clone (control) and 3 clones (patient and sister) each with 3-4 hiPSC-CM differentiations.

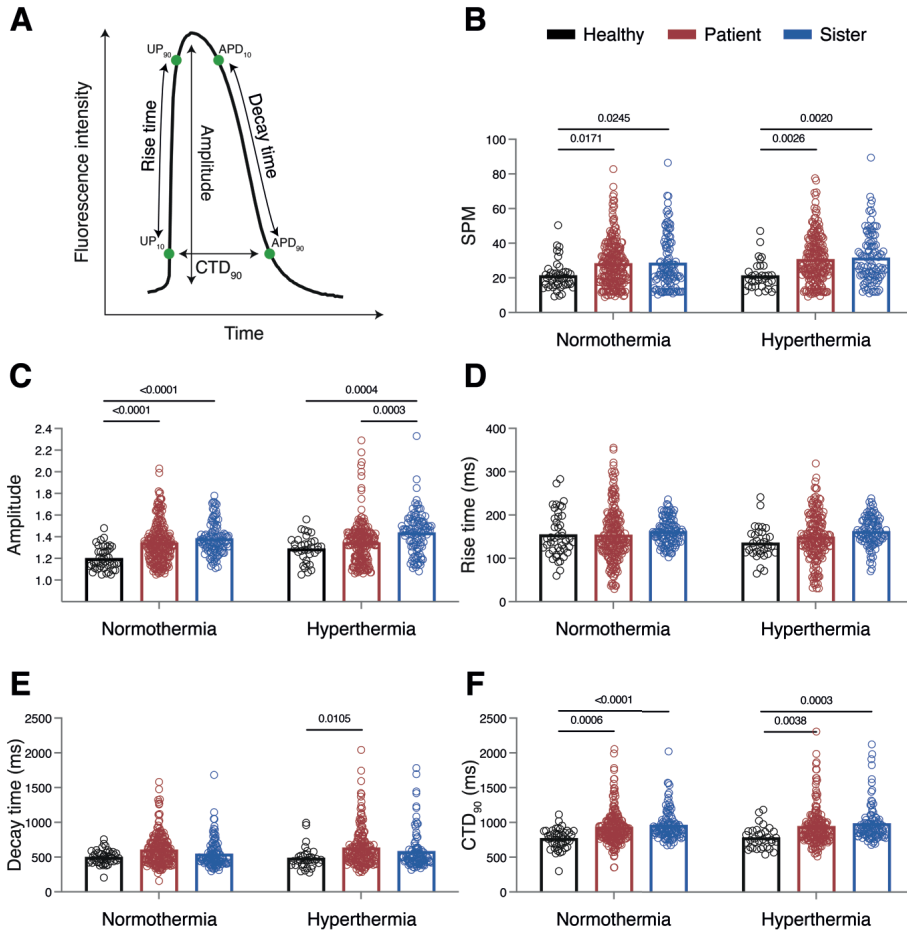


Figure 2. Calcium transient parameters indicating disturbed calcium handling. Calcium transient measurements were performed in hiPSC-CMs from the patient (red), sister (blue), and a healthy control (black) during normo- and hyperthermia. **(A)** Definitions of parameters based on 10% and 90% of the up- and downstroke of the fluorescence intensity. **(B)** Number of signal per minute (SPM). **(C)** Amplitude of the initial calcium release. **(D)** Rise time of the calcium signal, representing the release of calcium into the cytosol. **(E)** Decay time of the calcium signal, representing the removal of calcium from the cytosol. **(F)** 90% of the calcium transient duration (CTD), representing the duration of the entire calcium transient. $n=34$ -221 measured cell clusters, originating from one clone (control) and 3 clones (patient and sister) each with 3-4 hiPSC-CM differentiations.

In the control and patient lines, action potential duration (APD) was also measured using a voltage-sensitive dye, with the depolarization and repolarization as peak up- and downstrokes, respectively (**Figure 3A**). While the spontaneous beating rates were similar for the patient when compared to the CaT measurements, the beating rate for the control cells was also comparable in those APD measurements (**Figure 3B**). Interestingly, action potential repolarization was shorter in the patient (**Figure 3C, 3D**).

Together, these data suggest electrophysiological disturbances that could underly the clinical phenotype of the patient, while also indicating a potential issue for the sister, since both showed an aggravation of the disturbed calcium handling by a hyperthermic condition.

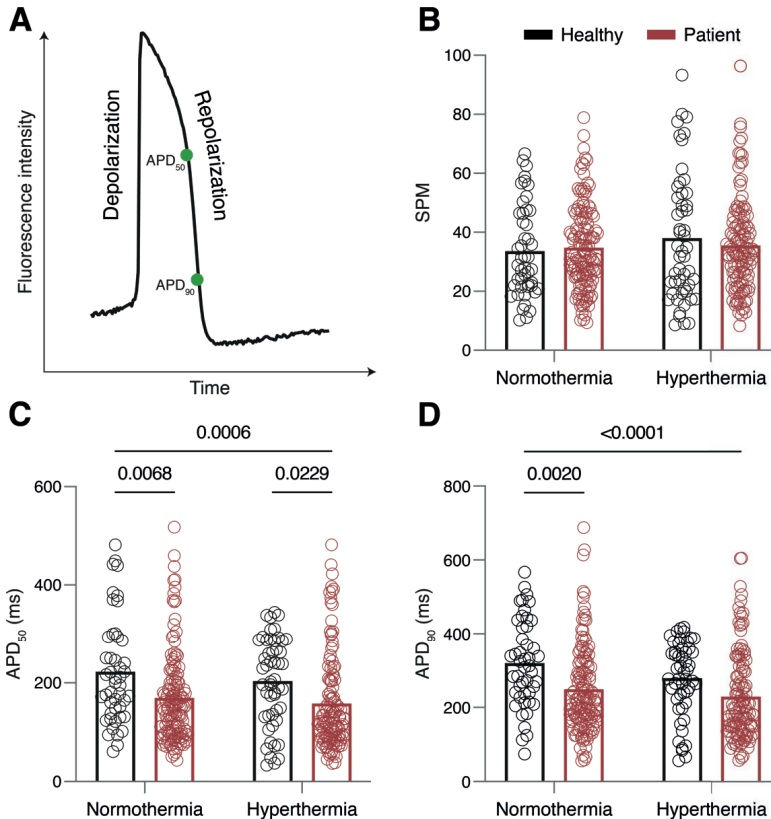


Figure 3. Shortened action potentials in patient hiPSC-CMs. Action potential measurements were performed in hiPSC-CMs from the patient (red) and a healthy control (black) during normo- and hyperthermia. (A) Definitions of parameters based on 50% and 90% of the downstroke of the fluorescence intensity. (B) Number of signal per minute (SPM). (C) 50% of the action potential duration (APD), representing early repolarization. (D) 90% of the APD, representing total repolarization. $n=47-135$ measured cell clusters, originating from one clone (control) and 3 clones (patient and sister) each with 3-4 hiPSC-CM differentiations.

3.2. Gene expression profile

While no genetic variations were identified in the patient, studying gene expression could aid in identifying a cause for the occurrence of EATs in both the patient and sister. Therefore, mRNA expression of electrophysiologically relevant genes was quantified in multiple clones and differentiations of the three individuals (Figure S4). Only calsequestrin (*CASQ2*) was upregulated in the sister, while *NCX1* and the

sodium channel (*SCN5A*) were downregulated in the patient, and the repolarization potassium channel (*KCNH2*) were downregulated in both patient and sister. *KCNJ2* mRNA expression was also low in both sisters but is known to be close to absent as generally reported in all hiPSC-CMs¹². Overall, both the patient and sister did not show alternate expression profiles, that could explain the electrophysiological phenotype.

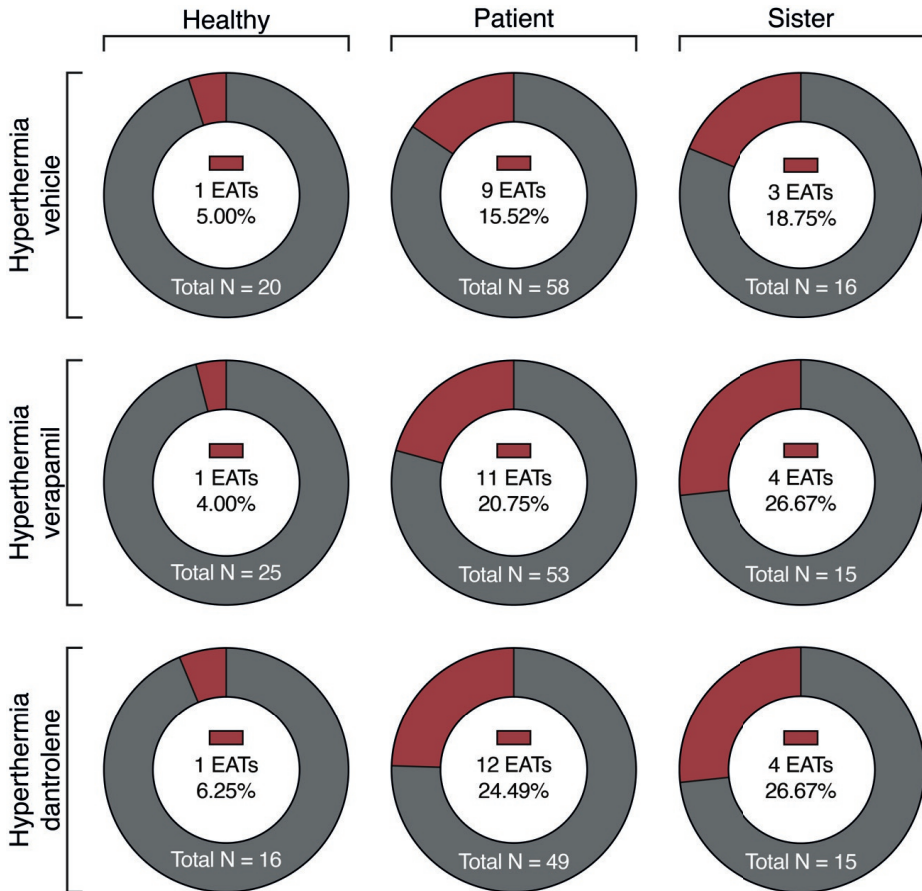


Figure 4. Occurrence of early after transients after pharmacological intervention. Calcium transient measurements were performed in hiPSC-CMs from the patient, sister, and a healthy control during hyperthermia after 24 hour incubation with either verapamil, dantrolene, or a vehicle. Compared to the prior experiment, the occurrence of early after transients (EATs) after drug administration did not alter in the vehicle group, while the patient and sister cells had a similar or increased percentage of EATs. n=number of measured cell clusters, originating from one clone (control) and 3 clones (patient and sister) each with 3-4 hiPSC-CM differentiations.

3.3. Hampered pharmacological screening

To investigate the effects of several drugs on the mechanisms behind the observed and aberrant EATs, cells from the three individuals were incubated with verapamil (a L-type calcium channel blocker) and dantrolene (a RyR2 blocker) for 24 hours. CaTs were measured under hyperthermic conditions and the occurrence of EATs was quantified. While only 1 EAT was observed in all control conditions (4-6.25%), the number of EATs in both patient and sister increased compared to the previous and baseline experiments (**Figure 4**). This indicates an even further disruption of the calcium kinetics in the hiPSC-CMs of specifically the patient and sister.

Quantification of the CaTs partly supported the effects of verapamil and dantrolene. Although the number of calcium signals and amplitude did not differ between control, patient, and sister cells, they seemed to be lower for the patient and sister when compared to the initial set of experiments (**Figure 5A, 5B**). However, release time was increased after verapamil administration in the patient, but otherwise similar or even shortened compared to previous measurements (**Figure 5C**). The CaT length was only influenced by dantrolene, which resulted mainly from those measurements that displayed extreme EATs (**Figure 5D, 5E**). Additionally, while dantrolene was not able to decrease the occurrence of EATs, amplitude of EATs seemed to be diminished in a majority of the measurements (**Figure S5**). All combined, the applied pharmacological screening did not result in improved calcium regulation, but in contrast even worsened the situation of disturbed calcium handling.

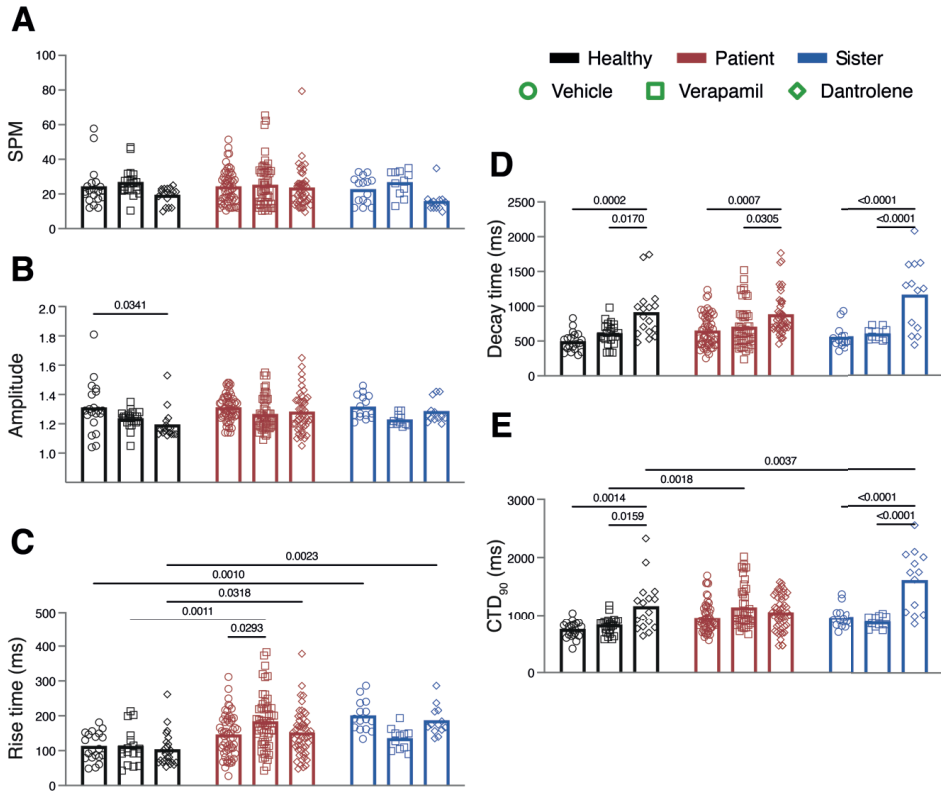


Figure 5. Calcium transient parameters after drug administration. Calcium transient measurements were performed in hiPSC-CMs from the patient (red), sister (blue), and a healthy control (black) during hyperthermia after 24 hour incubation with either verapamil, dantrolene, or a vehicle. (A) Number of signal per minute (SPM). (B) Amplitude of the initial calcium release. (C) Rise time of the calcium signal, representing the release of calcium into the cytosol. (D) Decay time of the calcium signal, representing the removal of calcium from the cytosol. (E) Calcium transient duration at 90% (CTD₉₀), representing the duration of 90% of the entire calcium transient. n=15-58 measured cell clusters, originating from one clone (control) and 3 clones (patient and sister) each with 3-4 hiPSC-CM differentiations.

4. Discussion

In this study, we generated hiPSC-CMs from a patient who suffered from out of hospital sudden cardiac arrest due to ventricular arrhythmias without a known cause. Additional cell lines were produced for the patient's sister, as well as a healthy age- and sex-matched control. Upon evaluating calcium handling in all hiPSC-CM lines, we found a striking occurrence of premature calcium releases, EATs, in both the patient and sister, which robustly increased under hyperthermic conditions. Further analysis of action potentials in the patient indicated a shortened APD, again in both normo- and hyperthermia. In general, mRNA expression was not different between the patient and sister, and did not clearly elucidate a mechanism

behind the EAT occurrence. We then performed a pharmacological screening to further study the pro-arrhythmic mechanism initiating the EATs, as well as to evaluate the effect of the current clinical treatment in the patient. Drug regimen was focused on controlling extracellular calcium load via the L-type calcium channel (by application of verapamil) and SR-calcium release (dantrolene). In contrast to what was expected, neither verapamil nor dantrolene ameliorated the incidence of EATs and even deteriorated the disturbed calcium handling, although it did seem to affect the calcium handling in terms of decreased amplitude and slowed CaT duration. In contrast, treatment of the control cells with those drugs did not worsen outcome. This study highlights the potential of patient-specific application and disease phenotyping using hiPSC-CMs.

4.1. Short-coupled Torsade de Pointes

As extra calcium is being released from the SR (EATs) without being triggered by a new AP, which can occur when the cardiac membrane potential is either still depolarized or completely repolarized, it can cause early or delayed after depolarizations (EADs and DADs), respectively¹³. These EADs and DADs are prematurely triggered action potentials, and in case that SR-calcium release is involved, are caused by increasing inward sodium current via the NCX1 in return for an outward calcium flux^{14,15}. In the experimental data from our patient, both APD shortening and EATs are observed, creating the ideal circumstance for DAD formation, which could result in triggered activity in the form of premature ventricular complexes (PVCs) and VF^{16,17}. However, it is important to note that the electrophysiological immaturity of hiPSC-CMs is mainly noticeable in the shorter AP, which could mean that the EATs observed in our study, might result in either EADs or DADs. Within our AP measurements we did not observe any DAD-like peaks; however, within spontaneously active hiPSC-CMs it is difficult to determine which signals are DAD-triggered action potentials.

Both EADs and DADs have been hypothesized as cause for the development of scTdP, although EADs are thought to be more likely, as patients often have normal QT intervals and PVC prior to the TdP is short coupled, which requires an early triggered AP¹⁸⁻²⁰. The PVCs present prior to scTdP in patients often originate from the Purkinje fiber network, which are especially likely to result in VF^{19,21}. As this seems to be the case in our patient, the experienced VF episodes developed are with a high degree of plausibility caused by early membrane depolarizations due to triggered extra calcium release from the SR. The use of verapamil has been shown to be effective in decreasing TdP occurrence, while not reducing the risk of SCD, leaving ICD implantation as advisable treatment^{18,20,22,23}. We also observed identical calcium disturbances in the sister, while she is currently clinically not under any consideration. Whether the hyperthermia in the patient has acted as a secondary trigger, which has been absent in the sister, or another secondary hit has yet to be identified remains elusive.

4.2. Pharmacological screening in diseased hiPSC-CMs

The pharmacological intervention, using verapamil en dantrolene, did not decrease the occurrence of EATs in either the patient or sister lines. While to a certain extend these drugs did show to be effective, both have limitations in term of preventing EATs. Verapamil is a L-type calcium channel blocker that can inhibit or delay calcium-induced calcium release (CICR), by lowering the calcium availability in the dyad between T-tubules and the SR. Blocking this channel would then prevent extra CICR-triggered releases in mature cardiomyocytes. However, hiPSC-CMs remain rather immature and are lacking the formation of T-tubules^{24,25}. This could potentially imply that the role of dyad calcium is dominated by general cytosolic calcium, obstructing the prevention of EATs by verapamil in hiPSC-CMS. Dantrolene is a RyR1 (present in skeletal muscle) blocker, used for treating muscular spasticity and malignant hyperthermia²⁶. However, it has been shown that dantrolene can also block RyR2 (the isoform primarily present in the heart)²⁷, and has proven to be effective in hiPSC-CM models of pathogenic *RYR2* variants^{28,29}. The binding of dantrolene to RyR2 is rather specific, where it is proposed to bind only the unzipped state of the protein in which the channel has an increased open probability, often caused by genetic variations³⁰. This would suggest that if dantrolene was effective in completely blocking the EATs, there would be a mechanistic link with RyR2 such as a genetic variation or chemical interaction. We observed only a decrease in EAT amplitude and not their occurrence. Moreover, we carefully checked the sequence of the *RYR2* gene in the patient but did not find any aberrancies. This could explain the only mild effect of dantrolene being merely based on incomplete blockade. In line with the sequence analysis of *RYR2*, we also cross-checked the sequence of *DPP6*, a gene involved in regulation of the transient outward potassium current in Purkinje fibers. This because overactivity of this gene due to genetic variations has been associated with the occurrence of VF originating from the Purkinje^{31,32}.

Performing drugs safety and application screenings in hiPSC-CMs, especially in engineered tissues, has for some drugs been shown to be effective and comparable to expected clinical outcome in both healthy and diseased cells^{33,34}. Unfortunately, the drug interventions in this study stresses the difficulties in testing therapeutic options in diseased hiPSC-CMs when there is no known or suggested cause of the disease. Not only is it difficult to evaluate which class of drugs could be relevant, our data also shows that intervening with indistinct calcium disturbances could exacerbate the phenotype. Further understanding of molecular pathogenesis or genetic involvement remains a prerequisite before assessment of patient-specific treatment option can be considered. In line with that, for an appropriate comparison with the calcium handling machinery is adult cardiomyocytes, It Is of utmost Importance that this aspects needs additional maturation In hiPSC-CM.

4.3. Clinical translationability of experimental hiPSC-CM phenotyping

Patient-specific disease phenotyping has become increasingly better and easier with the use and improvements of hiPSC-CMs. They can be widely implemented to investigate molecular and functional consequences of novel pathogenic variants and inherited cardiomyopathies³⁵⁻³⁹. The majority of the experimental studies are performed to associate a genetic predisposition to a general clinical phenotype in a patient population. However, this instigates the discussion on the role of experimental phenotyping of pathological electrophysiology in the absence of a genetic variation. In our case, we have identified an experimental phenotype in the patient reminiscent of the observed clinical presentation, but have additionally detected a similar electrophysiological disturbance in the sister, who has no clinical complications. The translationability of this disease model can partly be hampered by the mentioned immaturity of the hiPSC-CMs or technical limitations such as spontaneous beating rates⁴⁰. Nonetheless, the occurrence of these EATs is both pronounced and harmful, and an extensive collaboration between researchers and clinicians is required to determine a potential clinical response for the sister.

Since both the patient and the sister show a comparable electrophysiological phenotype, the involvement of a genetic component seems likely. Currently, only the patient was screened for a panel of genes associated with inherited arrhythmias. Proposed future work should include a more complete genetic screening of both patient and sister, as well as direct relatives, to identify a potential genetic cause. When this is discovered, further classical hiPSC-CM studies could be performed to mimic the phenotype and strengthen the hypothesized cause for the clinical presentation in the patient.

5. Conclusion

Here, we studied a patient-specific case of scTdP, in which the patient has suffered from multiple episodes of VF. Generation of hiPSC-CMs of the patient and her sister successfully recapitulated the clinical electrophysiological phenotype that could potentially be explained by the occurrence of premature electrical activity in the patient. Moreover our data identified the sister as a potential carrier for a similar phenotype. This study emphasizes the potential of hiPSC-CMs in studying cellular mechanisms and pharmacological interventions, while simultaneously describing the necessity for a delicate approach in translating the experimental results towards the clinics.

References

1. Jacoby D, McKenna WJ. Genetics of inherited cardiomyopathy. *Eur Heart J*. 2012;33(3):296-304.
2. Martinez HR, Beasley GS, Miller N, Goldberg JF, Jefferies JL. Clinical Insights Into Heritable Cardiomyopathies. *Front Genet*. 2021;12:663450.
3. Campuzano O, Sarquella-Brugada G, Brugada R, Brugada J. Genetics of channelopathies associated with sudden cardiac death. *Glob Cardiol Sci Pract*. 2015;2015(3):39.
4. Fernandez-Falgueras A, Sarquella-Brugada G, Brugada J, Brugada R, Campuzano O. Cardiac Channelopathies and Sudden Death: Recent Clinical and Genetic Advances. *Biology (Basel)*. 2017;6(1):7.
5. Li CJ, Chen CS, Yang GT, Tsai AP, Liao WT, Wu MY. Advanced Evolution of Pathogenesis Concepts in Cardiomyopathies. *J Clin Med*. 2019;8(4):520.
6. Burke MA, Cook SA, Seidman JG, Seidman CE. Clinical and Mechanistic Insights Into the Genetics of Cardiomyopathy. *J Am Coll Cardiol*. 2016;68(25):2871-2886.
7. Coll M, Perez-Serra A, Mates J, et al. Incomplete Penetrance and Variable Expressivity: Hallmarks in Channelopathies Associated with Sudden Cardiac Death. *Biology (Basel)*. 2017;7(1).
8. Dainis AM, Ashley EA. Cardiovascular Precision Medicine in the Genomics Era. *JACC Basic Transl Sci*. 2018;3(2):313-326.
9. Landstrom AP, Dobrev D, Wehrens XHT. Calcium Signaling and Cardiac Arrhythmias. *Circ Res*. 2017;120(12):1969-1993.
10. Eisner DA, Caldwell JL, Kistamas K, Trafford AW. Calcium and Excitation-Contraction Coupling in the Heart. *Circ Res*. 2017;121(2):181-195.
11. Bolhaqueiro ACF, Ponsioen B, Bakker B, et al. Ongoing chromosomal instability and karyotype evolution in human colorectal cancer organoids. *Nat Genet*. 2019;51(5):824-834.
12. Goversen B, van der Heyden MAG, van Veen TAB, de Boer TP. The immature electrophysiological phenotype of iPSC-CMs still hampers in vitro drug screening: Special focus on I(K1). *Pharmacol Ther*. 2018;183:127-136.
13. Nemeč J, Kim JJ, Salama G. The link between abnormal calcium handling and electrical instability in acquired long QT syndrome—Does calcium precipitate arrhythmic storms? *Prog Biophys Mol Biol*. 2016;120(1-3):210-221.
14. Fink M, Noble PJ, Noble D. Ca²⁺-induced delayed afterdepolarizations are triggered by dyadic subspace Ca²⁺ affirming that increasing SERCA reduces aftercontractions. *Am J Physiol Heart Circ Physiol*. 2011;301(3):H921-935.
15. Shiferaw Y, Aistrup GL, Wasserstrom JA. Intracellular Ca²⁺ waves, afterdepolarizations, and triggered arrhythmias. *Cardiovasc Res*. 2012;95(3):265-268.
16. Katta RP, Laurita KR. Cellular mechanism of calcium-mediated triggered activity in the heart. *Circ Res*. 2005;96(5):535-542.
17. Liu MB, de Lange E, Garfinkel A, Weiss JN, Qu Z. Delayed afterdepolarizations generate both triggers and a vulnerable substrate promoting reentry in cardiac tissue. *Heart Rhythm*. 2015;12(10):2115-2124.

18. Leenhardt A, Glaser E, Burguera M, Nurnberg M, Maison-Blanche P, Coumel P. Short-coupled variant of torsade de pointes. A new electrocardiographic entity in the spectrum of idiopathic ventricular tachyarrhythmias. *Circulation*. 1994;89(1):206-215.
19. Wang G, Zhong L, Chu H, Wang C, Zhu X. Short-coupled variant of torsade de pointes: A systematic review of case reports and case series. *Front Cardiovasc Med*. 2022;9:922525.
20. Shiga T, Shoda M, Matsuda N, et al. Electrophysiological characteristic of a patient exhibiting the short-coupled variant of torsade de pointes. *J Electrocardiol*. 2001;34(3):271-275.
21. Guillen RH, Chort C, Mantilla L, Sriram CS, Gonzalez MD. Short coupled torsade de pointes: Critical timing of the ventricular premature beats. *J Electrocardiol*. 2021;65:69-72.
22. Bogaard K, van der Steen MS, Tan HL, Tukkie R. Short-coupled variant of torsade de pointes. *Neth Heart J*. 2008;16(7-8):246-249.
23. Van den Branden B, Wever E, Boersma L. Torsade de pointes with short coupling interval. *Acta Cardiol*. 2010;65(3):345-346.
24. Parikh SS, Blackwell DJ, Gomez-Hurtado N, et al. Thyroid and Glucocorticoid Hormones Promote Functional T-Tubule Development in Human-Induced Pluripotent Stem Cell-Derived Cardiomyocytes. *Circ Res*. 2017;121(12):1323-1330.
25. Lundy SD, Zhu WZ, Regnier M, Laflamme MA. Structural and functional maturation of cardiomyocytes derived from human pluripotent stem cells. *Stem Cells Dev*. 2013;22(14):1991-2002.
26. Krause T, Gerbershagen MU, Fiege M, Weisshorn R, Wappler F. Dantrolene—a review of its pharmacology, therapeutic use and new developments. *Anaesthesia*. 2004;59(4):364-373.
27. Paul-Pletzer K, Yamamoto T, Ikemoto N, et al. Probing a putative dantrolene-binding site on the cardiac ryanodine receptor. *Biochem J*. 2005;387(Pt 3):905-909.
28. Jung CB, Moretti A, Mederos y Schnitzler M, et al. Dantrolene rescues arrhythmogenic RYR2 defect in a patient-specific stem cell model of catecholaminergic polymorphic ventricular tachycardia. *EMBO Mol Med*. 2012;4(3):180-191.
29. Kobayashi S, Yano M, Suetomi T, et al. Dantrolene, a therapeutic agent for malignant hyperthermia, markedly improves the function of failing cardiomyocytes by stabilizing interdomain interactions within the ryanodine receptor. *J Am Coll Cardiol*. 2009;53(21):1993-2005.
30. Yamamoto T, Ikemoto N. Spectroscopic monitoring of local conformational changes during the intramolecular domain-domain interaction of the ryanodine receptor. *Biochemistry*. 2002;41(5):1492-1501.
31. Xiao L, Koopmann TT, Ordog B, et al. Unique cardiac Purkinje fiber transient outward current beta-subunit composition: a potential molecular link to idiopathic ventricular fibrillation. *Circ Res*. 2013;112(10):1310-1322.
32. Ten Sande JN, Postema PG, Boekholdt SM, et al. Detailed characterization of familial idiopathic ventricular fibrillation linked to the DPP6 locus. *Heart Rhythm*. 2016;13(4):905-912.

33. Harris K, Aylott M, Cui Y, Louttit JB, McMahon NC, Sridhar A. Comparison of electrophysiological data from human-induced pluripotent stem cell-derived cardiomyocytes to functional preclinical safety assays. *Toxicol Sci.* 2013;134(2):412-426.
34. Goldfracht I, Efraim Y, Shinnawi R, et al. Engineered heart tissue models from hiPSC-derived cardiomyocytes and cardiac ECM for disease modeling and drug testing applications. *Acta Biomater.* 2019;92:145-159.
35. Stutzman MJ, Kim CSJ, Tester DJ, et al. Characterization of N-terminal RYR2 variants outside CPVT1 hotspot regions using patient iPSCs reveal pathogenesis and therapeutic potential. *Stem Cell Reports.* 2022;17(9):2023-2036.
36. Zhou Y, Huang W, Liu L, et al. Patient-specific induced pluripotent stem cell properties implicate Ca(2+)-homeostasis in clinical arrhythmia associated with combined heterozygous RYR2 and SCN10A variants. *Philos Trans R Soc Lond B Biol Sci.* 2023;378(1879):20220175.
37. Van Kampen SJ, Han SJ, van Ham WB, et al. PITX2 induction leads to impaired cardiomyocyte function in arrhythmogenic cardiomyopathy. *Stem Cell Reports.* 2023;18(3):749-764.
38. Badone B, Ronchi C, Lodola F, et al. Characterization of the PLN p.Arg14del Mutation in Human Induced Pluripotent Stem Cell-Derived Cardiomyocytes. *Int J Mol Sci.* 2021;22(24):13500.
39. Simons E, Loeyts B, Alaerts M. iPSC-Derived Cardiomyocytes in Inherited Cardiac Arrhythmias: Pathomechanistic Discovery and Drug Development. *Biomedicines.* 2023;11(2):334.
40. Van Mil A, Balk GM, Neef K, et al. Modelling inherited cardiac disease using human induced pluripotent stem cell-derived cardiomyocytes: progress, pitfalls, and potential. *Cardiovasc Res.* 2018;114(14):1828-1842.

Supplementary Materials

Table S1. List of gene probes for quantitative PCR.

Gene	protein	Assay	Supplier	ID
CASQ2	Calsequestrin-2	qPCR	Custom	FW GGTGATATTGTAGAAATTGCTGTG RV TGACTGGTCAACTCTTAGTGTGGT
SLC8A1	Sodium-calcium exchanger 1	qPCR	Custom	FW GCCCTTGTGGTTGGGACTAA RV CGTCATCATCTTCCCACGA
RYR2	Ryanodine receptor 2	qPCR	Custom	FW GCTGGTTGTGGACTGCAAAG RV AACACTCAGGCCCTCCGAATG
PLN	Phospholamban	qPCR	Custom	FW CCCCAGCTAAACACCGTAA RV CTTTTAGGTAGCCTTGGCAGC
CACNA1C	L-type calcium-channel	qPCR	Custom	FW GCCTTCAAACCCAAGGGTTACT RV TGCTGCCAATTACGATGAGGA
CACNB2	L-type calcium-channel	qPCR	Custom	FW GGTGGGAAGAAATGGACCGA RV CCGAACCATAGGACACCCG
ATP2A2	Sarcoendoplasmic reticulum ATPase 2a	qPCR	Custom	FW GGTGATATTGTAGAAATTGCTGTG RV TGACTGGTCAACTCTTAGTGTGGT
SCN5A	Voltage gate sodium channel 1.5	qPCR	Custom	FW AGGCCAGTGCATCTCAGG RV GGTGTGGTCATGTCTGCTG
KCNH2	Potassium voltage-gated channel subfamily H member 2	qPCR	Custom	FW GGCCAGAGCCGTAAGTTCAT RV AAGCCGTCGTTGCAGTAGAT
KCNJ2	Potassium inwardly rectifying channel subfamily J member 2	qPCR	Custom	FW ACCGCTACAGCATCGTCTCT RV TCCACACACGTGGTGAAGAT
CAMK2D	Calcium/calmodulin dependent protein kinase II delta	qPCR	Custom	FW GTCACTGAACAACATGATCGAAGC RV GAATCGGTGAAAATCCATCCCTT
ARP	Acidic ribosomal phosphor- protein PO	qPCR	Custom	FW CACCATTTGAAATCCTGAGTGATGT RV TGACCAGCCCAAAGGAGAAG

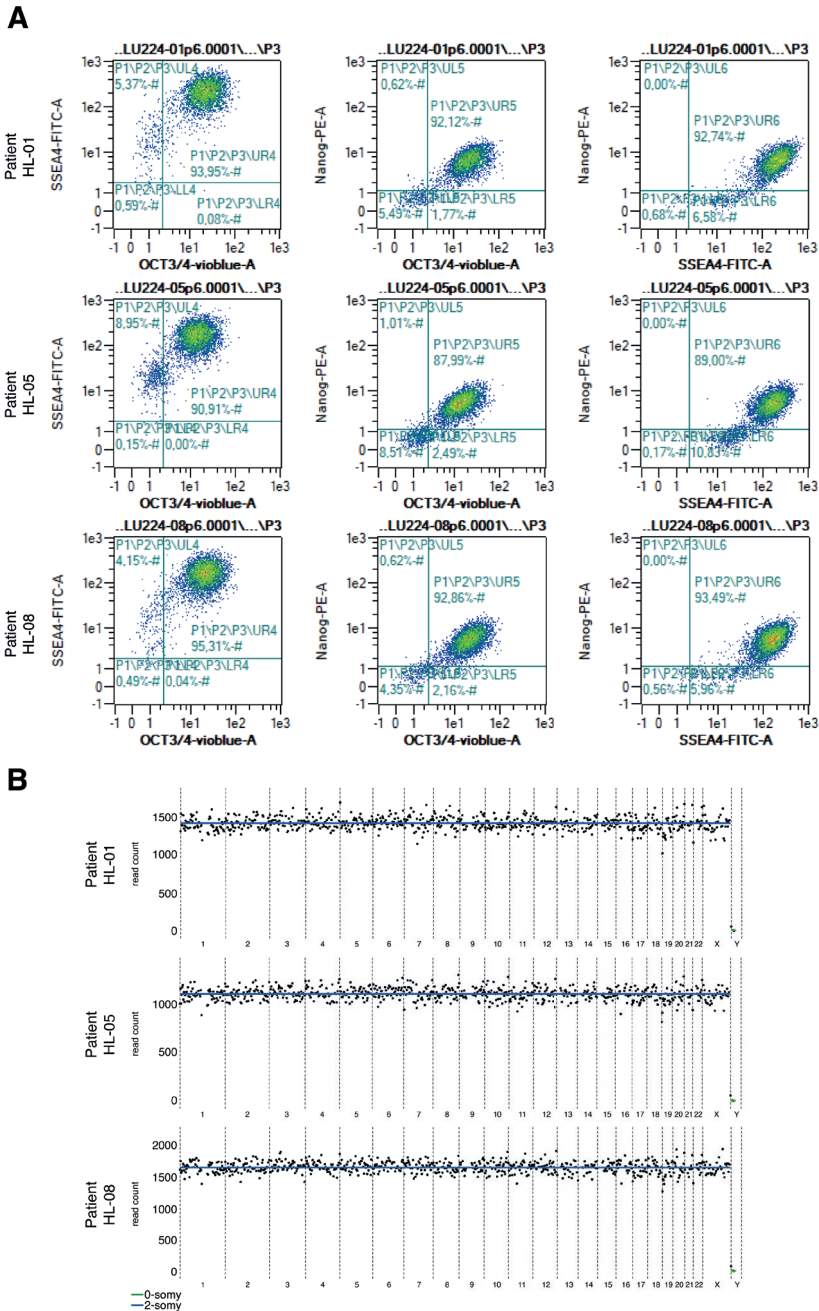
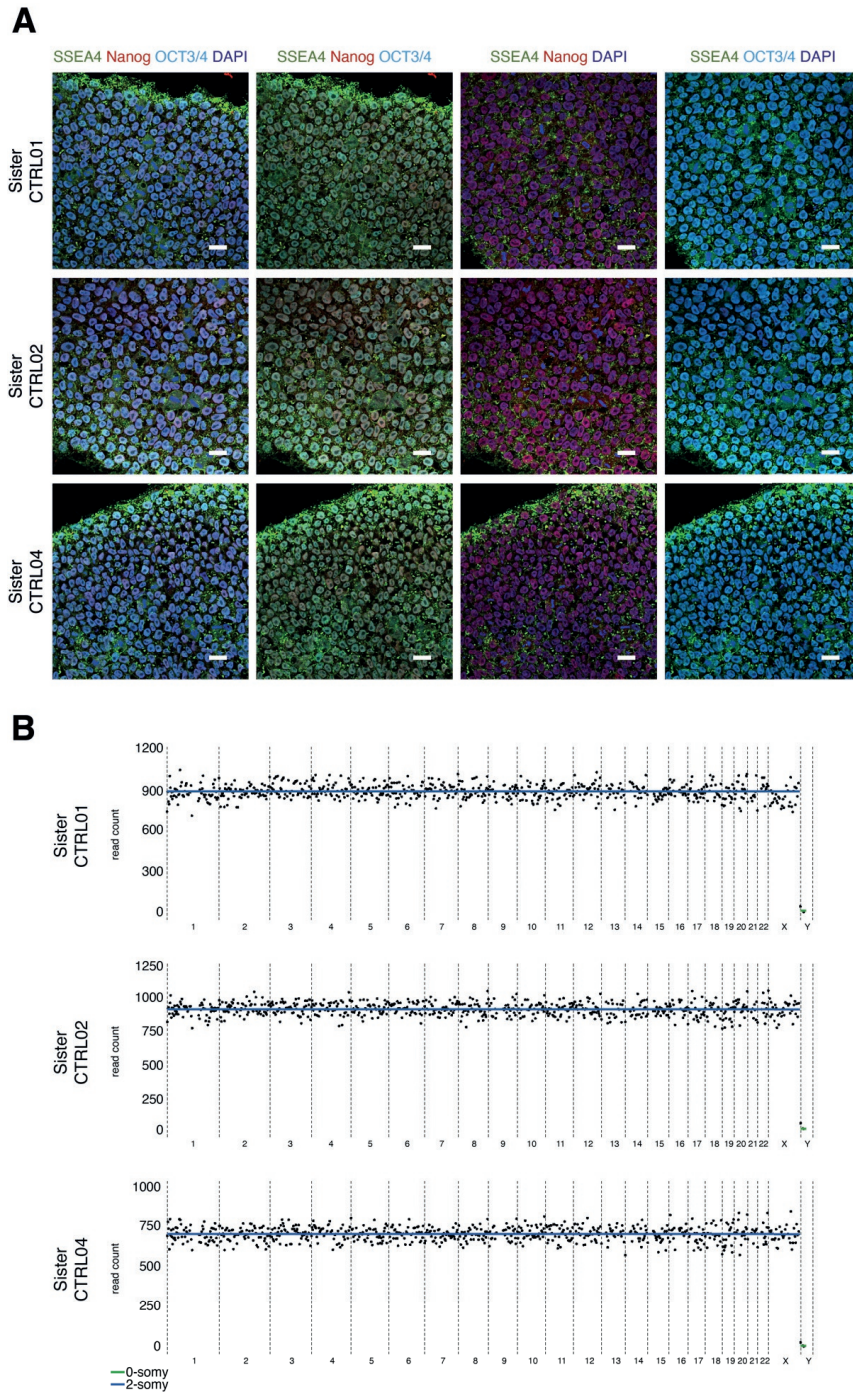


Figure S1. Patient hiPSC clones characteristics. Three independent patient hiPSC clones were generated from isolated peripheral blood mononuclear cells. **(A)** Representative merged immunofluorescence images of SSEA4, Nanog, OCT3/4, and DAPI. Scalebar represents 25 μ m. **(B)** Karyo-sequencing profiles.



V

Figure S2. Sister hiPSC clones characteristics. Three independent sister hiPSC clones were generated from isolated peripheral blood mononuclear cells. **(A)** FACS plots of SSEA4, Nanog, OCT3/4, and DAPI. **(B)** Karyo-sequencing profiles.

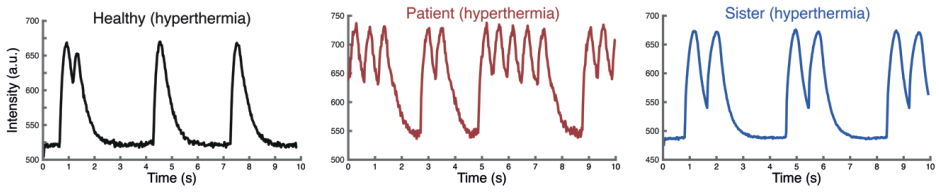


Figure S3. Example recordings of calcium transients in healthy, patient, and sister lines. Example calcium transient measurements performed in hiPSC-CMs from the patient (red), sister (blue), and a healthy control (black) during hyperthermia, indicating the occurrence of early after calcium transients.

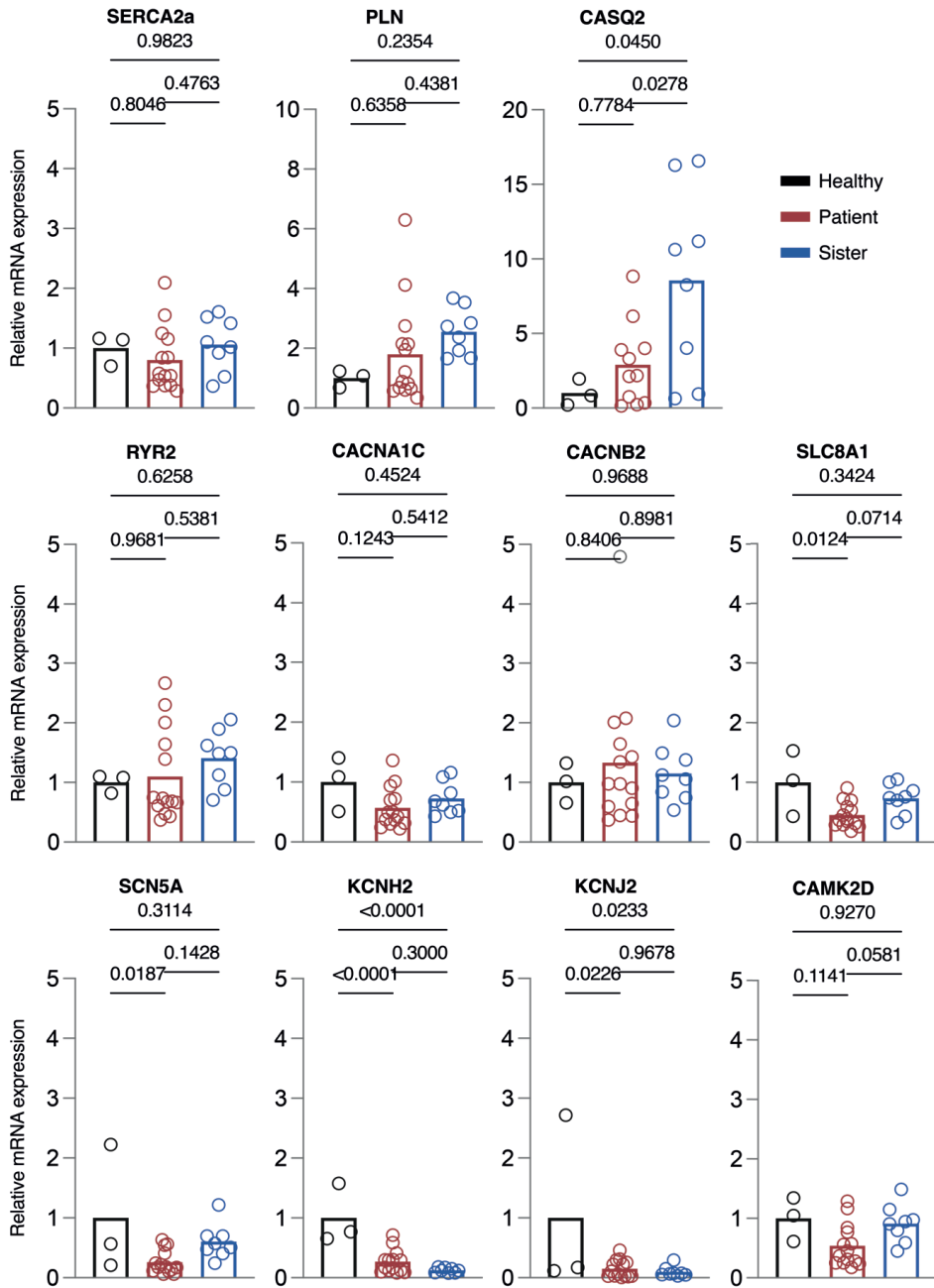


Figure S4. Gene expression changes underlying disturbed calcium handling. Quantification of mRNA expression of genes involved in cardiac electrophysiology in hiPSC-CMs from the patient (red), sister (blue), and a healthy control (black). In general, expression profiles of the patient and sister are similar, and do not indicate a clear explanation for the measured electrophysiological phenotype.

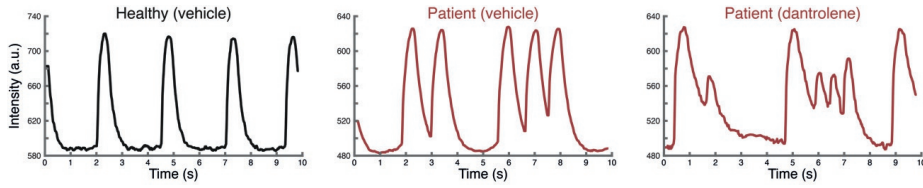


Figure S5. Example recordings of calcium transients after drug administration. Example calcium transient measurements performed in hiPSC-CMs from the patient (red) and a healthy control (black) during hyperthermia after dantrolene administration, indicating the diminished amplitude of early after calcium transients in the patient.

Willem B. van Ham¹

¹Department of Medical Physiology, University Medical Center Utrecht, The Netherlands

Chapter VI

Introduction

**Electrophysiological disturbances in
inherited and acquired
cardiomyopathies**

Arrhythmogenic and ischemic cardiomyopathy

Arrhythmogenic cardiomyopathy (ACM) is an inherited and progressive cardiac disease, with a prevalence between 1:1000 and 1:5000¹. Clinical diagnosis is complicated by an initiating concealed phase in disease presentation and incomplete penetrance of the associated genetic variants². ACM, including its progressive electrical and structural adaptations, often remains asymptomatic, but results in a high susceptibility for sudden cardiac death. Approximately 50% of patients diagnosed with ACM (or more specifically its former name ARVC) carry one or more pathogenic variants in genes encoding for desmosomal proteins, which are vital for cohesion between cardiomyocytes³. These include: plakophilin-2 (PKP2), plakoglobin (JUP), desmoplakin (DSP), desmoglein (DSG), and desmocollin (DSC)^{1,4,5}. Desmosomes are part of the cell-to-cell linkage termed intercalated discs (IDs), and interact closely with other components, such as gap junctions and numerous ion channels^{3,6-9}. Additionally, studies using a model of tamoxifen induced cardiomyocyte specific *Pkp2* deletion in adult mice demonstrated a compromised intracellular calcium handling in the absence of PKP2¹⁰⁻¹². In myocardial tissue obtained from ACM patients decreased levels of these desmosomal proteins have also been identified^{7,13-16}.

The transcription factor paired-like homeodomain 2 (PITX2) has been shown to influence a network of structural and ion channel-related genes and can therefore influence desmosomal protein expression²¹. Genetic variants of *PITX2* are also known to predispose patients to cardiac arrhythmias^{22,23}. Desmosomal protein levels and their localization is also influenced by protein degradation processes. These processes are vital for normal cell function as they assure that damaged or misfolded proteins will be degraded to prevent cardiotoxicity, mainly via the ubiquitin-proteasome system (UPS), the autophagy-lysosome pathway, or calcium dependent calpain and cathepsin proteases¹⁷. Genetic variants in both *PKP2* and *DSP* can lead to decreased protein stability and increased sensitivity towards calpain proteases^{18,19}, whereas ACM has also been linked with prevention of neddylation-directed proteasome degradation²⁰. Studying the role of PITX2 and protein degradation in ACM could potentially lead to the identification of novel therapeutic approaches to improve desmosomal protein function and consequently prevent electrophysiological and calcium handling disturbances.

Heart failure caused by the progressive deterioration of cardiac performance due to ischemic heart disease (IHD) is the most common and leading cause of death worldwide^{24,25}. IHD is caused by a complete or partial occlusion of coronary arteries, resulting in a decreased blood flow towards the myocardial tissue after the occlusion. During IHD the area of hypoxia-induced loss of cardiomyocytes is gradually replaced by fibrotic scar tissue, which hampers contractility due to the non-elastic nature of this tissue and the fact that through the loss of cardiomyocytes the contractile capacity of the myocardium is diminished^{26,27}. On top of that, this ischemic injury has been shown to cause intracellular calcium overload, leading to impaired contractility and relaxation which adds to cardiomyocyte dysfunction^{28,29}. Disturbed expression and

function of several calcium handling proteins can cause this pathological remodeling³⁰⁻³². Recently, Zinc finger E-box-binding homeobox 2 (ZEB2) was identified as a cardioprotective transcription factor, which is upregulated during hypoxia, but expression decreases with age^{33,34}. Studying the specific role of ZEB2 on cardiac ion channels and calcium homeostasis could aid in the development of IHD therapeutic options.

Studying cardiac electrophysiology and calcium homeostasis

Electrophysiological and calcium handling experiments and the resulting findings from three collaborative studies are extracted and described in this chapter. The complete abstract of each study and the methods regarding the electrophysiology experiments will be included. Molecular data originating from these studies will also be briefly summarized, to contextualize the highlighted electrophysiological data.

In **Part A** we used human induced pluripotent stem cell derived cardiomyocytes (hiPSC-CMs) to study a novel potentially pathogenic variant in *DSP*. The consequences for cellular electrophysiology, as well as the modulatory effects of *PITX2* overexpression and depletion, will be described. In **Part B** we studied calcium handling and the therapeutic potential of a UPS inhibitor using cardiomyocytes isolated from adult mouse hearts that expressed a patient-specific heterozygous variant of *Pkp2*. In **Part C** we analyzed calcium handling in isolated adult cardiomyocytes obtained from a cardiomyocyte-specific *Zeb2* overexpression mouse model. This chapter concludes with a **discussion** reflecting on the findings from those three studies.

References

1. Van der Voorn SM, Te Riele A, Basso C, Calkins H, Remme CA, van Veen TAB. Arrhythmogenic cardiomyopathy: pathogenesis, pro-arrhythmic remodelling, and novel approaches for risk stratification and therapy. *Cardiovasc Res.* 2020;116(9):1571-1584.
2. Marcus FI, McKenna WJ, Sherrill D, et al. Diagnosis of arrhythmogenic right ventricular cardiomyopathy/dysplasia: proposed modification of the task force criteria. *Circulation.* 2010;121(13):1533-1541.
3. Patel DM, Green KJ. Desmosomes in the heart: a review of clinical and mechanistic analyses. *Cell Commun Adhes.* 2014;21(3):109-128.
4. Corrado D, Link MS, Calkins H. Arrhythmogenic Right Ventricular Cardiomyopathy. *N Engl J Med.* 2017;376(1):61-72.
5. Austin KM, Trembley MA, Chandler SF, et al. Molecular mechanisms of arrhythmogenic cardiomyopathy. *Nat Rev Cardiol.* 2019;16(9):519-537.
6. Vermij SH, Abriel H, van Veen TA. Refining the molecular organization of the cardiac intercalated disc. *Cardiovasc Res.* 2017;113(3):259-275.
7. Kaplan SR, Gard JJ, Protonotarios N, et al. Remodeling of myocyte gap junctions in arrhythmogenic right ventricular cardiomyopathy due to a deletion in plakoglobin (Naxos disease). *Heart Rhythm.* 2004;1(1):3-11.
8. Vite A, Radice GL. N-cadherin/catenin complex as a master regulator of intercalated disc function. *Cell Commun Adhes.* 2014;21(3):169-179.
9. Sato PY, Coombs W, Lin X, et al. Interactions between ankyrin-G, Plakophilin-2, and Connexin43 at the cardiac intercalated disc. *Circ Res.* 2011;109(2):193-201.
10. Kim JC, Perez-Hernandez M, Alvarado FJ, et al. Disruption of Ca(2+)(i) Homeostasis and Connexin 43 Hemichannel Function in the Right Ventricle Precedes Overt Arrhythmogenic Cardiomyopathy in Plakophilin-2-Deficient Mice. *Circulation.* 2019;140(12):1015-1030.
11. Van Opbergen CJM, Bagwan N, Maurya SR, et al. Exercise Causes Arrhythmogenic Remodeling of Intracellular Calcium Dynamics in Plakophilin-2-Deficient Hearts. *Circulation.* 2022;145(19):1480-1496.
12. Cerrone M, Montnach J, Lin X, et al. Plakophilin-2 is required for transcription of genes that control calcium cycling and cardiac rhythm. *Nat Commun.* 2017;8(1):106.
13. Rasmussen TB, Nissen PH, Palmfeldt J, et al. Truncating plakophilin-2 mutations in arrhythmogenic cardiomyopathy are associated with protein haploinsufficiency in both myocardium and epidermis. *Circ Cardiovasc Genet.* 2014;7(3):230-240.
14. Tandri H, Asimaki A, Dalal D, Saffitz JE, Halushka MK, Calkins H. Gap junction remodeling in a case of arrhythmogenic right ventricular dysplasia due to plakophilin-2 mutation. *J Cardiovasc Electrophysiol.* 2008;19(11):1212-1214.

15. Vite A, Gandjbakhch E, Prost C, et al. Desmosomal cadherins are decreased in explanted arrhythmogenic right ventricular dysplasia/cardiomyopathy patient hearts. *PLoS One*. 2013;8(9):e75082.
16. Noorman M, Hakim S, Kessler E, et al. Remodeling of the cardiac sodium channel, connexin43, and plakoglobin at the intercalated disk in patients with arrhythmogenic cardiomyopathy. *Heart Rhythm*. 2013;10(3):412-419.
17. Wang C, Wang X. The interplay between autophagy and the ubiquitin-proteasome system in cardiac proteotoxicity. *Biochim Biophys Acta*. 2015;1852(2):188-194.
18. Kirchner F, Schuetz A, Boldt LH, et al. Molecular insights into arrhythmogenic right ventricular cardiomyopathy caused by plakophilin-2 missense mutations. *Circ Cardiovasc Genet*. 2012;5(4):400-411.
19. Ng R, Manring H, Papoutsidakis N, et al. Patient mutations linked to arrhythmogenic cardiomyopathy enhance calpain-mediated desmoplakin degradation. *JCI Insight*. 2019;5(14):e128643.
20. Liang Y, Lyon RC, Pellman J, et al. Desmosomal COP9 regulates proteome degradation in arrhythmogenic right ventricular dysplasia/cardiomyopathy. *J Clin Invest*. 2021;131(11):e137689.
21. Tao Y, Zhang M, Li L, et al. Pitx2, an atrial fibrillation predisposition gene, directly regulates ion transport and intercalated disc genes. *Circ Cardiovasc Genet*. 2014;7(1):23-32.
22. Chinchilla A, Daimi H, Lozano-Velasco E, et al. PITX2 insufficiency leads to atrial electrical and structural remodeling linked to arrhythmogenesis. *Circ Cardiovasc Genet*. 2011;4(3):269-279.
23. Van Ouwkerk AF, Hall AW, Kadow ZA, et al. Epigenetic and Transcriptional Networks Underlying Atrial Fibrillation. *Circ Res*. 2020;127(1):34-50.
24. Nowbar AN, Gitto M, Howard JP, Francis DP, Al-Lamee R. Mortality From Ischemic Heart Disease. *Circ Cardiovasc Qual Outcomes*. 2019;12(6):e005375.
25. Virani SS, Alonso A, Benjamin EJ, et al. Heart Disease and Stroke Statistics-2020 Update: A Report From the American Heart Association. *Circulation*. 2020;141(9):e139-e596.
26. Talman V, Ruskoaho H. Cardiac fibrosis in myocardial infarction-from repair and remodeling to regeneration. *Cell Tissue Res*. 2016;365(3):563-581.
27. Chiong M, Wang ZV, Pedrozo Z, et al. Cardiomyocyte death: mechanisms and translational implications. *Cell Death Dis*. 2011;2(12):e244.
28. Bers DM. Calcium cycling and signaling in cardiac myocytes. *Annu Rev Physiol*. 2008;70:23-49.
29. Wang R, Wang M, He S, Sun G, Sun X. Targeting Calcium Homeostasis in Myocardial Ischemia/Reperfusion Injury: An Overview of Regulatory Mechanisms and Therapeutic Reagents. *Front Pharmacol*. 2020;11:872.
30. Baskin KK, Makarewich CA, DeLeon SM, et al. MED12 regulates a transcriptional network of calcium-handling genes in the heart. *JCI Insight*. 2017;2(14):e91920.
31. Periasamy M, Reed TD, Liu LH, et al. Impaired cardiac performance in heterozygous mice with a null mutation in the sarco(endo)plasmic reticulum Ca²⁺-ATPase isoform 2 (SERCA2) gene. *J Biol Chem*. 1999;274(4):2556-2562.

32. Wolska BM, Stojanovic MO, Luo W, Kranias EG, Solaro RJ. Effect of ablation of phospholamban on dynamics of cardiac myocyte contraction and intracellular Ca²⁺. *Am J Physiol.* 1996;271(1 Pt 1):C391-397.
33. Gladka MM, Kohela A, Molenaar B, et al. Cardiomyocytes stimulate angiogenesis after ischemic injury in a ZEB2-dependent manner. *Nat Commun.* 2021;12(1):84.
34. Gladka MM, Johansen AKZ, van Kampen SJ, et al. Thymosin beta4 and prothymosin alpha promote cardiac regeneration post-ischaemic injury in mice. *Cardiovasc Res.* 2023;119(3):802-812.

Sebastiaan J. van Kampen¹

Su Ji Han¹

Willem B. van Ham²

Eirini Kyriakopoulou¹

Elizabeth W. Stouthart¹

Birgit Goversen^{2,3}

Jantine Monshouwer-Kloots¹

Ilaria Perini¹

Hesther de Ruiters¹

Petra van der Kraak⁴

Aryan Vink⁴

Linda W. van Laake⁵

Judith A. Groeneweg⁵

Teun P. de Boer²

Hoyee Tsui¹

Cornelis J. Boogerd¹

Toon A.B. van Veen²

Eva van Rooij^{1,5}

¹Hubrecht Institute, KNAW, University Medical Center Utrecht, The Netherlands

²Department of Medical Physiology, University Medical Center Utrecht, The Netherlands

³Department of Physiology, Amsterdam University Medical Centers, Location VU Medical Center, The Netherlands

⁴Department of Pathology, University Medical Center Utrecht, The Netherlands

⁵Department of Cardiology, University Medical Center Utrecht, The Netherlands

Chapter VI

Part A

This chapter contains extracts originating from:

**PITX2 induction leads to impaired
cardiomyocyte function in
arrhythmogenic cardiomyopathy**

Stem Cell Reports, 18(3), 749-764. (2023)

Abstract

Arrhythmogenic cardiomyopathy (ACM) is an inherited progressive disease characterized by electrophysiological and structural remodeling of the ventricular myocardium. However, the disease-causing molecular pathways, as a consequence of mutations in genes encoding desmosomal proteins, are poorly understood. Here, we identified a novel missense mutation within *desmoplakin* in a patient clinically diagnosed with ACM. Using CRISPRCas9, we corrected this mutation in patient-derived human induced pluripotent stem cells (hiPSCs) and generated an independent knockin hiPSC line carrying the same mutation. The generated cardiomyocytes displayed a decline in connexin 43, Nav1.5, and desmosomal proteins, which was accompanied by a prolonged action potential duration. Interestingly, paired-like homeodomain 2 (*PITX2*), a transcription factor that acts as a repressor of connexin 43, Nav1.5, and desmoplakin, was induced in mutant cardiomyocytes. We validated these results in control cardiomyocytes in which *PITX2* was either depleted or overexpressed. Importantly, knockdown of *PITX2* in patient-derived cardiomyocytes appeared sufficient to restore the levels of desmoplakin, connexin 43, and Nav1.5.

Keywords: *PITX2*; arrhythmogenic cardiomyopathy; desmoplakin; desmosome; induced pluripotent stem cells; cardiomyocyte

1. Measurements and analysis of action potentials

hiPSC-derived cardiomyocytes were seeded per 100,000 cells on Geltrex™-coated glass coverslips, to allow cluster formation. Coverslips were incubated for 15 minutes at 37 °C with 1:1000 voltage sensitive dye FluoVolt and 1:1000 Powerload (Thermo Fischer Scientific, F10488) in RPMI-1640-Medium-GlutaMAX™-Supplement-HEPES supplemented with B-27™ Supplement (50x)-serum free. During measurements, cells were immersed in a solution containing in mM: NaCl (130), KCl (4), CaCl₂ (1.8), MgCl₂ (1.2), NaHCO₃ (18), HEPES (10) and glucose (10), pH 7.4. A custom-build microscope (Cairn Research, Kent, UK) with a 10x objective was used for the recordings. Excitation of the dye was done by a blue light, using a 482/35 excitation filter (Semrock FF01-482/35-25), and captured with a high-speed camera (Andor Zyla 5.5.CL3, Oxford Instruments), using a 514 long-pass emission filter (Semrock LP02-514RU-25). A custom MATLAB script was used for analysis of the action potentials (DOI: 10.17605/OSF.IO/86UFE). Action potential durations were corrected for the beating rate using an adjustment of the Fredericia formula to correct the QT interval for heart rate: $APD_{corrected} = APD / (\sqrt[3]{(60/BPM)})^1$.

2.1. Heterozygous *DSP* p.Tyr1188His hiPSC-derived cardiomyocytes display reduced desmosomal protein levels and impaired function

To further understand the molecular consequences of this novel mutation, we reprogrammed patient skin fibroblasts to obtain human induced pluripotent stem cells (hiPSCs) bearing the heterozygous *DSP* c.3562T>C mutation. Next, we corrected the mutant allele utilizing CRISPR-Cas9 in combination with a singlestranded DNA template, yielding an isogenic control line (**Figure 1A**). Hereinafter, we refer to these lines as Pa. *DSP*^{WT/WT} and Pa. *DSP*^{p.Tyr1188His/WT}. Desmoplakin (DSP), plakoglobin (JUP), and plakophilin-2 (PKP2) correctly localized to the cell periphery in 1-month-old mutant cardiomyocytes (**Figure 1B**). However, molecular analyses revealed a significant reduction in DSP protein levels in mutant cardiomyocytes, whereas the mRNA levels were unaffected (**Figures 1C–1E**). Immunoblot analysis for the desmosomal proteins desmocollin (DSC), desmoglein (DSG), JUP, and PKP2 showed a significant decline for all proteins in Pa. *DSP*^{p.Tyr1188His/WT} hiPSC-derived cardiomyocytes when compared with the isogenic control (**Figures 1F and 1G**). As arrhythmogenic cardiomyopathy (ACM) patients display electrophysiological abnormalities including repolarization irregularities and arrhythmias, we performed electrophysiology assays on mutant hiPSC-derived cardiomyocytes. We observed a prolonged action potential duration (APD) at 50% and 90% of repolarization in mutant cardiomyocytes compared with control (**Figure 1H**). Together, cardiomyocytes bearing the novel *DSP* p.Tyr1188His mutation show reduced desmosomal protein levels and a prolonged APD.

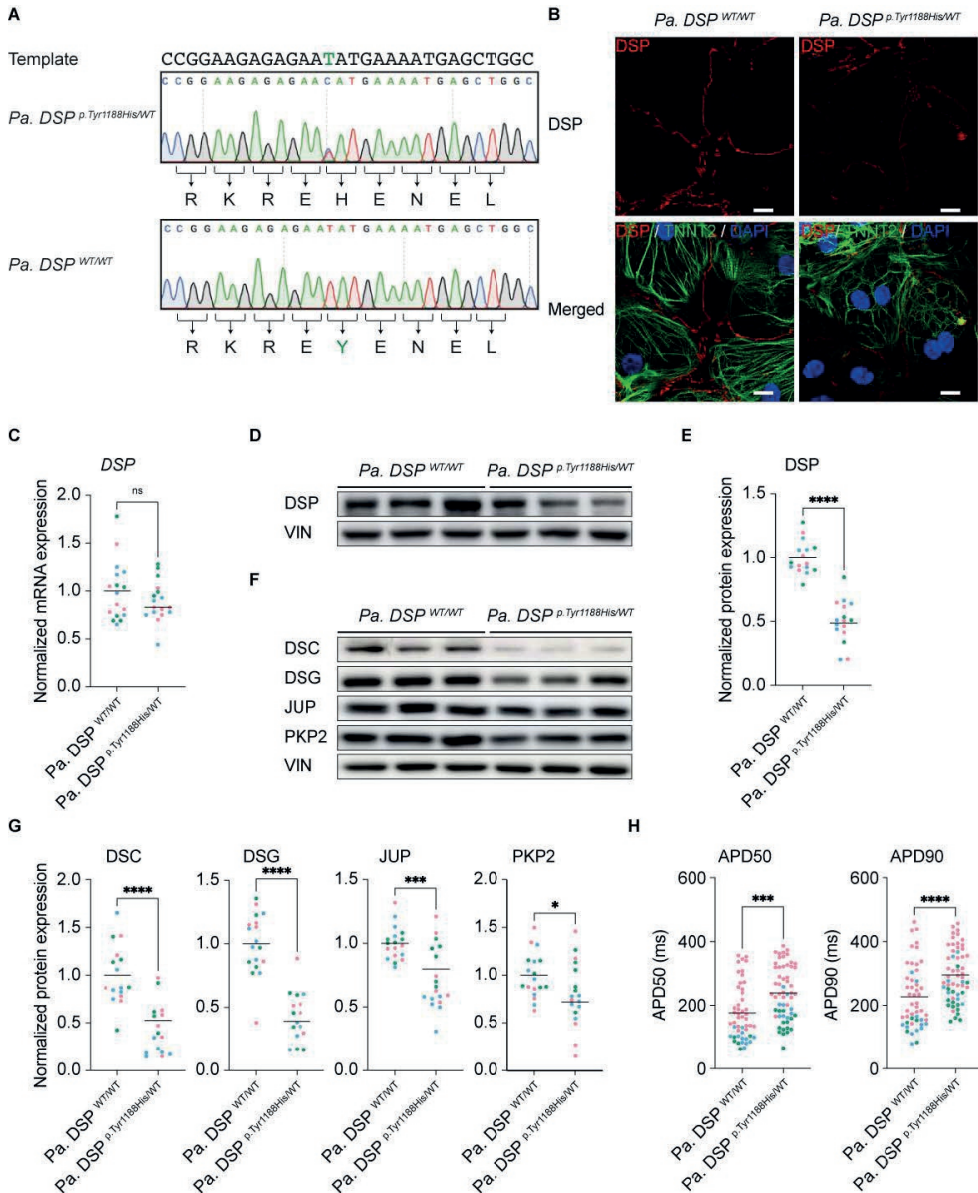


Figure 1. Heterozygous Pa. DSP^{p.Tyr1188His/WT} hiPSC-derived cardiomyocytes display reduced desmosomal protein levels and a prolonged action potential duration. (A) Sanger sequencing traces of the patient-derived and corrected isogenic control hiPSC lines. The DNA template used for CRISPR-Cas9-targeting, correcting the DSP p.Tyr1188His mutation (C > T), is shown. Intended mutation is indicated in green. (B–H) Molecular and functional analyses on 1-month-old hiPSC-derived cardiomyocytes obtained from three independent experiments. (B) Representative immunostainings for DSP. DSP in red; cardiac troponin T (TNNT2) in green; DAPI in blue. Scale bar: 10 mm. (C) Gene expression levels of DSP normalized to GUS. (D) Representative immunoblots for DSP. (E) Quantification of DSP protein levels normalized to VIN. (F) Representative immunoblots for DSC, DSG, JUP, PKP2, and VIN. (G) Quantification of protein levels normalized to VIN. (H) Quantification of action potential duration (APD) parameters.

JUP, and PKP2. **(G)** Quantification of the desmosomal protein levels. Values normalized to VIN. **(H)** Action potential duration (APD) measured at 50% and 90% of cardiomyocyte repolarization (Pa. DSP^{WT/WT}, n=50 cell clusters; Pa. DSP^{p.Tyr1188His/WT}, n=58 cell clusters). Data are plotted as mean. The dots in **(C, E, G, and H)** represent technical replicates, whereas the color of each dot indicates the experimental origin (3 independent experiments; 4–34 technical replicates). Significance has been assessed by a two-tailed unpaired Student's t test or two-tailed Mann-Whitney test when data were not normally distributed (*p < 0.05, ***p < 0.001, ****p < 0.0001, ns, not significant).

2.2. Knockin hiPSC-derived DSP p.Tyr1188His/WT cardiomyocytes corroborate findings observed in patient-derived cardiomyocytes

In an effort to exclude confounding effects, such as the presence of second genomic hits, we generated an independent knockin (KI) hiPSC line bearing the DSP p.Tyr1188His mutation. We used a healthy hiPSC line and followed the same targeting process as described above (**Figure 2A**). Hereafter, we refer to these lines as KI. DSP^{WT/WT} and KI. DSP^{p.Tyr1188His/WT}. Similar to Pa. DSP^{p.Tyr1188His/WT}, a decline in DSP protein levels was observed in the KI. DSP^{p.Tyr1188His/WT} cardiomyocytes (**Figures 2C and 2D**). Interestingly, also the mRNA levels of DSP were reduced, which is in contrast to the observation made in the patient-derived line (**Figure 2B**). Western blot analysis revealed a significant decline for DSC and JUP, whereas DSG and PKP2 were at a similar level compared with the isogenic control (**Figures 2E and 2F**). Importantly, the APD at 50% and 90% of cardiomyocyte repolarization was also prolonged in KI. DSP^{p.Tyr1188His/WT} cardiomyocytes (**Figure 2G**) in a fashion comparable to that seen in the patient line.

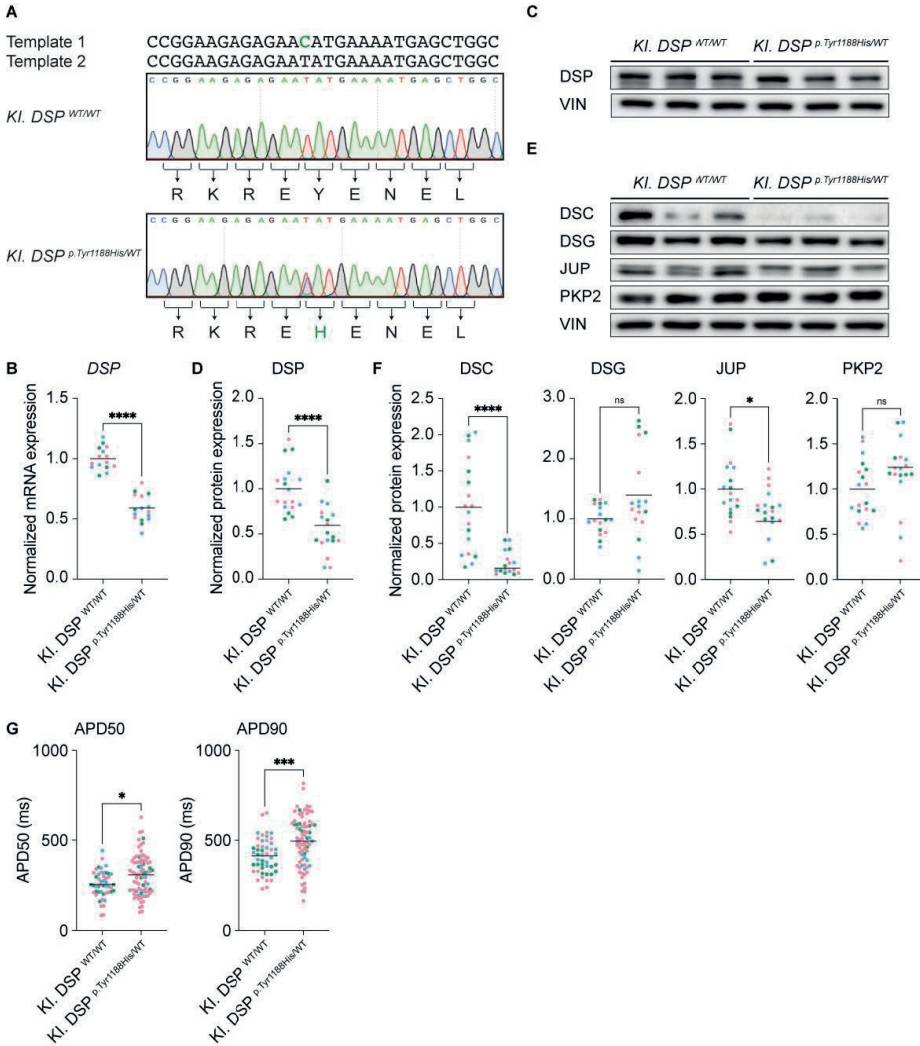


Figure 2. hiPSC-derived KI. DSP^{p.Tyr1188His/WT} cardiomyocytes corroborate findings observed in patient-derived cardiomyocytes. (A) Sanger sequencing traces of the control and knockin hiPSC lines. The two different DNA templates used to introduce the intended mutation are depicted. Intended mutation is indicated in green. **(B–G)** Molecular and functional analyses on 1-month-old hiPSC-derived cardiomyocytes obtained from three independent experiments. **(B)** Gene expression levels of *DSP* normalized to *GUS*. **(C)** Representative immunoblots for DSP. **(D)** Quantification of DSP protein levels normalized to VIN. **(E)** Representative immunoblots for DSC, DSG, JUP, and PKP2. **(F)** Quantification of the desmosomal protein levels. Values normalized to VIN. **(G)** APD measured at 50% and 90% (*KI. DSP^{WT/WT}*, n=48 cell clusters; *KI. DSP^{p.Tyr1188His/WT}*, n=81 cell clusters) of cardiomyocyte repolarization. Data are plotted as mean. The dots in **(B, D, F, and G)** represent technical replicates, whereas the color of each dot indicates the experimental origin (3 independent experiments; 4–60 technical replicates). Significance has been assessed by a two-tailed unpaired Student’s t test or two-tailed Mann-Whitney test when data were not normally distributed (*p < 0.05, ****p < 0.0001, ns, not significant).

2.3. PITX2 levels are increased in DSP p.Tyr1188His/WT cardiomyocytes and repress expression of structural and ion-handling genes

The observation that many ion channels, indispensable for proper electrophysiological function of the cardiomyocytes, were dysregulated in Pa. and KI. DSP^{p.Tyr1188His/WT} cardiomyocytes prompted us to investigate potential upstream effectors. Martin and coworkers previously reported that the transcription factor paired-like homeodomain 2 (PITX2) dictates a gene network in mouse postnatal atrial cardiomyocytes encompassing ion-channel and calcium handling genes as well as genes involved in stabilizing cell-cell junctions². In that study, the authors combined chromatin immunoprecipitation sequencing and transcriptomics on conditional *Pitx2* knockout mice, demonstrating that a loss of *Pitx2* in cardiomyocytes results in upregulation of *Dsp*, *Gja1*, and *Scn5a*, indicating that PITX2 acts as a repressor for these genes. In humans, mutations in genomic loci adjacent to or within *PITX2*, thereby affecting its expression, predisposes the heart to atrial arrhythmias³⁻⁶. mRNA analyses and subsequent validation experiments revealed an induction of *PITX2* in Pa. and KI. DSP^{p.Tyr1188His/WT} cardiomyocytes (**Figure 3A**), which was confirmed at the protein level (**Figures 3B–3D**). To evaluate whether PITX2 could evoke a similar response in an independent model, we used lentivirus to overexpress *PITX2* (lenti-PITX2) for 7 days in healthy hiPSC-derived control cardiomyocytes. *PITX2* levels were induced approximately 20-fold compared with the baseline condition (**Figures 4A and 4C**). The PITX2 targets *DSP*, *GJA1*, and *SCN5A* were all repressed in lenti-PITX2-treated cardiomyocytes (**Figures 4B and 4C**). On the protein level, we could confirm the induction of PITX2 and reduced levels of DSP and Cx43 (**Figures 3E and 3F**). Functionally, we observed a significant prolongation of the APD at 90% of cardiomyocyte repolarization (**Figure 3G**). On the contrary, knockdown of *PITX2* gene expression in control cardiomyocytes induced the expression of *DSP*, *GJA1*, and *SCN5A* (**Figures 4D–4F**). The APD was shortened in si-PITX2-treated cardiomyocytes at 50% and 90% of repolarization when compared with control (**Figure 4I**). These results demonstrate that PITX2 is induced in Pa. and KI. DSP^{p.Tyr1188His/WT} cardiomyocytes and that PITX2 represses genes vital for cardiomyocyte function.

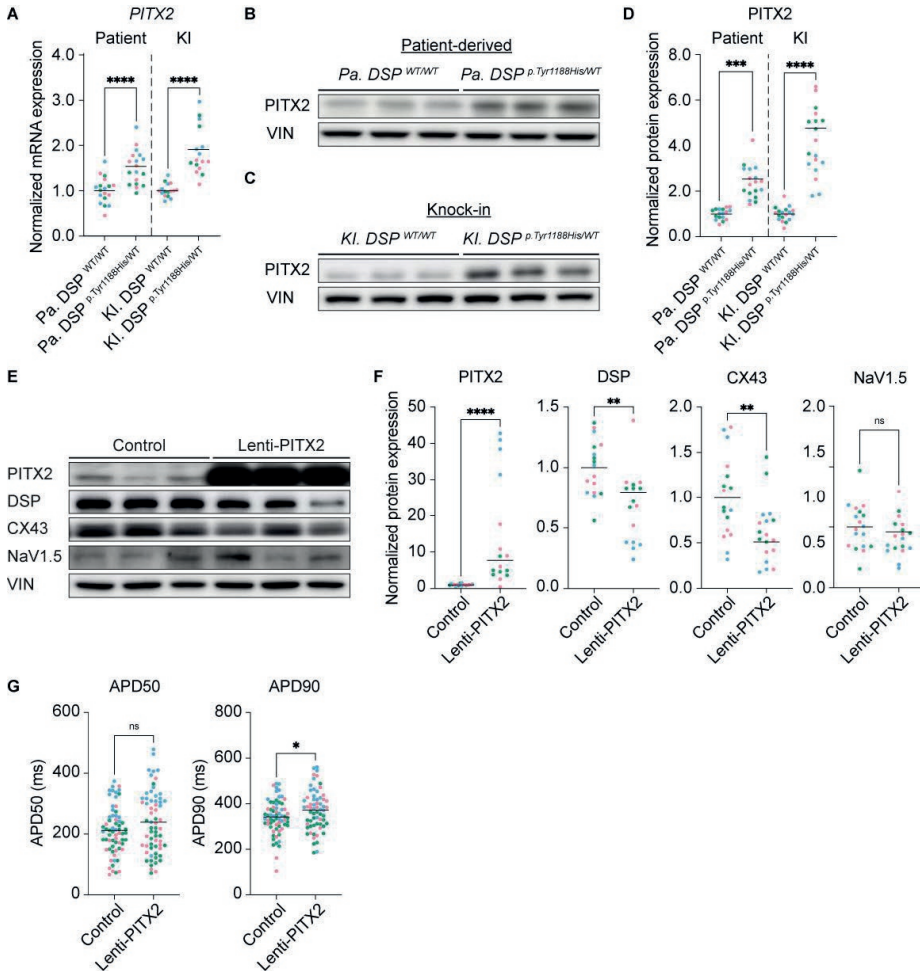


Figure 3. Paired-like homeodomain 2 levels are increased in mutant cardiomyocytes and repress expression of DSP, Cx43, and Nav1.5. (A–D) Molecular analyses on 1-month-old Pa. DSP^{p.Tyr1188His/WT}, KI. DSP^{p.Tyr1188His/WT}, and isogenic control cardiomyocytes. (A) Gene expression levels for PITX2 normalized to GUS. (B and C) Representative immunoblots for PITX2 in Pa. DSP^{p.Tyr1188His/WT} (B) and KI. DSP^{p.Tyr1188His/WT} (C) cardiomyocytes. (D) Quantification of PITX2 protein levels normalized to VIN. (E–G) Molecular and functional analyses on 1-month-old control hiPSC-derived cardiomyocytes treated with either empty viral particles or particles encoding for PITX2 (lenti-PITX2). (E) Representative immunoblots for PITX2, DSP, Cx43, and Nav1.5. (F) Protein levels of PITX2, DSP, Cx43, and Nav1.5 normalized to VIN. (G) APD measured at 50% and 90% (control, n=66 cell clusters; lenti-PITX2, n=64 cell clusters) of cardiomyocyte repolarization. Data are plotted as mean. The dots in (A, D, F, and G) represent technical replicates, whereas the color of each dot indicates the experimental origin (3 independent experiments; 4–29 technical replicates). Significance has been assessed by a two-tailed unpaired Student’s t test or two-tailed Mann-Whitney test when data were not normally distributed (*p < 0.05, **p < 0.01, ***p < 0.001, ****p < 0.0001, ns, not significant). KI, knockin; Pa., patient.

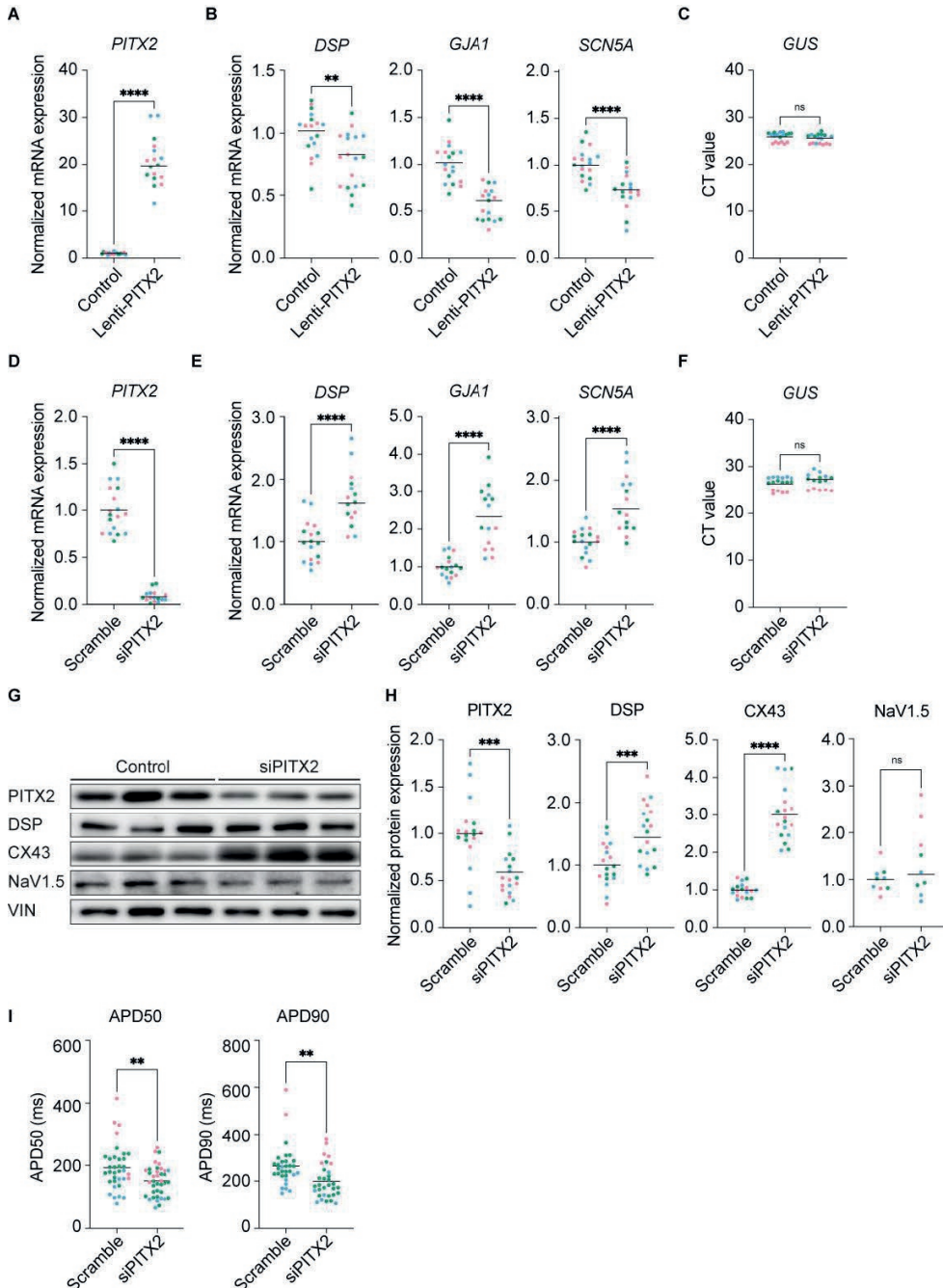


Figure 4. Overexpression and knockdown of paired-like homeodomain 2 in control cardiomyocytes represses and induces expression of cardiac ion- and structural-related genes, respectively. (A-C) Molecular analyses on one-month-old control hiPSC-derived cardiomyocytes treated with either control lentiviral particles or particles encoding for *PITX2* (Lenti-PITX2). Data obtained from three independent experiments. (A) Gene

expression levels for *PITX2*. **(B)** Gene expression levels for *DSP*, *GJA1* and *SCN5A*. **(C)** Cycle threshold (CT) levels for *GUS* in the corresponding experiments. **(D-I)** Molecular and functional analyses on one-month-old control hiPSC-derived cardiomyocytes treated with scramble or siRNA against *PITX2*. Data obtained from three independent experiments. **(D)** Gene expression levels for *PITX2*. **(E)** Gene expression levels for *DSP*, *GJA1* and *SCN5A* normalized to *GUS*. **(F)** Cycle threshold (CT) levels for *GUS* in the corresponding differentiations. **(G)** Representative immunoblots for *PITX2*, *DSP*, *Cx43* and *Nav1.5*. **(H)** Quantification of *PITX2*, *DSP*, *Cx43* and *Nav1.5* protein levels. Values normalized to *VIN*. **(I)** Action potential duration (APD) measured at 50% and 90% of repolarization (control, n=31 cell clusters; si*PITX2*, n=32 cell clusters). Data plotted as mean. The dots in **(A-F and H-I)** represent technical replicates, whereas the color of each dot indicates the experimental origin (3 independent experiments; 4-20 technical replicates). Significance has been assessed by a two-tailed unpaired Student's t-test or two-tailed Mann-Whitney test when data were not normally distributed (* P-value < 0.05, ** P-value < 0.01, *** P-value < 0.001, **** P-value < 0.0001, ns: not significant).

References

1. Blinova K, Stohman J, Vicente J, et al. Comprehensive Translational Assessment of Human-Induced Pluripotent Stem Cell Derived Cardiomyocytes for Evaluating Drug-Induced Arrhythmias. *Toxicol Sci.* 2017;155(1):234-247.
2. Tao Y, Zhang M, Li L, et al. Pitx2, an atrial fibrillation predisposition gene, directly regulates ion transport and intercalated disc genes. *Circ Cardiovasc Genet.* 2014;7(1):23-32.
3. Chinchilla A, Daimi H, Lozano-Velasco E, et al. PITX2 insufficiency leads to atrial electrical and structural remodeling linked to arrhythmogenesis. *Circ Cardiovasc Genet.* 2011;4(3):269-279.
4. Gudbjartsson DF, Arnar DO, Helgadóttir A, et al. Variants conferring risk of atrial fibrillation on chromosome 4q25. *Nature.* 2007;448(7151):353-357.
5. Kaab S, Darbar D, van Noord C, et al. Large scale replication and meta-analysis of variants on chromosome 4q25 associated with atrial fibrillation. *Eur Heart J.* 2009;30(7):813-819.
6. Van Ouwkerk AF, Hall AW, Kadow ZA, et al. Epigenetic and Transcriptional Networks Underlying Atrial Fibrillation. *Circ Res.* 2020;127(1):34-50.

Hoyee Tsui^{1*}
Sebastiaan J. van Kampen^{1*}
Su Ji Han¹
Viviana Meraviglia²
Willem B. van Ham³
Simona Casini⁴
Petra van der Kraak⁵
Aryan Vink⁵
Xiaohe Yin⁶
Manuel Mayr⁶
Alexandre Bossu³
Gerard A. Marchal⁴
Jantine Monshouwer-Kloots¹
Joep Eding¹
Danielle Versteeg¹
Hesther de Ruiter¹
Karel Bezstarosti⁷
Judith Groeneweg⁸
Sjoerd J. Klaasen⁹
Linda W. van Laake⁸
Jeroen A.A. Demmers⁷
Geert J.P.L. Kops⁹
Christine L. Mummery²
Toon A.B. van Veen³
Carol Ann Remme⁴
Milena Bellin²
Eva van Rooij^{1,8}

¹Hubrecht Institute, KNAW, University Medical Center Utrecht, The Netherlands

²Department of Anatomy and Embryology, Leiden University Medical Center, The Netherlands

³Department of Medical Physiology, University Medical Center Utrecht, The Netherlands

⁴Department of Clinical and Experimental Cardiology, University Medical Center Amsterdam, The Netherlands

⁵Department of Pathology, University Medical Center Utrecht, The Netherlands

⁶James Black Centre, King's College, University of London, United Kingdom

⁷Proteomics Center, Erasmus Medical Center Rotterdam, The Netherlands

⁸Department of Cardiology, University Medical Center Utrecht, The Netherlands

⁹Oncode Institute, Hubrecht Institute, KNAW, University Medical Center Utrecht, The Netherlands

*Hoyee Tsui and Sebastiaan J. van Kampen are shared first authors

Chapter VI

Part B

This chapter contains extracts originating from:

**Desmosomal protein degradation
as an underlying cause of
arrhythmogenic cardiomyopathy**

Abstract

Arrhythmogenic cardiomyopathy (ACM) is an inherited progressive cardiac disease. Many patients with ACM harbor mutations in genes encoding desmosomal proteins, predominantly in *plakophilin-2* (*PKP2*). Although the genetic basis of ACM is well characterized, the underlying disease-driving mechanisms remain unresolved. Explanted hearts from patients with ACM showed diminished PKP2 protein compared with healthy hearts, which correlated with reduced levels of desmosomal and adherens junction (AJ) proteins. These proteins were also disorganized in areas of fibrotic remodeling. *In vitro* data from human-induced pluripotent stem cell–derived cardiomyocytes and microtissues carrying the heterozygous *PKP2 c.2013delC* pathogenic mutation also displayed impaired contractility. Knock-in mice carrying the equivalent heterozygous *Pkp2 c.1755delA* mutation recapitulated the changes in desmosomal and AJ proteins and displayed cardiac dysfunction and fibrosis with age. Global proteomics analysis of 4-month-old heterozygous *Pkp2 c.1755delA* hearts indicated involvement of the ubiquitin-proteasome system (UPS) in the underlying pathogenesis. Inhibition of the UPS in mutant mice increased levels of proteins composing the area composita and improved calcium dynamics when measured in isolated cardiomyocytes. Additional proteomics analyses identified several lysine ubiquitination sites on the desmosomal proteins, which appeared more ubiquitinated in mutant mice. In summary, we show that a patient-specific *PKP2* mutation can lead to decreased desmosomal and AJ protein levels through a UPS-dependent mechanism, which preceded cardiac remodeling. These findings suggest that targeting protein degradation pathways and improving desmosomal protein stability may be a potential therapeutic strategy for treatment of ACM.

Keywords: PKP2; arrhythmogenic cardiomyopathy; desmosomes; adherens junctions; ubiquitin-proteasome system; protein degradation

1. Measurements and analysis of calcium transients

Isolation of the cardiomyocytes was performed by Langendorff perfusion as described previously¹. Prior to the measurements, cells were incubated in 1:1000 calcium sensitive dye Fluo-4-AM (ThermoFischer, F14201) in Tyrode solution containing: 130 mM NaCl, 4mM KCl, 1.8 mM CaCl₂, 1.2 mM MgCl₂, 18 mM NaHCO₃, 10 mM HEPES, 10 mM glucose, for 20 minutes at 37 °C. Stock solutions of 1 mM Fluo-4-AM were prepared in DMSO. Cells were placed in Tyrode solution during the recording of the calcium transients at 37 °C. Cells were additionally incubated with 1 μM isoproterenol for 5 minutes in Tyrode solution prior to recordings and were paced at a frequency of 1 Hz by field-stimulation. Recordings were made on a custom-build microscope (Cairn Research, Kent, UK) using a 20x objective. Blue light was used for excitation, using a 482/35 nm excitation filter (Semrock FF01-482/35-25), and captured with a high-speed camera (Andor Zyla 5.5.CL3, Oxford Instruments) using a 514 Long-Pass Emission Filter (Semrock LP02-514RU-25). A custom MATLAB script (DOI: 10.17605/OSF.IO/86UFE) was used for analysis.

2.1. Reduction of cardiac desmosomal and adherens junction protein levels in *Pkp2 c.1755delA/WT* mice

To start exploring disease driving mechanisms in response to the pathogenic *Pkp2* mutation, we performed proteomics analysis on 4-month-old heart lysates of *Pkp2 c.1755delA/WT* mice and WT littermates. This revealed a significant upregulation of 114 proteins and a downregulation of 31 proteins when compared to WT littermates (**Fig. 1A**, Fold Change > 1.25 or < 0.8 and a P-value < 0.05). In addition to plakophilin-2 (PKP2), proteomics data indicated a significant decrease in several other key desmosomal proteins, like plakoglobin (JUP), desmoplakin (DSP), and desmoglein (DSG) in *Pkp2 c.1755delA/WT* mouse heart tissue compared to WT (**Figure 1A and 1B**), which was further confirmed by immunoblot assays (**Figure 1C and 1D**). Although, desmocollin (DSC) was not detected in the proteomics data, immunoblots showed also a decline in DSC in *Pkp2 c.1755delA/WT* mice (**Figure 1C and 1D**).

In addition to desmosomal protein downregulation, proteomics also identified a significant decline in several AJ proteins, such as β-catenin (β-CAT), N-cadherin (N-CAD) and αE-catenin (αE-CAT) (**Figure 1A and 1B**), which could be validated by immunoblot analysis (**Figure 1E and 1F**). The exhibited decrease in AJ proteins is intriguing as maintenance of cell-to-cell adhesion between cardiomyocytes relies on a unique hybrid structure, known as the area composita, which comprises both adherens junction (AJ) and desmosome proteins²⁻⁵. In addition, β-CAT has been linked to the Wnt signaling pathway and inhibition of β-CAT has been shown to drive arrhythmogenic cardiomyopathy (ACM)⁶. Other ACM-related proteins, such as four and a half LIM domains-1 (FHL1) and LIM domain binding-3 (LDB3)⁷⁻¹¹, were also decreased in *Pkp2 c.1755delA/WT* mice compared to WT littermates (**Figure 1B, 1G and 1H**).

proteins involved in protein degradation (yellow) were plotted in a heatmap (n=4 mice per group). Representative immunoblots and the respective protein quantifications for desmosomal (**C and D**), adherens junction (**E and F**) and ACM-linked (**G and H**) proteins in eight-week-old mice (n=6 per group, VIN as loading control). Protein expression data (**D, F, and H**) plotted as mean \pm SEM. Significance has been assessed by a two-tailed Mann-Whitney test (* P-value < 0.05, ** P-value < 0.01, *** P-value < 0.001).

2.2. Proteasomal degradation as the underlying cause of protein decline induced by PKP2 haploinsufficiency

As a proof-of-concept to study the potential involvement of the UPS, we subjected *Pkp2 c.1755delA/WT* mice and control littermates to intraperitoneal injections of MG132, a peptide aldehyde inhibitor of the proteasome^{13,14}, at a dosage of 2 mg/kg/day for 10 consecutive days (**Figure 2A**). Intriguingly, our results demonstrated that MG132 treatment was able to revert the reduction in PKP2, JUP and DSP protein levels in *Pkp2 c.1755delA/WT* mice, while DSG and DSC protein levels remained unchanged (**Figure 2B and 2C**). In addition, protein level of α -CAT was also restored whilst β -CAT and N-CAD levels showed a strong trend of upregulation (**Figure 2D and 2E**).

Earlier studies utilized tamoxifen induced cardiomyocyte specific deletion of *Pkp2* in adult mice to illustrate that the absence of PKP2 protein caused: increased ryanodine receptor sensitivity towards calcium induction, enhanced sarcoplasmic reticulum calcium load, and an increase in the frequency and amplitude of spontaneous calcium release¹⁵⁻¹⁷. The data obtained in these studies, in combination with our proof-of-concept results presented above, led us to examine whether desmosomal protein upregulation achieved through UPS inhibition could also rescue the calcium dysfunction in *Pkp2 c.1755delA/WT* mice. Cardiomyocytes were isolated from Langendorff-perfused hearts from *Pkp2 c.1755delA/WT* mice and control littermates, post intraperitoneal injection of MG132 or saline. Subsequently, calcium transient measurements were recorded at baseline or upon acute isoproterenol induction. As shown in **Figure 2F**, cardiomyocytes from saline treated *Pkp2 c.1755delA/WT* mice, at baseline, show an increased calcium amplitude and a reduction in top peak width (10% of total peak duration) when compared to control littermates. In addition, these cardiomyocytes also displayed a lack of response towards acute isoproterenol induction. These calcium irregularities were rescued in cardiomyocytes derived from MG132 treated *Pkp2 c.1755delA/WT* mice, demonstrated by a reduction of the baseline calcium amplitude and an increase in top peak width, as well as recovery of the acute isoproterenol response (**Figure 2F**).

We recognized that due to potential toxicity caused by chronic UPS inhibition, non-specific inhibition would not be a viable treatment option, and instead, a more specific inhibition target would be required¹⁸. Thus, following up on the lessons learned from our proof-of-concept data, we aimed to identify the specific protein ubiquitination sites on the target proteins in the presence of this pathological mutation.

Ubiquitination of the target protein involves three ligase enzymes, E1 (ubiquitin activating), E2 (ubiquitin conjugating) and E3 (substrate binding) ligases, where substrate specificity is conferred by the latter^{19,20}. Due to the low stoichiometry of ubiquitinated proteins, efforts to decipher the cardiac ubiquitinome through mass spectrometry proteomics has been challenging¹⁹. Enrichment for ubiquitinated proteins through genetically engineered tagged ubiquitin has proven to be laborious and suffers from interference through endogenous proteins^{21,22}. In this study, we took advantage of highly specific antibodies that recognize the residual di-glycine remnant present at substrate ubiquitination lysine sites post-trypsin cleavage, allowing us to enrich for ubiquitinated proteins preceding mass spectrometry analysis^{22,23}. By performing ubiquitin proteomics analysis on *Pkp2 c.1755delA/WT* mouse heart samples, we identified a total of 1920 differentially regulated ubiquitinated protein sites when compared to control littermates. A total of 1722 protein sites (from 534 proteins) demonstrated increased ubiquitination in *Pkp2 c.1755delA/WT* hearts compared to WT littermates. Furthermore, we could identify the exact lysine (K) ubiquitination site(s) on the target proteins, PKP2 (K134), JUP (K57) and DSP (K166, K871, K1045, K1166, K1206, K2373, K2535, K2614, K2715, K2738 and K2808), N-CAD (K766) and α -CAT (K12, K16, K45, K163, K577 and K683) (**Figure 2G**).

Together these data indicate that the observed protein degradation in *Pkp2 c.1755delA/WT* mice is, at least in part, mediated by the UPS consequent to ubiquitination on target proteins. This is intriguing as increased ubiquitination on PKP2, in response to a haploinsufficient pathogenic *Pkp2* variation, indicates that the quantity of functioning PKP2 could be lower than the originally expected 50%. Identification of the specific ubiquitination site on PKP2 generates the opportunity for modulating these site-specific events in an effort to stabilize PKP2 to sufficient levels and thus prevention of the deleterious downstream effects.

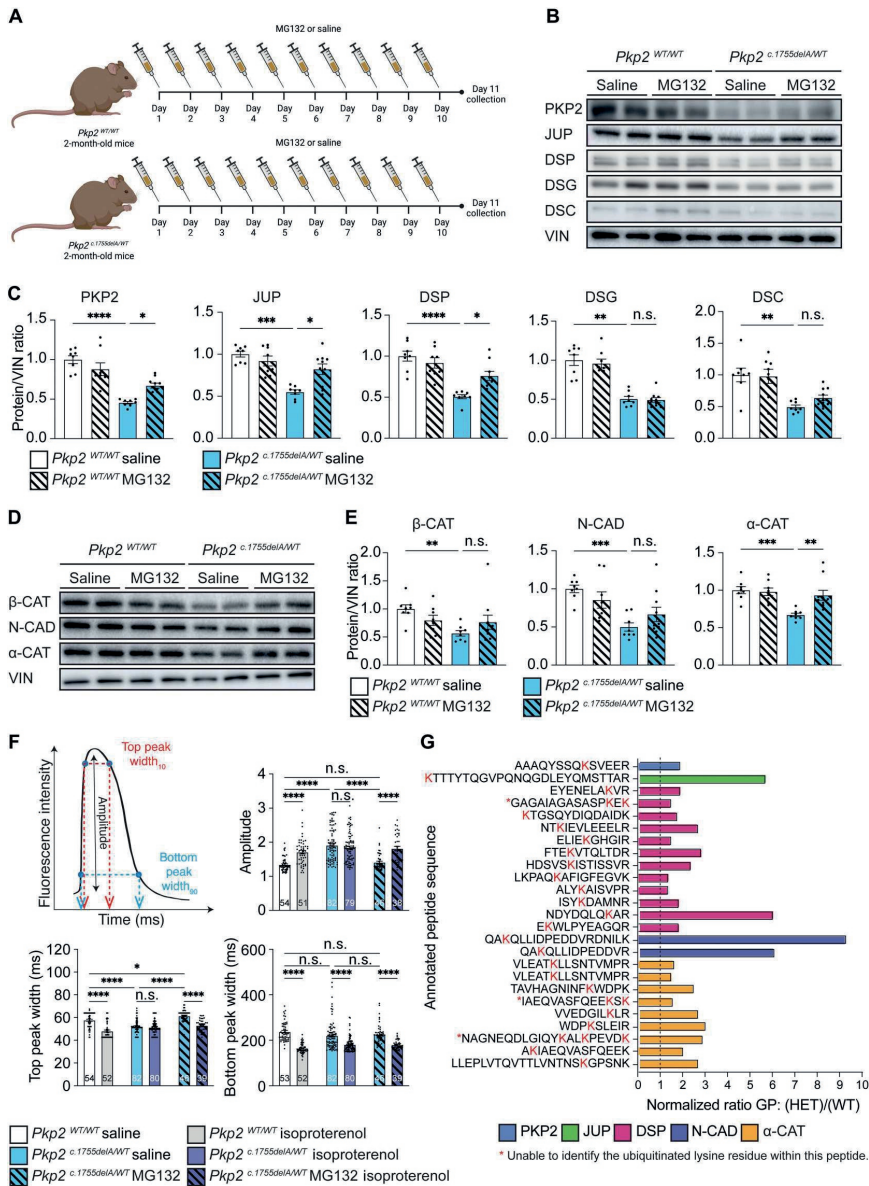


Figure 2. UPS inhibition in *Pkp2*^{c.1755delA/WT} mice increases desmosomal protein abundance and improves calcium dysregulation. **(A)** Schematic outlining UPS inhibition treatment with MG132 in 8-week-old mice. **(B-E)** Representative immunoblots ($n=2$ per group) and the respective quantification for desmosomal **(B and C)** and AJ **(D and E)** proteins on ventricular tissue obtained from mice treated with saline or MG132 ($n=8$ to 10 mice per group). **(F)** Assessment of calcium transients in cardiomyocytes obtained from Langendorff-perfused mouse hearts treated with saline or MG132 ($n=3$ mice per group). Isolated cardiomyocytes were treated with either vehicle or isoproterenol. Shown are the calcium transient amplitude, top peak width (10% of total peak duration),

and bottom peak width (90% of total peak duration). **(G)** Abundance of desmosomal and AJ protein ubiquitination in ventricular tissue obtained from *Pkp2* *WT/WT* and *Pkp2* *c.1755delA/WT* mice using proteomics combined with enrichment for diglycine peptides (ubiquitinated proteins). Lysine (K) residues marked in red were ubiquitinated. Protein expression and electrophysiology data **(C, E, and F)** were plotted as means \pm SEM. **(C and E)**, and significance has been assessed by a Kruskal-Wallis test with Dunn's multiple comparison test; $\alpha=0.05$. For **(F)**, significance has been assessed by an ordinary two-way ANOVA test with Tukey's multiple comparison test with a single pooled variance (*P < 0.05; **P < 0.01; ***P < 0.001; ****P < 0.0001). GP, global proteome abundance; HET, *Pkp2* *c.1755delA/WT* mice; WT, *Pkp2* *WT/WT* mice.

References

1. Louch WE, Sheehan KA, Wolska BM. Methods in cardiomyocyte isolation, culture, and gene transfer. *J Mol Cell Cardiol.* 2011;51(3):288-298.
2. Patel DM, Green KJ. Desmosomes in the heart: a review of clinical and mechanistic analyses. *Cell Commun Adhes.* 2014;21(3):109-128.
3. Franke WW, Borrmann CM, Grund C, Pieperhoff S. The area composita of adhering junctions connecting heart muscle cells of vertebrates. I. Molecular definition in intercalated disks of cardiomyocytes by immunoelectron microscopy of desmosomal proteins. *Eur J Cell Biol.* 2006;85(2):69-82.
4. Sato PY, Coombs W, Lin X, et al. Interactions between ankyrin-G, Plakophilin-2, and Connexin43 at the cardiac intercalated disc. *Circ Res.* 2011;109(2):193-201.
5. Nekrasova O, Green KJ. Desmosome assembly and dynamics. *Trends Cell Biol.* 2013;23(11):537-546.
6. Chen SN, Gurha P, Lombardi R, Ruggiero A, Willerson JT, Marian AJ. The hippo pathway is activated and is a causal mechanism for adipogenesis in arrhythmogenic cardiomyopathy. *Circ Res.* 2014;114(3):454-468.
7. Mayosi BM, Fish M, Shaboodien G, et al. Identification of Cadherin 2 (CDH2) Mutations in Arrhythmogenic Right Ventricular Cardiomyopathy. *Circ Cardiovasc Genet.* 2017;10(2):e001605.
8. Sheikh F, Chen Y, Liang X, et al. alpha-E-catenin inactivation disrupts the cardiomyocyte adherens junction, resulting in cardiomyopathy and susceptibility to wall rupture. *Circulation.* 2006;114(10):1046-1055.
9. Chiarella SE, Rabin EE, Ostilla LA, Flozak AS, Gottardi CJ. alphaT-catenin: A developmentally dispensable, disease-linked member of the alpha-catenin family. *Tissue Barriers.* 2018;6(2):e1463896.
10. San Roman I, Navarro M, Martinez F, et al. Unclassifiable arrhythmic cardiomyopathy associated with Emery-Dreifuss caused by a mutation in FHL1. *Clin Genet.* 2016;90(2):171-176.
11. Lopez-Ayala JM, Ortiz-Genga M, Gomez-Milanes I, et al. A mutation in the Z-line Cypher/ZASP protein is associated with arrhythmogenic right ventricular cardiomyopathy. *Clin Genet.* 2015;88(2):172-176.
12. Zientara-Rytter K, Subramani S. The Roles of Ubiquitin-Binding Protein Shuttles in the Degradative Fate of Ubiquitinated Proteins in the Ubiquitin-Proteasome System and Autophagy. *Cells.* 2019;8(1):40.
13. Kisselev AF, Goldberg AL. Proteasome inhibitors: from research tools to drug candidates. *Chem Biol.* 2001;8(8):739-758.
14. Zhang XM, Li YC, Chen P, et al. MG-132 attenuates cardiac deterioration of viral myocarditis via AMPK pathway. *Biomed Pharmacother.* 2020;126:110091.
15. Kim JC, Perez-Hernandez M, Alvarado FJ, et al. Disruption of Ca(2+)(i) Homeostasis and Connexin 43 Hemichannel Function in the Right Ventricle Precedes Overt Arrhythmogenic Cardiomyopathy in Plakophilin-2-Deficient Mice. *Circulation.* 2019;140(12):1015-1030.

16. Van Opbergen CJM, Bagwan N, Maurya SR, et al. Exercise Causes Arrhythmogenic Remodeling of Intracellular Calcium Dynamics in Plakophilin-2-Deficient Hearts. *Circulation*. 2022;145(19):1480-1496.
17. Cerrone M, Montnach J, Lin X, et al. Plakophilin-2 is required for transcription of genes that control calcium cycling and cardiac rhythm. *Nat Commun*. 2017;8(1):106.
18. Das A, Dasgupta S, Gong Y, et al. Cardiotoxicity as an adverse effect of immunomodulatory drugs and proteasome inhibitors in multiple myeloma: A network meta-analysis of randomized clinical trials. *Hematol Oncol*. 2022;40(2):233-242.
19. Chen PC, Na CH, Peng J. Quantitative proteomics to decipher ubiquitin signaling. *Amino Acids*. 2012;43(3):1049-1060.
20. Pickart CM. Back to the future with ubiquitin. *Cell*. 2004;116(2):181-190.
21. Jeon HB, Choi ES, Yoon JH, et al. A proteomics approach to identify the ubiquitinated proteins in mouse heart. *Biochem Biophys Res Commun*. 2007;357(3):731-736.
22. Udeshi ND, Mertins P, Svinkina T, Carr SA. Large-scale identification of ubiquitination sites by mass spectrometry. *Nat Protoc*. 2013;8(10):1950-1960.
23. Van der Wal L, Bezstarosti K, Sap KA, et al. Improvement of ubiquitylation site detection by Orbitrap mass spectrometry. *J Proteomics*. 2018;172:49-56.

Monika M. Gladka^{1,2}

Arwa Kohela^{1,3}

Anne de Leeuw¹

Bas Molenaar¹

Danielle Versteeg¹

Lieneke Kooijman¹

Mariska van Geldorp¹

Willem B. van Ham⁴

Jody J. Haigh⁵

Toon A.B. van Veen⁴

Eva van Rooij^{1,6}

¹Hubrecht Institute, KNAW, University Medical Center Utrecht, The Netherlands

²Department of Medical Biology, Amsterdam University Medical Center, The Netherlands

³School of Biotechnology, Nile University, Egypt

⁴Department of Medical Physiology, University Medical Center Utrecht, The Netherlands

⁵Department of Pharmacology and Therapeutics, University of Manitoba, Canada

⁶Department of Cardiology, University Medical Center Utrecht, The Netherlands

Chapter VI

Part C

This chapter contains extracts originating from:

Hypoxia-responsive ZEB2 regulates a network of calcium handling genes in the injured heart

Submitted

Abstract

Intracellular calcium (Ca^{2+}) overload is known to play a critical role in the development of cardiac dysfunction. Despite the remarkable improvement in managing the progression of heart disease, developing effective therapies for heart failure (HF) remains a challenge. A better understanding of the molecular mechanisms that threat physiological Ca^{2+} homeostasis and contractility in the injured heart could be of therapeutic value. Here, we report that transcription factor Zinc finger E-box-binding homeobox 2 (ZEB2) is induced by Hypoxia-inducible factor 1-alpha (HIF1a) in hypoxic cardiomyocytes and this factor regulates a network of genes involved in Ca^{2+} -handling and contractility during ischemic heart disease. Gain- and loss-of-function studies in genetically engineered mouse models revealed that *Zeb2* expression in cardiomyocytes is necessary and sufficient to protect the heart against ischemia-induced diastolic dysfunction and structural remodeling. Moreover, RNA sequencing (RNA-seq) of *Zeb2*-overexpressing (*Zeb2* cTg) hearts post-injury implicated ZEB2 in regulating numerous Ca^{2+} -handling and contractility-related genes. Mechanistically, *Zeb2* overexpression increased the phosphorylation of phospholamban (PLN) at both serine-16 and threonine-17, implying enhanced activity of sarcoplasmic reticulum Ca^{2+} -ATPase (SERCA2a), thereby augmenting sarcoplasmic reticulum (SR) Ca^{2+} uptake and contractility. Furthermore, we observed a decrease in the activity of Ca^{2+} -dependent calcineurin/NFAT signaling in *Zeb2* cTg hearts, which is the main driver of pathological cardiac remodeling. On a post-transcriptional level, we showed that ZEB2 expression can be regulated by the cardiomyocyte-specific microRNA-208a (miR-208a). Blocking the function of miR-208a with anti-miR-208a increased *Zeb2* expression in the heart and effectively protected the development of pathological cardiac hypertrophy. Together, we present ZEB2 as a central regulator of contractility and Ca^{2+} -homeostasis in the mammalian heart. Further mechanistic understanding of the role of ZEB2 in regulating Ca^{2+} homeostasis in cardiomyocytes is an essential step towards the development of improved therapies for HF.

Keywords: ZEB2; ischemic heart disease; HIF1a; calcium handling; contractility

1. Measurements and analysis of calcium transients

Cardiomyocytes were isolated as described before¹. Cells were subsequently incubated in 1:1000 calcium-sensitive dye Fluo-4-AM (ThermoFischer, F14201) in Tyrode solution containing (mM): NaCl (130), KCl (4), CaCl₂ (1.8), MgCl₂ (1.2), NaHCO₃ (18), HEPES (10), glucose (10), for 15 minutes at 37 °C. Cells were placed in Tyrode solution during the recording of the calcium transients and were paced at 1Hz, 3Hz, and 5Hz by field stimulation. Recordings were made on a custom-built microscope (Cairn Research, Kent, UK) using a 10x objective. Blue light was used for excitation, using a 482/35 excitation filter (Semrock FF01-482/35-25), and captured with a high-speed camera (Andor Zyla 5.5.CL3, Oxford Instruments) using a 514 long-pass emission filter (Semrock LP02-514RU-25). Analysis was performed using a custom MATLAB script (DOI: 10.17605/OSF.IO/86UFE).

2.1. Cardiomyocyte-specific ZEB2 overexpression protects from ischemia-reperfusion induced pathological hypertrophy and contractile dysfunction

To study the *in vivo* effects of Zinc finger E-box-binding homeobox 2 (ZEB2) induction in cardiomyocytes, we generated cardiomyocyte-specific *Zeb2*-overexpressing mice (*Zeb2* cTg) as described previously², and subjected them to ischemia reperfusion (IR) injury. Functional and molecular analysis 14 days after surgery confirmed the upregulation of ZEB2 at mRNA and protein levels in *Zeb2* cTg mice compared to their wild-type littermates (*Zeb2* WT) (**Figure 1A-1D**). Echocardiographical measurements showed an improvement in function and a better preserved cardiac morphology in *Zeb2* cTg mice (**Figure 1E-1G**). Additionally, heart weight to tibia length ratio (HW/TL) indicated a reduction in pathological hypertrophy in *Zeb2* cTg mice post-IR compared to WT controls (**Figure 1H**). This was confirmed by a reduction in the surface area of cardiomyocytes localized in the border zone and remote areas of the injured hearts (**Figure 1I-1J**).

Calcineurin is a phosphatase that upon increased levels of cytosolic Ca²⁺ dephosphorylates nuclear factor of activated T cells (NFAT), which in turn translocates to the nucleus to activate a hypertrophic gene program^{3,4}. While several NFAT isoforms have been detected in the heart^{5,6}, NFATc3 plays a dominant role in cardiac hypertrophic signaling⁷. In line with the pro-hypertrophic role of the Calcineurin/NFAT signaling pathway, we observed significantly higher levels of NFATc3 phosphorylation (p-NFATc3) in *Zeb2* cTg post-IR hearts compared to the *Zeb2* WT group while total NFATc3 remained unaltered (t-NFATc3) (**Figure 1K-1M**), implying less calcineurin activity upon increased ZEB2 levels. Since Calcineurin is activated during an intracellular increase in Ca²⁺^{8,9}, we next examined whether the Ca²⁺ handling machinery was affected in *Zeb2*-overexpressing hearts. Phospholamban (PLN) is a key regulator of cardiac contractility that modulates Ca²⁺ sequestration in the sarcoplasmic reticulum (SR) via modulation of the Sarco/endoplasmic reticulum Ca²⁺ (SERCA2a) activity. Phosphorylation of PLN relieves the natural inhibitory effect of PLN on SERCA2a, which leads to a faster relaxation and an

increase in force of contraction^{10,11}. This can occur through beta-adrenergic stimulation which leads to enhanced cyclic AMP-dependent protein kinase A activity and subsequent phosphorylation of PLN at serine 16 (S16) or the activation of the Ca²⁺/calmodulin dependent CamKII

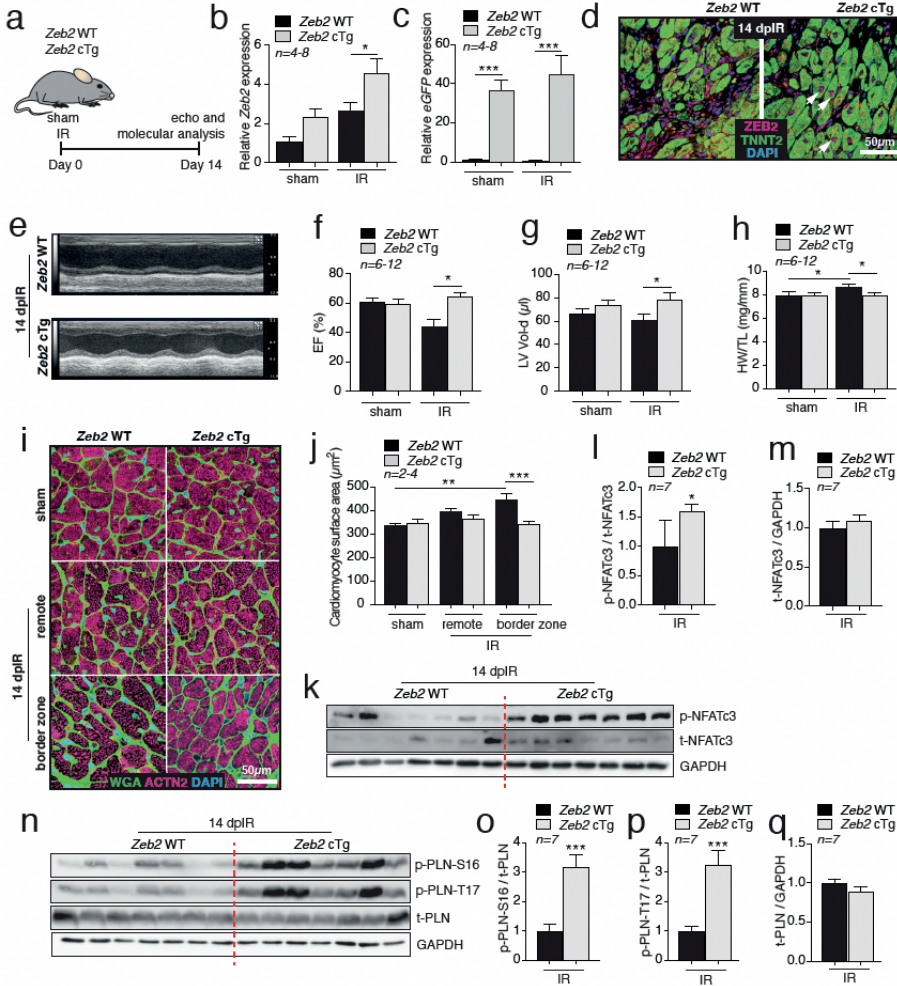


Figure 1. Cardiomyocyte-specific ZEB2 overexpression protects from ischemia-induced pathological hypertrophy and contractile dysfunction. (A) Study design. (B and C) qPCR analysis of (B) Zeb2 and (C) eGFP (Ct values) in hearts from Zeb2 WT and Zeb2 cTg mice post sham or IR surgeries. (D) Representative immunofluorescence staining of ZEB2 and TNNT2 in hearts from Zeb2 WT and Zeb2 cTg mice 14 days post-IR (dpIR). (E) Representative M-mode images of Zeb2 WT and Zeb2 cTg mice 14 dpIR. (F-H) Quantification of (F) ejection fraction (EF), (G) left ventricular volume in diastole (LV Vol-d), (H) heart weight to tibia length ratio (HW/TL) in Zeb2 WT and Zeb2 cTg mice post-surgery. (I) WGA staining to show cardiomyocyte surface area and (J) its quantification. (K-Q) Western blot analysis of (K and N) the indicated proteins and (L, M, O-Q) their

quantification in *Zeb2* WT and *Zeb2* cTg mice 14 dpIR. n (biological replicates) is indicated in the figures. White arrows show ZEB2-positive cardiomyocytes. Data are represented as mean \pm SEM, * p < 0.05, ** p < 0.01, *** p < 0.001 using one-way ANOVA followed by Sidak's multiple comparison test (**B, C, F, G, and H**), compared to sham using one-way ANOVA followed by Dunnett's multiple comparison test (**J**) or compared to *Zeb2* WT using unpaired, two-tailed Student's t-test (**L, M, O, P, and Q**).

resulting in phosphorylation at threonine 17 (T17)^{12,13}. Cardiomyocyte-specific overexpression of *Zeb2* increased PLN phosphorylation at both S16 and T17 (**Figure 1N-1Q**), likely contributing to the enhanced cardiac contractility observed in these mice after injury. Together, these data indicate that *Zeb2* overexpression in cardiomyocytes prevents cardiac dysfunction and cardiomyocyte hypertrophy post-ischemic injury.

2.2. ZEB2 improves Ca²⁺ handling in cardiomyocytes after injury

Given the observed changes in contractility and expression of Ca²⁺-handling genes, we next measured Ca²⁺ levels in adult cardiomyocytes isolated from *Zeb2* WT and *Zeb2* cTg mice post-IR. Isolated cardiomyocytes were incubated with the Ca²⁺-sensitive dye Fluo-4-AM, after which changes in signal intensity, indicative of Ca²⁺ transients, were measured at different pacing frequencies (1, 3, and 5 Hz) (**Figure 2A-2C**). *Zeb2*-overexpressing cardiomyocytes showed increased transient amplitudes at all applied frequencies (**Figure 2D-2F**). While no differences were seen in rising time, longer decay times were observed in cells from *Zeb2* cTg mice at 1Hz and 3Hz (**Figure 2G-2I**). The increased decay time reflected an increased amount of Ca²⁺ in the cytosol at these frequencies, as the difference in decay time was absent at 5Hz. Interestingly, the regression slope of the decay time in cardiomyocytes from *Zeb2* cTg mice at all pacing frequencies showed a steeper slope, indicating a shorter decay time at higher frequencies (**Figure 2J-2K**). These data demonstrate that cardiomyocytes isolated from *Zeb2* cTg hearts have improved Ca²⁺ reuptake after IR injury, which can potentially be contributing to the overall enhanced cardiac function.

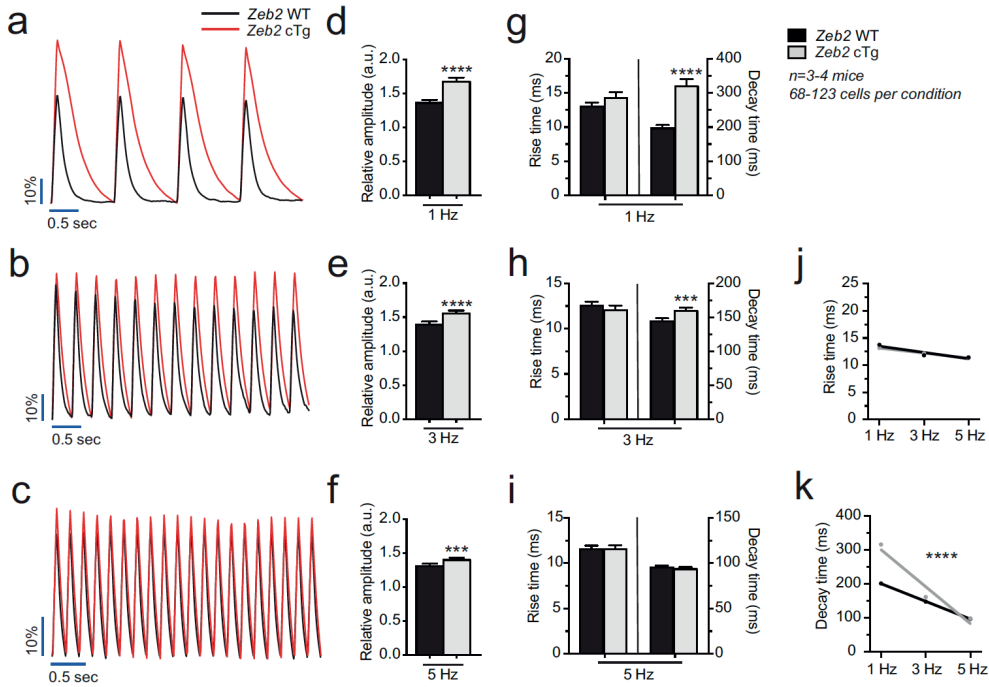


Figure 2. ZEB2 overexpression improves Ca²⁺ handling in cardiomyocytes after injury. (A-C) Representative analysis of Ca²⁺ transients in cardiomyocytes isolated from Zeb2 WT and Zeb2 cTg mice 14 days post-IR (dpIR) exposed to a Ca²⁺-sensitive dye after different stimulation frequencies. (D-F) Quantification of relative Ca transient amplitude. (G-I) Quantification of rise time, defined as the time from baseline to transient peak, and decay time, defined as the time from the transient peak back to baseline. (J and K) Slope of frequency-dependency of rise and decay time. n (biological replicates) is indicated in the figures. Data are represented as mean ± SEM, ***p < 0.001, ****p < 0.0001 compared to Zeb2 WT using unpaired, two-tailed Student's t-test (D, E, F, G, H, and I). Linear regression analysis was performed for slope comparisons (J and K).

References

1. Louch WE, Sheehan KA, Wolska BM. Methods in cardiomyocyte isolation, culture, and gene transfer. *J Mol Cell Cardiol.* 2011;51(3):288-298.
2. Gladka MM, Kohela A, Molenaar B, et al. Cardiomyocytes stimulate angiogenesis after ischemic injury in a ZEB2-dependent manner. *Nat Commun.* 2021;12(1):84.
3. Wilkins BJ, Dai YS, Bueno OF, et al. Calcineurin/NFAT coupling participates in pathological, but not physiological, cardiac hypertrophy. *Circ Res.* 2004;94(1):110-118.
4. Molkenin JD, Lu JR, Antos CL, et al. A calcineurin-dependent transcriptional pathway for cardiac hypertrophy. *Cell.* 1998;93(2):215-228.
5. Rinne A, Kapur N, Molkenin JD, et al. Isoform- and tissue-specific regulation of the Ca(2+)-sensitive transcription factor NFAT in cardiac myocytes and heart failure. *Am J Physiol Heart Circ Physiol.* 2010;298(6):H2001-2009.
6. Pu WT, Ma Q, Izumo S. NFAT transcription factors are critical survival factors that inhibit cardiomyocyte apoptosis during phenylephrine stimulation in vitro. *Circ Res.* 2003;92(7):725-731.
7. Wilkins BJ, De Windt LJ, Bueno OF, et al. Targeted disruption of NFATc3, but not NFATc4, reveals an intrinsic defect in calcineurin-mediated cardiac hypertrophic growth. *Mol Cell Biol.* 2002;22(21):7603-7613.
8. Wilkins BJ, Molkenin JD. Calcium-calcineurin signaling in the regulation of cardiac hypertrophy. *Biochem Biophys Res Commun.* 2004;322(4):1178-1191.
9. Creamer TP. Calcineurin. *Cell Commun Signal.* 2020;18(1):137.
10. Haghghi K, Bidwell P, Kranias EG. Phospholamban interactome in cardiac contractility and survival: A new vision of an old friend. *J Mol Cell Cardiol.* 2014;77:160-167.
11. Koss KL, Kranias EG. Phospholamban: a prominent regulator of myocardial contractility. *Circ Res.* 1996;79(6):1059-1063.
12. Zhang YH, Zhang MH, Sears CE, et al. Reduced phospholamban phosphorylation is associated with impaired relaxation in left ventricular myocytes from neuronal NO synthase-deficient mice. *Circ Res.* 2008;102(2):242-249.
13. Akaike T, Du N, Lu G, Minamisawa S, Wang Y, Ruan H. A Sarcoplasmic Reticulum Localized Protein Phosphatase Regulates Phospholamban Phosphorylation and Promotes Ischemia Reperfusion Injury in the Heart. *JACC Basic Transl Sci.* 2017;2(2):160-180.

Willem B. van Ham¹

¹Department of Medical Physiology, University Medical Center Utrecht, The Netherlands

Chapter VI

Discussion

**Electrophysiological disturbances in
inherited and acquired
cardiomyopathies**

Arrhythmogenic and ischemic cardiomyopathy

In this chapter, we described two studies in which arrhythmogenic cardiomyopathy (ACM)-associated patient-specific variants in the desmosomal proteins desmoplakin (DSP) and plakophilin-2 (PKP2) were integrated in human induced pluripotent stem cell derived cardiomyocyte (hiPSC-CM) lines and a mouse model, respectively. Using the DSP hiPSC-CM lines, we were able to show that this patient-specific pathogenic variant causes a general disturbance of protein levels of components that form the intercalated disc (ID), which seems to contribute to the clinical ACM phenotype. Both patient and knock-in mutated DSP lines had increased levels of the transcription factor paired-like homeodomain 2 (PITX2) protein, which has been linked to arrhythmogenic predisposition^{1,2}. We observed prolonged action potentials in these hiPSC-CM lines, which through modulation of PITX2 could be reproduced and reversed. In the mutated *Pkp2* mouse hearts, again numerous ID protein levels were decreased similarly as the hiPSC-CM lines that we studied. In addition, components of the ubiquitin-proteasome system (UPS) were increased, identifying the importance of protein degradation in ACM. Using the proteasome inhibitor MG132, we were able to demonstrate the reversal of desmosomal protein degradation, which also led to improved calcium handling in isolated cardiomyocytes.

In the third study described in this chapter, we studied the intervention of cardiomyocyte dysfunction in ischemic heart disease (IHD). The observed calcium overload in IHD leads to cardiac dysfunction by means of impaired contractility and relaxation^{3,4}. Importantly, the cardioprotective transcription factor Zinc finger E-box-binding homeobox 2 (ZEB2) regulates a network of calcium handling genes. Our data show that overexpression of *Zeb2* in a mouse model of ischemia and reperfusion resulted in improved cardiac contractility and relaxation. Additionally, calcium removal from the cytosol, resulting in improved calcium handling, was enhanced in isolated cardiomyocytes.

The use of hiPSC-CMs allows for introduction of patient-specific genetic variants and experimental phenotyping of disease pathologies⁵⁻⁷. Although we observed prolonged action potentials in all mutated DSP lines, hinting towards the electrical disturbances seen in ACM patients, the cause of this lengthening is still unknown. To completely understand the mechanics behind action potential alterations, the lack of knowledge on the effects of e.g. repolarization currents and calcium homeostasis should be resolved. However, while hiPSC-CMs have been shown to recapitulate many aspects of ACM⁸, their morphological and electrophysiological properties still remain immature, hampering these investigations. The use of adult mouse cardiomyocytes only partly solves this issue, as they are electromechanically mature, but substantially differ from human adult cardiomyocytes in ion current composition and action potential formation⁹.

Complete inhibition of the UPS like we experimentally applied, will not be a feasible treatment option, as removal of mis-folded proteins is essential in the prevention of proteotoxicity¹⁰. However, the identified specific ubiquitination sites on desmosomal proteins could aid in developing small molecule inhibitors against these sites or specific ligases. The application of gene editing in these disease models also allows for potential future therapeutic strategies in inherited cardiomyopathies such as ACM. Tremendous strides have been made regarding these techniques, but are mainly limited by precise targeting and delivery, which still lead to potentially toxic and inefficient applications¹¹. While PITX2 suppression could become a therapeutic approach in ACM patients, the viral delivery of healthy genes, e.g. *PKP2*, offers a possibility to restore functional protein levels of mutated genes. Preclinical data in a cardiomyocyte-specific conditional *PKP2* knockout mouse model has already confirmed the promising potential of viral *PKP2* delivery in both early and advanced stages of ACM¹².

While overexpression of *Zeb2* could technically also be achieved in a similar fashion using viral transduction, the use of microRNAs and anti-microRNAs could also prove beneficial^{13,14}. Although not described in this chapter, in this particular study we also evaluated the use of anti-microRNA-208, which is cardiomyocyte-specific, to regulate *ZEB2* expression. Blocking the activity of microRNA-208 resulted in increased *ZEB2* protein levels and improved calcium handling, albeit to a lesser extent when compared to transgenic overexpression of *Zeb2*. However, while this establishes a cardioprotective effect in the remote myocardium, during IHD a part of this myocardium will also be replaced by scar tissue which obviously remains an irreversible condition.

Studying cardiac electrophysiology and calcium homeostasis

In this chapter, we furthermore highlighted the overarching role of electrophysiology and calcium homeostasis in studying patient-specific pathogenic variants of inherited and acquired cardiomyopathies. Where genotypical and phenotypical characteristics of cardiac diseases can vary extensively, disturbances in ion currents are observed in the majority of these pathologies, resulting in altered cardiomyocyte excitability, contractility, relaxation, proliferation, hypertrophy, and toxicity. Expression and functioning of the desmosomal proteins *PKP2* and *DSP* not only influence cell-to-cell contacts, but also regulates e.g. ion channel and gap junction expression, influencing both contractility and electrical conductivity of the myocardium¹⁵⁻¹⁷. The ID proteins β -catenin and N-cadherin were also decreased in our *Pkp2* mutated mouse model and are key players in cell signaling such as the YAP and Wnt pathways. Disruption of these ID components inhibits the activation of these pathways, hampering cardiomyocyte development and survival, and has been implicated in ACM¹⁸⁻²⁰. The effects on calcium handling indicate not only impaired contraction and relaxation, but e.g. calcium overload can also lead to calcium-induced mitochondrial dysfunction, resulting in a hampered metabolic capacity and elevated cell stress which can culminate in cell death. Such metabolic complications have already been identified as an additional mechanism involved

in ACM²¹. Additionally, increased intracellular calcium levels also lead to the activation of the NFAT pathway, responsible for pathological remodeling observed in IHD and general heart failure²²⁻²⁵. Understanding more about calcium handling and disturbances that lead to calcium overload will illuminate exact mechanisms around calcium as central player in these cardiomyopathies.

In all three studies, we utilized the high-throughput applicability of voltage- and calcium sensitive dyes. However, with these dyes parameters are only obtained as arbitrary fluorescence intensities, meaning that absolute values of current densities, voltages, and concentrations cannot be recorded. This can be especially troublesome in diseases like ACM, where cytosolic calcium and calcium overload seem to play an important role^{26,27}. In addition, measuring contractility and relaxation in isolated cardiomyocytes or monolayers of hiPSC-CM lines is not providing very useful information. Using both voltage- and calcium sensitive dyes simultaneously in measurements already improves the data quality, while also clarifying the interconnection between the formation of the action potential and calcium handling. On the opposite, application of the patch clamp technique results in more precise and exact data in terms of ion current densities and action potential formation, which can aid to specific effects on electrophysiological mechanisms once fluorescent dyes have identified e.g. action potential alterations. Automated patch clamp techniques, which are often proposed in studying larger numbers of drugs during cardiotoxicity screenings^{28,29}, are also valuable in phenotyping different patient-specific hiPSC-CMs at a larger scale. Preferably, the use of patient-specific hiPSC-CM should progressively be implemented in more complex three-dimensional cell systems to study acquired and especially inherited cardiomyopathies. Standardizing electrophysiological phenotyping in several disease models within a study, collectively supports the understanding of disease mechanisms and the value of potential therapeutic approaches.

References

1. Chinchilla A, Daimi H, Lozano-Velasco E, et al. PITX2 insufficiency leads to atrial electrical and structural remodeling linked to arrhythmogenesis. *Circ Cardiovasc Genet*. 2011;4(3):269-279.
2. Van Ouwkerk AF, Hall AW, Kadow ZA, et al. Epigenetic and Transcriptional Networks Underlying Atrial Fibrillation. *Circ Res*. 2020;127(1):34-50.
3. Bers DM. Calcium cycling and signaling in cardiac myocytes. *Annu Rev Physiol*. 2008;70:23-49.
4. Wang R, Wang M, He S, Sun G, Sun X. Targeting Calcium Homeostasis in Myocardial Ischemia/Reperfusion Injury: An Overview of Regulatory Mechanisms and Therapeutic Reagents. *Front Pharmacol*. 2020;11:872.
5. Van Mil A, Balk GM, Neef K, et al. Modelling inherited cardiac disease using human induced pluripotent stem cell-derived cardiomyocytes: progress, pitfalls, and potential. *Cardiovasc Res*. 2018;114(14):1828-1842.
6. Casini S, Verkerk AO, Remme CA. Human iPSC-Derived Cardiomyocytes for Investigation of Disease Mechanisms and Therapeutic Strategies in Inherited Arrhythmia Syndromes: Strengths and Limitations. *Cardiovasc Drugs Ther*. 2017;31(3):325-344.
7. Poirier M, Fedida D. The Emergence of Human Induced Pluripotent Stem Cell-Derived Cardiomyocytes (hiPSC-CMs) as a Platform to Model Arrhythmogenic Diseases. *Int J Mol Sci*. 2020;21(2):657.
8. Higo S. Disease modeling of desmosome-related cardiomyopathy using induced pluripotent stem cell-derived cardiomyocytes. *World J Stem Cells*. 2023;15(3):71-82.
9. London B. Cardiac arrhythmias: from (transgenic) mice to men. *J Cardiovasc Electrophysiol*. 2001;12(9):1089-1091.
10. Gilda JE, Gomes AV. Proteasome dysfunction in cardiomyopathies. *J Physiol*. 2017;595(12):4051-4071.
11. Kyriakopoulou E, Monnikhof T, van Rooij E. Gene editing innovations and their applications in cardiomyopathy research. *Dis Model Mech*. 2023;16(5):dmm050088.
12. Van Opbergen CJ, Narayanan B, Sacramento CB, et al. AAV-mediated Delivery of Plakophilin-2a Arrests Progression of Arrhythmogenic Right Ventricular Cardiomyopathy in Murine Hearts: Preclinical Evidence Supporting Gene Therapy in Humans. *bioRxiv*. 2023:2023.2007.2012.548590.
13. Shang R, Lee S, Senavirathne G, Lai EC. microRNAs in action: biogenesis, function and regulation. *Nat Rev Genet*. 2023;24(12):816-833.
14. Lagerbauer B, Engelhardt S. MicroRNAs as therapeutic targets in cardiovascular disease. *J Clin Invest*. 2022;132(11):e159179.
15. Vreeker A, van Stuijvenberg L, Hund TJ, Mohler PJ, Nikkels PG, van Veen TA. Assembly of the cardiac intercalated disk during pre- and postnatal development of the human heart. *PLoS One*. 2014;9(4):e94722.
16. Vermij SH, Abriel H, van Veen TA. Refining the molecular organization of the cardiac intercalated disc. *Cardiovasc Res*. 2017;113(3):259-275.

17. Vite A, Radice GL. N-cadherin/catenin complex as a master regulator of intercalated disc function. *Cell Commun Adhes.* 2014;21(3):169-179.
18. Garcia-Gras E, Lombardi R, Giocondo MJ, et al. Suppression of canonical Wnt/beta-catenin signaling by nuclear plakoglobin recapitulates phenotype of arrhythmogenic right ventricular cardiomyopathy. *J Clin Invest.* 2006;116(7):2012-2021.
19. Guo H, Lu YW, Lin Z, et al. Intercalated disc protein Xinbeta is required for Hippo-YAP signaling in the heart. *Nat Commun.* 2020;11(1):4666.
20. Hu Y, Pu WT. Hippo activation in arrhythmogenic cardiomyopathy. *Circ Res.* 2014;114(3):402-405.
21. Kim C, Wong J, Wen J, et al. Studying arrhythmogenic right ventricular dysplasia with patient-specific iPSCs. *Nature.* 2013;494(7435):105-110.
22. Wilkins BJ, Dai YS, Bueno OF, et al. Calcineurin/NFAT coupling participates in pathological, but not physiological, cardiac hypertrophy. *Circ Res.* 2004;94(1):110-118.
23. Wilkins BJ, Molkentin JD. Calcium-calcineurin signaling in the regulation of cardiac hypertrophy. *Biochem Biophys Res Commun.* 2004;322(4):1178-1191.
24. Sanna B, Bueno OF, Dai YS, Wilkins BJ, Molkentin JD. Direct and indirect interactions between calcineurin-NFAT and MEK1-extracellular signal-regulated kinase 1/2 signaling pathways regulate cardiac gene expression and cellular growth. *Mol Cell Biol.* 2005;25(3):865-878.
25. Rinne A, Kapur N, Molkentin JD, et al. Isoform- and tissue-specific regulation of the Ca(2+)-sensitive transcription factor NFAT in cardiac myocytes and heart failure. *Am J Physiol Heart Circ Physiol.* 2010;298(6):H2001-2009.
26. Lyon A, van Opbergen CJM, Delmar M, Heijman J, van Veen TAB. In silico Identification of Disrupted Myocardial Calcium Homeostasis as Proarrhythmic Trigger in Arrhythmogenic Cardiomyopathy. *Front Physiol.* 2021;12:732573.
27. Sutanto H, Lyon A, Lumens J, Schotten U, Dobrev D, Heijman J. Cardiomyocyte calcium handling in health and disease: Insights from in vitro and in silico studies. *Prog Biophys Mol Biol.* 2020;157:54-75.
28. Obergrussberger A, Rinke-Weiss I, Goetze TA, et al. The suitability of high throughput automated patch clamp for physiological applications. *J Physiol.* 2022;600(2):277-297.
29. Obergrussberger A, Goetze TA, Brinkwirth N, et al. An update on the advancing high-throughput screening techniques for patch clamp-based ion channel screens: implications for drug discovery. *Expert Opin Drug Discov.* 2018;13(3):269-277.

Willem B. van Ham¹

Stephanie M. van der Voorn¹

Aryan Vink²

Selina M.W. Teurlings¹

Chantal J.M. van Opbergen³

Feddo P. Kirkels⁴

Karim Taha⁴

Anneline S.J.M. te Riele^{4#}

Jordi Heijman⁵

Mario Delmar³

Joost Lumens⁶

Aurore Lyon^{1,6*}

Toon A.B. van Veen^{1*}

¹Department of Medical Physiology, University Medical Center Utrecht, The Netherlands

²Department of Pathology, University Medical Center Utrecht, The Netherlands

³Leon H Charney Division of Cardiology, New York University School of Medicine, USA

⁴Department of Cardiology, University Medical Center Utrecht, The Netherlands

⁵Department of Cardiology, CARIM, Maastricht University, The Netherlands

⁶Department of Biomedical Engineering, CARIM, Maastricht University, The Netherlands

[#]Member of the European Reference Network for rare, low prevalence and complex diseases of the heart: ERN GUARD-Heart (ERN GUARD HEART; <http://guardheart.ern-net.eu>)

*Aurore Lyon and Toon A.B. van Veen are shared senior authors

Chapter VII

**Patient-specific modeling of
disrupted calcium handling and
cardiomyocyte electromechanics in
arrhythmogenic cardiomyopathy**

In preparation

Abstract

Patients with arrhythmogenic cardiomyopathy (ACM) may suffer from life-threatening arrhythmias and progressive contractile dysfunction. Previous research identified calcium handling abnormalities as a disease-initiating mechanism in mice, but whether this mechanism translates to humans remains unknown. Here, we characterized disturbed molecular regulators of intracellular calcium in ACM patients and predicted their effects on human cardiomyocyte electromechanics in left and right ventricle (LV, RV) using a computer model. Protein levels were analyzed in LV and RV tissue samples from five PKP2 ACM patients and five controls without cardiac disease. Additionally, patients with end-stage heart failure due to phospholamban (n=5), dilated (n=3), and hypertrophic (n=4) cardiomyopathy were included. Experimentally-characterized protein level changes were implemented in our electromechanical human cardiomyocyte computer model. Calcium transients and cardiomyocyte tension were simulated and compared to controls. Protein levels varied between the PKP2 ACM patients and between individual LV and RV samples, but the sodium-calcium exchanger (NCX1) was consistently lower in patients versus controls. ACM-associated differences in protein levels in patients differed significantly from data in mice. These differences also contrasted with those in dilated and hypertrophic cardiomyopathies, indicating a specific association with ACM rather than a generalized heart failure phenotype. All simulated calcium transients and tension showed longer relaxation times and elevated diastolic levels due to lower NCX1 activity. Selectively restoring NCX1 activity in the *in silico* ACM patients prevented the calcium overload phenotype, resulting in improved relaxation. We identified a pronounced calcium handling protein remodeling in human ACM myocardium, distinct from results in mice and other inherited cardiomyopathies. By integrating these data in a human computer model, the electromechanical effects of patient-specific changes were quantified. Our results reveal an important role for decreased NCX1 function in driving impaired relaxation in cardiomyocytes of ACM patients, suggesting its potential as a future therapeutic target.

Keywords: arrhythmogenic cardiomyopathy; computational electromechanical modeling; calcium handling; human cardiac tissue; sodium-calcium exchanger (NCX)

1. Introduction

Individuals with arrhythmogenic cardiomyopathy (ACM) suffer from an increased risk of ventricular arrhythmias and sudden cardiac death (SCD), which often occurs in young adults at an early stage of the disease^{1,2}. As the disease progresses, contractile impairment further deteriorates cardiac performance. Early detection of ACM remains challenging³⁻⁵, so a better understanding of the mechanisms underlying ACM is needed to identify markers of early disease and potential therapeutic targets. ACM is often caused by pathogenic variants in genes coding for desmosomal proteins, such as PKP2, which encodes the protein plakophilin-2 (PKP2). PKP2 is present in the intercalated discs of cardiomyocytes and plays a vital role in cell-to-cell adhesion, but is also a component of the connexome, and therefore influences various molecular pathways⁶. The consequences of PKP2 dysfunction in cardiomyocytes remain complex, but recent studies have identified a crucial role for PKP2 in translating signals originating at the cell junction into intracellular signals controlling structural and electrical cardiomyocyte components, especially relating to calcium homeostasis⁷⁻⁹. These recent insights have highlighted the pro-arrhythmic and contractile consequences of such disturbances in calcium handling in genetically engineered mouse models^{8,10}, but how these changes alter the contractile function and force generation, and whether they are also present in ACM patients remains poorly understood.

Measuring levels of proteins involved in calcium homeostasis in human early-stage disease cardiac tissue can provide important insights in disturbed calcium handling caused by pathogenic variants in PKP2 in this stage of the disease. However, such human cardiac material from early stages of the disease is difficult to obtain, due to a general late detection of the disease in patients and the inability to safely take sufficiently large cardiac biopsies for protein isolation. Acquiring such an amount of human ventricular tissue is mainly limited to specimen taken from explanted hearts, which only occurs in patients with end-stage heart failure. Due to the worsened quality of the myocardium, it becomes difficult to attribute individual experimentally observed molecular alterations to the disease rather than the overall and complex deterioration of the myocardium caused by progressive heart failure. However, the classical form of ACM (formerly also mentioned as ARVC) differs in pathological background and phenotype from other inherited cardiomyopathies, such as dilated and hypertrophic cardiomyopathy (DCM and HCM)^{11,12}. Even more complex, other cardiomyopathies may show mixed phenotypes, such as phospholamban (PLN-p.Arg14del) cardiomyopathy, which includes features reminiscent of both ACM and DCM¹³. Comparing the molecular signature of explanted failing heart tissue from these cardiomyopathies to ACM therefore allows to distinguish molecular changes that are specific to ACM from the general changes resulting from end-stage heart failure.

Understanding how pathogenic variants trigger the onset and progression of disease or lead to changes in protein levels, impaired ion channel- and electromechanical function, and their downstream clinical phenotypes is challenging. Computational models can help to address part of this challenge by translating alterations at the molecular level to cellular dynamics. Additionally, these models provide a controlled environment to evaluate the influence of individual parameters on cellular electromechanics and pinpoint underlying disease mechanisms. They have shown to provide mechanistic insights into the dysregulation of cardiomyocyte calcium handling¹⁴, and to capture the individual and combined consequences of electromechanical changes such as changes in sarcomere length and the effects of adrenergic stimulations¹⁵. In a previous study, we used computer models to identify the underlying mechanisms by which calcium-handling abnormalities due to *Pkp2* loss-of-function may lead to arrhythmias in a mouse model which appeared reminiscent of the pathophysiology of ACM as seen in patients¹⁶.

In this study, we investigated for the first time in human cardiac tissue, how pathogenic variants in *PKP2* may affect levels of proteins relevant for cardiomyocyte calcium handling in ACM patients. We compared protein profiles to data acquired in a *Pkp2* knockout mouse model, as well as human protein levels derived from patients diagnosed with cardiomyopathies other than ACM. By integrating these experimental data into an electromechanical human cardiomyocyte computer model, we were able to study the functional consequences of this calcium handling remodeling on electromechanical cellular phenotype in terms of calcium and force generation.

2. Methods

2.1. Cardiac material

Cryo-frozen patient material was acquired from the pathology department, derived from cardiac biopsies or explanted hearts at the University Medical Center Utrecht, The Netherlands. Tissue material was obtained from healthy controls and ACM (harboring different pathogenic *PKP2* variants), PLN (PLN p.Arg14del), DCM, and HCM diagnosed patients (**Table 1**). This study is part of the UCC-UNRAVEL biobank¹⁷, a single-center research data platform that combines routine electronic health records enriched with deep phenotyping, genetic data, and standardized biobanking to facilitate research in (inherited) heart diseases (www.unravelrdp.nl). Healthy control material was gratefully obtained from prof. dr. I.R. Efimov, Department of Biomedical Engineering and Medicine, Northwestern University, Chicago, Illinois. The study was approved by the local institutional ethics review board (University Medical Center Utrecht, protocol UCC-UNRAVEL #12-387).

Cardiac tissue (snap-frozen) from a cardiomyocyte-specific tamoxifen-induced *Pkp2* knockout mouse model were obtained from (4-5 months old) mice at 28 days post tamoxifen injection and compared to our previously reported data at 21 days post injection⁷.

Table 1. Patient characteristics tissue material.

Category	Patient	Sex	Age	Origin
Control	C1	M	52	LV/RV
	C2	F	59	LV/RV
	C3	F	56	LV/RV
	C4	F	58	LV/RV
	C5	M	48	LV/RV
ACM	A1	M	66	LV/RV
	A2	M	47	LV/RV
	A3	M	61	LV/RV
	A4	F	56	LV/RV
	A5	M	55	LV/RV
PLN	P1	F	66	LV/RV
	P2	F	37	LV/RV
	P3	F	58	LV/RV
	P4	F	55	LV/RV
	P5	M	72	LV/RV
DCM	D1	M	44	LV
	D2	M	64	LV
	D3	M	54	LV
HCM	H1	M	69	LV
	H2	F	77	LV
	H3	F	77	LV
	H4	M	77	LV

2.2. Western immunoblotting

All cardiac tissue, stored at -80 °C, was pulverized at -21 °C with pestle and mortar, and subsequently thoroughly dissolved in RIPA lysis buffer (20 mM Tris, 150 mM NaCl, 10 mM Na₂HPO₄, 1 mM EDTA, 50 mM NaF, 1% Triton X100, 1% Na-deoxycholate, 0.1% SDS, supplemented with 0.2% aprotinin and 1 mM PMSF). SDS-PAGE was performed using 30 µg of protein sample, followed by a transfer onto nitrocellulose membranes. Equal loading was determined by GAPDH (control vs. ACM and PLN) labeling and ponceau staining (control vs. DCM and HCM). Primary antibodies and secondary HRP-conjugated antibodies (**Table S1**) were diluted in 5% protifar TBST (20 mM Tris, 150 mM NaCl, 0.05% Tween-20) and incubated at 4 °C overnight or at room temperature for 90 min. An ECL detection kit (Cytiva, RPN2232), a ChemiDoc Molecular Imager and ImageLab software v.6.1. (Bio-Rad) were used to image and analyze the results.

2.3. Quantitative PCR

Total RNA was extracted from the pulverized cardiac tissue using TRIzol reagent (ThermoFischer) and subsequently treated with DNase I (Promega). DNase-treated RNA was then converted into complement DNA (cDNA) with reverse transcriptase (Invitrogen) according to the protocol of the manufacturer. Real time-qPCR was performed using TaqMan gene expression assays (Applied Biosystems by Life Technologies Corp) in a MyiQ2 Real-Time PCR Detection System (Bio-Rad Laboratories). mRNA

levels were determined for genes involved in calcium handling relative to housekeeping controls (**Table S2**). The $2^{(-\Delta\Delta CT)}$ method was applied to calculate fold changes in gene expression.

2.4. Computational modeling

The electromechanical cardiomyocyte computer model developed by Lyon et al. 2020 was used¹⁵. In brief, this model couples the O’Hara-Rudy model¹⁸ of detailed ventricular cardiomyocyte electrophysiology with the MechChem model^{19,20} of sarcomere contraction, describing the cooperative nature of myocardial contraction through mechanochemical interactions. This bidirectional coupling is executed through the buffering of calcium by troponin. Validated on a range of experimental protocols from human and large mammals, this electromechanical cardiomyocyte computer model has shown its ability to recapitulate the complex bidirectional relationship between cardiac cellular electrophysiology and mechanics¹⁵. For each ACM, DCM, and HCM patient, the relative deviations in protein level from the mean control value ($n=5$, normalized to 1) were included in the LV and RV versions of the model when available. Several parameters involved in calcium handling were modified according to the experimentally measured deviations in the relative protein levels. The current density of the L-type calcium current was multiplied by the relative change in L-type calcium channel (Cav1.2) protein levels. Maximal calcium fluxes through the sarcoplasmic reticulum calcium ATP-ase (SERCA2a) pump and ryanodine receptors (RyR2) were multiplied by the relative change in SERCA2a and RyR2 protein levels, respectively. Maximum calsequestrin (CSQ2) concentration was multiplied by the relative change in CSQ2 protein level. The model’s basal SERCA2a affinity for cytosolic calcium and its modulation by calcium/calmodulin-dependent protein kinase II (CaMKII) were scaled based on changes in PLN expression, with lower PLN expression resulting in a higher affinity (i.e., lower K_m value). Finally, the maximum transport rate of the sodium-calcium exchanger (NCX1) was multiplied by the relative change in NCX1 protein levels. These model parameters are listed in **Table 2** (with patient-specific protein values as displayed in **Tables S3** and **S4**). For each patient, calcium transients, action potentials, and tension during isometric twitches at initial sarcomere length of $2.1 \mu\text{m}$ were simulated, after pre-pacing for 300 beats at 1 Hz.

Table 2. Computer model ACM parameter changes.

Model parameter	Interpretation
ICaL_i	Current density of the L-type calcium current
Jup	Maximal calcium uptake flux through the SERCA2a pump
JRel	Maximal calcium release flux through RyR2
csqlmax	Maximum calsequestrin concentration
Jup,CaMK (scaling of 0.00092 and 0.00017)	SERCA2a basal affinity and CamKII effect
Gncx	Maximum conductance of sodium-calcium exchanger (NCX)

2.5. Statistical analysis

All statistical analyses were performed using GraphPad Prism software, v.9. The assumption was made that variations of data within each group would follow a normal distribution. Therefore, comparisons were made using a student's T-test or one-way ANOVA, with Tukey's post-hoc test to correct for multiple comparisons. Data are reported as means \pm SEM for western immunoblotting and quantitative PCR. *p* values < 0.05 were considered significant.

3. Results

3.1. Calcium handling in ACM

Six of the most prominent proteins involved in calcium handling (*Cav1.2*, *RyR2*, *SERCA2a*, *PLN*, *CSQ2*, and *NCX1*) were analyzed in lysates derived from human cardiac tissue, comparing PKP2 ACM patients to healthy controls (**Figure 1 and Figure S1**). In general, protein levels varied considerably within each patient group, and no clear differences were observed between LV and RV. Of those six evaluated proteins, detected protein levels were not significantly different between the ACM patients and controls, except for *PLN* and *NCX1*, which were both severely decreased in ACM (pentameric *PLN*: LV -92% and RV -92%, *NCX1*: LV -67% and RV -53% in ACM vs control). mRNA expression levels of calcium handling proteins were also measured in the same patient samples (**Figure S2**). The mRNA expression was largely similar between control and ACM, and no clear relation between mRNA expression and protein levels in the individual samples could be found. Therefore, measured experimental changes introduced in the computer model were based on protein levels only.

To better understand how previous results reported in genetically engineered mice with an inducible deletion of *Pkp2* translate and compare to those results in humans, we evaluated the molecular data from a cardiomyocyte-specific tamoxifen-induced *Pkp2* knockout mouse model to the human data presented here. We analyzed cardiac mouse material derived from an advanced heart failure stage and compared that to data obtained from the early-stage of cardiac remodeling that we described before⁷. Interestingly, almost all levels of calcium handling proteins were decreased in the late-stage mice in a pattern very reminiscent to that observed in the early-stage timepoints in this mouse model (**Figure S3**). In contradiction, when compared to the alterations seen in the PKP2 ACM human samples, the mouse data appeared to have an alternative protein profile in which most of the six protein levels were significantly decreased.

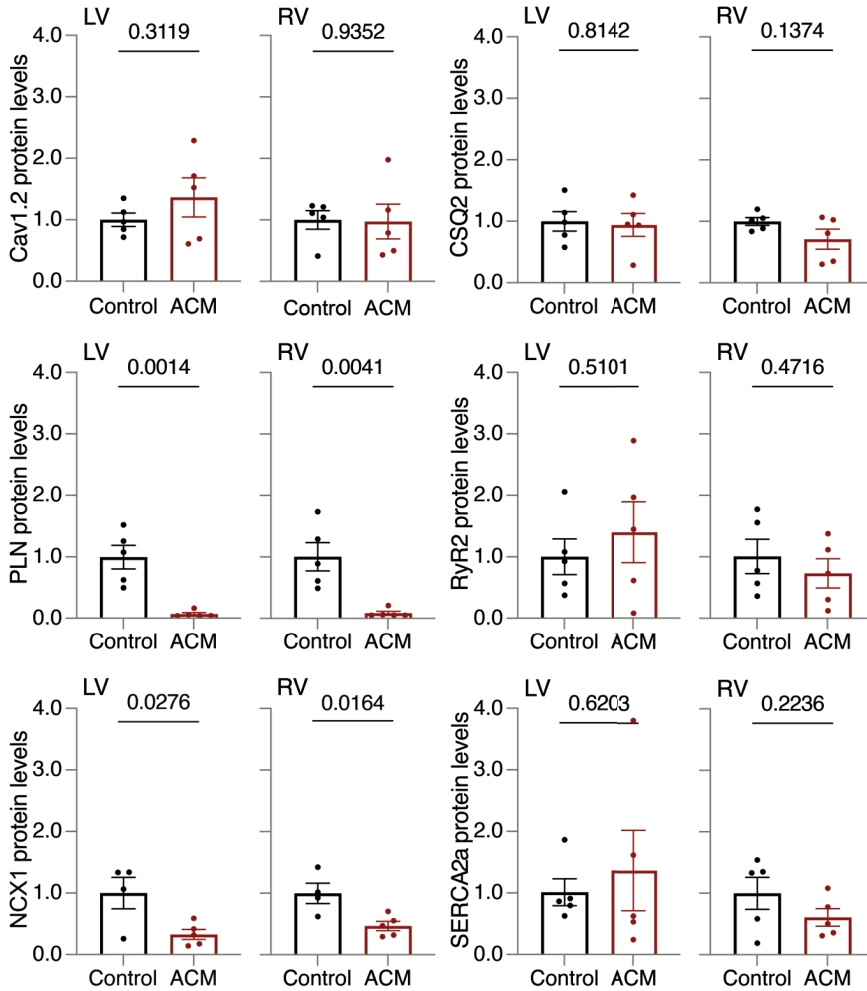


Figure 1. Protein levels of calcium handling related proteins in ACM patient material. Protein levels were measured in human cardiac biopsies originating from the left and right ventricle (LV and RV) of 5 healthy control and 5 arrhythmogenic cardiomyopathy (ACM) patients. Of the six major proteins involved in calcium handling, only the levels of phospholamban (pentameric PLN) and the sodium-calcium exchanger (NCX1) were severely diminished in ACM patients. All protein levels were normalized to GAPDH protein levels.

3.2. Computer simulations of cellular electromechanics in ACM

Raw protein levels of both control and PKP2 ACM patients (**Table S3**) were implemented in the electromechanical human cardiomyocyte computer model. Each control or patient was modeled individually, allowing for assessment of both patient-specific electromechanical consequences and average effects (**Figure 2**). Interestingly, in all patients, simulations showed increased systolic and diastolic calcium in PKP2 ACM patients, and increased force generation with a slower decay, suggesting impaired

relaxation. In patient A3-LV, these changes even led to a hypercontractile cardiomyocyte, indicating profound shortening of the sarcomere. These effects were more pronounced in LV compared to RV. While SERCA2a protein levels were also slightly decreased in some ACM patients, the generally diminished NCX1 levels exacerbated the impaired removal of cytosolic calcium.

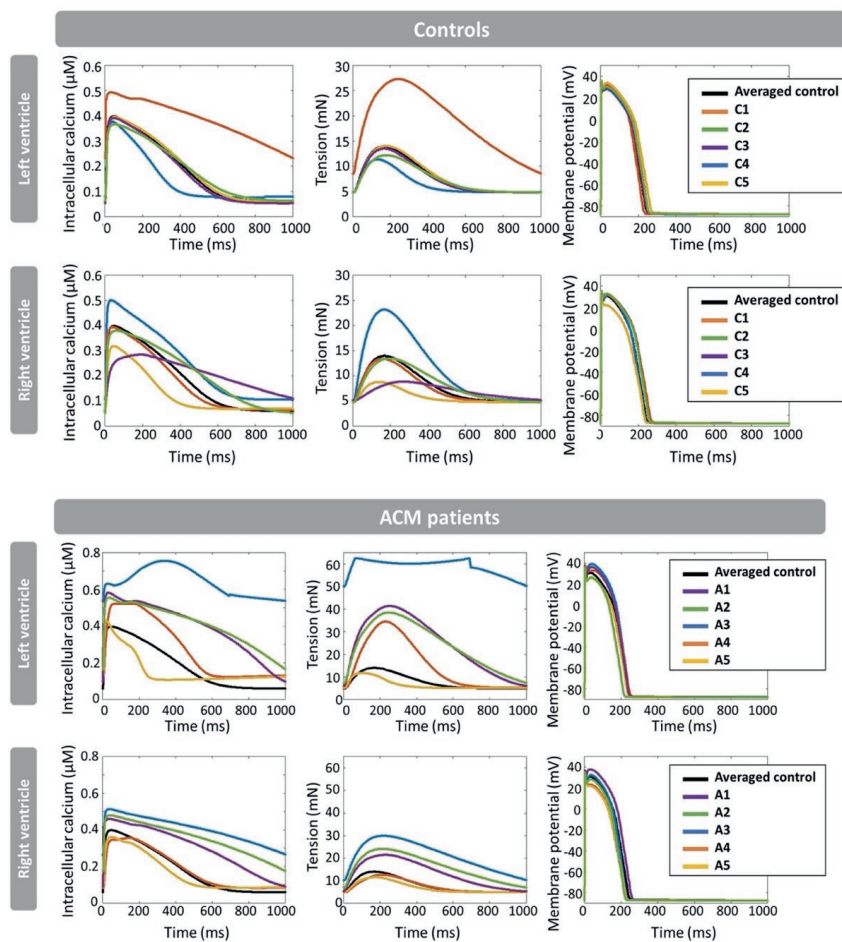


Figure 2. Computational modeling of calcium, tension, and action potentials in control and ACM patients. Protein level data was implemented in a human electromechanical cardiomyocyte model, and calcium transients, tension, and action potentials were simulated. Individual control and arrhythmogenic cardiomyopathy (ACM) patients were modeled (colored lines), as well as an averaged control (no deviation in calcium protein levels, black line), for both the left and right ventricle (LV and RV).

3.3. Molecular and computational analysis of DCM and HCM

To identify whether the electromechanical changes identified in PKP2 ACM are specific for this disease, and therefore different from other cardiomyopathies or a general end-stage heart failure phenomena, protein levels were additionally determined in cardiac LV and RV samples from PLN cardiomyopathy patients (**Figure S1 and S4**), and LV samples from DCM and HCM patients (**Figure 3 and Figure S5**).

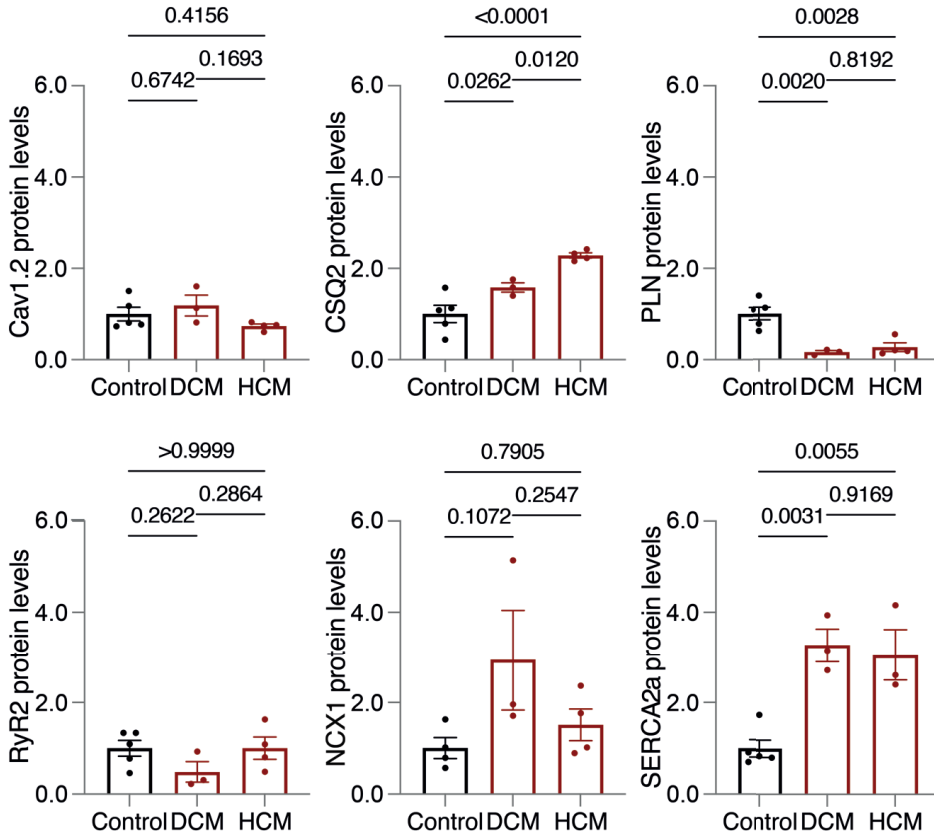


Figure 3. Protein levels of calcium handling related proteins in DCM and HCM patient material. Protein levels were measured in human cardiac biopsies originating from the left ventricle of 3 dilated cardiomyopathy (DCM) and 4 hypertrophic cardiomyopathy (HCM) patients, as well as earlier presented healthy controls. Calcium handling related protein levels mainly indicated an increased trend, except for the ryanodine receptor (RyR2) in DCM and phospholamban (pentameric PLN) in both DCM and HCM. All protein levels were normalized to ponceau.

The majority of the calcium handling-related proteins in both DCM and HCM either remained unchanged or were even increased compared to controls (**Figure 3**). Only PLN was, similar to PKP2 ACM, largely diminished (-85% and -74% for DCM and HCM, respectively), resulting in diminished PLN as common

deviant across the four cardiomyopathies. Importantly, average NCX1 levels were robustly amplified in both cardiomyopathies compared to control (+193% and +51% for DCM and HCM vs. control respectively), although these differences did not reach statistical significance due to the large inter-patient variability. Interestingly, while PLN patients are commonly diagnosed as either ACM or DCM, or even show a phenotype with characteristics of both diseases, a large overlap in molecular signature was identified between ACM and PLN patients (Figure S4) but not with DCM. Given this molecular similarity of PLN and PKP2 ACM patients, we did not further analyze the PLN profile in the modeling.

Implementing the DCM and HCM protein level data into the computer model led to a different cellular electromechanical phenotype from that observed in PKP2 ACM (Figure 4). Both DCM and HCM indicated enhanced removal of cytosolic calcium during diastole, represented by the faster decay of tension. In HCM, calcium and tension amplitudes were maintained due to sufficient functionality of RyR2 and Cav1.2. In DCM, calcium transient and tension amplitudes were lower. In conclusion, both profiles in DCM and HCM were clearly different from PKP2 ACM in terms of cellular electromechanics.

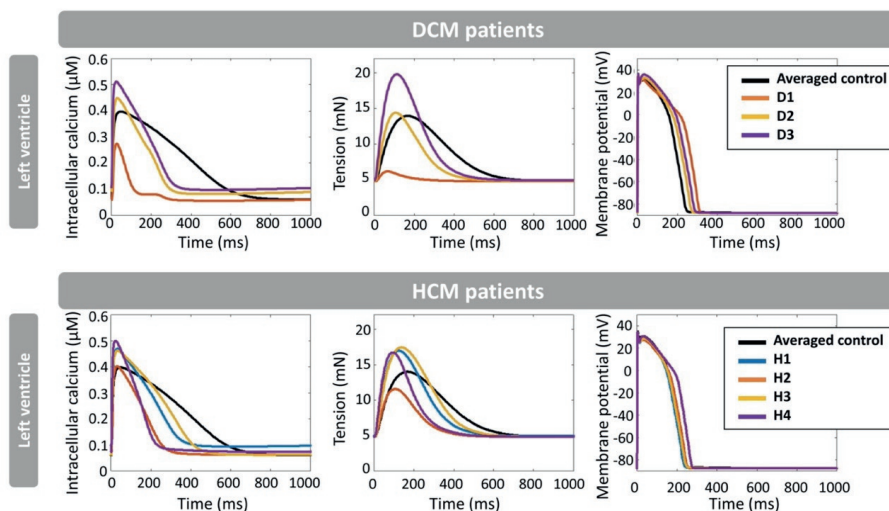


Figure 4. Computational modeling of calcium, tension, and action potentials in DCM and HCM patients. Protein level data were implemented in the computer model, and calcium transients, tension, and action potentials were simulated. Individual dilated cardiomyopathy (DCM) and hypertrophic cardiomyopathy (HCM) patients were modeled (colored lines), as well as an averaged control (no deviation in calcium protein levels, black line), for the left ventricle (LV).

3.4. Molecular and computational analysis of DCM and HCM

To further pinpoint the critical role of NCX1 in driving the cellular electromechanical changes observed in ACM, additional simulations were performed for PKP2 ACM patients in whom NCX1 function was selectively restored to control values (Figure 5). These simulations indicated that diastolic calcium levels were vastly decreased when NCX1 functionality was restored (e.g. from 0.16 μM to 0.04 μM in A2, and from 0.55 μM to 0.13 μM in A3), which resulted in appropriate relaxation of cardiomyocytes (calcium transient duration shortened, e.g. 616 ms to 455 ms in A4, 994 ms to 789 ms in A1). Calcium transient durations remained slightly prolonged in patients in whom SERCA2a levels were decreased additionally to that of NCX1.

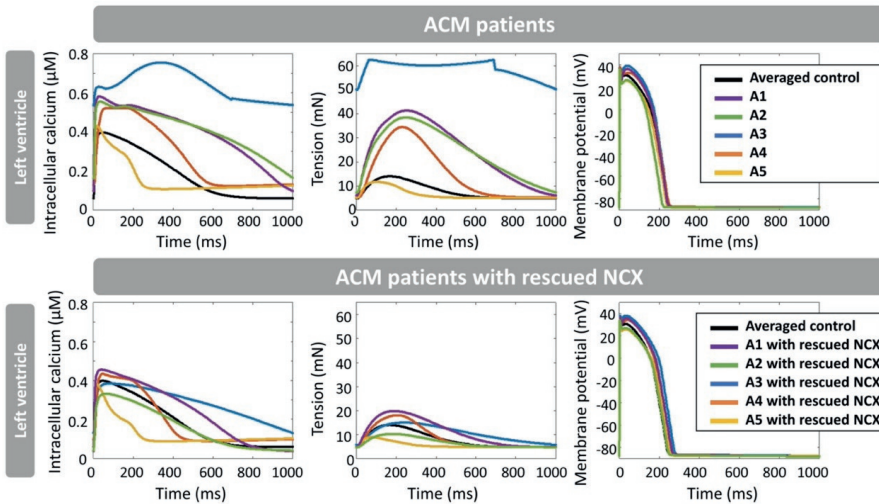


Figure 5. Importance of NCX1 in ACM. Protein levels from the left ventricle from 5 arrhythmogenic cardiomyopathy (ACM) patient were implemented in the computational model, both the original simulations (top panel) and with normalized sodium-calcium exchanger (NCX1) values (bottom panel). Diastolic calcium levels were reduced in all patients compared to the original simulations, with subsequent improved relaxation. Individual ACM patients were modeled (colored lines) together with an averaged control (no deviation in calcium protein levels, black line).

4. Discussion

In this study, we characterized the manifestation of disturbed calcium handling in PKP2 ACM patients and investigated its electromechanical consequences using a novel approach combining experimental data obtained from human cardiac explant tissue with a human electromechanical computer model. By incorporating experimentally measured differences in calcium handling protein levels into simulations of calcium transients and tension, this study showed that disturbed calcium handling in ACM may translate into slower relaxation with elevated diastolic calcium in the cardiomyocytes. We also showed here that

molecular profiles and cellular electromechanics of ACM, DCM, and HCM patients are distinct, suggesting that the experimentally characterized calcium-handling remodeling reported here is not a general feature of end-stage heart failure, but is specific to PKP2 ACM. In addition, our data highlight that NCX1 dysfunction may be a key driver of impaired relaxation in cardiomyocytes of ACM patients. Indeed, when NCX1 function was normalized in the computer simulations, this rescued the calcium overload phenotype, resulting in more appropriate relaxation in ACM.

4.1. Importance of NCX1 in ACM

By isolating the contribution of NCX1 changes in cellular electromechanics in ACM, the computer simulations showed that the increased diastolic calcium levels and impaired relaxation phenotype are primarily a consequence of diminished functional NCX1 protein levels. Interestingly, previous modeling work showed that decreased NCX1 function together with increased diastolic calcium caused delayed after depolarizations (DADs) by reactivation of the RyR2 activity in mice¹⁶. The results from our current study are in line with those findings and highlight, beyond the pro-arrhythmic effects described previously¹⁶, a potential contractile dysfunction caused by abnormal NCX1 in ACM.

Interestingly, ACM patients respond well to flecainide²¹, a sodium channel and RyR2 inhibitor which indirectly increases NCX1 activity. The applicability of flecainide in treatment of ACM has recently successfully been studied in a clinical trial²². Amongst the genetic cardiomyopathies this would mainly be relevant for ACM, as NCX1 protein levels and functionality seem increased in other types of heart failure²³. Several neurodegenerative diseases, such as Parkinson disease, Alzheimer disease, and multiple sclerosis, also involve disturbed calcium handling due to affected NCX expression²⁴. Similar to the potential for application of NCX activators in these diseases²⁴, amelioration of NCX1 function might be a promising therapeutic target against arrhythmias and disease progression in ACM.

4.2. Translation of ACM pathology in mouse models

Several studies of PKP2 in relation to ACM have been performed in genetically engineered mouse models, consisting of complete knock-out or inducible cardiomyocyte-specific *Pkp2* deletion^{7,8,25,26}, haploinsufficiency models²⁶⁻²⁸, and heterozygous knock-in of a human pathological PKP2 variants^{29,30}. While these models have provided important insights in understanding the relation between PKP2 and ACM disease progression in general, translation of these models to the human situation remains challenging. Even though many models are genetically exaggerated, as clinically mostly heterozygous pathogenic variants are observed^{9,31}, fibrofatty replacement of the myocardium (a hallmark of ACM) is often absent (particularly the aspect of fat) and the role of aberrant PKP2 expression during development/progression of the disease is only rarely studied^{26,29}. However, previous work on a *Pkp2* conditional knockout mouse model showed an impressive alignment of disease manifestations between

those seen in this model and those seen in ACM patients. Moreover, these studies highlighted an important role of increased diastolic calcium in relation to arrhythmic incidence^{7,10}. However, the levels of proteins crucial for calcium homeostasis that were reported in the *Pkp2* conditional knockout mice, at both 21 and 28 days post tamoxifen injection as highlighted in our previous data⁷ and this current study, differed significantly from the human ACM data presented in this current study. This suggests that employing these mouse models to understand human pathology or predict clinical outcomes of pathological genetic variants requires caution. Indeed, there are well established differences in calcium handling between rodents and larger mammals, including a much smaller role for NCX1-mediated calcium extrusion in rodents¹⁴. Moreover, the mentioned alterations observed in the mouse model reflect those that were present at the onset of disease manifestation, while the human data that we present are derived from explanted end-stage disease hearts. To address this potential confounding factor, we repeated the analysis regarding the proteins involved in calcium cycling in near-end-stage failing *Pkp2* conditional knockout mouse hearts. Interestingly, these data show that the alterations in the early stage persist in the end-stage of the disease, while still being different from end-stage PKP2 ACM disease in humans. To study the disease progression in humans, human induced pluripotent stem cell-derived cardiomyocyte (hiPSC-CM) models of patient-specific pathogenic variations are increasingly being developed over the past years, and recapitulate many aspects of the ACM phenotype (reviewed in ³²). However, in addition to known challenges of hiPSC-CMs (e.g. premature phenotype and structural organization), translation from the cell system towards clinical phenotypes is also limited, and the implementation of this type of experimental data in computational modeling has yet to be validated.

To follow up on experimental studies, we showed how computational modeling can help to scale and predict the effects of these changes in humans (from molecular changes to adult human cardiomyocyte phenotype). Multiscale models linking cell to whole-system and circulation will, in future work, allow an even larger degree of translation from molecular changes to clinical observations³³⁻³⁵.

4.3. Translating molecular changes to clinical phenotypes

Understanding how pathogenic variants trigger the onset and progression of disease or lead to changes in protein levels, impaired ion channel and cellular electromechanical function, and their downstream clinical phenotypes is challenging, and yet crucial for personalized diagnosis and mechanism-based treatment of genetic cardiomyopathy patients. Indeed, clinical diagnosis of genetic cardiomyopathies is based on cardiac structure and function, which, together with molecular profiles as demonstrated by the data presented here, can also overlap. However, our experimental contractile function is modeled at a cellular level, which might not translate to whole-heart performance. This is especially relevant in an *in vivo* situation such as sympathetic stimulation, where increased SERCA2a function may limit the impact of decreased NCX1. Disturbed diastolic calcium levels on the other hand, are a favorable substrate for arrhythmias³⁶.

Additionally, both calcium overload and pathogenic *PKP2* variations can cause fibrofatty replacement of the myocardium³⁷⁻⁴⁰, which together with arrhythmias, are major hallmarks of ACM in patients.

Especially PLN patients, diagnosed either as DCM or ACM, seem to exhibit characteristics spanning both diseases⁴¹, which fuels the suggestion that genetic cardiomyopathies require a genotype-categorized diagnosis based on specific pathogenic variants within each inherited cardiomyopathy phenotype. While this might complicate diagnostic procedures, it is of importance for clinical prognosis, as genetic background amongst ACM patients also influences prognosis and disease progression². This is exemplified by the fact that ACM patients with pathogenic variants in *PKP2* mainly present an initial right ventricular remodeling while ACM patients with a *DSP* variant show a LV phenotype⁴².

In the case of ACM, structural alterations such as fibrofatty replacement and cardiomyocyte death only arise when the disease is already advanced to an irreversible and complex situation, whereas life-threatening arrhythmias are often early signs of the disease^{31,43}. Detection of disease progression, for example by cardiac imaging, is mainly performed in family members of carriers with an established pathogenic variant due to the incomplete penetrance, but lacks sensitivity in early ACM⁴⁴. We also observed calcium overload and impaired relaxation in our modeling. While diastolic dysfunction is not a well-known characteristic of ACM and often only observed in later stages of progressive heart failure, it is also an ongoing challenge to standardize classification of diastolic dysfunction in clinical practice. While algorithms have been developed for classification of LV diastolic dysfunction⁴⁵, standardized indices of RV diastolic function are lacking. Interestingly, echocardiographic analysis in pre-symptomatic PLN p.Arg14del patients has also indicated compromised relaxation of the myocardium, presumably caused by calcium overload⁴⁶. These clinical data fits with the results obtained in the current study using a cellular electromechanical model.

This study initiates the possibility for using patient-specific experimental data to model clinical phenotypes, emphasized by dissimilarities in protein level changes amongst end-stage heart failure material from different patient populations. Indeed, our approach allows the prediction of the cellular electromechanical signature based on relative protein level differences in an individual ACM patient, solving one step of the complex molecular to clinical phenotype challenge. However, direct clinical translation remains restricted by the large and complex gap between molecular alterations, intertwined cellular pathways, patient symptoms, and clinical diagnostics. A previous attempt at bridging clinical and tissue findings in ACM patients applied a top-down approach by modeling phenomenological potential mechanisms underlying clinically observed phenotypes (e.g. reduced contractility, increased myocardial stiffness), but could not establish a causative molecular mechanism responsible for these changes⁴⁷. Our bottom-up method is currently still restricted to a cellular computational model, which cannot be directly converted to whole-

heart simulations. This for now hampers the direct link between our results and clinical patient characteristics. However, the upcoming use of multiscale computer models linking cellular, whole-heart, and system function will allow to bridge this gap in future work and holds great promise in translating experimental findings to clinical observations.

5. Conclusion

Calcium handling protein levels measured in ACM patients showed pronounced differences compared to controls. These differences were distinct from results obtained in mouse models, strongly highlighting the challenges in translating findings in animal models to humans and the importance of studying human samples. Alterations in ACM calcium handling protein levels also differed from those observed in other genetic human cardiomyopathies, suggesting an ACM-specific remodeling. By integrating these data in a human computer model, the electromechanical effects of patient-specific changes in calcium handling were quantified and showed a potential role for decreased NCX1 function in driving compromising cardiac contractility in ACM. Future work that combines experimental data from ACM models with multiscale computational electromechanical models to simulate clinical phenotypes could aid in predicting cardiac function adaptations independent of heart failure.

References

1. Groeneweg JA, Bhonsale A, James CA, et al. Clinical Presentation, Long-Term Follow-Up, and Outcomes of 1001 Arrhythmogenic Right Ventricular Dysplasia/Cardiomyopathy Patients and Family Members. *Circ Cardiovasc Genet.* 2015;8(3):437-446.
2. Protonotarios A, Anastasakis A, Panagiotakos DB, et al. Arrhythmic risk assessment in genotyped families with arrhythmogenic right ventricular cardiomyopathy. *Europace.* 2016;18(4):610-616.
3. Corrado D, Link MS, Calkins H. Arrhythmogenic Right Ventricular Cardiomyopathy. *N Engl J Med.* 2017;376(1):61-72.
4. Bosman LP, Te Riele A. Arrhythmogenic right ventricular cardiomyopathy: a focused update on diagnosis and risk stratification. *Heart.* 2022;108(2):90-97.
5. De Brouwer R, Bosman LP, Gripenstedt S, et al. Value of genetic testing in the diagnosis and risk stratification of arrhythmogenic right ventricular cardiomyopathy. *Heart Rhythm.* 2022;19(10):1659-1665.
6. Nielsen MS, van Opbergen CJM, van Veen TAB, Delmar M. The intercalated disc: a unique organelle for electromechanical synchrony in cardiomyocytes. *Physiol Rev.* 2023;103(3):2271-2319.
7. Cerrone M, Montnach J, Lin X, et al. Plakophilin-2 is required for transcription of genes that control calcium cycling and cardiac rhythm. *Nat Commun.* 2017;8(1):106.
8. Kim JC, Perez-Hernandez M, Alvarado FJ, et al. Disruption of Ca(2+)(i) Homeostasis and Connexin 43 Hemichannel Function in the Right Ventricle Precedes Overt Arrhythmogenic Cardiomyopathy in Plakophilin-2-Deficient Mice. *Circulation.* 2019;140(12):1015-1030.
9. Austin KM, Trembley MA, Chandler SF, et al. Molecular mechanisms of arrhythmogenic cardiomyopathy. *Nat Rev Cardiol.* 2019;16(9):519-537.
10. Van Opbergen CJM, Bagwan N, Maurya SR, et al. Exercise Causes Arrhythmogenic Remodeling of Intracellular Calcium Dynamics in Plakophilin-2-Deficient Hearts. *Circulation.* 2022;145(19):1480-1496.
11. Brownrigg JR, Leo V, Rose J, et al. Epidemiology of cardiomyopathies and incident heart failure in a population-based cohort study. *Heart.* 2022;108(17):1383-1391.
12. Ciarambino T, Menna G, Sansone G, Giordano M. Cardiomyopathies: An Overview. *Int J Mol Sci.* 2021;22(14):7722.
13. Van der Zwaag PA, van Rijsingen IA, Asimaki A, et al. Phospholamban R14del mutation in patients diagnosed with dilated cardiomyopathy or arrhythmogenic right ventricular cardiomyopathy: evidence supporting the concept of arrhythmogenic cardiomyopathy. *Eur J Heart Fail.* 2012;14(11):1199-1207.
14. Sutanto H, Lyon A, Lumens J, Schotten U, Dobrev D, Heijman J. Cardiomyocyte calcium handling in health and disease: Insights from in vitro and in silico studies. *Prog Biophys Mol Biol.* 2020;157:54-75.
15. Lyon A, Dupuis LJ, Arts T, et al. Differentiating the effects of beta-adrenergic stimulation and stretch on calcium and force dynamics using a novel electromechanical cardiomyocyte model. *Am J Physiol Heart Circ Physiol.* 2020;319(3):H519-H530.

16. Lyon A, van Opbergen CJM, Delmar M, Heijman J, van Veen TAB. In silico Identification of Disrupted Myocardial Calcium Homeostasis as Proarrhythmic Trigger in Arrhythmogenic Cardiomyopathy. *Front Physiol.* 2021;12:732573.
17. Sammani A, Jansen M, Linschoten M, et al. UNRAVEL: big data analytics research data platform to improve care of patients with cardiomyopathies using routine electronic health records and standardised biobanking. *Neth Heart J.* 2019;27(9):426-434.
18. O'Hara T, Virag L, Varro A, Rudy Y. Simulation of the undiseased human cardiac ventricular action potential: model formulation and experimental validation. *PLoS Comput Biol.* 2011;7(5):e1002061.
19. Dupuis LJ, Lumens J, Arts T, Delhaas T. High tension in sarcomeres hinders myocardial relaxation: A computational study. *PLoS One.* 2018;13(10):e0204642.
20. Dupuis LJ, Lumens J, Arts T, Delhaas T. Mechano-chemical Interactions in Cardiac Sarcomere Contraction: A Computational Modeling Study. *PLoS Comput Biol.* 2016;12(10):e1005126.
21. Ermakov S, Gerstenfeld EP, Svetlichnaya Y, Scheinman MM. Use of flecainide in combination antiarrhythmic therapy in patients with arrhythmogenic right ventricular cardiomyopathy. *Heart Rhythm.* 2017;14(4):564-569.
22. Zareba W, Tichnell C, Rosero SZ, et al. CE-452779-3 randomized placebo-controlled trial of flecainide in patients with arrhythmogenic right ventricular cardiomyopathy. *Heart Rhythm.* 2023.
23. Sipido KR, Volders PG, Vos MA, Verdonck F. Altered Na/Ca exchange activity in cardiac hypertrophy and heart failure: a new target for therapy? *Cardiovasc Res.* 2002;53(4):782-805.
24. Annunziato L, Secondo A, Pignataro G, Scorziello A, Molinaro P. New perspectives for selective NCX activators in neurodegenerative diseases. *Cell Calcium.* 2020;87:102170.
25. Moncayo-Arlandi J, Guasch E, Sanz-de la Garza M, et al. Molecular disturbance underlies to arrhythmogenic cardiomyopathy induced by transgene content, age and exercise in a truncated PKP2 mouse model. *Hum Mol Genet.* 2016;25(17):3676-3688.
26. Grossmann KS, Grund C, Huelsken J, et al. Requirement of plakophilin 2 for heart morphogenesis and cardiac junction formation. *J Cell Biol.* 2004;167(1):149-160.
27. Van Opbergen CJM, Noorman M, Pfenniger A, et al. Plakophilin-2 Haploinsufficiency Causes Calcium Handling Deficits and Modulates the Cardiac Response Towards Stress. *Int J Mol Sci.* 2019;20(17):4076.
28. Cerrone M, Noorman M, Lin X, et al. Sodium current deficit and arrhythmogenesis in a murine model of plakophilin-2 haploinsufficiency. *Cardiovasc Res.* 2012;95(4):460-468.
29. Tsui H, van Kampen SJ, Han SJ, et al. Desmosomal protein degradation as an underlying cause of arrhythmogenic cardiomyopathy. *Sci Transl Med.* 2023;15(688):eadd4248.
30. Camors EM, Roth AH, Alef JR, et al. Progressive Reduction in Right Ventricular Contractile Function Attributable to Altered Actin Expression in an Aging Mouse Model of Arrhythmogenic Cardiomyopathy. *Circulation.* 2022;145(21):1609-1624.

31. van der Voorn SM, Te Riele A, Basso C, Calkins H, Remme CA, van Veen TAB. Arrhythmogenic cardiomyopathy: pathogenesis, pro-arrhythmic remodelling, and novel approaches for risk stratification and therapy. *Cardiovasc Res.* 2020;116(9):1571-1584.
32. Higo S. Disease modeling of desmosome-related cardiomyopathy using induced pluripotent stem cell-derived cardiomyocytes. *World J Stem Cells.* 2023;15(3):71-82.
33. Arts T, Delhaas T, Bovendeerd P, Verbeek X, Prinzen FW. Adaptation to mechanical load determines shape and properties of heart and circulation: the CircAdapt model. *Am J Physiol Heart Circ Physiol.* 2005;288(4):H1943-1954.
34. Lumens J, Delhaas T, Kirn B, Arts T. Three-wall segment (TriSeg) model describing mechanics and hemodynamics of ventricular interaction. *Ann Biomed Eng.* 2009;37(11):2234-2255.
35. Walmsley J, Arts T, Derval N, et al. Fast Simulation of Mechanical Heterogeneity in the Electrically Asynchronous Heart Using the MultiPatch Module. *PLoS Comput Biol.* 2015;11(7):e1004284.
36. Van Opbergen CJ, Delmar M, van Veen TA. Potential new mechanisms of pro-arrhythmia in arrhythmogenic cardiomyopathy: focus on calcium sensitive pathways. *Neth Heart J.* 2017;25(3):157-169.
37. Costa S, Cerrone M, Saguner AM, Brunckhorst C, Delmar M, Duru F. Arrhythmogenic cardiomyopathy: An in-depth look at molecular mechanisms and clinical correlates. *Trends Cardiovasc Med.* 2021;31(7):395-402.
38. Maione AS, Faris P, Iengo L, et al. Ca(2+) dysregulation in cardiac stromal cells sustains fibro-adipose remodeling in Arrhythmogenic Cardiomyopathy and can be modulated by flecainide. *J Transl Med.* 2022;20(1):522.
39. Sommariva E, Brambilla S, Carbucicchio C, et al. Cardiac mesenchymal stromal cells are a source of adipocytes in arrhythmogenic cardiomyopathy. *Eur Heart J.* 2016;37(23):1835-1846.
40. Gadicherla AK, Wang N, Bulic M, et al. Mitochondrial Cx43 hemichannels contribute to mitochondrial calcium entry and cell death in the heart. *Basic Res Cardiol.* 2017;112(3):27.
41. McKenna WJ, Judge DP. Epidemiology of the inherited cardiomyopathies. *Nat Rev Cardiol.* 2021;18(1):22-36.
42. DeWitt ES, Chandler SF, Hylind RJ, et al. Phenotypic Manifestations of Arrhythmogenic Cardiomyopathy in Children and Adolescents. *J Am Coll Cardiol.* 2019;74(3):346-358.
43. Kohela A, van Rooij E. Fibro-fatty remodelling in arrhythmogenic cardiomyopathy. *Basic Res Cardiol.* 2022;117(1):22.
44. Towbin JA, McKenna WJ, Abrams DJ, et al. 2019 HRS expert consensus statement on evaluation, risk stratification, and management of arrhythmogenic cardiomyopathy. *Heart Rhythm.* 2019;16(11):e301-e372.
45. Nagueh SF, Smiseth OA, Appleton CP, et al. Recommendations for the Evaluation of Left Ventricular Diastolic Function by Echocardiography: An Update from the American Society of Echocardiography and the European Association of Cardiovascular Imaging. *J Am Soc Echocardiogr.* 2016;29(4):277-314.

46. Taha K, Te Rijdt WP, Verstraelen TE, et al. Early Mechanical Alterations in Phospholamban Mutation Carriers: Identifying Subclinical Disease Before Onset of Symptoms. *JACC Cardiovasc Imaging*. 2021;14(5):885-896.
47. Mast TP, Teske AJ, Walmsley J, et al. Right Ventricular Imaging and Computer Simulation for Electromechanical Substrate Characterization in Arrhythmogenic Right Ventricular Cardiomyopathy. *J Am Coll Cardiol*. 2016;68(20):2185-2197.

Supplementary materials

Table S1. List of antibodies for western immunoblotting.

Antibody	Species	Dilution	Supplier	Product ID
Ankyrin B	Mouse	1:500	Biologend	821-501
Calsequestrin	Rabbit	1:1000	Invitrogen	PA1-913
Cav1.2	Mouse	1:500	Sigma	MAB13170
GAPDH	Mouse	1:500	Sigma	MAB374
NCX1	Rabbit	1:1000	Abcam	ab177952
Phospholamban	Mouse	1:1000	Invitrogen	MA3-922
Ryanodine receptor 2	Mouse	1:1000	Invitrogen	MA3-916
SERCA2a	Rabbit	1:1000	Invitrogen	PA5-97481
Triadin	Mouse	1:1500	Invitrogen	MA3-927
Anti-mouse HRP	Goat	1:7000	Jackson	115-035-003
Anti-rabbit HRP	Goat	1:7000	Bio-Rad	170-6515

Table S2. List of gene probes for quantitative PCR.

Gene	protein	Assay	Supplier	ID
CASQ2	Calsequestrin-2	Taqman	Thermo Fisher	Hs00154286_m1
ANK2	Ankyrin B	Taqman	Thermo Fisher	Hs00153998_m1
RYR2	Ryanodine Receptor 2	Taqman	Thermo Fisher	Hs00892891_m1
Triadin	TRDN	Taqman	Thermo Fisher	Hs00952568_m1
PLN	Phospholamban	Taqman	Thermo Fisher	Hs01848144_s1
CACNA1C	L-type Ca ²⁺ -channel	Taqman	Thermo Fisher	Hs00167681_m1
ATP2A2	SERCA2a	Taqman	Thermo Fisher	Hs01564013_m1
SLC8A1	NCX1	Taqman	Thermo Fisher	Hs01062258_m1
PPIA	Peptidylprolyl Isomerase A	Taqman	Thermo Fisher	Hs04194521_s1
RPL32	60S Ribosomal Protein L32	Taqman	Thermo Fisher	Hs00851655_g1
TBP	TATA-binding Protein	Taqman	Thermo Fisher	Hs00427620_m1

Table S3. Raw data values of protein levels in control and ACM patients for computational modeling.

Patient tissue	Cav1.2		PLN		NCX1		SERCA2a		CSQ2		RyR2	
	Protein fold	Protein fold	Protein fold	Protein fold	Protein fold	Protein fold	Protein fold	Protein fold	Protein fold	Protein fold	Protein fold	Protein fold
C1 Control	1.1246762025	1.7090434222	0.2592534911	0.6144945059	0.7794096478	2.0524157642	0.6144945059	0.7794096478	2.0524157642	0.7794096478	2.0524157642	2.0524157642
C2 Control	0.9645088943	1.0159408602	1.0638079484	0.7858701338	0.5798979585	0.9264788393	0.7858701338	0.5798979585	0.9264788393	0.5798979585	0.9264788393	0.9264788393
C3 Control	0.8446896087	0.5058560859	1.0000000000	0.8974536081	1.1444619026	1.0793450806	0.8974536081	1.1444619026	1.0793450806	1.1444619026	1.0793450806	1.0793450806
C4 Control	0.7160510044	1.1978733380	1.3401404427	1.8499408306	0.9865168241	0.5681430216	1.8499408306	0.9865168241	0.5681430216	0.9865168241	0.5681430216	0.5681430216
C5 Control	1.3500742901	0.5712862938	1.3367981178	0.8522409215	1.5097136670	0.3736172943	0.8522409215	1.5097136670	0.3736172943	1.5097136670	0.3736172943	0.3736172943
A1 ACM	1.7135695835	0.0469124818	0.3186354471	0.6173638404	1.4237978536	2.8789367479	0.6173638404	1.4237978536	2.8789367479	1.4237978536	2.8789367479	2.8789367479
A2 ACM	0.6893993397	0.0485793558	0.1398856271	0.5213348846	0.9495452302	1.9595327860	0.5213348846	0.9495452302	1.9595327860	0.9495452302	1.9595327860	1.9595327860
A3 ACM	2.2871693737	0.0504852099	0.1759790511	0.2305287401	0.9376511483	1.4451057189	0.2305287401	0.9376511483	1.4451057189	0.9376511483	1.4451057189	1.4451057189
A4 ACM	1.5217875871	0.1710650003	0.4143651043	1.6081093778	1.1084581675	0.0798717252	1.6081093778	1.1084581675	0.0798717252	1.1084581675	0.0798717252	0.0798717252
A5 ACM	0.6068988616	0.0675622822	0.5886538945	3.7958848187	0.2829589780	0.6114782285	3.7958848187	0.2829589780	0.6114782285	0.2829589780	0.6114782285	0.6114782285
C1 Control	1.1088492597	2.0652972489	1.4269188344	1.3484448205	0.8381308432	1.5486898686	1.3484448205	0.8381308432	1.5486898686	0.8381308432	1.5486898686	1.5486898686
C2 Control	1.2281738401	0.8139165150	1.0196828259	0.5866624830	0.8887559190	1.7637881661	0.5866624830	0.8887559190	1.7637881661	0.8887559190	1.7637881661	1.7637881661
C3 Control	1.2103039499	0.4459395276	1.0000000000	0.1909902218	1.0525594356	0.5615152611	0.1909902218	1.0525594356	0.5615152611	1.0525594356	0.5615152611	0.5615152611
C4 Control	1.0397411011	1.1411007157	0.6236375291	1.5436091262	1.1980332566	0.7708105345	1.5436091262	1.1980332566	0.7708105345	1.1980332566	0.7708105345	0.7708105345
C5 Control	0.4129318492	0.5337459928	0.9297608106	1.33022933485	1.0225205455	0.3551961697	1.33022933485	1.0225205455	0.3551961697	1.0225205455	0.3551961697	0.3551961697
A1 ACM	1.9806735410	0.2096498315	0.7046590959	0.5060727855	0.8080226126	1.3691120893	0.5060727855	0.8080226126	1.3691120893	0.8080226126	1.3691120893	1.3691120893
A2 ACM	0.7891442573	0.0490361309	0.2952239796	0.3583469521	1.0247508236	1.1110982978	0.3583469521	1.0247508236	1.1110982978	1.0247508236	1.1110982978	1.1110982978
A3 ACM	1.1627173286	0.0519945037	0.3205430818	0.3112964283	1.0682353363	0.7246639468	0.3112964283	1.0682353363	0.7246639468	1.0682353363	0.7246639468	0.7246639468
A4 ACM	0.5002166469	0.0574627209	0.4716075066	0.7782304660	0.3045289423	0.1180140770	0.7782304660	0.3045289423	0.1180140770	0.3045289423	0.1180140770	0.1180140770
A5 ACM	0.4327984559	0.0509674228	0.5546312560	1.0846431397	0.3525351915	0.2999025853	1.0846431397	0.3525351915	0.2999025853	0.3525351915	0.2999025853	0.2999025853

Table S4. Raw data values of protein levels in control, DCM, and HCM patients for computational modeling.

Patient tissue	Cav1.2	PLN	NCX1	SERCA2a	CSQ2		RyR2	
					Protein fold	Protein fold	Protein fold	Protein fold
C1 Control LV	1.1767792851	0.7746722924	0.5700355060	0.8042120877	0.7860735380	1.3344257925		
C2 Control LV	0.8125816931	1.3916959778	1.6258662377	0.8396949753	0.4356832970	1.0945023257		
C3 Control LV	0.7714323803	0.6204852124	1.0000000000	0.7054226915	1.124303548	1.3358688837		
C4 Control LV	0.7319428206	1.1246001344	1.0153659557	1.7404668675	1.0807882172	0.7752072691		
C5 Control LV	1.5072638209	1.0885463830	0.7887323006	0.9102033781	1.5731515930	0.4599957290		
D1 DCM LV	0.8169018514	0.206866484	5.1262882970	3.9195516820	1.3993390697	0.2204071939		
D2 DCM LV	1.1353414801	0.090161798	1.7038569243	2.7259097608	1.7539234551	0.3057195751		
D3 DCM LV	1.6095565582	0.162121524	1.9512626560	3.1409784068	1.5816434623	0.9286351471		
H1 HCM LV	0.7496607677	0.547451154	0.8917053083	2.6187116454	2.4168930190	0.4902665171		
H2 HCM LV	0.6089769189	0.178549025	1.7580904914	2.4096372627	2.3173055927	0.8062286435		
H3 HCM LV	0.7623283483	0.194644462	1.0156946765	1.6571678385	2.2258245840	1.0858654076		
H4 HCM LV	0.8225729403	0.125313005	2.3584268299	4.1378823409	2.1570185693	1.6288645076		

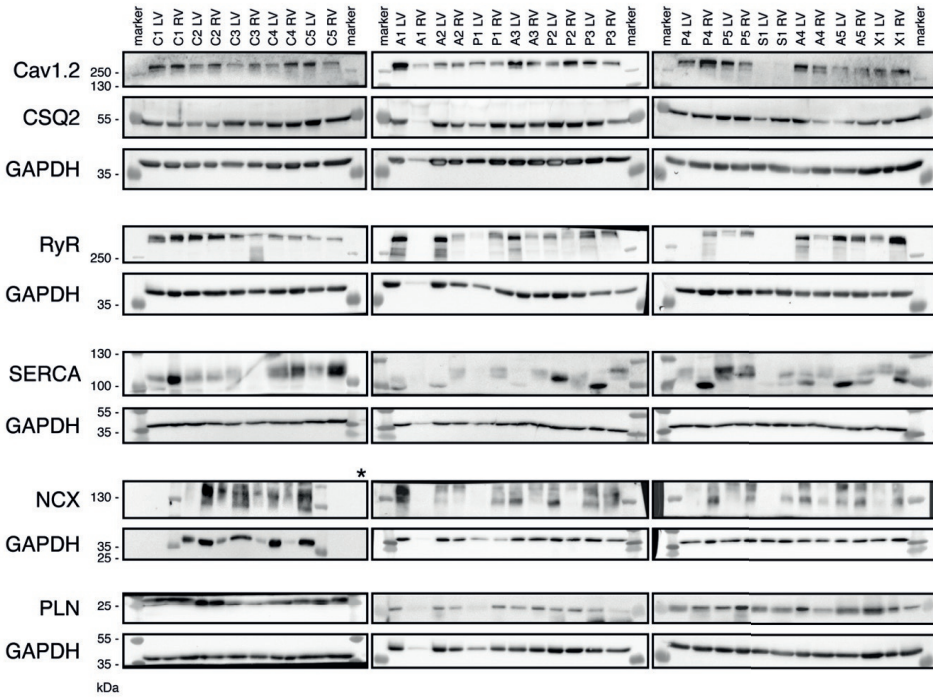


Figure S1. Western immunoblotting of calcium handling proteins in ACM. Western immunoblots of human cardiac biopsy samples originating from the left and right ventricle (LV and RV) of 5 healthy control (C1-C5), 5 arrhythmogenic cardiomyopathy (ACM, A1-A5), and 5 phospholamban cardiomyopathy (PLN, P1-P5) patients. LV and RV samples of two unrelated patients (S1 and X1) were excluded from analysis. GAPDH levels were determined to correct for equal sample loading.

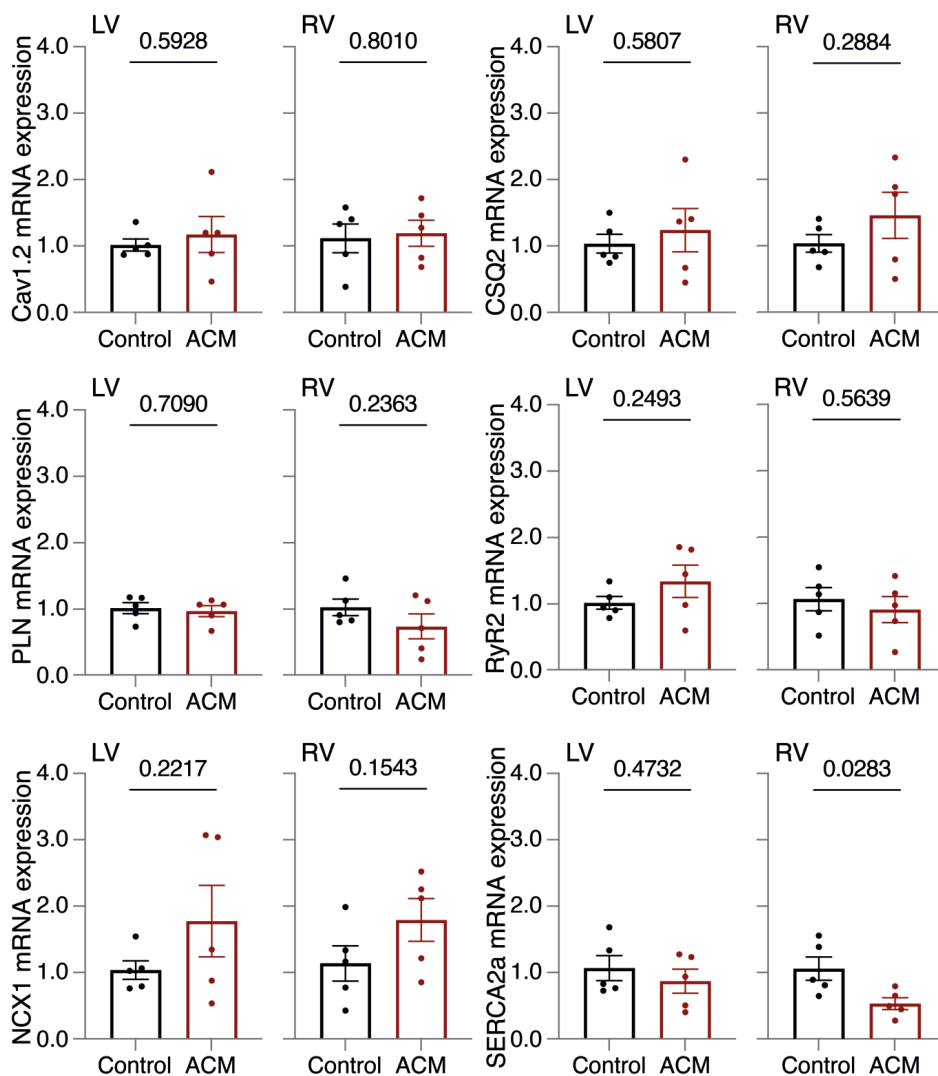


Figure S2. Gene expression of calcium handling related proteins in ACM patient material. Calcium handling related gene expression was measured in human cardiac biopsies originating from the left and right ventricle (LV and RV) of 5 healthy control and 5 arrhythmogenic cardiomyopathy (ACM) patients. Interestingly, no clear relation between protein levels and gene expression in the patient material could be observed that is applicable to all proteins.

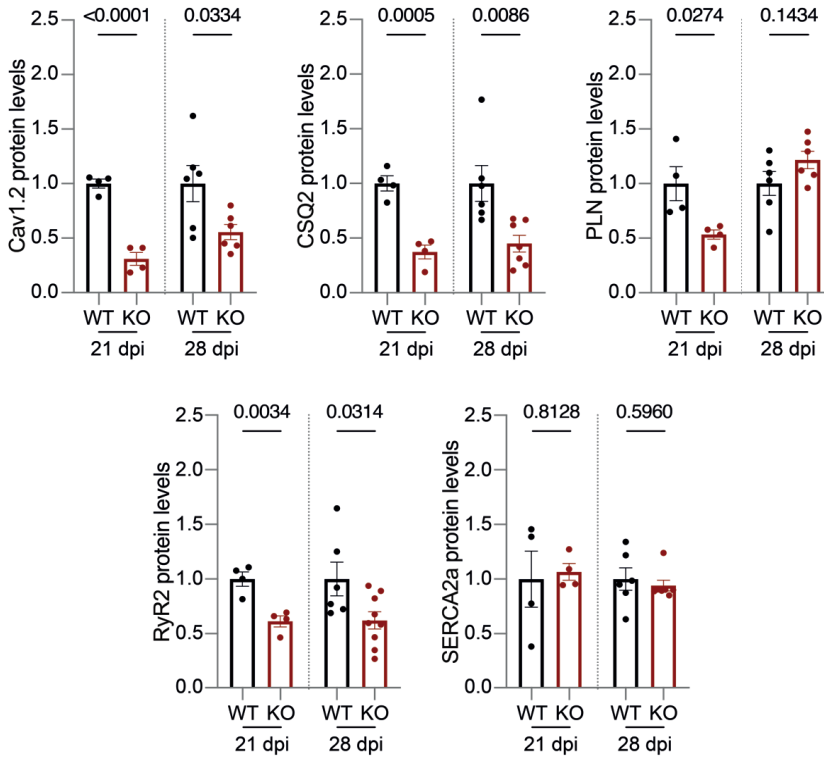


Figure S3. Western immunoblotting of calcium handling proteins in an inducible *Pkp2* knock-out mouse model. Protein levels were measured in mouse cardiac biopsies originating from the left (LV) of 4-6 wild-type (WT), and 4-8 cardiomyocyte-specific tamoxifen-induced *PKP2* knock-out (KO) mice. Biopsies were obtained at 21 and 28 days post tamoxifen injection (dpi). Data from the 21 dpi mice were obtained from prior experiments⁷. Protein levels of calcium handling proteins was similar between both timepoints. All protein levels were normalized to poncau.

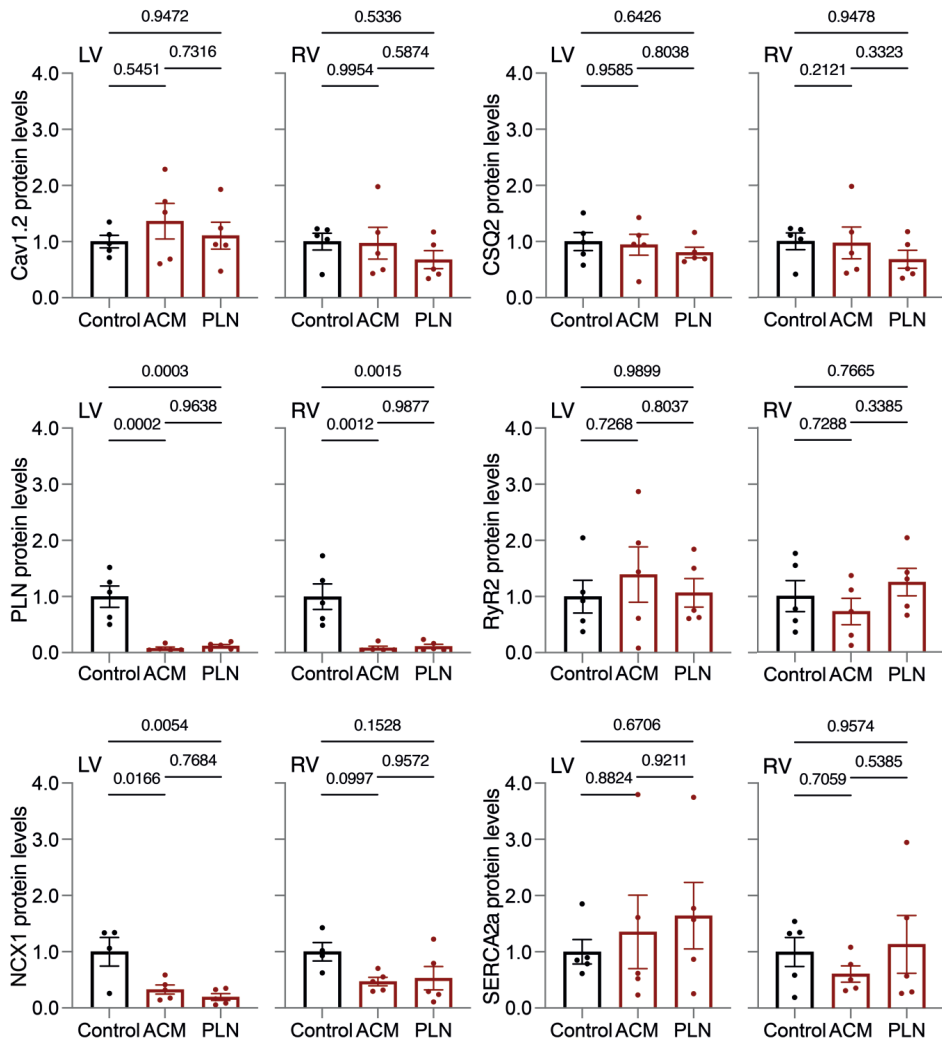


Figure S4. Protein levels of calcium handling proteins in ACM and PLN. Protein levels were measured in human cardiac biopsies originating from the left and right ventricle (LV and RV) of 5 healthy control, 5 phospholamban cardiomyopathy (PLN), and 5 arrhythmogenic cardiomyopathy (ACM) patients. Protein levels of calcium handling proteins were not different between PLN and ACM samples. All protein levels were normalized to GAPDH protein levels.

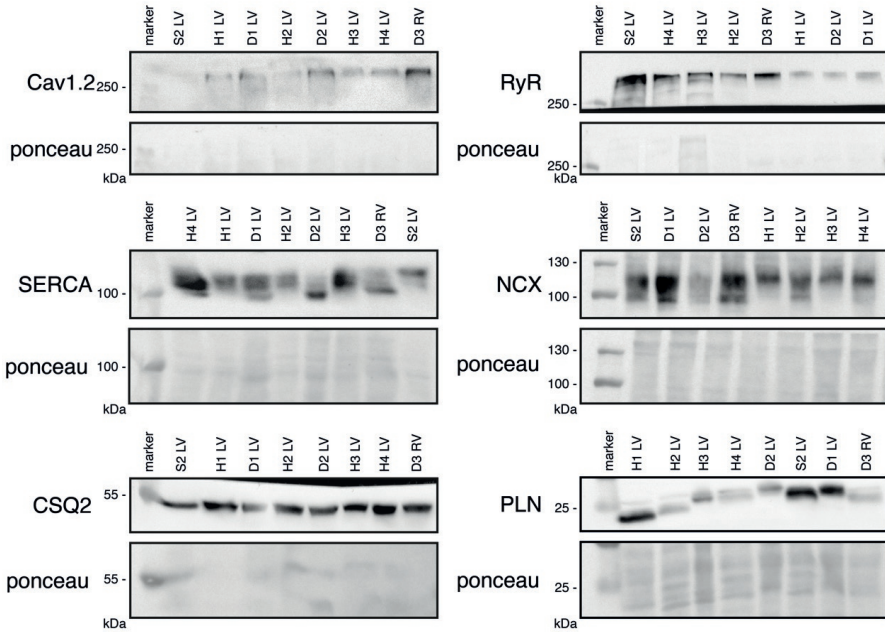


Figure S5. Western immunoblotting of calcium handling proteins in DCM and HCM. Western immunoblots of human cardiac biopsy samples originating from the left ventricle (LV) of 3 dilated cardiomyopathy (DCM, D1-D3) and 4 hypertrophic cardiomyopathy (HCM, H1-H4) patients. Ponceau stainings were determined to correct for equal sample loading and normalization of all protein levels. Samples were compared to control material originating from Figure S1, also normalized to ponceau.

Willem B. van Ham¹

¹Department of Medical Physiology, University Medical Center Utrecht, The Netherlands

Chapter VIII

General discussion

Cellular substrates of arrhythmogenicity in inherited and acquired cardiomyopathies

Pro-arrhythmic substrates can develop from genetic predisposition to dysfunctional proteins, as seen in arrhythmogenic cardiomyopathy (ACM), or cardiac and systemic pathologies, such as ischemic heart disease (IHD) and chronic kidney disease (CKD). ACM (formerly known as ARVC) is an inherited disease, represented by progressive deterioration of cardiac performance and increased susceptibility to cardiac arrhythmias. On the other hand, cardiac dysfunction in CKD and IHD are acquired due to dysfunction of the kidneys or coronary arteries, respectively. Consequently, increased uremic toxin (UT) concentrations, inflammatory responses, cell death, and fibrosis formation can affect cardiac performance. In this thesis, we included studies that investigated molecular and electrophysiological mechanisms behind increased arrhythmogenicity in inherited and acquired cardiomyopathies.

Part I - Cardiorenal syndrome

Approximately 10% of the global population suffers from kidney disease, especially CKD¹. Amongst the advanced stages of CKD, particularly during end-stage kidney disease (ESKD), the prevalence of sudden cardiac death (SCD) is estimated as high as 40%^{2,3}. Rather remarkably, the incidence of sudden cardiac arrest (SCA) during dialysis sessions is not elevated despite electrolyte fluxes and fluid disturbances, although it was observed that 60% of patients who were resuscitated after SCA during dialysis died within 48 hours⁴. The influence of electrolyte fluxes on SCD is further demoted by the prevalence of SCD in peritoneal dialysis patients, who do not undergo rapid electrolyte changes⁵. Moreover, SCD rates in non-dialysis and young CKD patients add to the uncertainty of dialysis being the sole cause of cardiac arrhythmias⁶⁻⁸. A study of almost 400 SCA cases in dialysis clinics showed that two-thirds of occurring arrhythmias were non-shockable, though a defibrillator was only applied on 50% of the SCA patients^{3,9}. Additionally, recent studies indicate that SCA in ESKD patients is more often caused by bradyarrhythmia and asystole^{10,11}. Logically, these statistics highlight the uncertainty of applying preventive implantable cardioverter defibrillators in the ESKD population. This has been proven to be unsuccessful, as implantation of these devices does not only fail to influence SCD or total mortality rates, but the implantation also brings many additional technical, physical, and emotional complications^{12,13}. Altogether, this emphasizes that arrhythmias in CKD have an extremely high prevalence and are difficult to treat, and future research should focus on preventing patients from reaching this endpoint.

Alongside the evident prevalence of SCA in CKD patients, various CKD mouse models show increased arrhythmogenicity¹⁴⁻¹⁷, but research on the exact mechanisms remains scarce. In **Chapter II** we have described the process of UT accumulation during CKD and associated cardiac issues. Concentrations of these UTs are increasing alongside the progressing stages of CKD, indicating that they play an important role in the development and aggravation of both renal and cardiac symptoms. Aside from the effects of

UTs on oxidative stress, inflammation, and fibrosis formation, we have highlighted the lack of knowledge on direct cardiac electrophysiological effects by summarizing electrophysiological UT research performed in both animals and humans. We further stress this by measuring the repolarization current I_{Kr} and action potentials (AP) after UT exposure, as described in **Chapter III**. The most commonly investigated UTs caused a decreased I_{Kr} current and subsequent AP prolongation after chronic, but not acute, exposure at clinically relevant concentrations. The latter was also reversible using a I_{Kr} activating compound, which indicates a potential pharmaceutical option to prevent repolarization issues in patients.

Although many studies report the occurrence of atrial fibrillation in CKD patients^{18,19}, CKD can also lead to ventricular arrhythmias^{8,20,21}. Increased fibrosis formation and inflammation play an important role in developing arrhythmias^{20,22}, whereas volume overload in CKD patients can also result in increased cardiac hypertrophy and therefore fuel susceptibility to arrhythmias and SCD^{21,23}. While we have now applied single UTs on human induced pluripotent stem cell derived cardiomyocytes (hiPSC-CMs), upscaling to more advanced cellular systems consisting of multiple cell types, and exposure to cocktails of multiple UTs or patient serum, is required to take the systemic effects into account. Most importantly, the development of CKD and occurrence of arrhythmias in young individuals should become a prime topic in preventing both kidney and cardiac related deaths in the future.

As the possibilities of transplantation of either a kidney or a heart are still very limited, therapeutic options are constricted to slowing CKD progression²⁴. Whereas initial effectiveness of the oral absorbent AST-120, which binds and neutralizes UTs but also suppresses inflammation, was proven in the Japanese CKD population^{25,26}, other population studies were proven unsuccessful in slowing CKD progression²⁷⁻²⁹. In future therapeutic studies it remains important to include not only analysis of drug or therapy effectiveness on CKD progression, but also on their ability to limit cardiac pathologies^{30,31}. For example, tolvaptan, a vasopressin V2-receptor antagonist was shown to hamper CKD progression effectively in polycystic kidney disease patients, because it limited volume overload and consequently improved cardiac function even in chronic heart failure patients^{32,33}. Similarly, pharmacological interventions developed for different diseases, such as cholesterol-lowering and anti-hypertension drugs, or sodium-glucose cotransporter 2 (SGLT2) inhibitors could also aid in treatment of the complex pathology in CKD patients^{8,34,35}. Explored options for UT removal from plasma, including a double layer mixed matrix membrane that facilitates both dialysis and UT adsorption^{36,37}, should be used to study the effects on cardiac remodeling and electrophysiology pre- and post-dialysis. When studying treatment applications, effectiveness is often determined by measuring the most essential UTs, i.e. UTs with the highest concentrations in patients. However, to efficiently evaluate these applications, effectiveness should be based on removal of the most detrimental UTs, of which the electrophysiological effects as determined in our study are a major element.

Part II - Patient-specific disease modeling of inherited and acquired cardiomyopathies

During cardiac development, the complex mechanical structure between cardiomyocytes named the intercalated disc (ID), regulates not only cell-to-cell contact formation, but also cell proliferation. In **Chapter III** we discussed the inappropriate localization of N-cadherin (N-CAD) and other ID proteins, which seemingly resulted in cardiac hyperplasia rather than hypertrophy shortly after birth. Unfortunately, as cardiac material from these pediatric patients is very scarce, only morphological analysis could be performed and since there was no clinical rationale for genetic screening at the time of death, we can only speculate on whether localization of N-CAD was the primary dysfunction. However, N-CAD is presumed to be a primary regulator of electromechanical maturation of the ID^{38,39}, meaning that these patients might have been carriers of pathogenic variants in *CDH2*, the gene encoding for N-CAD. Alternatively, genetic variants in genes encoding for proteins involved in proper localization of N-CAD cannot be excluded. Interestingly, these aberrancies also resemble the pathogenicity of ACM, as there are ACM patients harboring pathogenic *CDH2* variants^{40,41}. Unfortunately, no immunohistological stainings are available for these cases, so no comparisons with our patients can be made. The molecular mechanism behind the arrhythmias in these patients has not been investigated but has been assumed to be consequential of dislocation and dysfunction of sodium channels and gap junctions, which are influenced by appropriate ID formation⁴². Further research on N-CAD dysfunction, e.g. using hiPSC-CM-based models, could determine the precise effects on electrophysiological disruption, cardiomyocyte maturation, fibrosis formation, and lipid accumulation.

Studying patient-specific disease mechanisms can be realized potently, and at a large scale, with the use of hiPSC-CMs, as shown in our patient case in **Chapter V**. While clinical and genetic diagnostics could not identify the cause of arrhythmias in this patient, experimentally we were able to show a disturbed calcium homeostasis in terms of early after transients (EATs). Additionally, we showed a similar but less pronounced experimental phenotype in the patient's sister, who we initially included as healthy control. This is a phenomenon that fits with the phenotype of short-coupled Torsade de Pointes (scTdP) arrhythmias like observed in the patient. This phenotype is based on premature ventricular complexes seemingly originating from the Purkinje fibers as noticed in multiple scTdP patients⁴³. This is supported by the measured shortened action potentials, where the EATs potentially culminate in the formation of delayed afterdepolarizations, a described mechanism in Purkinje fibers^{44,45}. We now postulated a mechanism that could be instigated by alternate cardiac ryanodine receptor functionality, as a similarly speculated mechanism in several scTdP cases⁴⁶⁻⁴⁸. Alternatively, as pathogenic variants in *SCN5A* and *DPP6* are also linked to scTdP and short-coupled idiopathic ventricular fibrillation⁴⁹⁻⁵¹, the involvement of the sodium current and the transient outward potassium current cannot be excluded in our study. This study intriguingly demonstrated the basis of experimentally phenotyping patient-specific cardiac

pathologies. Although now only calcium handling was studied as an initial approach following the clinical diagnosis of scTdP, standardizing the electrophysiological phenotyping of both calcium regulation, individual ion currents, and AP morphology could be beneficial in all patient-specific cardiomyopathy research. The current study is limited herein, as more elaborate action potential and sodium, calcium, and potassium current data could be useful to further understand the mechanism of arrhythmogenicity. Furthermore, if more extensive whole exome sequencing can be performed, these results need to be analyzed across family members to possibly identify a pathogenic variant. If this would happen, further knockin hiPSC-CM studies could aid in reproducing the occurrence of EATs and potentially establish a novel pathogenic variant associated with scTdP. Simultaneously, it instigates the ethical discussion surrounding the value of experimental data in determining a clinical diagnosis. Currently, a certain degree of skepticism on translationability is valid based on e.g. immaturity of hiPSC-CMs and the fact that it concerns only a single patient. However, the majority of cardiac research aims at establishing early diagnostic tools and preventative treatments, but use of patient material is often limited to end-stage heart failure. Identifying potential disease carriers such as our patient's sister using cell-based disease models remains a major achievement.

Approximately 60% of ACM patients harbor pathogenic variants in genes encoding for desmosomal proteins, such as *plakoglobin* (*JUP*), *desmoplakin* (*DSP*), and most frequently *plakophilin-2* (*PKP2*)^{52,53}. Therefore, in **Chapter VI** we described parts of three studies that we performed in collaborations, which all revolved around disturbed cellular electrophysiology and calcium handling. In **Part A** we were able to identify a novel *DSP* variant in hiPSC-CMs and identified the transcription factor paired-like homeodomain 2 (*PITX2*) as regulator of electrophysiological disturbance and predisposition to ACM. In our performed efforts, molecular focus remained limited to protein levels of connexin 43 (*Cx43*) and the sodium channel (*Nav1.5*), which cannot entirely explain the prolongation of the measured action potentials. However, in the setting of ACM, decreased levels of *Cx43* and *Nav1.5* combined with the diminished desmosomal proteins indicate the impaired electromechanical coupling between cardiomyocytes. Proteins and current densities that are responsible for action potential repolarization (e.g. *Kv11.1* conducting I_{Kr} , *Kir2.1* conducting I_{K1} , and *Nav1.5* conducting I_{Na}) are more likely to explain the action potential lengthening, but their involvement in *PITX2* dysregulation is currently limited to a small and rather inconclusive number of studies in atrial cardiomyocytes^{54,55}. In **Part B**, investigating a heterozygous mouse model of a pathogenic and patient-specific *Pkp2* variant, we presented an additional mechanism behind diminished ID protein levels in ACM, and demonstrated a proof-of-concept method to inhibit protein degradation which prohibited the phenotype of molecular- and calcium dysfunction. This model only partially shows the electrophysiological consequences seen in ACM, but considers the genetic background comparable to patients. Generally, ACM mouse models are often either genotypically

or phenotypically comparable to the representing human disease. Where the conditional *Pkp2* knock-out mouse clearly resembles electrical and calcium handling deficiencies, the complete depletion of PKP2 after cardiac development does not represent the human disease given the fact that genetic variants in patients generally have a heterozygous character^{56,57}. Application of additional triggers, e.g. a high fat diet shown to increase lipid accumulation and inflammation in a heterozygous *Pkp2* knock-out mouse⁵⁸, in our genotypically comparable ACM mouse could increase the effects on cardiac electrophysiology. In **Part C**, exploring a mouse model of IHD, we showed that overexpression of the transcription factor Zinc finger E-box-binding homeobox 2 (ZEB2) improved calcium homeostasis and cardiac function. Therapeutic modulation of ZEB2 can be achieved by inhibiting mircoRNA-208a, which regulates expression of many cardiac genes. Alternatively, viral delivery of ZEB2 can also be effective and precise, and has also been shown to preserve cardiac function⁵⁹. In recent years, both viral delivery and extracellular vesicles have been increasingly popular for their application in gene editing due to their rather low immunogenicity and high precision⁶⁰⁻⁶². Viral delivery of PKP2 has recently been shown to prevent ACM progression in mice⁶³, paving the road for a promising future for the application of these techniques in humans.

Chapter VII included the molecular analysis of cardiac biopsies from patients diagnosed with PKP2 ACM, but also other inherited cardiomyopathies, being dilated (DCM), hypertrophic (HCM), and *phospholamban* (PLN) cardiomyopathy. In these patients, we showed differences in profiles of proteins involved in maintenance of normal calcium homeostasis and implemented them in a computational model of human cellular electromechanics. We highlighted the sodium-calcium exchanger (NCX1) as key regulator in the identified calcium overload and dysfunction of cellular relaxation in ACM patients. Interestingly, where increased NCX1 functionality can also result in arrhythmias⁶⁴, our ACM patients had significantly decreased NCX1 protein levels. Under physiological conditions, NCX1 transports three sodium ions for one potassium ion and is dependent on both membrane potential and intracellular calcium⁶⁵. Arrhythmias induced by increased NCX1 activity are most likely caused by enhanced calcium efflux and sodium influx, culminating in a potentially premature depolarizing current that can induce pro-arrhythmic afterdepolarizations. However, in our modeling study we did not focus on arrhythmogenicity in terms of ectopic activity, but mainly highlighted the calcium dysregulation. Potentially, decreased NCX1 protein levels could lead to increased diastolic calcium, with subsequent impaired relaxation and enhanced mitochondrial calcium uptake. Mitochondrial calcium overload could eventually lead to calcium-mediated cardiomyocyte stress and death, the latter being a phenomenon also observed in ACM patients^{66,67}. With this study we also reinforced the suggestion to cluster patients based on genotype rather than phenotype. A limitation of this study, however, is the direct translation from protein levels to protein function in the computational model. Unfortunately, no direct translation exists, but protein levels remain more suitable than gene expression. In time, bridging the gap between experimental and clinical data could be achieved

with the use of computational modeling, as a previous study already linked computational to clinical data⁶⁸. This would require more complex multiscale models, an exploration that is currently ongoing⁶⁹⁻⁷¹.

Disease modeling and phenotyping

Studying pathological mechanisms, performing pharmacological safety analyses, and estimating the potency of new therapeutic approaches requires the selection of the optimal disease models. While animal models are mainly chosen to mimic systemic consequences and cellular models to study exact mechanics in a controlled environment, both have their own claim on clinical translationability. The use of hiPSC-CMs has significantly improved over the years and allows for precise and patient-specific approaches that can be modulated in terms of model complexity. This is especially important in the aim to reduce animal-use in scientific research⁷², and the fact that these cells are of human origin suggests that the influence of differences in species can be excluded. Where hiPSC-CMs were originally applied mainly in a two dimensional fashion (i.e. cell clusters and monolayers), development of multicellular engineered heart tissues⁷³, vascularized microtissues⁷⁴, and organ-on-a-chip systems⁷⁵ have introduced intricate options to improve *in vitro* research and to proceed in bridging the gap towards original human tissue. Especially when connecting both cardiac microtissues with kidney organoids in a micro-fluid system⁷⁶, disease models are elevated in terms of complexity, interdisciplinarity, and translationability. However, the use of single cells is still important in studying specific ion currents for example. To study cardiac pathophysiology, these complex systems can be used first for general optical electrophysiological and contractility screenings to establish a broad disease phenotype, after which follow-up analyses can be designed for specific mechanisms of interest and therapeutic interventions. Bridging the cellular studies to the clinical setting still remains difficult and computational models can aid in translationability, especially when cellular, whole-heart, and systemic computer models are linked in a multi-scale model^{71,77,78}.

In recent years, tremendous strides have also been made in slicing, cultivating, and handling of human cardiac tissue slices, and recent improvements are highly promising⁷⁹⁻⁸¹. When acquiring human biopsies, e.g. during implantation of an assist device, partial resectioning, or a complete heart transplant, thin slices can be prepared and cultured for several weeks. Currently, these studies are restricted to end-stage failing hearts, which still limits the extensiveness of the concept. Ultimately, developing strategies to handle and cultivate post-mortem heart tissue would substantially increase availability of human material. These slices can be used for serial contractility and optical electrophysiology research, as well as screening drug applications. Subsequently, tissue stainings and biochemical analyses can also be performed, covering both molecular and functional parameters in a human model.

Conclusion

The complex interaction between electrical activity, calcium handling, contractility, cell-to-cell coupling, and conduction demands a variety of research approaches to fully understand the mechanisms behind cardiac arrhythmias. Where novel sophisticated techniques and cell models will aid in translationability of patient-focused experimental findings, basic research remains vital in understanding underlying mechanisms. In the upcoming years the use of animal models will likely be heavily restricted if not nonexistent in the foreseeable future, whether we are ready for it or not. On the other hand, the question remains how to study e.g. chronic effects of newly developed drugs without the availability of a systemic (animal) model. The use of hiPSC-CMs, tissue engineering, computational modeling, and increased availability of human tissue has created an abundance of alternatives for disease modeling. In this thesis, we made use of some of these options to perform patient-specific and translationable studies. Much progress can still be made in our research, especially in terms of novel techniques and approaches, but the described patient populations are a valuable target for reducing arrhythmia occurrence and other cardiovascular diseases. As they are not cardiac patients from onset on, improving the treatment options for the CKD population will significantly affect the success of arrhythmia prevention. Similarly, patient-specific research in patients of inherited cardiomyopathies and their family members could increase the number of identified individuals at risk. This will also create a challenging situation in which decisions need to be prepared for a clinical handling of these (sometimes not yet symptomatic) individuals.

References

1. Jager KJ, Kovesdy C, Langham R, Rosenberg M, Jha V, Zoccali C. A single number for advocacy and communication-worldwide more than 850 million individuals have kidney diseases. *Kidney Int.* 2019;96(5):1048-1050.
2. Schuett K, Marx N, Lehrke M. The Cardio-Kidney Patient: Epidemiology, Clinical Characteristics and Therapy. *Circ Res.* 2023;132(8):902-914.
3. Genovesi S, Boriani G, Covic A, et al. Sudden cardiac death in dialysis patients: different causes and management strategies. *Nephrol Dial Transplant.* 2021;36(3):396-405.
4. Karnik JA, Young BS, Lew NL, et al. Cardiac arrest and sudden death in dialysis units. *Kidney Int.* 2001;60(1):350-357.
5. Genovesi S, Porcu L, Luise MC, et al. Sudden Death in End Stage Renal Disease: Comparing Hemodialysis versus Peritoneal Dialysis. *Blood Purif.* 2017;44(1):77-88.
6. Caravaca F, Chavez E, Alvarado R, Garcia-Pino G, Luna E. Sudden cardiac death in non-dialysis chronic kidney disease patients. *Nefrologia.* 2016;36(4):404-409.
7. Svane J, Nielsen JL, Stampe NK, et al. Nationwide study of mortality and sudden cardiac death in young persons diagnosed with chronic kidney disease. *Europace.* 2022;24(10):1599-1607.
8. Pun PH. The interplay between CKD, sudden cardiac death, and ventricular arrhythmias. *Adv Chronic Kidney Dis.* 2014;21(6):480-488.
9. Pun PH, Dupre ME, Starks MA, et al. Outcomes for Hemodialysis Patients Given Cardiopulmonary Resuscitation for Cardiac Arrest at Outpatient Dialysis Clinics. *J Am Soc Nephrol.* 2019;30(3):461-470.
10. Sacher F, Jesel L, Borni-Duval C, et al. Cardiac Rhythm Disturbances in Hemodialysis Patients: Early Detection Using an Implantable Loop Recorder and Correlation With Biological and Dialysis Parameters. *JACC Clin Electrophysiol.* 2018;4(3):397-408.
11. Roy-Chaudhury P, Tumlin JA, Koplan BA, et al. Primary outcomes of the Monitoring in Dialysis Study indicate that clinically significant arrhythmias are common in hemodialysis patients and related to dialytic cycle. *Kidney Int.* 2018;93(4):941-951.
12. Pun PH, Hellkamp AS, Sanders GD, et al. Primary prevention implantable cardioverter defibrillators in end-stage kidney disease patients on dialysis: a matched cohort study. *Nephrol Dial Transplant.* 2015;30(5):829-835.
13. Jukema JW, Timal RJ, Rotmans JI, et al. Prophylactic Use of Implantable Cardioverter-Defibrillators in the Prevention of Sudden Cardiac Death in Dialysis Patients. *Circulation.* 2019;139(23):2628-2638.
14. Fontes MS, Papazova DA, van Koppen A, et al. Arrhythmogenic Remodeling in Murine Models of Deoxycorticosterone Acetate-Salt-Induced and 5/6-Subtotal Nephrectomy-Salt-Induced Cardiorenal Disease. *Cardiorenal Med.* 2015;5(3):208-218.
15. Thomsen MB, Nielsen MS, Aarup A, Bisgaard LS, Pedersen TX. Uremia increases QRS duration after beta-adrenergic stimulation in mice. *Physiol Rep.* 2018;6(13):e13720.

16. King BMN, Mintz S, Lin X, et al. Chronic Kidney Disease Induces Proarrhythmic Remodeling. *Circ Arrhythm Electrophysiol.* 2023;16(1):e011466.
17. Laurita KR, Khan S, McMahon T, et al. Ventricular arrhythmias in mouse models of diabetic kidney disease. *Sci Rep.* 2021;11(1):20570.
18. Huang SY, Chen YA, Chen SA, Chen YJ, Lin YK. Uremic Toxins - Novel Arrhythmogenic Factor in Chronic Kidney Disease - Related Atrial Fibrillation. *Acta Cardiol Sin.* 2016;32(3):259-264.
19. Yamagami F, Tajiri K, Yumino D, Ieda M. Uremic Toxins and Atrial Fibrillation: Mechanisms and Therapeutic Implications. *Toxins (Basel).* 2019;11(10):597.
20. Green D, Roberts PR. Ventricular arrhythmias and sudden death in patients with chronic kidney disease. *J Ren Care.* 2010;36 Suppl 1:54-60.
21. Di Lullo L, Rivera R, Barbera V, et al. Sudden cardiac death and chronic kidney disease: From pathophysiology to treatment strategies. *Int J Cardiol.* 2016;217:16-27.
22. Galli F. Protein damage and inflammation in uraemia and dialysis patients. *Nephrol Dial Transplant.* 2007;22 Suppl 5:v20-36.
23. Kitano Y, Kasuga H, Watanabe M, et al. Severe coronary stenosis is an important factor for induction and lengthy persistence of ventricular arrhythmias during and after hemodialysis. *Am J Kidney Dis.* 2004;44(2):328-336.
24. Larmour K, Levin A. Slowing Progression in CKD: DAPA CKD and Beyond. *Clin J Am Soc Nephrol.* 2021;16(7):1117-1119.
25. Hatakeyama S, Yamamoto H, Okamoto A, et al. Effect of an Oral Adsorbent, AST-120, on Dialysis Initiation and Survival in Patients with Chronic Kidney Disease. *Int J Nephrol.* 2012;2012:376128.
26. Shoji T, Wada A, Inoue K, et al. Prospective randomized study evaluating the efficacy of the spherical adsorptive carbon AST-120 in chronic kidney disease patients with moderate decrease in renal function. *Nephron Clin Pract.* 2007;105(3):c99-107.
27. Schulman G, Berl T, Beck GJ, et al. Randomized Placebo-Controlled EPPIC Trials of AST-120 in CKD. *J Am Soc Nephrol.* 2015;26(7):1732-1746.
28. Cha RH, Kang SW, Park CW, et al. A Randomized, Controlled Trial of Oral Intestinal Sorbent AST-120 on Renal Function Deterioration in Patients with Advanced Renal Dysfunction. *Clin J Am Soc Nephrol.* 2016;11(4):559-567.
29. Schulman G, Berl T, Beck GJ, et al. Risk factors for progression of chronic kidney disease in the EPPIC trials and the effect of AST-120. *Clin Exp Nephrol.* 2018;22(2):299-308.
30. Nakai K, Fujii H, Kono K, Goto S, Fukagawa M, Nishi S. Effects of AST-120 on left ventricular mass in predialysis patients. *Am J Nephrol.* 2011;33(3):218-223.
31. Asanuma H, Chung H, Ito S, et al. AST-120, an Adsorbent of Uremic Toxins, Improves the Pathophysiology of Heart Failure in Conscious Dogs. *Cardiovasc Drugs Ther.* 2019;33(3):277-286.
32. Kinugawa K, Sato N, Inomata T. Effects of Tolvaptan on Volume Overload in Patients with Heart Failure. *Int Heart J.* 2018;59(6):1368-1377.

33. Gheorghiadu M, Niazi I, Ouyang J, et al. Vasopressin V2-receptor blockade with tolvaptan in patients with chronic heart failure: results from a double-blind, randomized trial. *Circulation*. 2003;107(21):2690-2696.
34. Zoccali C, Mallamaci F, Adamczak M, et al. Cardiovascular complications in chronic kidney disease - A review from the European Renal and Cardiovascular Medicine Working Group (EURECA-m) of the European Renal Association (ERA). *Cardiovasc Res*. 2023;119(11):2017-2032.
35. The E-KCG, Herrington WG, Staplin N, et al. Empagliflozin in Patients with Chronic Kidney Disease. *N Engl J Med*. 2023;388(2):117-127.
36. Faria J, Ahmed S, Stamatialis D, et al. Bioengineered Kidney Tubules Efficiently Clear Uremic Toxins in Experimental Dialysis Conditions. *Int J Mol Sci*. 2023;24(15):12435.
37. Pavlenko D, van Geffen E, van Steenbergen MJ, et al. New low-flux mixed matrix membranes that offer superior removal of protein-bound toxins from human plasma. *Sci Rep*. 2016;6:34429.
38. Vite A, Radice GL. N-cadherin/catenin complex as a master regulator of intercalated disc function. *Cell Commun Adhes*. 2014;21(3):169-179.
39. Linask KK, Knudsen KA, Gui YH. N-cadherin-catenin interaction: necessary component of cardiac cell compartmentalization during early vertebrate heart development. *Dev Biol*. 1997;185(2):148-164.
40. Ghidoni A, Elliott PM, Syrris P, et al. Cadherin 2-Related Arrhythmogenic Cardiomyopathy: Prevalence and Clinical Features. *Circ Genom Precis Med*. 2021;14(2):e003097.
41. Mayosi BM, Fish M, Shaboodien G, et al. Identification of Cadherin 2 (CDH2) Mutations in Arrhythmogenic Right Ventricular Cardiomyopathy. *Circ Cardiovasc Genet*. 2017;10(2):e001605.
42. Vermij SH, Abriel H, van Veen TA. Refining the molecular organization of the cardiac intercalated disc. *Cardiovasc Res*. 2017;113(3):259-275.
43. Wang G, Zhong L, Chu H, Wang C, Zhu X. Short-coupled variant of torsade de pointes: A systematic review of case reports and case series. *Front Cardiovasc Med*. 2022;9:922525.
44. Maruyama M, Joung B, Tang L, et al. Diastolic intracellular calcium-membrane voltage coupling gain and postshock arrhythmias: role of purkinje fibers and triggered activity. *Circ Res*. 2010;106(2):399-408.
45. Bergeman AT, Postema PG, Wilde AAM, van der Werf C. Pharmacological treatment of short-coupled idiopathic ventricular fibrillation: A review. *Indian Pacing Electrophysiol J*. 2023;23(3):77-83.
46. Hirose S, Murayama T, Tetsuo N, et al. Loss-of-function mutations in cardiac ryanodine receptor channel cause various types of arrhythmias including long QT syndrome. *Europace*. 2022;24(3):497-510.
47. Fujii Y, Itoh H, Ohno S, et al. A type 2 ryanodine receptor variant associated with reduced Ca(2+) release and short-coupled torsades de pointes ventricular arrhythmia. *Heart Rhythm*. 2017;14(1):98-107.
48. Cheung JW, Meli AC, Xie W, et al. Short-coupled polymorphic ventricular tachycardia at rest linked to a novel ryanodine receptor (RyR2) mutation: leaky RyR2 channels under non-stress conditions. *Int J Cardiol*. 2015;180:228-236.

49. Kajiyama T, Miyazawa K, Kondo Y, Nakano M, Kobayashi Y. SCN5A mutation and a short coupled variant of Torsades de Pointes originating from the right ventricle: A case report. *J Cardiol Cases*. 2020;21(3):104-105.
50. Sonoda K, Ohno S, Shimizu Y, et al. SCN5A mutation identified in a patient with short-coupled variant of torsades de pointes. *Pacing Clin Electrophysiol*. 2020;43(5):456-461.
51. Xiao L, Koopmann TT, Ordog B, et al. Unique cardiac Purkinje fiber transient outward current beta-subunit composition: a potential molecular link to idiopathic ventricular fibrillation. *Circ Res*. 2013;112(10):1310-1322.
52. Corrado D, Basso C, Judge DP. Arrhythmogenic Cardiomyopathy. *Circ Res*. 2017;121(7):784-802.
53. Groeneweg JA, van der Heijden JF, Dooijes D, van Veen TA, van Tintelen JP, Hauer RN. Arrhythmogenic cardiomyopathy: diagnosis, genetic background, and risk management. *Neth Heart J*. 2014;22(7-8):316-325.
54. Mechakra A, Footz T, Walter M, et al. A Novel PITX2c Gain-of-Function Mutation, p.Met207Val, in Patients With Familial Atrial Fibrillation. *Am J Cardiol*. 2019;123(5):787-793.
55. Schulz C, Lemoine MD, Mearini G, et al. PITX2 Knockout Induces Key Findings of Electrical Remodeling as Seen in Persistent Atrial Fibrillation. *Circ Arrhythm Electrophysiol*. 2023;16(3):e011602.
56. Kim JC, Perez-Hernandez M, Alvarado FJ, et al. Disruption of Ca(2+)(i) Homeostasis and Connexin 43 Hemichannel Function in the Right Ventricle Precedes Overt Arrhythmogenic Cardiomyopathy in Plakophilin-2-Deficient Mice. *Circulation*. 2019;140(12):1015-1030.
57. Cerrone M, Montnach J, Lin X, et al. Plakophilin-2 is required for transcription of genes that control calcium cycling and cardiac rhythm. *Nat Commun*. 2017;8(1):106.
58. Sommariva E, Stadiotti I, Casella M, et al. Oxidized LDL-dependent pathway as new pathogenic trigger in arrhythmogenic cardiomyopathy. *EMBO Mol Med*. 2021;13(9):e14365.
59. Gladka MM, Kohela A, Molenaar B, et al. Cardiomyocytes stimulate angiogenesis after ischemic injury in a ZEB2-dependent manner. *Nat Commun*. 2021;12(1):84.
60. Whitley JA, Cai H. Engineering extracellular vesicles to deliver CRISPR ribonucleoprotein for gene editing. *J Extracell Vesicles*. 2023;12(9):e12343.
61. Harisa GI, Faris TM, Sherif AY, et al. Gene-editing technology, from macromolecule therapeutics to organ transplantation: Applications, limitations, and prospective uses. *Int J Biol Macromol*. 2023:127055.
62. Evers MJW, van de Wakker SI, de Groot EM, et al. Functional siRNA Delivery by Extracellular Vesicle-Liposome Hybrid Nanoparticles. *Adv Healthc Mater*. 2022;11(5):e2101202.
63. Van Opbergen CJ, Narayanan B, Sacramento CB, et al. AAV-mediated Delivery of Plakophilin-2a Arrests Progression of Arrhythmogenic Right Ventricular Cardiomyopathy in Murine Hearts: Preclinical Evidence Supporting Gene Therapy in Humans. *bioRxiv*. 2023:2023.2007.2012.548590.
64. Wang X, Song J, Yuan Y, et al. Downregulation of FKBP5 Promotes Atrial Arrhythmogenesis. *Circ Res*. 2023;133(1):e1-e16.

65. Eisner DA, Caldwell JL, Trafford AW, Hutchings DC. The Control of Diastolic Calcium in the Heart: Basic Mechanisms and Functional Implications. *Circ Res.* 2020;126(3):395-412.
66. Rasola A, Bernardi P. Mitochondrial permeability transition in Ca(2+)-dependent apoptosis and necrosis. *Cell Calcium.* 2011;50(3):222-233.
67. De Stefani D, Rizzuto R, Pozzan T. Enjoy the Trip: Calcium in Mitochondria Back and Forth. *Annu Rev Biochem.* 2016;85:161-192.
68. Mast TP, Teske AJ, Walmsley J, et al. Right Ventricular Imaging and Computer Simulation for Electromechanical Substrate Characterization in Arrhythmogenic Right Ventricular Cardiomyopathy. *J Am Coll Cardiol.* 2016;68(20):2185-2197.
69. Walmsley J, Arts T, Derval N, et al. Fast Simulation of Mechanical Heterogeneity in the Electrically Asynchronous Heart Using the MultiPatch Module. *PLoS Comput Biol.* 2015;11(7):e1004284.
70. Lumens J, Delhaas T, Kirn B, Arts T. Three-wall segment (TriSeg) model describing mechanics and hemodynamics of ventricular interaction. *Ann Biomed Eng.* 2009;37(11):2234-2255.
71. Arts T, Delhaas T, Bovendeerd P, Verbeek X, Prinzen FW. Adaptation to mechanical load determines shape and properties of heart and circulation: the CircAdapt model. *Am J Physiol Heart Circ Physiol.* 2005;288(4):H1943-1954.
72. Van der Velden J, Asselbergs FW, Bakkens J, et al. Animal models and animal-free innovations for cardiovascular research: current status and routes to be explored. Consensus document of the ESC Working Group on Myocardial Function and the ESC Working Group on Cellular Biology of the Heart. *Cardiovasc Res.* 2022;118(15):3016-3051.
73. Goldfracht I, Efraim Y, Shinnawi R, et al. Engineered heart tissue models from hiPSC-derived cardiomyocytes and cardiac ECM for disease modeling and drug testing applications. *Acta Biomater.* 2019;92:145-159.
74. Arslan U, Brescia M, Meraviglia V, et al. Vascularized hiPSC-derived 3D cardiac microtissue on chip. *Stem Cell Reports.* 2023;18(7):1394-1404.
75. Goldrick C, Guri I, Herrera-Oropeza G, et al. 3D multicellular systems in disease modelling: From organoids to organ-on-chip. *Front Cell Dev Biol.* 2023;11:1083175.
76. Gabbin B, Meraviglia V, Mummery CL, et al. Toward Human Models of Cardiorenal Syndrome in vitro. *Front Cardiovasc Med.* 2022;9:889553.
77. Van Osta N, Kirkels FP, van Loon T, et al. Uncertainty Quantification of Regional Cardiac Tissue Properties in Arrhythmogenic Cardiomyopathy Using Adaptive Multiple Importance Sampling. *Front Physiol.* 2021;12:738926.
78. Lyon A, Dupuis LJ, Arts T, et al. Differentiating the effects of beta-adrenergic stimulation and stretch on calcium and force dynamics using a novel electromechanical cardiomyocyte model. *Am J Physiol Heart Circ Physiol.* 2020;319(3):H519-H530.
79. Wang K, Lee P, Mirams GR, et al. Cardiac tissue slices: preparation, handling, and successful optical mapping. *Am J Physiol Heart Circ Physiol.* 2015;308(9):H1112-1125.

80. Meki MH, Miller JM, Mohamed TMA. Heart Slices to Model Cardiac Physiology. *Front Pharmacol.* 2021;12:617922.
81. Hamers J, Sen P, Merkus D, Seidel T, Lu K, Dendorfer A. Preparation of Human Myocardial Tissue for Long-Term Cultivation. *J Vis Exp.* 2022(184).

Appendix

Samenvatting in het Nederlands

Dankwoord

List of publications

Curriculum vitae

Cellulaire substraten van aritmogeniteit in erfelijke en verworven hartspierziekten

Samenvatting in het Nederlands

Introductie

Elektrische activiteit en stroomgeleiding in het hartspierweefsel liggen ten grondslag aan de samentrekking van het hart. Verschillende ionstromen die zich verplaatsen over het celmembraan via ionkanalen veroorzaken de elektrische activatie (depolarisatie) en inactivatie (repolarisatie) van hartspiercellen. De opsomming van al deze ionstromen reflecteert zich in de cardiale actiepotentiaal. Vlak na de depolarisatie leiden bepaalde ionstromen tot de vrijlating van calcium uit de calciumopslag binnen in de hartspiercel, wat vervolgens de samentrekking (contractie) van die cel faciliteert. De opvolgende repolarisatie en heropname van calcium in de calciumopslag brengen de hartspiercel weer in rust (relaxatie). Actiepotentialen kunnen van cel op cel doorgegeven worden doordat de hartspiercellen mechanisch stevig aan elkaar verbonden zijn door middel van intercalaire schijven (intercalated discs, IDs). Op die manier kan het gehele hart op een georganiseerde manier samentrekken. De elektromechanische koppeling tussen hartspiercellen en de calciumhuishouding in deze cellen zijn van cruciaal belang voor het waarborgen van een gezond hartritme en verstoringen in deze processen kunnen leiden tot hartritmestoornissen.

Twee algemene concepten zijn van belang in het ontstaan van hartritmestoornissen, namelijk ongeleide spontane activiteit (ectopic activity) en ontregelde voortgeleiding van de elektrische impuls (reentry). Spontane activiteit is het gevolg van vervroegde en spontane depolarisatie van de hartspiercel, doordat ionstromen in foutieve hoeveelheden over het celmembraan bewegen of wanneer de calcium regulatie verstoord is. Reentry ontstaat zodra actiepotentialen incorrect over het hartspierweefsel kunnen voortgeleiden, doordat er bijvoorbeeld een lokale blokkade van collageenweefsel is ontstaan tussen cellen en daardoor het patroon van de voortgeleiding anders zal verlopen dan normaal. In beide processen kunnen hartspiercellen worden geactiveerd op ongecontroleerde momenten, waarbij er dus een ritmestoornis ontstaat in het hart. Een hartritmestoornis kan een mild karakter hebben zonder grote of langdurige consequenties, maar indien de stoornis langer aanhoudt of de contractiliteit van het hart ernstig belemmerd wordt, kan dit ook fatale gevolgen hebben.

Om de mechanismen die ten grondslag liggen aan hartritmestoornissen te kunnen onderzoeken, moeten deze twee mogelijke oorzaken meegenomen worden in het kiezen van geschikte modellen. Waar individuele of clusters van cellen gebruikt kunnen worden voor het onderzoeken van ionstromen en calciumhuishouding, is intact hartspierweefsel nodig om voortgeleiding te kunnen bestuderen. Gezien dat het gebruik van diermodellen veelal ontmoedigd wordt, vindt er veel ontwikkeling plaats op het gebied

van cellulaire modellen. Binnen hartonderzoek worden vooral hartspiercellen gebruikt afkomstig van stamcellen (human induced pluripotent stem cell derived cardiomyocytes, hiPSC-CMs) voor de ontwikkeling van geavanceerde en complexere modellen. Daarbij is het materiaal afkomstig uit mensen en bevatten de hiPSC-CMs veel, maar niet alle, karakteristieken van originele humane hartspiercellen. Het gebruik van humane hartplakjes gesneden van explantaat materiaal of harten afkomstig uit diersmodellen blijft echter van belang voor onderzoek gericht op stroomgeleiding in het hart.

Verschillende van deze cellulaire substraten onderliggend aan hartritmestoornissen kunnen verworven worden gedurende het leven van een individu. Een voorbeeld hiervan is chronische nierziekte (chronic kidney disease, CKD). Patiënten die lijden aan CKD hebben vaak ook last van hart- en vaatproblemen, en zeker in de vergevorderde fases overlijden veel patiënten aan plotse hartoortdood. De functionaliteit van het hart en de nieren zijn met elkaar verbonden, bijvoorbeeld bij de bloeddrukregulatie en huishouding van ion concentraties in het bloed. Met deze kennis is het aannemelijk dat nierziekten ook effect hebben op de elektrische activiteit van hartspiercellen, maar onderzoek hierover is nog zeer beperkt. Alternatief hieraan zijn substraten voor hartritmestoornissen, waarbij een genetische achtergrond bepalend is. Een voorbeeld hiervan is aritmogene cardiomyopathie (ACM). Deze erfelijke hartspierziekte wordt gekarakteriseerd door ritmestoornissen en vervanging van spierweefsel voor collageen- en vetweefsel. Genetische veranderingen in de genen coderend voor de desmosomale eiwitten plakophilin-2 en desmoplakin, betrokken in de vorming van de ID, komen het meest voor binnen de ACM-patiëntenpopulatie. Het hebben van een genetische variatie heeft echter niet altijd een ziekteontwikkeling als gevolg, wat de voorspelling voor het ontstaan, de ernst en de progressie van de ziekte per patiënt verschillend maakt. Er is relatief veel aandacht voor ACM, maar nieuwe genetische kennis en een onvolledig begrip van de rol van de calciumhuishouding in dit ziekteproces vereisen voortzetting van onderzoek.

Dit proefschrift

In dit proefschrift hebben we onderzoek uitgevoerd om de mechanismen te begrijpen die ten grondslag liggen aan het ontstaan van hartritmestoornissen in diverse modellen van hartspierziekten. In **hoofdstuk I** beschrijven we de basis van cellulaire elektrofyfiologie en calciumregulatie in hartspiercellen, worden de ziekten CKD en ACM geïntroduceerd en bespreken we de elektrofyfiologische fenotypering binnen ziektemodellering. We scheiden de overige hoofdstukken in dit proefschrift vervolgens in twee delen.

Deel I draait om de interactie tussen hart- en nierziekten, het cardiorenaal syndroom (CRS). **Hoofdstuk II** introduceert en beschrijft de kenniskloof die bestaat rondom de effecten van in het bloed accumulerende uremische toxines op de elektrofyfiologie van het hart in CKD-patiënten. In deze literatuurstudie geven we overzichten van onderzoeksmodellen en klinische studies die de koppeling

tussen CKD en elektrische verstoringen in het hart beschreven hebben. Verder stellen we een overzicht voor waarin concentraties van toxines staan om te gebruiken in toekomstig onderzoek, gebaseerd op concentraties van uremische toxines zoals die gemeten zijn in patiënten met verschillende stadia van CKD. Vervolgens gebruiken we enkele van deze individuele uremische toxines en hun bijbehorende concentraties in **hoofdstuk III** om het effect van deze stoffen op actiepotentialen en onderliggende ionstromen te bestuderen. We laten zien dat onder andere indoxyl sulfaat, een van de meest onderzochte uremische toxines, actiepotentialen van hiPSC-CMs verlengt en dat dit veroorzaakt wordt door vermindering van de repolarisatiestroom I_{Kr} . We tonen aan dat dit effect waarschijnlijk veroorzaakt wordt door een verminderde hoeveelheid eiwitten die deze stroom faciliteren.

Deel II van dit proefschrift beschrijft verschillende patiënt-specifieke studies waarin de ID, cellulaire elektrofysiologie en calciumregulatie een rol spelen in het veroorzaken van elektromechanische verstoringen. In **hoofdstuk IIII** hebben we hartweefsel bekeken van twee pediatrie patiënten die op een leeftijd van respectievelijk vier en zes weken na geboorte plotseling overleden zijn. Wij tonen aan dat het hartspierweefsel van deze patiënten veel meer hartspiercellen bevat als gebruikelijk en dat ID-vorming verstoord is vergeleken met een gezonde leeftijdscontrole. Onze data benadrukt dat de ID niet alleen van belang is bij de elektromechanische koppeling tussen de hartspiercellen, maar ook een belangrijke rol speelt in het ontwikkelingsproces van het hartspierweefsel. We postuleren dat in deze patiënten de immature ID-vorming de wisseling van hyperplasie (celvermeerdering) naar hypertrofie (celvergroting) verhinderd heeft, wat nodig is om goed en geëordineerd samentrekkend spierweefsel te vormen.

We beschrijven in **hoofdstuk V** een studie waarbij we onderzoeken hoe bij een ogenschijnlijk gezonde en jonge patiënt meerdere malen zeer ernstige ritmestoornissen zijn voorgekomen. Deze patiënt had geen geschiedenis van hartproblemen of structurele deformaties in het hart en standaard genetische doorlichting van genen betrokken bij aangeboren ritmestoornissen identificeerde geen enkele verandering in die betreffende genen. We tonen aan dat in hiPSC-CMs die we geproduceerd hebben van de patiënt, de regulatie van de interne calcium huishouding is verstoord. Deze cellen laten opnieuw calcium vrij uit de calciumopslag, terwijl de voorgaande vrijlating nog terug opgenomen dient te worden in de opslag. Ook laten we zien dat hiPSC-CMs van de zus van de patiënt dit fenomeen ook laten zien, wat mogelijk betekent dat de zus een asymptomatische drager zou kunnen zijn van een vergelijkbaar ziektebeeld.

Enkele studies betreffende hartspierziekten die we in samenwerking met andere onderzoekers uitgevoerd hebben staan beschreven in **hoofdstuk VI**. Deze projecten zijn uitgevoerd in hiPSC-CMs en muismodellen, waarbij wij de functionele elektrofysiologische analyses hebben uitgevoerd en beschreven hebben in dit proefschrift. In **deel A** onderzoeken we in hiPSC-CMs de effecten van een patiënt-specifieke genetische verandering in het gen coderend voor het desmosomale eiwit desmoplakin. In deze studie laten

we zien dat als gevolg van de mutatie de actiepotentialen verlengd worden indien desmoplakin verstoord is ongeacht de gevolgde technische interventies in de hiPSC-CMs. Ook komt naar voren dat deze verlenging gemoduleerd lijkt te worden door een eiwit (PITX2) dat verschillende ionkanalen reguleert. Bij **deel B** moduleren we nogmaals ACM, maar dan via een muismodel met een genetische aanpassing in plakophilin-2. We laten zien dat als gevolg van de effecten op dit eiwit andere ID-eiwitten ook beïnvloed worden door verstoorde plakophilin-2 functionaliteit. Daarnaast komt ook naar voren dat als we afbraak van eiwitten verhinderen met afbraakremmer, deze eiwitten onverstoord blijven en op een normale manier te vinden zijn in de hartspiercellen. Toepassing van deze remmer leidde ook tot behoud van de calciumhuishouding in geïsoleerde hartspiercellen, welke in eerste instantie wel verstoord was na introductie van de genetische verandering in plakophilin-2. In de derde studie, **deel C**, beschrijven we de rol van calcium in een situatie van ischemische hartspierziekte en hartregeneratie. In een overexpressie muis model van een transcriptiefactor (ZEB2) dat betrokken is bij de regulatie van calciumhuishouding en ionkanalen, laten we zien dat de hartfunctie behouden blijft na het induceren van ischemische hartschade. Ook in geïsoleerde hartspiercellen van deze overexpressie muizen bleek de calciumregulatie beter na de aangebrachte hartschade.

In **hoofdstuk VII** onderzoeken we veranderingen in eiwitten betrokken bij de calciumhuishouding in het hartspierweefsel van ACM-patiënten, waarbij we moleculair onderzoek implementeren in een humaan hartspiercel computermodel. Hiermee zoeken we naar een methode om de vertaalslag van resultaten naar patiënten te verbeteren ten opzichte van data verkregen uit cel- of diermodellen. We identificeren een vermindering van een ion transporteiwit (NCX) specifiek in ACM-weefsel en benadrukken, na implementatie van de eiwitniveaus in het computermodel, de functionele consequenties voor de hartspiercellen. Herstel van enkel het betreffende ion transporteiwit voorkomt ook de verslechterde functionaliteit in het model.

Hoofdstuk VIII sluit alle studies af door ze te verbinden met elkaar en we bespreken zowel limitaties van de studies als toekomstige visies.

Conclusie

In dit proefschrift beschrijven we verschillende erfelijke en verworven hartspierziekten met een focus op de cellulaire substraten van aritmogeniteit. De complexe interacties tussen elektrische activiteit, calciumhuishouding, contractiliteit, mechanische cel koppeling en voortgeleiding vereisen verscheidene manieren van onderzoek om de mechanismen van hartritmestornissen beter te begrijpen. Ontwikkelingen in cellulaire modellen hebben geleid tot translationeel en patiënt-specifiek onderzoek, maar verdere verbeteringen van technieken en interdisciplinair onderzoek zijn nodig om het verminderde gebruik van diermodellen te verantwoorden. De beschreven patiëntpopulaties uit dit proefschrift zijn

uitermate geschikt voor het verminderen van het aantal toekomstige hartziekten patiënten. Onderzoek gericht op CKD-patiënten of familieleden van patiënten met een (mogelijk) erfelijke hartspierziekte kunnen veel succes hebben in het verminderen van hartritme stoornissen in deze patiëntgroepen. Dit zal ook nieuwe en ingewikkelde situaties met zich meebrengen, waarbij beslissingen gemaakt moeten worden rondom het klinisch behandelen van deze (soms nog niet symptomatische) individuen.

Dankwoord

De laatst geschreven, maar vaak eerst gelezen, pagina's van elk proefschrift. Hiermee wil ik graag alle mensen bedanken die bijgedragen hebben aan mijn promotietraject, werkervaring en algemene mentale gesteldheid.

Prof. dr. **Vos, Marc**, je hebt altijd de successen van je onderzoeken en promovendi terecht met trots gedragen. Ik heb jarenlang de vrijheid en autonomie gekregen over mijn werk en wetenschappelijke interesses, waarbij wij elkaar vooral spraken over toekomstplannen en persoonlijke gebeurtenissen. Jouw praktische blik op academisch onderzoek heeft mede geholpen in het ontwikkelen van mijn eigen visie en ambitie. Mijn dank.

Dr. **Van Veen, Toon**, al snel leerde ik dat wij persoonlijk goed met elkaar overweg kunnen. Gesprekken zijn bij ons vaak rechtdoorzee, voorspelbaar omdat we vooraf al kunnen bedenken wat de ander gaat zeggen en ze zitten vol met platte en unieke uitspraken. Je vertrouwde jarenlang mijn onderzoeksrichting volledig ondanks mijn koppigheid, maar stuurde bij waar nodig of indien ik er naar vroeg. Tijdens lokale meetings en buitenlandse congressen introduceerde jij mij aan onderzoekers uit ons vakgebied, deelden we direct de nieuwtjes die we hoorden en konden we goed lachen. We hebben ook vaak genoeg het glas geheven, iets waar ik goed op terugkijk. Heel erg bedankt.

Graag wil ik mijn beoordelingscommissie, bestaande uit prof. dr. **Jeroen Bakkers**, prof. dr. **Roos Masereeuw**, prof. dr. **Christine Mummery**, prof. dr. **Joost Sluijter**, prof. dr. **Arthur Wilde**, bedanken voor het kritisch doorlezen en beoordelen van mijn proefschrift.

Uiteraard dragen de collega's op de vloer bij aan de ervaring van het werk en dat is bij de Medische Fysiologie niet anders. **Marcel**, al sinds mijn masterstage ben jij een fijne en stabiele rots in de branding. Door jouw goede begeleiding, bezoeken in Wenen, zomerborrels in jouw tuin en jouw hart voor onderzoek ben je onmisbaar. We zitten vrij vaak op dezelfde lijn en (ten koste van onze collega's?) lachen wat af. Mijn dank is groot. **Teun**, je bent niet alleen een vraagbaak voor veel discussies over elektronica en elektrofysiologie, je hebt ook een grote passie voor diezelfde (voor velen moeilijke) thema's. Ik waardeer dat je naast het hobbyen in het lab ook altijd mensen wilt helpen. **Marti**, wat heb ik genoten van onze dagelijkse koffiemomenten en gezellige gesprekken. Je bent een rolmodel binnen het onderwijs en het was super om voor en met jou onderwijs te mogen geven. **Sanne**, mijn eerste rondje op de Medische Fysiologie was dankzij jou toen ik nog in de 5^e klas op de middelbare school zat. Jij creëert dankzij je openheid en betrokkenheid een fijne en gezellige studie- en werkomgeving. **Linda**, een dag zonder kletsen op jouw kantoor is een dag niet gewerkt. Je bent altijd betrokken, bovenmaats behulpzaam en gezellig. Je bent er

altijd om mijn gezeur aan te horen, roddeltjes te delen, een steek onder de riem te geven of te zoeken naar de beste hotels en vluchten. Het was erg leuk om samen evenementen te organiseren, over alles en niets te praten en te flauwekullen. Erg bedankt. **Vera**, je hebt op alles een uniek perspectief en daar heb ik vaak veel aan gehad. Het was genieten om samen de BKO, BHV en Papendal trainingen te volgen. We konden altijd meedenken over elkaars werk en daarnaast gezellig borrelen en uit eten. Dankjewel. **Meye**, het ging ons goed af te verdwalen in discussies over diepgaande elektrofysiologie, onderwijs of de afdeling, vaak zonder echte conclusie. Je bent betrokken en neemt verantwoordelijkheid voor het lab en dat is heel fijn. Daarnaast ben je een van de mensen wie het al het langst met mij uitgehouden heeft op hetzelfde kantoor en daar moet je toch best robuust voor zijn. Dankje. **Encan**, it is really nice to see you found your own balance in the lab and at the conferences we went to together. You always work hard, but also remain very excited and kind to everyone around you. **Nathalie**, met jou kwam er ook een frisse wind over de werkvloer en dat was fijn. Al in een korte tijd zaten we best veel met elkaar opgezadeld en daar heb ik erg van genoten. Bedankt dat je elke dag de tijd nam om werk en interesses te bespreken en om samen te lachen. **Marien**, al komen we allemaal vaak voor technische en inhoudelijk hulp op het lab naar je toe, voor goede (maar soms wel bizarre) verhalen binnen en buiten het lab ben jij voor mij ook zeker een goede keuze. We konden altijd tussendoor even kletsen over spellen of het internet, en alle momenten op het elektrofysiologie lab waren genieten. Dankjewel. **Emmy**, je paste in een korte tijd toch al goed in onze groep en daar zijn wij ook beter van geworden. Heel fijn hoe je hard werkt, anderen helpt en je inzet om met het lab leuke dingen te gaan doen.

Mijn waardering is zeker niet gelimiteerd tot huidige leden van Medische Fysiologie, maar gaat ook uit naar mijn oud-collega's. **Joanne**, vanaf mijn eerste dag was jij betrokken, loyaal aan de mensen om je heen en in voor gezelligheid. Het was enorm waardevol en vaak een plezier om, al dan niet los van elkaar, zoveel samen te werken en mee te maken. Het was een eer om jou te mogen en kunnen helpen de afgelopen jaren, en om ook jouw hulp te ontvangen voor mijn promotietraject en daarbuiten. We kunnen altijd goed sparren, muggenziften op alles en dingen delen met elkaar, waardoor jouw standpunten en mentaliteit in mijn achterhoofd zullen hangen bij elke discussie die ik weer met mezelf voer. Ontzettend bedankt. **Birgit**, ik ben erg blij dat ik mijn eerste jaren in het lab zoveel op je kon rekenen, niet alleen inhoudelijk en technisch, maar vooral ook voor gezelligheid, gekkigheid en wederzijdse waardering. Na onze gezamenlijk tijd op het lab bleef dat gelukkig ook zo, en proberen we zo nu en dan nog samen te komen. Gelukkig kan ik nog steeds op jouw kennis, karakter en humor rekenen. Dankjewel. **Stephanie**, over de jaren hebben we de Toon groep goed in stand gehouden door de begeleiding van veel studenten, leuke borrels en etentjes en een mooi aantal gezellige congressen. Je bent altijd goedgezind en behulpzaam. Dat maakte niet alleen de afdeling een prettige plek, maar dat maakt je ook erg geschikt voor je gekozen loopbaan. **Aurore**, while we could occasionally find each other in complaining about everything, I will always be

envious of how much motivation you have for working, reading, and exercising so much. I valued all the conversations we had about experiences and career options in academia and science. I really enjoyed our conferences, dinners, projects, and time together. **Alexandre**, your departure allowed for my arrival, and I will always be grateful for your continuing support throughout and after that transition. In a relatively short time you taught and guided me immensely, but also combined it with greatly enjoyable patch clamp evenings and lunches. Thank you. **Jet**, ondanks dat ik geen dag met jou op de werkvloer heb gestaan, heb ik immens genoten van onze momenten samen. Van gezellig lunchen of borrelen op de afdeling tot promoties en een autotrip naar Tilburg in het midden van de nacht (en voor veel van deze evenementen ook zeker dank aan Esther). Dankjewel voor je interesse en hulp. **Agnieszka**, ook al hebben wij nooit inhoudelijk samen gewerkt, we hebben veel leuke en mooie momenten mee mogen maken. Bij jou thuis, op de afdeling of zelfs jouw bruiloftsfeest, gezellige borrels met jou waren er genoeg. Jouw daadkracht, interesse en persoonlijke betrokkenheid zijn inspirerend om mee te maken. **Valerie**, of we nu aan aaneengesloten bureaus zaten, aparte kantoren hadden of moesten bellen tussen Utrecht en Los Angeles, we konden elkaar altijd even vinden om mee te denken, te flauwekullen of te haten op alles en iedereen. Ik kijk altijd op naar hoe jaloersmakend slim en gedreven jij bent. Wel nog even doorwerken, ik heb de roze toga al besteld. **Leonie**, jij gaf veel structuur op het lab en wist van aanpakken. Je hielp met experimenten en was altijd paraat voor gezellige onderonsjes, daar heb ik van genoten. **Tonny**, al waren mijn eerste jaren op de afdeling jouw laatste jaren, toch hebben we nog veel over alles en niets gekletst. Het was erg fijn om altijd een plekje te vinden om het even niet over werk te hebben.

Een van mijn meest waardevolle taken was het begeleiden van studenten en dan niet (alleen) omdat er verdacht vaak koffie voor me werd gehaald. **Liza**, you were the first student I guided and helped a lot with developing my style of supervision while you worked on heart-kidney projects. I was happy to hear when you said you started a PhD project and wish you the best. **Carlijn**, van essay student tot bachelor- en masterstage student heb jij veel meegeholpen aan het uitdenken en uitvoeren van onze hart-nier projecten. Je bent prettig in de omgang en weet van doorpakken, ik wens je alle succes met verdere keuzes in je carrière. **Esmeralda**, vanaf jouw eerste stagedag was jij gepassioneerd en hardwerkend aan de slag gegaan met meerdere projecten. Het was een eer om jouw master laudatio te mogen geven en zoals beloofd blijf ik uiteraard met veel plezier jouw PhD traject en verdere carrière volgen. **Merel**, je voelde je vanaf het eerste moment al thuis in de groep en hebt veel bijgedragen aan de afronding van meerdere projecten. Jouw sociale karakter en nette werkstijl zullen goed van pas komen bij de uitvoering van je welverdiende PhD positie. **Ellis**, je zet het werk rondom onze hart-nier projecten voort en helpt mee met het uitzetten van de toekomstige projecten daarvan. Je bent scherpzinnig en bereid om hard te werken, heel fijn. **Nina**, je startte op een relatief nieuw onderzoeksgebied voor ons, maar wilde en kon al snel je eigen draai geven aan je project en experimenten. Je bent gedreven en zet je in voor de groep, heel fijn. **Zoë**, het was erg

leuk om een keer een student met een andere opleidingsachtergrond te mogen begeleiden. In de paar maanden dat je bij ons was, liet je zien dat je leergierig en enthousiast bent, ga zo door. **Sophie**, al was ik officieel niet jouw begeleider, ik heb jouw stagejaar met plezier van dichtbij meegemaakt. Jouw creatieve vermogen en nuchterheid zullen je goed helpen bij het vinden van een geschikte werkplek. **Kristina**, ook jij viel niet onder mijn begeleiding, maar tijdens jouw stage en ook daarna maakten we aardig wat van elkaars werk mee. Je bent gepassioneerd en werkt hard, en ik wens je veel plezier met je PhD traject.

I participated in several collaborations (some of which were only single experiments or discussions rather than predetermined projects) with people from different labs, which I enjoyed tremendously. From the Van Rooij group at the Hubrecht Institute. Prof. dr. **Van Rooij, Eva**, het was een eer om mee te kunnen denken en helpen met de projecten uit jullie groep. Dank voor het vertrouwen die je in mij had om het werk uit te voeren en het bieden van een rechte doorzetter perspectief in ons gemeenschappelijke onderzoek. **Monika**, it was wonderful to work on the isolations with you in my first year. Not only did you have the patience to allow me to train the required skills, but we also had a lot of fun in the lab. Encounters after that still allowed for quick discussions, exchange of advice, and enormously amusing times. Thank you. **Jenny**, we briefly met in my first year, but actually connected during the isolations for your project. I am genuinely happy we worked so well together and laughed endlessly. After that, we always stayed personally in touch and it remains a great pleasure to share coffee meetings, borrels, dinners, and keeping each other generally up-to-date. Many thanks. **Jantine**, je hebt met enthousiasme ontzettend veel gedaan voor ons gezamenlijke project. Het was altijd fijn samen te werken door de makkelijke communicatie en je consistente bijdrage en interesse. **Brian**, stiekem hebben we nog behoorlijk wat experimenten uitgevoerd voor jouw project, maar het was zeker de moeite waard. Ontzettend fijn dat je daarnaast altijd bereid was om nog wat cellen aan te leveren voor mijn hobbyprojecten. **Eirini**, although I eventually could not aid you in your project, we tried our best and expanded our experiences and collaborations. Your enthusiasm and kindness make it a pleasure every time we encounter each other. **Su Ji**, we only performed a few experiments, which unfortunately did not help you and your project. Luckily, we could always catch up when we encountered each other during a borrel or meeting.

From the lab of Experimental Cardiology at the UMCU. Prof. dr. **Sluiter, Joost**, voornamelijk in de laatste maanden van mijn promotietraject en in de tijd daarna hebben we regelmatig gepraat over onderzoek, onderwijs, begeleiding en onze kijk op de toekomst. Dank voor de uitdagingen om verder te denken en het bieden van vertrouwen in mijn keuzes en aanpak. **Elise**, het moest te doen zijn om een masterschrijfpodracht tot een publiceerbaar review om te zetten als we toch het lab niet op konden, al liep het wel een beetje uit. Ik ben erg blij hoe jij me meegenomen hebt in alle stappen en keuzes rondom artikelen schrijven en publiceren. Dankjewel. **Jort**, waar het in het begin vaker ging over technische onderwerpen, veranderden onze gesprekken al gauw naar kennisuitwisselingen, inzichten van elkaars lab

en andere onderzoekers of gewoon flauwekul. Je was altijd bereid om te helpen, een ander perspectief te bieden of te borrelen. Dankjewel. **Vasco**, it was always a delight when you visited our lab, with or without your horde of students and visitors. Before, during, and after you did your experiments there was always time for a nice chat or discussion, which I really enjoyed. **Renee**, het was fijn om te bespreken hoe we beiden in het onderzoek en samenwerkingen stonden. Ik ben blij dat ik mee kon denken met jouw analyses en technische opties, terwijl jij mij kon helpen met kennis en cellen voor mijn hobbyprojecten.

Het was erg leuk en verfrissend om af en toe inzicht te krijgen in promotietrajecten uit het verre België. **Evelien**, door jou forceer ik mezelf vaker om de goeie kant van mensen overheersend in gedachten te houden (al laat ik dat in de praktijk niet vaak aan die mensen merken). Je bent uitzonderlijk sympathiek, slim en hartelijk, en het is een eer om daar een deel van te ontvangen. Bedankt. **Fatima**, er zijn weinig mensen die lekker kunnen haten op alles en iedereen zoals dat wij dat kunnen. Het was ook goed de leuke kanten van België en een PhD te bespreken, al dan niet met een cynische ondertoon. Ik heb waardering voor hoe uitgesproken, slim en direct jij bent. Dankje.

During my time in Utrecht I met several great people for whom I will always be grateful. **Anoushka** (and **Marnix**), the dark humor we share is something I thoroughly enjoy and we always find a way to use it in any conversation. I admire how hard you have fought to be where you are now. The mix of topics like jokes, life experiences, science, and politics makes it a pleasure every time we have drinks together. Thank you. **Betzabel** (en **Seymour**), elke keer als we even in de kantine samen kwamen, we met de groep wat gingen drinken of wanneer jij weer heerlijk voor ons kookte, combineer jij sarcasme met eerlijkheid en vriendelijkheid. Je hebt tijdens je eigen drukte mij ontzettend geholpen met de opmaak van dit proefschrift en daar ben ik heel blij mee. Bedankt. **Li Ting** (and **Kai**), although you try to convince us that is not the case, it seems you have already figured out how to have a stable life. It is a blast when you are around, as you are always in for a laugh. I envy your cheerfulness and attentiveness.

Caroline, vanaf onze studententijd en de opvolgende jaren ben jij persoonlijk en inhoudelijk erg betrokken geweest. Het was altijd fijn om irritaties te bespreken, perspectieven van elkaars lab en personeel te vergelijken of gewoon een kopje koffie of pilsje te drinken (al ben ik toch elke keer blij dat ik het weer overleefd heb als ik uit jouw auto stap nadat ik mee kon rijden). We hebben altijd gezocht naar een project waarin we inhoudelijk kunnen samenwerken, wellicht komt die er ooit nog. Erg bedankt. **Doreth**, jij hebt jouw liefde voor pizza (waarvan ik de intensiteit onderschat had) over de jaren heen veel gedeeld met ons. Ondanks dat ik het idee heb dat jij vrijwel altijd op vakantie bent, heb je jezelf in een mooie loopbaan gewerkt. Ik geniet er elke keer van als we bijkletsen onder het genot van een borreltje en flauwe grappen.

In Tilburg is er altijd een thuishaven. **CV 't Schôrstintje** (ofwel **Pim, Tom, Jort, Thomas, Thom, Merijn, Daan, Thomas, Thio, Job**), de heren van het goede leven. Ik waardeer hoe wij als groep altijd

voor elkaar klaarstaan. Onder het genot van een borreltje is het voor mij altijd genieten en als vanouds als we samenkomen voor carnaval, vergaderingen, lunchmiddagen of huisbezoekjes. Immens bedankt. **Ward**, bijna wekelijkse lunches of avondjes in het café waren een zeer goed idee. In verhalen over vroeger, inzichten in onze banen of onze ergernissen aan hoe organisaties en mensen functioneren (of dus juist niet) kunnen we elkaar goed vinden. Mijn dank. **Stijn**, jij speelt het burgerlijke leven sneller uit dan de meesten van ons en dat is je gegund. Het is altijd gezellig om even samen te komen, online of fysiek en vrijwel altijd onder het genot van een pilsje, waarbij we kunnen terugblikken op vroeger en altijd dezelfde grappen kunnen maken. Dankjewel. **Roef**, jij hebt altijd interesse getoond in wat ik doe en afgevraagd hoe mijn werk mogelijk invloed kan hebben op de toekomst van patiënten. Via kaarten, digitale berichten of bezoeken ben je altijd betrokken bij onze hele familie en dat waardeer ik enorm. Dankjewel.

Mijn paranimfen en tevens goede vrienden. Niet alleen hebben jullie mij geholpen met mijn promotie, we hebben met zijn drieën samen carnaval gevierd, concerten bezocht, lekker geluncht, geborreld en een mooie vakantie in Lissabon gehad (en technisch gezien ook in Dublin, maar daar praten we niet meer over). **Erik**, vrijwel elke gebeurtenis gedurende mijn promotie heb jij jarenlang indirect ook meegemaakt en je hebt flink wat van mijn gezeur aangehoord. Je hebt altijd veel interesse getoond in mijn promotie en de perikelen eromheen en bij alles rond mijn verdediging en dit boekje stond je paraat om te helpen. Ondanks mijn koppige tegenzin om nieuwe dingen te doen, heb je mij vaak genoeg meegesleept naar feestjes of concerten waarvan ik vooraf nog niet wist dat ik het leuk zou vinden. Over de jaren heen hebben we een behoorlijk aantal sportsessies, lunches, en biertjes gedeeld en daar ben ik ontzettend blij mee. Waanzinnig bedankt. **Pim**, alleen in de laatste maanden hebben wij meer inhoudelijk over mijn promotie gesproken, daarvoor hebben we jarenlang heel vaak glaasjes gedronken, geluncht, gefeest en vakanties gedeeld. Onze gezamenlijke Brabantse nuchterheid helpt altijd goed mee om werkzaken even in perspectief te plaatsen en zelfs tijdelijk te vergeten. Dagen op pad in Spanje, Portugal, Zeeland of Utrecht met jou erbij zijn altijd gevuld met keet schoppen, jouw barbaarse en mijn zotte gedrag, humor en mooie verhalen. Je staat altijd klaar om te helpen en daarna doen we een lekker glaasje. Waanzinnig bedankt.

Een van de voordelen van het hebben van veel broers en zussen is dat ik veel kan afkijken van het leven. Ontzettend bedankt voor alles. **Barbara**, of het nu vakantie-reizen, vriendenuitjes of familiedagen zijn, jij regelt het alsof het niets is en weet iedereen mee te krijgen in je enthousiasme. Op eigen kracht heb jij een passie omgezet in werk en draagt dat graag over op anderen. Jij bent een voorbeeld van spontaniteit en tegelijkertijd controle hebben over de situatie. **Thijs**, terwijl je aangaf er niets van te begrijpen, keken jij en **Fabio** toch altijd op een afstandje met mijn werk mee. Bij elke stap van mijn opleidingen en loopbaan was jij ervan overtuigd dat ik grof geld ging verdienen, al was het alleen maar om mij te motiveren (of er zelf wat profijt aan over te houden). Jij bent een voorbeeld van oprechtheid en doordachte humor. **Floortje**, ondanks dat er vaak ook makkelijkere routes openliggen, besluit jij meer uit jezelf te halen en door te

pakken. Hoe jij kunt blijven jongleren met nieuwe studies, je werk, je leven en **Keano** is bewonderenswaardig. Jij bent een voorbeeld van iemand die echt hard kan werken en veel voor anderen over heeft. **Daan**, jij en **Emmy** zitten nauwelijks stil, gaan op veel (hoe dan?) mooie vakanties, sporten met vrienden en genieten hier en daar van een borreltje. We kunnen altijd samen praten over alle serieuze en onzinnige onderwerpen die we meemaken of tegenkomen. Al geloof ik best dat je ook goed in je werk zult zijn, jij bent een voorbeeld van hoe je daarbuiten hoort te genieten van alles. **Jesse**, jij en **Jeremy** durven risico's te nemen, zoeken op die manier jullie eigen weg en hebben er vertrouwen in dat het goed gaat komen. Of het nu in Nederland of het zonnige zuiden is, jullie werken om te genieten en genieten van het werken. Jij bent een voorbeeld van je eigen weg volgen en doorpakken.

Papa, al haakte je (terecht) al af bij de titels, als mijn naam op een nieuw artikel stond ging je het toch regelmatig even opzoeken. Je begon steeds meer begrip te krijgen van promoveren naarmate de concrete afrondingsfase inging. Vanaf dat moment kon je ook veel meer meedenken over mijn boekje, de verdediging en mijn, zoals jij ze noemt, secondanten (wat ik overigens een mooier en gepaster woord vind dan paranimfen, want laten we eerlijk zijn, promoveren is meer een gevecht dan een huwelijk). Ik ben heel erg blij dat je lekker op pad gaat met de camper en geniet van je tijd zoals je dat zelf wilt, maar toch ook altijd een paar dagen Nederland in je planning houdt zodat ik altijd met een gerust hart op huis aan kan gaan. Je bent er altijd voor het bijkletsen, het gezeur aanhoren, de spontane telefoontjes en de praktische trucjes van het leven. Oneindig bedankt.

Mama, je was de eerste die ik had willen vertellen dat dit alles gelukt is. Je wilde alles aanhoren en dacht altijd met me mee, vroeg wat nodig was voor mijn werk en promotie en bood jezelf vaak genoeg aan als proefpersoon. Jouw wens was dat we als familie elkaar op diezelfde manier blijven steunen en altijd voor elkaar klaar staan, iets waar we allemaal voor zullen blijven vechten. Jij was misschien niet waarom ik bepaalde onderzoeken begonnen ben, maar bent wel de reden waarom ik door zou willen blijven gaan. Oneindig bedankt.

List of publications

Publications included in this thesis:

van Ham, W.B., Cornelissen, C.M., & van Veen, T.A.B. Uremic toxins in chronic kidney disease highlight a fundamental gap in understanding their detrimental effects on cardiac electrophysiology and arrhythmogenesis. *Acta Physiologica (Oxford, England)*, 236(3), e13888. (2022).

van Ham, W.B., Cornelissen, C.M., Polyakova, E., van der Voorn, S.M., Ligtermoet, M.L., Monshouwer-Kloots, J., Vos, M.A., Bossu, A., van Rooij, E., van der Heyden, M.A.G., & van Veen, T.A.B. Pro-arrhythmic potential of accumulated uremic toxins is mediated via vulnerability of action potential repolarization. *International Journal of Molecular Sciences*, 24(6), 5373. (2023).

van Ham, W.B., Meijboom, E.E.M., Ligtermoet, M.L., Nikkels, P.G.J., van Veen, T.A.B. Maturation and function of the intercalated disc: report of two pediatric cases focusing on cardiac development and myocardial hyperplasia. *Journal of Cardiovascular Development and Disease*, 10(8), 354. (2023).

van Kampen, S.J., Han, S.J., **van Ham, W.B.**, Kyriakopoulou, E., Stouthart, E.W., Goversen, B., Monshouwer-Kloots, J., Perini, I., de Ruiter, H., van der Kraak, P., Vink, A., van Laake, L.W., Groeneweg, J.A., de Boer, T.P., Tsui, H., Boogerd, C.J., van Veen, T.A.B., & van Rooij, E. PITX2 induction leads to impaired cardiomyocyte function in arrhythmogenic cardiomyopathy. *Stem Cell Reports*, 18(3), 749–764. (2023).

Tsui, H., van Kampen, S.J., Han, S.J., Meraviglia, V., **van Ham, W.B.**, Casini, S., van der Kraak, P., Vink, A., Yin, X., Mayr, M., Bossu, A., Marchal, G.A., Monshouwer-Kloots, J., Eding, J., Versteeg, D., de Ruiter, H., Bezstarosti, K., Groeneweg, J., Klaasen, S.J., van Laake, L.W., Demmers, J.A.A., Kops, G.J.P.L., Mummery, C.L., van Veen, T.A.B., Remme, C.A., Bellin, M., & van Rooij, E. Desmosomal protein degradation as an underlying cause of arrhythmogenic cardiomyopathy. *Science Translational Medicine*, 15(688), eadd4248. (2023).

Submitted manuscripts included in this thesis:

Gladka, M.M., Kohela, A., de Leeuw, A., Molenaar, B., Versteeg, D., Kooijman, L., van Geldrop, M., **van Ham, W.B.**, Haigh, J.J., van Veen, T.A.B., & van Rooij, E. Hypoxia-responsive ZEB2 regulates a network of calcium handling genes in the injured heart.

Manuscripts in preparation included in this thesis:

van Ham, W.B., Meijboom, E.E.M., Ligtermoet, M.L., Monshouwer-Kloots, J., te Riele, A.S.J.M., Asselbergs, F.W., van Rooij, E., Bourfiss, M., & van Veen, T.A.B. An hiPSC-CM approach for electrophysiological phenotyping of a patient-specific case of short-coupled TdP.

van Ham, W.B., van der Voorn, S.M., Vink, A., Teurlings, S.M.W., van Opbergen, C.J.M., Kirkels, F.P., Taha, K., te Riele, A.S.J.M., Heijman, J., Delmar, M., Lumens, J., Lyon, A., & van Veen, T.A.B. Patient-specific modeling of disrupted calcium handling and cardiomyocyte electromechanics in arrhythmogenic cardiomyopathy.

Other publications:

van Ham, W.B., Kessler, E.L., Oerlemans, M.I.F.J., Handoko, M.L., Sluijter, J.P.G., van Veen, T.A.B., den Ruijter, H.M., & de Jager, S.C.A. Clinical phenotypes of heart failure with preserved ejection fraction to select preclinical animal models. **JACC. Basic to Translational Science**, 7(8), 844–857. (2022).

Li, E., Loen, V., van Ham, W.B., Kool, W., van der Heyden, M.A.G., & Takanari, H. Quantitative analysis of the cytoskeleton's role in inward rectifier $K_{IR}2.1$ forward and backward trafficking. **Frontiers in Physiology**, 12, 812572. (2022).

Qile, M., Ji, Y., Golden, T.D., Houtman, M.J.C., Romunde, F., Fransen, D., van Ham, W.B., IJzerman, A. P., January, C.T., Heitman, L.H., Stry-Weinzinger, A., Delisle, B.P., & van der Heyden, M.A.G. LUF7244 plus dofetilide rescues aberrant $K_v11.1$ trafficking and produces functional $I_{Kv11.1}$. **Molecular Pharmacology**, 97(6), 355–364. (2020).

Qile, M., Beekman, H.D.M., Sprenkeler, D.J., Houtman, M.J.C., van Ham, W.B., Stry-Weinzinger, A., Beyl, S., Hering, S., van den Berg, D.J., de Lange, E.C.M., Heitman, L.H., IJzerman, A.P., Vos, M.A., & van der Heyden, M.A.G. LUF7244, an allosteric modulator/activator of $K_v11.1$ channels, counteracts dofetilide-induced Torsades de Pointes arrhythmia in the chronic atrioventricular block dog model. **British Journal of Pharmacology**, 176(19), 3871–3885. (2019).

Dierich, M., van Ham, W.B., Stry-Weinzinger, A., & Leitner, M.G. Histidine at position 462 determines the low quinine sensitivity of ether-à-go-go channel superfamily member $K_v12.1$. **British Journal of Pharmacology**, 176(15), 2708–2723. (2019).

Curriculum vitae

Willem was born on the 1st of February 1995 in Tilburg to Nicoline Blankert and Frans-Jozef van Ham. He grew up together with his siblings Barbara, Thijs, Floortje, Daan, and Jesse. He followed his pre-university education at St. Odulphus Lyceum in Tilburg, where he already developed an interest in human physiology. He started his bachelor Biomedical Sciences at Utrecht University in 2013, mainly focusing on molecular and cellular cardiac (patho)physiology. He continued his studies with the master program Biology of Disease at Utrecht University in 2017. During this time he developed a clear interest in cardiac electrophysiology, represented by internships on ion channel trafficking



(Department of Medical Physiology, UMC Utrecht) and computational modeling of drug-ion channel interactions (Vienna University, Austria). After his studies in 2019, Willem acquired a research position at the Department of Medical Physiology at UMC Utrecht, where he worked for one year gaining experience in the theory and techniques of cardiac cellular electrophysiology. This time was extended into a PhD position, during which he continued his work focusing on cellular substrates of arrhythmogenicity in the setting of inherited and acquired cardiomyopathies. The work performed during his time at the Department of Medical Physiology is presented in this thesis. Along with research, Willem has been involved in education and obtained his Basiskwalificatie Onderwijs (BKO). From September 2023, Willem continued his scientific career as postdoctoral researcher at the Department of Medical Physiology at UMC Utrecht.

